Advancing host-directed therapy for Mycobacterium avium infection: identification of drug candidates and potential host targets

Kilinc, G.

Advancing host-directed therapy for *Mycobacterium avium* infection: identification of drug candidates and potential host targets

Gül Kilinç

Advancing host-directed therapy for *Mycobacterium avium* infection: identification of drug candidates and potential host targets

Gül Kilinç

Advancing host-directed therapy for *Mycobacterium avium* infection: identification of drug candidates and potential host targets
Doctoral thesis, Leiden University, Leiden, The Netherlands

Author: Gül Kilinç
Cover and chapter page images: Jeremy Thomas (jeremythomasphoto) and Jongsun Lee (sarahleejs) (Unsplash)
Layout and design: Gül Kilinç
Printed by: Gildeprint
ISBN: 978-94-6496-474-5

The research presented in this thesis was funded by the Innovative Medicines Initiative 2 Joint Undertaking (IMI2 JU) (www.imi.europa.eu) under the RespiriNTM (grant N° 853932) project within the IMI AntiMicrobial Resistance (AMR) Accelerator program.

Advancing host-directed therapy for *Mycobacterium avium* infection: identification of drug candidates and potential host targets

Proefschrift

ter verkrijging van
de graad van doctor aan de Universiteit Leiden,
op gezag van rector magnificus prof. dr. ir. H. Bijl,
volgens besluit van het college voor promoties
te verdedigen op donderdag 6 november 2025
klokke 13.00 uur

door

Gülandem Kilinç
geboren te Sas van Gent
In 1996

Promotor:	Prof. Dr. T.H.M. Ottenhoff
Copromotor:	Dr. A. Saris
Promotiecommissie:	Prof. Dr. H.H. Smits Prof. Dr. M.G.J. de Boer Prof. Dr. A.H. Meijer (Leiden University) Dr. A. van Laarhoven (Radboud University Medical Center) Dr. C.P. Kuijl (Amsterdam University Medical Center)

per aspera ad astra
through hardships to the stars

Table of contents


Chapter
1

General introduction

Gül Kilinç[1]

[1] Leiden University Center for Infectious Diseases, Leiden University Medical Center, Leiden, The Netherlands

Background & milestones NTM research

Tuberculosis (TB) is an ancient disease characterized by the presence of tubercles in tissues like the lungs and therefore historically described to be caused by ‘’tubercle bacilli’’. In 1882, Robert Koch isolated and identified the causative pathogen of TB and renamed it *Mycobacterium tuberculosis* (*Mtb*), which is the main cause of human infections due to *Mycobacterium* species (1). Following Koch’s discovery, other species of *Mycobacterium* were increasingly identified, which were referred to by several names, including ‘atypical mycobacteria’ and ‘nontuberculous mycobacteria’ (NTM). The earliest report of NTM was in the late 1880s when Alvarez and Tavil described the smegma bacillus (currently known as *Mycobacterium smegmatis*) found in human secretions (2). Nonetheless, it was already in 1868 in England, when Crisp observed seemingly TB in chicken (avian), later classified as *Mycobacterium tuberculosis avium* that mimicked the disease seen in humans, which was the first probable description of a bacterium now known as *Mycobacterium avium* (*Mav*) (**Figure 1**) (3). Koch initially stated that *Mav* was rather a variant of *Mtb* in animals, but more and more evidence became available to counteract his argument (3). According to Maffucci’s reports in 1890 and 1892, Rivolta suggested in 1883 and eventually also showed by experimental methods in 1889 that there was a difference between bovine TB and *Mav* found in chickens. In his reports, Maffucci described that *Mav* was definitely distinct from *Mtb* in the sense of cultural and pathogenic aspects, which was also confirmed by Cadiot, Gilbert, and Roger. However, since guinea pigs injected with *Mav* did not develop disease, *Mav* was believed not to cause disease in humans (3, 4). The development of improved culture techniques resulted in more accurate diagnoses of mycobacterial disease. In 1933, Branch reported the recognition of human-derived (pathogenic) *Mav* strains, and in 1943 Feldman et al. described a virulent *Mav* strain isolated from a patient with lung disease (5, 6). In 1949, a report by Cuttino and McCabe described a case of disseminated disease caused by a bacterial species, which was first named Nocardia intracellularis, later renamed to *Mycobacterium intracellulare* (*Min*) (7). Since *Mav* and *Min* are genetically very similar and not distinguishable by common laboratory examinations, they were together referred to as the *Mav* complex (MAC) (8). By 1953, more cases of MAC were described (9), and MAC was considered the most common cause of chronic lung infection due to NTM worldwide in the 1970s, which is still the case in many geographical regions. Interest in NTM increased in 1982, when disseminated infection, particularly caused by *Mav*, was dramatically more often observed in human immunodeficiency virus (HIV)-infected patients. While initially extremely rare, the recognition of *Mav* in patients with acquired immunodeficiency syndrome (AIDS) increased the number of disseminated cases strongly (10). Initially treated with solely *Mtb*-specific drugs, the implementation of clarithromycin in the 1990s marked a significant breakthrough in managing MAC disease. Meanwhile, the occurrence of MAC infections in AIDS patients was the first indication of the current knowledge that host immunity, specifically cell-mediated immunity, is critical for protection against MAC.

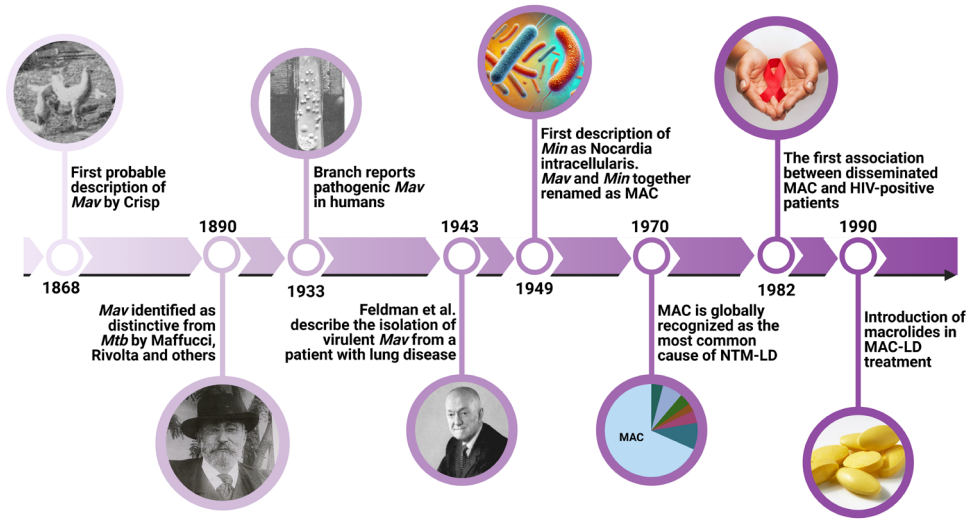

Figure 1. History of *Mav* (complex). *Mav*: *Mycobacterium avium*, *Mtb*: *Mycobacterium tuberculosis*, *Min*: *Mycobacterium intracellulare*, MAC: *Mycobacterium avium* complex, NTM: nontuberculous mycobacteria, LD: lung disease, HIV: human immunodeficiency virus. Created with BioRender.

MAC pathogenesis

Entry in, and recognition by host cells of the immune system

Given the airway-oriented nature of NTM infections, *Mav* may invade the mucosal barrier by interacting with bronchial epithelial cells to cause infection (11). Recognition and uptake of *Mav* by immune cells begins with the interaction of pattern recognition receptors (PRRs) on the cell surface that bind to pathogen-associated molecular patterns (PAMPs) to initiate a protective innate immune response against the mycobacteria. Characterization of the adhesions on *Mav* cell surface associated with the ability to interact with epithelial cells has identified the bacterial fibronectin attachment protein (FAP). FAP interacts with fibronectin to bind to integrin receptors on the surface of bronchial epithelial cells (12, 13). Once *Mav* reaches the alveolar space, it interacts with alveolar epithelial cells. Once recognized, *Mav* is taken up by epithelial cells requiring structural modifications of the cytoskeleton and proactive engagement of the cell (14). It is believed that *Mav*, by inducing biofilm formation and impairing the induction of an inflammatory response, may establish a chronic lung infection using the alveolar epithelial cells as a niche (15-17). While the mechanisms of escaping epithelial cells are unknown, it has been shown that *Mav* leaving epithelial mucosa has a different phenotype resulting in more efficient invasion of macrophages (18).

The mycobacteria may also directly, without interaction with epithelial cells, reach mononuclear phagocytes like monocytes and macrophages in the airways (19). There is a general consensus that macrophages represent the main reservoir of mycobacteria in the host (20, 21). Macrophages have a wide range of activation states with different functions, which can be broadly classified into two polar ends of the activation spectrum: pro-inflammatory macrophages (M1), involved in fighting infections, and

anti-inflammatory macrophages (M2), which play a role in resolving inflammation and promoting tissue repair (22-24). In the healthy ''resting'' state, human alveolar macrophages may possess an M1 or M2 phenotype (25, 26). During bacterial infections, however, host responses are skewing toward an M1 signature, which is associated with the control of acute infections. In contrast, the persistence of bacterial pathogens is linked to macrophage reprogramming to the M2 signature (27).

Macrophages express a wide variety of PRRs (28, 29), including Fc receptors, integrins, complement receptors (CR), C-type lectins, mannose and scavenger receptors. In addition to recognition, toll-like receptors (TLRs) are also involved in the induction of intracellular signaling cascades and pro-inflammatory responses. In particular TLR2, potentially by forming heterodimers with TLR1 and TLR6, plays a pivotal role in innate immune protection against *Mav* infection (30, 31). NTM, including *Mav*, express glycopeptidolipids (32), a major cell surface component that shields cell wall phosphatidyl-myo-inositol mannosides, thereby weakening recognition by TLR2 (33). Moreover, TLR6 and TLR9 are indispensable for managing *Mav* infection in mice (34, 35).

Host-pathogen interactions: macrophages vs. *Mav*

Once *Mav* is recognized, the macrophage membrane encapsulates and phagocytoses the mycobacteria, causing *Mav* to be targeted to cytoplasmic vacuoles called phagosomes. These phagosomes engage with the endosomal compartment to promote phagosome maturation (36). Phagosomes ultimately fuse with lysosomes that contain enzymes for bacterial killing (**Figure 2**). However, MAC can prevent its killing for example by impairing phagosome maturation by, using its secretory protein MAV_2941, interfering with vesicle trafficking and consequently fusion with lysosomes (37, 38). Moreover, mycobacterial membrane protein large 4 (MMPL4) participates in preventing phagosome maturation in *Mav*-infected cells by mechanisms not yet understood (39). Mycobacteria like *Mtb* and *Mycobacterium marinum* (*Mmar*) are known to be able to escape from the phagosome into the cytosol (40), where they can be targeted to autophagosomes to be degraded in a process called autophagy (or xenophagy) (41). In the same study, *Mav* remained phagosomal and showed no translocation to the cytosol, but the possibility of phagosomal escape has not been conclusively disproven.

In addition to direct recognition of *Mav*, macrophages can further be activated by IFN-γ released by CD4+ T helper 1 (Th1) cells induced by dendritic cells (DCs) via amongst others IL-12 (42). By presenting antigens and inducing T-cell responses, DCs link innate and adaptive immunity (43), in which the CD4+ T cell subset is essential for the host immunity against *Mav* (44, 45). Activation of the macrophage results in the TLR2-mediated production of pro-inflammatory cytokines, like IL-12, IL-23, and TNF (46, 47). IL-12 and IL-23 secreted by macrophages bind to their receptors on Th1 cells, promoting an increase in IFN-γ production. Furthermore, TNF induces apoptosis upon binding to its receptor TNFR1 (48). While most research indicates (TNF-mediated) host cell apoptosis as a host defense mechanism against mycobacterial, including *Mav*, infection (49-52), apoptosis can also be considered as a virulence mechanism of the bacteria as apoptotic macrophages have also been shown to result in the release and dissemination of *Mav* infection (53, 54). *Mav* expresses the MAV_2054 protein, which is known to induce macrophage apoptosis that can therefore be either host-protective or host-detrimental during *Mav* infection (55). Finally, macrophages generate reactive

oxygen species (ROS) and reactive nitrogen species (RNS) upon activation. While *Mav* tolerates RNS (56), ROS has been described to be involved in the killing of *Mav* by macrophages (57, 58). Taken together, while macrophages are the first-line defenders against *Mav* infection, bacteria can modulate host immune function to establish an intracellular replication niche that facilitates their replication and survival and evades immune detection.

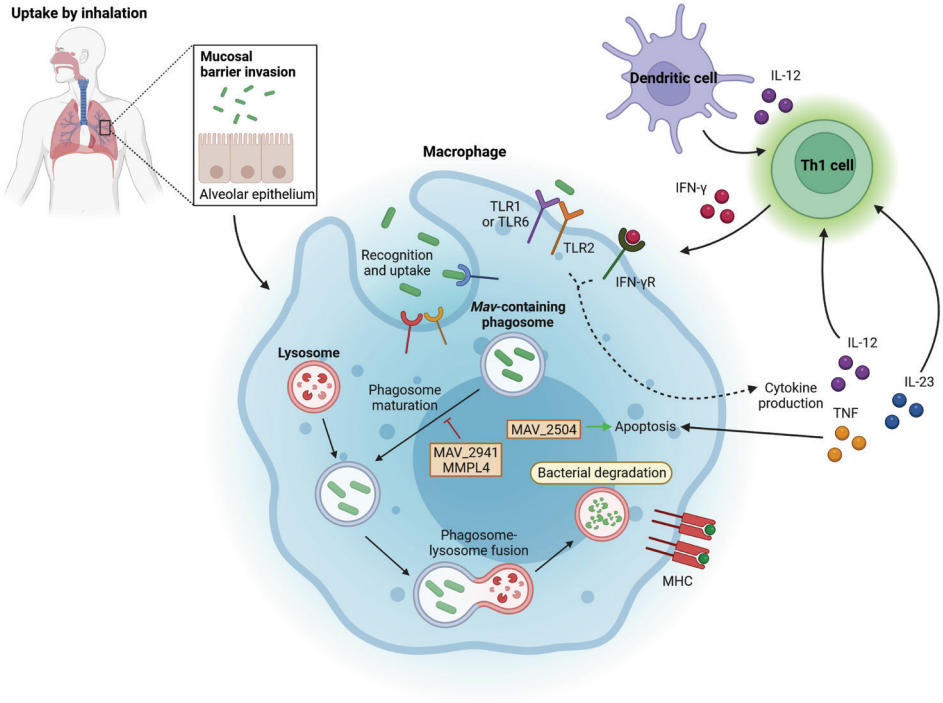

Figure 2. Phagocytosis and elimination of *Mav* by alveolar macrophages. Created with BioRender.

Mav exposure and risk factors

Environmental factors

While there is some evidence of human-to-human transmission (59), this type of transmission is extremely rare. Reasons may be the opportunistic nature of *Mav*, limiting infection in healthy individuals, and for example the lack of human-specific adaptations required for widespread transmission. Hence, it is believed that human disease due to *Mav* is acquired from environmental exposures. *Mav* and other NTM have been isolated from various environmental habitats, including both natural and treated water sources (e.g. drinking water distribution systems, hospitals, and household plumbing) (**Figure 3**), which are shared with humans and animals and have been associated with *Mav* disease (60-63). In addition to water, bacteria aerosolized as dust from potting soil has also been shown to be a risk factor for the development of disease due to *Mav* (64, 65). While the isolation of NTM from the environment is similar among different geographic areas (66, 67), higher risks for NTM infection and disease were identified in areas

characterized by higher population densities and higher household education and income levels. These factors tend to cluster in more urbanized areas, which previously have been linked to NTM disease (68-70).

The major factor that permits the persistence of *Mav* and other NTM in environmental sources is their hydrophobic, lipid-rich outer membrane (71, 72). The hydrophobic characteristic of these bacteria enables their attachment to surfaces (73), which prevents bacteria from being washed out and allows them to form biofilms (74). Both the character of a thick cell wall and biofilm formation result in the increased tolerance of NTM to antibiotics and disinfectants.

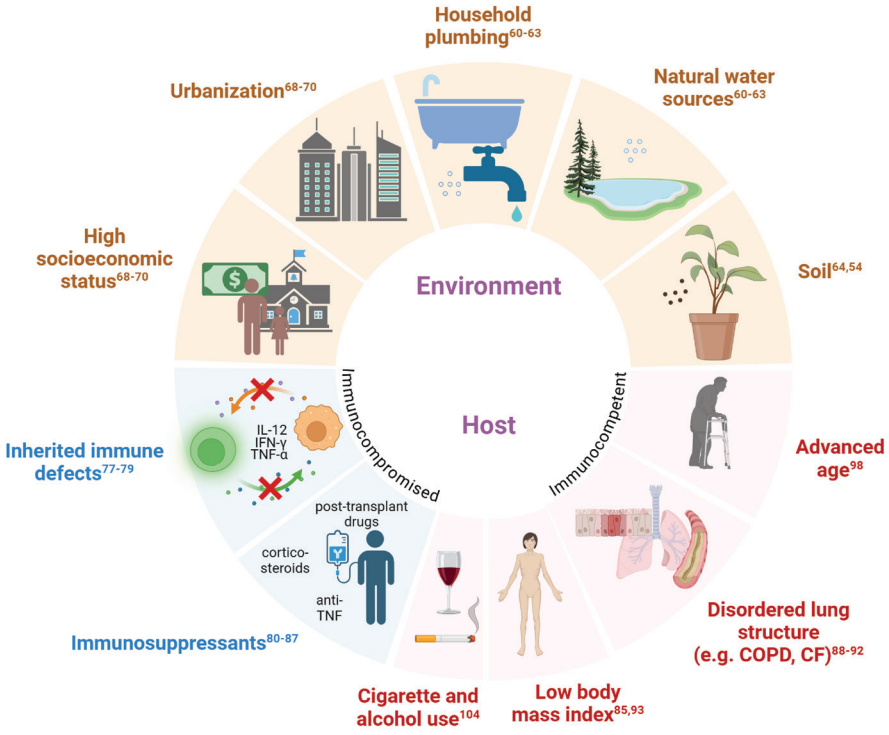

Figure 3. Environmental and host risk factors for MAC-LD. Created with BioRender.

Host factors

Due to their abundance, nearly everyone is presumed to be exposed to NTM, including *Mav*. Nevertheless, most people do not develop clinical signs or disease, indicating that host factors must also be involved in the outcome of exposure and infection. This was first reflected by the well-established association between disseminated NTM infections, particularly by *Mav*, in AIDS patients (75, 76), while the incidence of disseminated disease in this group was reduced by the administration of antiretroviral therapy. The key role of host immunity in the outcome of *Mav* infection is further supported by the development of lung disease (*Mav*-LD) in other immunocompromised phenotypes.

Inherited defects in the IFN-γ/IL-12 signaling pathways are known to be associated with increased susceptibility to mycobacterial infection and diseases, including *Mav* (77-79) (**Figure 3**), indicating that IFN-γ and IL-12 are both crucial elements in the host defense against NTM. Another pro-inflammatory cytokine induced upon *Mav* infection is TNF and its important role in controlling intracellular mycobacteria is shown by anti-TNF therapy; in several autoimmune diseases, targeting the TNF pathway with anti-TNF therapies, such as infliximab, adalimumab, and etanercept, increases the risk of the development of active TB (80), but also of *Mav* disease (81, 82). Similar to subjects receiving TNF blockers, patients receiving immunosuppressive drugs like corticosteroids (83-85), but also medication (e.g. tacrolimus) provided following organ transplantation (86), have higher rates of *Mav*-LD. Furthermore, individuals with solid tumors are at an elevated risk of developing lung disease caused by NTM, likely due to immune dysfunction associated with the disease or the immunosuppressive effects of chemotherapy (87).

However, *Mav* infections can also occur in hosts who are apparently healthy, without systemic immunosuppression, but often have (pre-existing) lung diseases or specific host characteristics (88). For example, cystic fibrosis (CF), an inherited disorder caused by mutations in the *CFTR* gene, leads to a reduced mucus layer and impaired mucociliary clearance, heightening the risk of the establishment of bacterial infection (89). Similarly, individuals with chronic obstructive pulmonary disease (COPD) or a history of pulmonary TB often have damaged lung structures, associated with a higher occurrence of *Mav*-LD (86, 90-92). Furthermore, lower body fat mass and BMI correlate with faster progression of *Mav*-LD (85, 93), which may be explained by the higher adiponectin and lower leptin levels expressed by fat cells, which have immunomodulatory effects (94-97). Furthermore, aging also increases susceptibility to *Mav* infection (98). This may be due to the simple fact that predisposing factors for *Mav* infection are more common with aging. However, independent of these underlying predisposing conditions, aging is also associated with immunosenescence that can affect key host defenses (99). With regards to gender, middle-aged (post-menopausal) females have a higher risk for *Mav*-LD (100-102), which may be related to the lower levels of estrogen as this has been shown to enhance the clearance of MAC in mice (103), although human data remain inconclusive (86, 87). In addition, middle-aged males with a history of smoking, alcohol use or aforementioned underlying lung diseases also have an increased risk for *Mav*-LD (104).

Although associations with some predisposing conditions are noticeably clear, predicting which individuals will develop *Mav* disease is not feasible. Nevertheless, factors that affect the host's susceptibility to MAC infection have enhanced our understanding of the pathogenesis of MAC, underscoring the significant role of the host's immune system in MAC infection.

Clinical presentations of *Mav* infection

Overall, *Mav* disease displays a range of clinical manifestations, from localized to systemic disease, largely influenced by the host's immune status and underlying risk factors. The most common site of *Mav* disease is the lung. *Mav*-LD can have two distinct forms (105, 106). Fibrocavitary lung disease, traditionally recognized as TB lung disease, is the severe form of *Mav*-LD and is characterized by areas of cavitation,

pleural thickening, volume loss, and fibrosis, mostly in the upper lobes of the lung. This form is more commonly seen in middle-aged males. Without appropriate treatment, fibrocavitary disease progresses within a few years and can result in respiratory failure or destruction (107, 108). Alternatively, *Mav*-LD can present as nodular-bronchiectatic disease, which is more commonly observed in slender and middle-aged women, affecting mainly the middle lobe of the lung with small nodules and bronchiectasis (109). Although this form has a much slower progression rate, long-term follow-up is nevertheless warranted, as progression still may lead to death.

Another manifestation of *Mav* is disseminated disease (106), which develops upon infection via inhalation or ingestion (gastrointestinal route), and mainly occurs in severely immunocompromised (CD4+ T cells counts < 100/uL) AIDS patients (45). Presently, the occurrence of disseminated *Mav* disease in AIDS patients has become rare due to effective antiviral therapies (110), however, disseminated disease remains life-threatening if untreated (19). Treatment of *Mav* in these cases is often considered lifelong unless immune function is restored.

Furthermore, *Mav* infection in children frequently presents as lymphadenitis, most likely acquired via ingestion and which primarily affects the cervical lymph nodes. Since antibiotics are typically less effective, excision by surgery, with generally high success rates, is the treatment of choice (104, 106).

Finally, while mainly caused by rapidly growing NTM like *Mycobacterium fortuitum* and *Mycobacterium abscessus, Mav* can also cause localized infections involving the skin, soft tissues, or bones, often developed upon exposure to contaminated water, trauma, or surgical wounds (111). Diagnosis and treatment are often hindered due to the failure to recognize rare organisms as the cause of infection and the infrequent routine performance of mycobacterial cultures for surgical wound infections. Once diagnosed, patients frequently receive both drugs and undergo excisional surgery.

Challenges in the management of *Mav*

Diagnosis and epidemiology of *Mav*-LD

Based on the 2007 guidelines from the American Thoracic Society and Infectious Diseases Society of America (ATS/IDSA), the diagnosis of *Mav*-LD necessitates compatible clinical symptoms, compatible radiographic findings, and repeated microbiological detection of the species (104). The symptoms of *Mav*-LD, however, can be variable and non-specific such as chronic and recurring cough, and may also include weight loss, fever, chest pain, or fatigue. Since such symptoms usually overlap with underlying lung diseases mentioned above, it is often difficult to recognize them as symptoms of *Mav*-LD. Hence, it is essential to exclude other diseases such as TB for which IFN-γ release assay may assist (112). The radiographic features of *Mav*-LD are dependent on whether it is fibrocavitary or nodular-bronchiectatic. Radiographic features can be assessed with a chest X-ray or, if cavitation is not observed, a chest high-resolution computer tomography (HRCT) scan. Since these physical and radiographic features are not sufficient to distinguish *Mav*-LD from other lung disorders like TB, microbiological confirmation is the third criterion for accurate diagnosis and treatment decisions. Identification of the causative pathogen can be achieved by molecular assays like 16S rRNA sequencing using a minimum of three sputum specimens

collected on separate days (113). In individuals who do not clearly meet the diagnostic criteria, a lung biopsy for diagnosing *Mav*-LD may be required (104). Diagnosing *Mav* infection requires the fulfillment of the equally important clinical, radiographic, and microbiologic criteria. Nevertheless, the diagnosis of *Mav* infection is often delayed due to non-specific symptoms, insufficient bacterial presence in sputum (114), resulting in late or incorrect treatment.

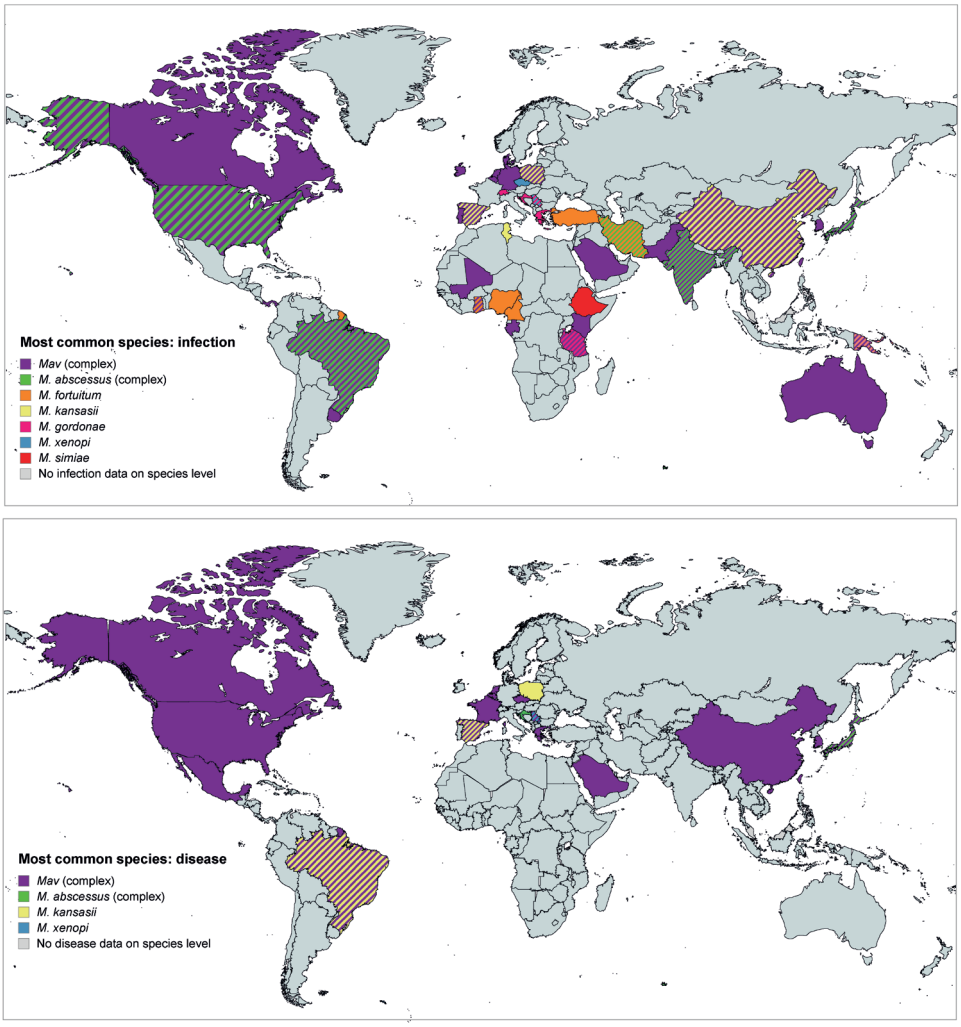

Figure 4. MAC is the most common species for NTM lung infection and disease worldwide. Created with MapChart.

Building on the challenges of diagnosing NTM, their reporting to public health authorities remains inconsistent. While NTM cases are seen in most industrialized countries, they are mandatorily reported in only a few states in the United States of America and Australia (115-117). The absence of a standardized global surveillance system limits the ability to accurately assess the burden of NTM to identify regional and national patterns

that would allow insight into potential individual or environmental risk factors for *Mav* infection and concomitant disease. Nevertheless, by using microbiological data from centralized public health institutions and administrative claims, a comprehensive review by Dahl et al. revealed that across numerous studies from more than 18 countries, the majority reported an overall increase in NTM lung infection (82%) and in lung disease (66.7-78%, depending on the case definition criteria used) (118). The most frequently isolated NTM was MAC with increased trends of infection and disease in 78.9% and 83.9% of the studies, respectively. While other NTM species can be more frequent in certain countries, MAC predominates for both NTM lung infection and disease (**Figure 4**) in most geographical regions (45, 119).

The overall increase in prevalence of *Mav* has likely multifactorial causes. Obvious reasons may be increased awareness or improved microbiologic detection techniques (105). Moreover, the occurrence of *Mav* cases may also increase as the aging population, associated with specific risk factors for *Mav* disease, as described above, is growing in certain countries such as the Netherlands (69, 120, 121). Finally, it has been suggested that by inducing protective immunity, TB infection provides cross-protection to NTM and the increasing number of diseases caused by NTM may be due to a decrease in TB cases (122). However, regardless of the reasons for the increase in NTM, the increase in the number of *Mav* infections and disease highlights the importance of documentation of NTM cases in a standardized manner to monitor and better manage these complicated infections.

Unsatisfactory treatment outcomes for *Mav*-LD

The recommended treatment of *Mav*-LD involves a combination of antibiotics, including a macrolide like clarithromycin or azithromycin, along with companion anti-TB drugs like ethambutol and a rifamycin to prevent the emergence of macrolide resistance (104). The goal of treatment is clinical improvement within 3-6 months and negative sputum cultures for 12 months while on therapy (123). However, the extensive and intensive nature of these antibiotic regimens may also hamper treatment adherence and increase the risk of developing drug resistance, complicating effective disease management. Despite a consensus statement in 2018 regarding treatment outcome definitions (124), there is a lack of widely accepted definitions of treatment success. The lack of such definitions, combined with different disease severities as well as different drug regimens and dosages included in MAC-LD clinical trials has resulted in inconsistent treatment success rates. Based on various systematic reviews and meta-analyses, Kwon et al. reported relatively poor pooled treatment success rates of 32-65% for MAC-LD (125). Successful treatment of MAC infection with a macrolide-based therapy is associated with the development of macrolide-resistant MAC strains (6.6-20% of treated patients) (126), for which the treatment regimens are far less successful (sputum conversion rates of 15-36%) (125). Even after initial success, 50% of the treated patients had a relapse (refractory infection) resulting in a positive sputum culture while receiving the same treatment (127, 128). Hence, the overall treatment success rate of the combinatorial antibiotic regime for MAC-LD has been unsatisfactory.

Several factors can interfere with successful treatment, which includes the lack of adherence to guidelines-based therapy (129), lack of treatment compliance or tolerance (77), lack of response to the regimen, the emergence of macrolide resistance, and

lack of effective treatment for macrolide-resistant disease (130-132). Moreover, MAC has also been associated with reinfection, which occurs in 25-48% of patients (133). Currently, only a small number of drugs, of which the majority have been repurposed, are evaluated in clinical trials for NTM-LD (134). This is likely a result of poor incentives, such as the lower profitability compared to communicable diseases like TB. Hence, new treatment strategies are urgently needed to potentiate, shorten and/or simplify current treatment strategies and improve treatment outcomes.

Antimicrobial susceptibility testing

For many years, antimicrobial susceptibility testing (AST) has long been conducted to predict the clinical effectiveness of antibiotics in treating NTM isolates. For MAC, the Clinical and Laboratory Standard Institute (CLSI) recommends using broth-based testing with both microdilution (multi-well plate) or macrodilution (radiometric BACTEC/Mycobacteria growth indicator tube (MGIT) system) (135, 136). However, unlike *Mtb* or rapidly growing mycobacteria (136, 137), it has long been known that for infections with slow growers like MAC, the correlation between *in vitro* susceptibility and good treatment outcomes for drugs is poor (138). Only *in vitro* susceptibility testing results for clarithromycin or clarithromycin-containing regimens correlated with *in vivo* efficacy (104), while the clinical response of MAC to ethambutol, rifampicin, and isoniazid using AST could not be predicted (139). Hence, the CLSI states that for MAC isolates only AST for clarithromycin is recommended.

The important discrepancies between AST results and the clinical response may stem from challenges in the laboratory process of AST, as well as the lack of standardized procedures and interpretation of the results. However, differential susceptibility *in vitro* versus *in vivo* may also be the result of specific bacterial behavior in a different setting. Suboptimal drug exposure and selection *in vivo* may differentially affect the interplay between tolerance and acquired resistance of bacteria interfering with susceptibility, which is not observed *in vitro* (140). Moreover, mycobacteria are known to be both intracellular and extracellular pathogens. Within cells, mycobacteria may adjust their metabolism or even become metabolically inactive (i.e. dormant) to prevent immune activation, possibly resulting in lower susceptibility to certain antibiotics that target active bacterial processes. Furthermore, *in vivo* bacteria might also reside in granulomas and biofilms which may affect their susceptibility to drugs. Hence, *in vitro* susceptibility testing of bacteria in conditions (more) resembling their physiological environment may improve the ability to translate the efficacy of drugs from *in vitro* to *in vivo*.

An alternative treatment strategy: boosting the host immune system

As reflected throughout this chapter, host immunity plays a crucial role in the outcome of *Mav* infection. Enhancing the host immune response to infection using host-directed therapy (HDT) may therefore be an alternative (adjunctive) treatment strategy to treat mycobacterial infections like *Mav*. HDT targets host processes to either reduce pathology caused by excessive inflammation or to enhance the host control of (intracellular) infection. The building knowledge on the host-pathogen interactions during *Mtb* infection has provided insights required for the development of HDT. By targeting host immunity rather than the pathogen, HDT has major advantages compared to conventional antibiotics including avoiding direct selective pressure on bacteria and

thus reducing the risk of *de novo* development of drug resistance, but also the potential to shorten the duration or decreasing the dosage of current treatment regimens, which may reduce adverse drug effects. Although HDT offers the potential to treat infections, the development of HDT for *Mav* is yet limited. The potential of HDT to boost the macrophage's ability to fight MAC infection has been shown *in vitro* with for example cytokines like GM-CSF or IFN-γ (141). Acquiring a more thorough understanding of how the host and pathogen interact during MAC infection may allow the development of other, more potent, HDTs.

Outline of this thesis

Given the challenges of current antibiotic treatments for *Mav*, this thesis focuses on developing HDTs to combat *Mav* infections. To this end, human cell-based infection models were developed to identify HDT candidates that improved host control of intracellular *Mav* infection. Using these models, also the host response to *Mav* infection was studied, improving our fundamental understanding of *Mav* infection and further aiding the development of HDTs against *Mav*.

First, we provide a comprehensive literature overview of HDTs under investigation for mycobacteria in **chapter 2**. As the development of HDTs for *Mav* is limited, this review mainly reports HDTs that have shown efficacy in treating *Mtb* infections. Moreover, we also propose potential intracellular host factors that may be targeted by HDT to improve host infection control of mycobacteria. In **chapter 3**, we developed human cell-based infection models for *Mav*, using the phagocytic MelJuSo cell line and primary human macrophages, to enable the identification of potential HDT candidates that can improve the antimycobacterial activity of host cells against intracellular *Mav*. These models can also be used to study host-pathogen interactions during *Mav* infection. By using the primary human macrophage model in **chapter 4** and **chapter 5**, we identified amiodarone and phenothiazines as potential HDT candidates for *Mav* infection. We showed that amiodarone most likely acts by enhancing the host autophagy pathway to impair intracellular survival of *Mav,* while phenothiazines impair intracellular *Mav* survival by enhancing cellular ROS production and additional mechanisms that remained undiscovered. In **chapter 6**, we performed transcriptomic analysis of primary human macrophages infected with *Mav* alongside *Mtb* to compare the host response between *Mav* and *Mtb* and to facilitate the rapid extrapolation of relevant findings from *Mtb* to *Mav*. The results described in **chapter 6** not only enhance our understanding of the host transcriptomic response to both pathogens, but they also provide insights into host factors that may be exploited for the development of HDT for *Mav*. Finally, the findings of this thesis were summarized and discussed in **chapter 7.**

References

1. Koch R. Classics in infectious diseases. The etiology of tuberculosis: Robert Koch. Berlin, Germany 1882. Rev Infect Dis. 1982;4(6):1270-4.
2. Wallace RJ, Jr., Nash DR, Tsukamura M, Blacklock ZM, Silcox VA. Human disease due to Mycobacterium smegmatis. J Infect Dis. 1988;158(1):52-9.
3. Feldman WH. Avian tuberculosis infections. Baltimore: The Williams & Wilkins company; 1938. 3 p. l., v-ix, 483 p. p.
4. Maffucci A. Die Hühnertuberculose. Zeitschrift für Hygiene und Infektionskrankheiten. 1892;11(1):445-86.
5. Branch A. A study of acid-fast organisms other than mammalian tubercle bacilli isolated from disease in man: The occurrence of avian tubercle bacillus infection of men and the diagnosis of avirulent

avian tubercle bacilli. Tubercle. 1933;14(8):337-53.
6. Feldman W, Davies R, Moses H, Andberg W. An Unusual Mycobacterium isolated from Sputum of a Man suffering from Pulmonary Disease of Long Duration. American Review of Tuberculosis and Pulmonary Diseases. 1943;48(2):82–93.
7. Cuttino JT, Mc CA. Pure granulomatous nocardiosis, a new fungus disease distinguished by intracellular parasitism; a description of a new disease in man due to a hitherto undescribed organism, Nocardia intracellularis, n. sp., including a study of the biologic and pathogenic properties of this species. Am J Pathol. 1949;25(1):1-47.
8. Wolinsky E. Nontuberculous mycobacteria and associated diseases. Am Rev Respir Dis. 1979;119(1):107-59.
9. Fogan L. Atypical mycobacteria. Their clinical, laboratory, and epidemiologic significance. Medicine (Baltimore). 1970;49(3):243-55.
10. Horsburgh CR, Jr., Mason UG, 3rd, Farhi DC, Iseman MD. Disseminated infection with Mycobacterium avium-intracellulare. A report of 13 cases and a review of the literature. Medicine (Baltimore). 1985;64(1):36-48.
11. Honda JR, Knight V, Chan ED. Pathogenesis and risk factors for nontuberculous mycobacterial lung disease. Clin Chest Med. 2015;36(1):1-11.
12. Schorey JS, Holsti MA, Ratliff TL, Allen PM, Brown EJ. Characterization of the fibronectin-attachment protein of Mycobacterium avium reveals a fibronectin-binding motif conserved among mycobacteria. Mol Microbiol. 1996;21(2):321-9.
13. Middleton AM, Chadwick MV, Nicholson AG, Dewar A, Groger RK, Brown EJ, et al. The role of Mycobacterium avium complex fibronectin attachment protein in adherence to the human respiratory mucosa. Mol Microbiol. 2000;38(2):381-91.
14. Bermudez LE, Young LS. Factors affecting invasion of HT-29 and HEp-2 epithelial cells by organisms of the Mycobacterium avium complex. Infect Immun. 1994;62(5):2021-6.
15. Bermudez LE, Goodman J. Mycobacterium tuberculosis invades and replicates within type II alveolar cells. Infect Immun. 1996;64(4):1400-6.
16. Carter G, Wu M, Drummond DC, Bermudez LE. Characterization of biofilm formation by clinical isolates of Mycobacterium avium. J Med Microbiol. 2003;52(Pt 9):747-52.
17. Li YJ, Danelishvili L, Wagner D, Petrofsky M, Bermudez LE. Identification of virulence determinants of Mycobacterium avium that impact on the ability to resist host killing mechanisms. J Med Microbiol. 2010;59(Pt 1):8-16.
18. Sangari FJ, Goodman J, Bermudez LE. Mycobacterium avium enters intestinal epithelial cells through the apical membrane, but not by the basolateral surface, activates small GTPase Rho and, once within epithelial cells, expresses an invasive phenotype. Cell Microbiol. 2000;2(6):561-8.
19. Nightingale SD, Cameron DW, Gordin FM, Sullam PM, Cohn DL, Chaisson RE, et al. Two controlled trials of rifabutin prophylaxis against Mycobacterium avium complex infection in AIDS. N Engl J Med. 1993;329(12):828-33.
20. Crowle AJ, Dahl R, Ross E, May MH. Evidence that vesicles containing living, virulent Mycobacterium tuberculosis or Mycobacterium avium in cultured human macrophages are not acidic. Infect Immun. 1991;59(5):1823-31.
21. Inderlied CB, Kemper CA, Bermudez LE. The Mycobacterium avium complex. Clin Microbiol Rev. 1993;6(3):266-310.
22. Gordon S, Martinez FO. Alternative activation of macrophages: mechanism and functions. Immunity. 2010;32(5):593-604.
23. Martinez FO, Sica A, Mantovani A, Locati M. Macrophage activation and polarization. Front Biosci. 2008;13:453-61.
24. Hussell T, Bell TJ. Alveolar macrophages: plasticity in a tissue-specific context. Nat Rev Immunol. 2014;14(2):81-93.
25. Alber A, Howie SE, Wallace WA, Hirani N. The role of macrophages in healing the wounded lung. Int J Exp Pathol. 2012;93(4):243-51.
26. Mitsi E, Kamng'ona R, Rylance J, Solorzano C, Jesus Reine J, Mwandumba HC, et al. Human alveolar macrophages predominately express combined classical M1 and M2 surface markers in steady state. Respir Res. 2018;19(1):66.
27. Benoit M, Desnues B, Mege JL. Macrophage polarization in bacterial infections. J Immunol. 2008;181(6):3733-9.
28. Bermudez LE, Young LS, Enkel H. Interaction of Mycobacterium avium complex with human macrophages: roles of membrane receptors and serum proteins. Infect Immun. 1991;59(5):1697-702.
29. Shamaei M, Mirsaeidi M. Nontuberculous Mycobacteria, Macrophages, and Host Innate Immune

Response. Infect Immun. 2021;89(8):e0081220.
30. Gomes MS, Florido M, Cordeiro JV, Teixeira CM, Takeuchi O, Akira S, et al. Limited role of the Toll-like receptor-2 in resistance to Mycobacterium avium. Immunology. 2004;111(2):179-85.
31. Gomes MS, Sousa Fernandes S, Cordeiro JV, Silva Gomes S, Vieira A, Appelberg R. Engagement of Toll-like receptor 2 in mouse macrophages infected with Mycobacterium avium induces non-oxidative and TNF-independent anti-mycobacterial activity. Eur J Immunol. 2008;38(8):2180-9.
32. Bhatnagar S, Schorey JS. Elevated mitogen-activated protein kinase signalling and increased macrophage activation in cells infected with a glycopeptidolipid-deficient Mycobacterium avium. Cell Microbiol. 2006;8(1):85-96.
33. Neupane AS, Willson M, Chojnacki AK, Vargas ESCF, Morehouse C, Carestia A, et al. Patrolling Alveolar Macrophages Conceal Bacteria from the Immune System to Maintain Homeostasis. Cell. 2020;183(1):110-25 e11.
34. Carvalho NB, Oliveira FS, Duraes FV, de Almeida LA, Florido M, Prata LO, et al. Toll-like receptor 9 is required for full host resistance to Mycobacterium avium infection but plays no role in induction of Th1 responses. Infect Immun. 2011;79(4):1638-46.
35. Marinho FA, de Paula RR, Mendes AC, de Almeida LA, Gomes MT, Carvalho NB, et al. Toll-like receptor 6 senses Mycobacterium avium and is required for efficient control of mycobacterial infection. Eur J Immunol. 2013;43(9):2373-85.
36. Lee HJ, Woo Y, Hahn TW, Jung YM, Jung YJ. Formation and Maturation of the Phagosome: A Key Mechanism in Innate Immunity against Intracellular Bacterial Infection. Microorganisms. 2020;8(9).
37. Danelishvili L, Bermudez LE. Mycobacterium avium MAV_2941 mimics phosphoinositol-3-kinase to interfere with macrophage phagosome maturation. Microbes Infect. 2015;17(9):628-37.
38. Sturgill-Koszycki S, Schlesinger PH, Chakraborty P, Haddix PL, Collins HL, Fok AK, et al. Lack of acidification in Mycobacterium phagosomes produced by exclusion of the vesicular proton-ATPase. Science. 1994;263(5147):678-81.
39. Danelishvili L, Chinison JJJ, Pham T, Gupta R, Bermudez LE. The Voltage-Dependent Anion Channels (VDAC) of Mycobacterium avium phagosome are associated with bacterial survival and lipid export in macrophages. Sci Rep. 2017;7(1):7007.
40. Houben D, Demangel C, van Ingen J, Perez J, Baldeon L, Abdallah AM, et al. ESX-1-mediated translocation to the cytosol controls virulence of mycobacteria. Cell Microbiol. 2012;14(8):1287-98.
41. Sharma V, Verma S, Seranova E, Sarkar S, Kumar D. Selective Autophagy and Xenophagy in Infection and Disease. Front Cell Dev Biol. 2018;6:147.
42. Harding CV, Boom WH. Regulation of antigen presentation by Mycobacterium tuberculosis: a role for Toll-like receptors. Nat Rev Microbiol. 2010;8(4):296-307.
43. Jiao X, Lo-Man R, Guermonprez P, Fiette L, Deriaud E, Burgaud S, et al. Dendritic cells are host cells for mycobacteria in vivo that trigger innate and acquired immunity. J Immunol. 2002;168(3):1294-301.
44. Appelberg R, Leal IS, Pais TF, Pedrosa J, Florido M. Differences in resistance of C57BL/6 and C57BL/10 mice to infection by Mycobacterium avium are independent of gamma interferon. Infect Immun. 2000;68(1):19-23.
45. Daley CL. Mycobacterium avium Complex Disease. Microbiol Spectr. 2017;5(2).
46. Underhill DM, Ozinsky A, Smith KD, Aderem A. Toll-like receptor-2 mediates mycobacteria-induced proinflammatory signaling in macrophages. Proc Natl Acad Sci U S A. 1999;96(25):14459-63.
47. Wang T, Lafuse WP, Zwilling BS. Regulation of toll-like receptor 2 expression by macrophages following Mycobacterium avium infection. J Immunol. 2000;165(11):6308-13.
48. Rodrigues MF, Alves CC, Figueiredo BB, Rezende AB, Wohlres-Viana S, Silva VL, et al. Tumour necrosis factor receptors and apoptosis of alveolar macrophages during early infection with attenuated and virulent Mycobacterium bovis. Immunology. 2013;139(4):503-12.
49. Behar SM, Martin CJ, Booty MG, Nishimura T, Zhao X, Gan HX, et al. Apoptosis is an innate defense function of macrophages against Mycobacterium tuberculosis. Mucosal Immunol. 2011;4(3):279-87.
50. Fratazzi C, Arbeit RD, Carini C, Remold HG. Programmed cell death of Mycobacterium avium serovar 4-infected human macrophages prevents the mycobacteria from spreading and induces mycobacterial growth inhibition by freshly added, uninfected macrophages. J Immunol. 1997;158(9):4320-7.
51. Keane J, Shurtleff B, Kornfeld H. TNF-dependent BALB/c murine macrophage apoptosis following Mycobacterium tuberculosis infection inhibits bacillary growth in an IFN-gamma independent manner. Tuberculosis (Edinb). 2002;82(2-3):55-61.
52. Shundo Y, On R, Matsumoto T, Ouchi H, Fujita M. TNFR1 Mediated Apoptosis Is Protective against Mycobacterium avium in Mice. Microorganisms. 2023;11(3).
53. Early J, Fischer K, Bermudez LE. Mycobacterium avium uses apoptotic macrophages as tools for spreading. Microb Pathog. 2011;50(2):132-9.

54. Bermudez LE, Danelishvili L, Babrack L, Pham T. Evidence for genes associated with the ability of Mycobacterium avium subsp. hominissuis to escape apoptotic macrophages. Front Cell Infect Microbiol. 2015;5:63.
55. Lee KI, Whang J, Choi HG, Son YJ, Jeon HS, Back YW, et al. Mycobacterium avium MAV2054 protein induces macrophage apoptosis by targeting mitochondria and reduces intracellular bacterial growth. Sci Rep. 2016;6:37804.
56. Gomes MS, Florido M, Pais TF, Appelberg R. Improved clearance of Mycobacterium avium upon disruption of the inducible nitric oxide synthase gene. J Immunol. 1999;162(11):6734-9.
57. Rost LM, Louet C, Bruheim P, Flo TH, Gidon A. Pyruvate Supports RET-Dependent Mitochondrial ROS Production to Control Mycobacterium avium Infection in Human Primary Macrophages. Front Immunol. 2022;13:891475.
58. Bermudez LE, Young LS. Oxidative and non-oxidative intracellular killing of Mycobacterium avium complex. Microb Pathog. 1989;7(4):289-98.
59. Bryant JM, Grogono DM, Greaves D, Foweraker J, Roddick I, Inns T, et al. Whole-genome sequencing to identify transmission of Mycobacterium abscessus between patients with cystic fibrosis: a retrospective cohort study. Lancet. 2013;381(9877):1551-60.
60. Guidotti TL, Ragain L. Communicating with healthcare providers. J Water Health. 2008;6 Suppl 1:53-61.
61. Nishiuchi Y, Maekura R, Kitada S, Tamaru A, Taguri T, Kira Y, et al. The recovery of Mycobacterium avium-intracellulare complex (MAC) from the residential bathrooms of patients with pulmonary MAC. Clin Infect Dis. 2007;45(3):347-51.
62. Prevots DR, Marshall JE, Wagner D, Morimoto K. Global Epidemiology of Nontuberculous Mycobacterial Pulmonary Disease: A Review. Clin Chest Med. 2023;44(4):675-721.
63. Tzou CL, Dirac MA, Becker AL, Beck NK, Weigel KM, Meschke JS, et al. Association between Mycobacterium avium Complex Pulmonary Disease and Mycobacteria in Home Water and Soil. Ann Am Thorac Soc. 2020;17(1):57-62.
64. Maekawa K, Ito Y, Hirai T, Kubo T, Imai S, Tatsumi S, et al. Environmental risk factors for pulmonary Mycobacterium avium-intracellulare complex disease. Chest. 2011;140(3):723-9.
65. Reed C, von Reyn CF, Chamblee S, Ellerbrock TV, Johnson JW, Marsh BJ, et al. Environmental risk factors for infection with Mycobacterium avium complex. Am J Epidemiol. 2006;164(1):32-40.
66. von Reyn CF, Waddell RD, Eaton T, Arbeit RD, Maslow JN, Barber TW, et al. Isolation of Mycobacterium avium complex from water in the United States, Finland, Zaire, and Kenya. J Clin Microbiol. 1993;31(12):3227-30.
67. Falkinham JO, 3rd. Nontuberculous mycobacteria in the environment. Tuberculosis (Edinb). 2022;137:102267.
68. O'Brien RJ, Geiter LJ, Snider DE, Jr. The epidemiology of nontuberculous mycobacterial diseases in the United States. Results from a national survey. Am Rev Respir Dis. 1987;135(5):1007-14.
69. Olivier KN, Weber DJ, Wallace RJ, Jr., Faiz AR, Lee JH, Zhang Y, et al. Nontuberculous mycobacteria. I: multicenter prevalence study in cystic fibrosis. Am J Respir Crit Care Med. 2003;167(6):828-34.
70. Adjemian J, Olivier KN, Seitz AE, Falkinham JO, 3rd, Holland SM, Prevots DR. Spatial clusters of nontuberculous mycobacterial lung disease in the United States. Am J Respir Crit Care Med. 2012;186(6):553-8.
71. Hoffmann C, Leis A, Niederweis M, Plitzko JM, Engelhardt H. Disclosure of the mycobacterial outer membrane: cryo-electron tomography and vitreous sections reveal the lipid bilayer structure. Proc Natl Acad Sci U S A. 2008;105(10):3963-7.
72. Brennan PJ, Nikaido H. The envelope of mycobacteria. Annu Rev Biochem. 1995;64:29-63.
73. Bendinger B, Rijnaarts HH, Altendorf K, Zehnder AJ. Physicochemical cell surface and adhesive properties of coryneform bacteria related to the presence and chain length of mycolic acids. Appl Environ Microbiol. 1993;59(11):3973-7.
74. Steed KA, Falkinham JO, 3rd. Effect of growth in biofilms on chlorine susceptibility of Mycobacterium avium and Mycobacterium intracellulare. Appl Environ Microbiol. 2006;72(6):4007-11.
75. Horsburgh CR, Jr., Gettings J, Alexander LN, Lennox JL. Disseminated Mycobacterium avium complex disease among patients infected with human immunodeficiency virus, 1985-2000. Clin Infect Dis. 2001;33(11):1938-43.
76. Horsburgh CR, Jr., Selik RM. The epidemiology of disseminated nontuberculous mycobacterial infection in the acquired immunodeficiency syndrome (AIDS). Am Rev Respir Dis. 1989;139(1):4-7.
77. Field SK, Fisher D, Cowie RL. Mycobacterium avium complex pulmonary disease in patients without HIV infection. Chest. 2004;126(2):566-81.
78. de Jong R, Altare F, Haagen IA, Elferink DG, Boer T, van Breda Vriesman PJ, et al. Severe mycobacterial

and Salmonella infections in interleukin-12 receptor-deficient patients. Science. 1998;280(5368):1435-8.
79. Dorman SE, Holland SM. Interferon-gamma and interleukin-12 pathway defects and human disease. Cytokine Growth Factor Rev. 2000;11(4):321-33.
80. Yeh JJ, Wang YC, Sung FC, Kao CH. Rheumatoid arthritis increases the risk of nontuberculosis mycobacterial disease and active pulmonary tuberculosis. PLoS One. 2014;9(10):e110922.
81. Winthrop KL, Chang E, Yamashita S, Iademarco MF, LoBue PA. Nontuberculous mycobacteria infections and anti-tumor necrosis factor-alpha therapy. Emerg Infect Dis. 2009;15(10):1556-61.
82. Winthrop KL, Baxter R, Liu L, Varley CD, Curtis JR, Baddley JW, et al. Mycobacterial diseases and antitumour necrosis factor therapy in USA. Ann Rheum Dis. 2013;72(1):37-42.
83. Brode SK, Jamieson FB, Ng R, Campitelli MA, Kwong JC, Paterson JM, et al. Increased risk of mycobacterial infections associated with anti-rheumatic medications. Thorax. 2015;70(7):677-82.
84. Liu VX, Winthrop KL, Lu Y, Sharifi H, Nasiri HU, Ruoss SJ. Association between Inhaled Corticosteroid Use and Pulmonary Nontuberculous Mycobacterial Infection. Ann Am Thorac Soc. 2018;15(10):1169-76.
85. Dirac MA, Horan KL, Doody DR, Meschke JS, Park DR, Jackson LA, et al. Environment or host?: A case-control study of risk factors for Mycobacterium avium complex lung disease. Am J Respir Crit Care Med. 2012;186(7):684-91.
86. Loebinger MR, Quint JK, van der Laan R, Obradovic M, Chawla R, Kishore A, et al. Risk Factors for Nontuberculous Mycobacterial Pulmonary Disease: A Systematic Literature Review and Meta-Analysis. Chest. 2023;164(5):1115-24.
87. Chen YM, Lin CH, Chen HH, Chao WC, Chen DY, Lin CC, et al. Risk of mycobacterial disease among cancer patients: A population-based cohort study in a TB endemic area. Cancer Epidemiol. 2019;59:64-70.
88. Chan ED, Iseman MD. Slender, older women appear to be more susceptible to nontuberculous mycobacterial lung disease. Gend Med. 2010;7(1):5-18.
89. Martiniano SL, Nick JA. Nontuberculous mycobacterial infections in cystic fibrosis. Clin Chest Med. 2015;36(1):101-15.
90. Matesanz Lopez C, Loras Gallego C, Cacho Calvo J, Thuissard Vasallo IJ, Rio Ramirez MT. Patients with non-tuberculous mycobacteria in respiratory samples: a 5-year epidemiological study. Rev Esp Quimioter. 2021;34(2):120-5.
91. Munjal S, Munjal S, Gao J, Venketaraman V. Exploring Potential COPD Immunosuppression Pathways Causing Increased Susceptibility for MAC Infections among COPD Patients. Clin Pract. 2021;11(3):619-30.
92. Sterling TR, Moore RD, Graham NM, Astemborski J, Vlahov D, Chaisson RE. Mycobacterium tuberculosis infection and disease are not associated with protection against subsequent disseminated M. avium complex disease. AIDS. 1998;12(12):1451-7.
93. Kim SJ, Yoon SH, Choi SM, Lee J, Lee CH, Han SK, et al. Characteristics associated with progression in patients with of nontuberculous mycobacterial lung disease : a prospective cohort study. Bmc Pulm Med. 2017;17(1):5.
94. Mustafa T. Does leptin have a role in immunity to tuberculosis? Indian J Med Res. 2008;128(6):691-3.
95. Naylor C, Petri WA, Jr. Leptin Regulation of Immune Responses. Trends Mol Med. 2016;22(2):88-98.
96. Tasaka S, Hasegawa N, Nishimura T, Yamasawa W, Kamata H, Shinoda H, et al. Elevated serum adiponectin level in patients with Mycobacterium avium-intracellulare complex pulmonary disease. Respiration. 2010;79(5):383-7.
97. Luo Y, Liu M. Adiponectin: a versatile player of innate immunity. J Mol Cell Biol. 2016;8(2):120-8.
98. Park HE, Lee W, Choi S, Jung M, Shin MK, Shin SJ. Modulating macrophage function to reinforce host innate resistance against Mycobacterium avium complex infection. Front Immunol. 2022;13:931876.
99. Lake MA, Ambrose LR, Lipman MC, Lowe DM. '"Why me, why now?" Using clinical immunology and epidemiology to explain who gets nontuberculous mycobacterial infection. BMC Med. 2016;14:54.
100. Mirsaeidi M, Hadid W, Ericsoussi B, Rodgers D, Sadikot RT. Non-tuberculous mycobacterial disease is common in patients with non-cystic fibrosis bronchiectasis. Int J Infect Dis. 2013;17(11):e1000-4.
101. Kim RD, Greenberg DE, Ehrmantraut ME, Guide SV, Ding L, Shea Y, et al. Pulmonary nontuberculous mycobacterial disease: prospective study of a distinct preexisting syndrome. Am J Respir Crit Care Med. 2008;178(10):1066-74.
102. Prevots DR, Shaw PA, Strickland D, Jackson LA, Raebel MA, Blosky MA, et al. Nontuberculous mycobacterial lung disease prevalence at four integrated health care delivery systems. Am J Respir Crit Care Med. 2010;182(7):970-6.
103. Tsuyuguchi K, Suzuki K, Matsumoto H, Tanaka E, Amitani R, Kuze F. Effect of oestrogen on Mycobacterium avium complex pulmonary infection in mice. Clin Exp Immunol. 2001;123(3):428-34.

104. Griffith DE, Aksamit T, Brown-Elliott BA, Catanzaro A, Daley C, Gordin F, et al. An official ATS/IDSA statement: diagnosis, treatment, and prevention of nontuberculous mycobacterial diseases. Am J Respir Crit Care Med. 2007;175(4):367-416.
105. McShane PJ, Glassroth J. Pulmonary Disease Due to Nontuberculous Mycobacteria: Current State and New Insights. Chest. 2015;148(6):1517-27.
106. Tortoli E. Clinical manifestations of nontuberculous mycobacteria infections. Clin Microbiol Infect. 2009;15(10):906-10.
107. Johnson MM, Odell JA. Nontuberculous mycobacterial pulmonary infections. J Thorac Dis. 2014;6(3):210-20.
108. Pulmonary disease caused by Mycobacterium avium-intracellulare in HIV-negative patients: five-year follow-up of patients receiving standardised treatment. Int J Tuberc Lung Dis. 2002;6(7):628-34.
109. Prince DS, Peterson DD, Steiner RM, Gottlieb JE, Scott R, Israel HL, et al. Infection with Mycobacterium avium complex in patients without predisposing conditions. N Engl J Med. 1989;321(13):863-8.
110. Kaplan JE, Masur H, Holmes KK, Usphs, Infectious Disease Society of A. Guidelines for preventing opportunistic infections among HIV-infected persons--2002. Recommendations of the U.S. Public Health Service and the Infectious Diseases Society of America. MMWR Recomm Rep. 2002;51(RR-8):1-52.
111. Ford MB, Okulicz JF, Salinas JR, Kiley JL. Epidemiology, clinical characteristics, and outcomes of nontuberculous mycobacterial skin, soft tissue, and bone infections from a single center over a 10-year period. J Clin Tuberc Other Mycobact Dis. 2023;33:100403.
112. Hermansen TS, Thomsen VO, Lillebaek T, Ravn P. Non-tuberculous mycobacteria and the performance of interferon gamma release assays in Denmark. PLoS One. 2014;9(4):e93986.
113. McNabb A, Eisler D, Adie K, Amos M, Rodrigues M, Stephens G, et al. Assessment of partial sequencing of the 65-kilodalton heat shock protein gene (hsp65) for routine identification of Mycobacterium species isolated from clinical sources. J Clin Microbiol. 2004;42(7):3000-11.
114. Xu K, Bi S, Ji Z, Hu H, Hu F, Zheng B, et al. Distinguishing nontuberculous mycobacteria from multidrug-resistant Mycobacterium tuberculosis, China. Emerg Infect Dis. 2014;20(6):1060-2.
115. Grigg C, Jackson KA, Barter D, Czaja CA, Johnston H, Lynfield R, et al. Epidemiology of Pulmonary and Extrapulmonary Nontuberculous Mycobacteria Infections at 4 US Emerging Infections Program Sites: A 6-Month Pilot. Clin Infect Dis. 2023;77(4):629-37.
116. Mercaldo RA, Marshall JE, Cangelosi GA, Donohue M, Falkinham JO, 3rd, Fierer N, et al. Environmental risk of nontuberculous mycobacterial infection: Strategies for advancing methodology. Tuberculosis (Edinb). 2023;139:102305.
117. Thomson R, Donnan E, Konstantinos A. Notification of Nontuberculous Mycobacteria: An Australian Perspective. Ann Am Thorac Soc. 2017;14(3):318-23.
118. Dahl VN, Molhave M, Floe A, van Ingen J, Schon T, Lillebaek T, et al. Global trends of pulmonary infections with nontuberculous mycobacteria: a systematic review. Int J Infect Dis. 2022;125:120-31.
119. Hoefsloot W, van Ingen J, Andrejak C, Angeby K, Bauriaud R, Bemer P, et al. The geographic diversity of nontuberculous mycobacteria isolated from pulmonary samples: an NTM-NET collaborative study. Eur Respir J. 2013;42(6):1604-13.
120. van Ingen J, Hoefsloot W, Dekhuijzen PN, Boeree MJ, van Soolingen D. The changing pattern of clinical Mycobacterium avium isolation in the Netherlands. Int J Tuberc Lung Dis. 2010;14(9):1176-80.
121. Al-Houqani M, Jamieson F, Mehta M, Chedore P, May K, Marras TK. Aging, COPD, and other risk factors do not explain the increased prevalence of pulmonary Mycobacterium avium complex in Ontario. Chest. 2012;141(1):190-7.
122. Brode SK, Daley CL, Marras TK. The epidemiologic relationship between tuberculosis and non-tuberculous mycobacterial disease: a systematic review. Int J Tuberc Lung Dis. 2014;18(11):1370-7.
123. Wallace RJ, Jr., Brown BA, Griffith DE, Girard WM, Murphy DT. Clarithromycin regimens for pulmonary Mycobacterium avium complex. The first 50 patients. Am J Respir Crit Care Med. 1996;153(6 Pt 1):1766-72.
124. van Ingen J, Aksamit T, Andrejak C, Bottger EC, Cambau E, Daley CL, et al. Treatment outcome definitions in nontuberculous mycobacterial pulmonary disease: an NTM-NET consensus statement. Eur Respir J. 2018;51(3).
125. Kwon YS, Koh WJ, Daley CL. Treatment of Mycobacterium avium Complex Pulmonary Disease. Tuberc Respir Dis (Seoul). 2019;82(1):15-26.
126. Heifets LB, Iseman MD. Individualized therapy versus standard regimens in the treatment of Mycobacterium avium infections. Am Rev Respir Dis. 1991;144(1):1-2.
127. Dutt AK, Stead WW. Long-term results of medical treatment in Mycobacterium intracellulare infection. Am J Med. 1979;67(3):449-53.

128. Yeager H, Jr., Raleigh JW. Pulmonary disease due to Mycobacterium intracellulare. Am Rev Respir Dis. 1973;108(3):547-52.
129. Adjemian J, Prevots DR, Gallagher J, Heap K, Gupta R, Griffith D. Lack of adherence to evidence-based treatment guidelines for nontuberculous mycobacterial lung disease. Ann Am Thorac Soc. 2014;11(1):9-16.
130. Tanaka E, Kimoto T, Tsuyuguchi K, Watanabe I, Matsumoto H, Niimi A, et al. Effect of clarithromycin regimen for Mycobacterium avium complex pulmonary disease. Am J Respir Crit Care Med. 1999;160(3):866-72.
131. Morimoto K, Namkoong H, Hasegawa N, Nakagawa T, Morino E, Shiraishi Y, et al. Macrolide-Resistant Mycobacterium avium Complex Lung Disease: Analysis of 102 Consecutive Cases. Ann Am Thorac Soc. 2016;13(11):1904-11.
132. Griffith DE, Brown-Elliott BA, Langsjoen B, Zhang Y, Pan X, Girard W, et al. Clinical and molecular analysis of macrolide resistance in Mycobacterium avium complex lung disease. Am J Respir Crit Care Med. 2006;174(8):928-34.
133. Nguyen MH, Daley CL. Treatment of Mycobacterium avium Complex Pulmonary Disease: When Should I Treat and What Therapy Should I Start? Clin Chest Med. 2023;44(4):771-83.
134. Dartois V, Dick T. Therapeutic developments for tuberculosis and nontuberculous mycobacterial lung disease. Nat Rev Drug Discov. 2024;23(5):381-403.
135. Siddiqi SH, Heifets LB, Cynamon MH, Hooper NM, Laszlo A, Libonati JP, et al. Rapid broth macrodilution method for determination of MICs for Mycobacterium avium isolates. J Clin Microbiol. 1993;31(9):2332-8.
136. Woods GL, Brown-Elliott BA, Conville PS, Desmond EP, Hall GS, Lin G, et al. Susceptibility Testing of Mycobacteria, Nocardiae, and Other Aerobic Actinomycetes. CLSI Standards: Guidelines for Health Care Excellence. 2nd ed. Wayne (PA)2011.
137. Brown-Elliott BA, Nash KA, Wallace RJ, Jr. Antimicrobial susceptibility testing, drug resistance mechanisms, and therapy of infections with nontuberculous mycobacteria. Clin Microbiol Rev. 2012;25(3):545-82.
138. Cowman S, Burns K, Benson S, Wilson R, Loebinger MR. The antimicrobial susceptibility of non-tuberculous mycobacteria. J Infect. 2016;72(3):324-31.
139. Research Committee of the British Thoracic S. First randomised trial of treatments for pulmonary disease caused by M avium intracellulare, M malmoense, and M xenopi in HIV negative patients: rifampicin, ethambutol and isoniazid versus rifampicin and ethambutol. Thorax. 2001;56(3):167-72.
140. van Ingen J, Boeree MJ, van Soolingen D, Mouton JW. Resistance mechanisms and drug susceptibility testing of nontuberculous mycobacteria. Drug Resist Updat. 2012;15(3):149-61.
141. Rose RM, Fuglestad JM, Remington L. Growth inhibition of Mycobacterium avium complex in human alveolar macrophages by the combination of recombinant macrophage colony-stimulating factor and interferon-gamma. Am J Respir Cell Mol Biol. 1991;4(3):248-54.

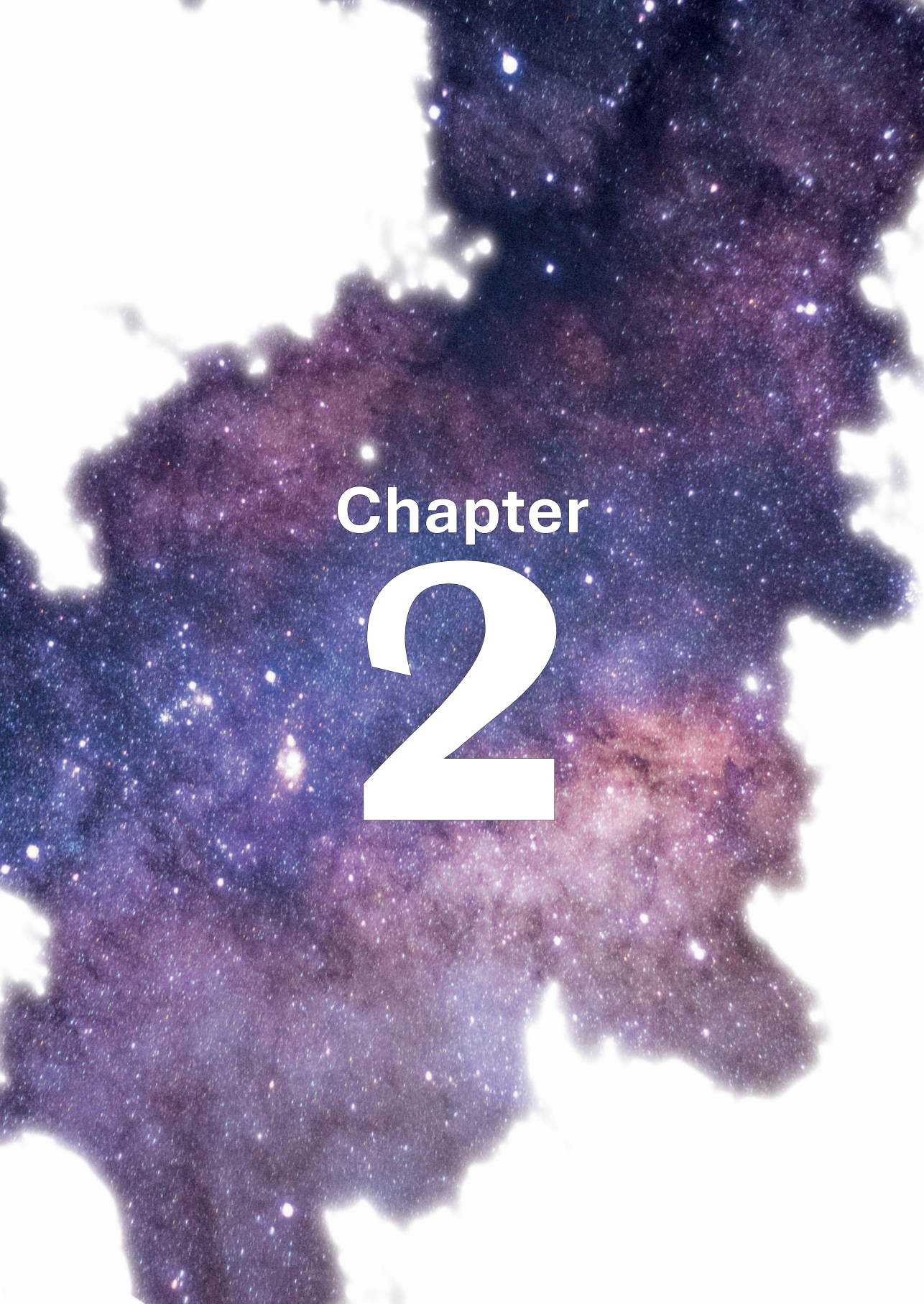
Chapter
2

Host-directed therapy to combat mycobacterial infections

Gül Kilinç[1,#], Anno Saris[1,#], Tom H. M. Ottenhoff[1] and Mariëlle C. Haks[1]

[1] Department of Infectious Diseases, Leiden University Medical Center, Leiden, The Netherlands
[#] These authors contributed equally to this work

Immunol Rev. 2021 Feb 9;301(1):62–83

Summary

Upon infection, mycobacteria such as *Mycobacterium tuberculosis* (*Mtb*) and nontuberculous mycobacteria (NTM), are recognized by host innate immune cells, triggering a series of intracellular processes that promote mycobacterial killing. Mycobacteria, however, have developed multiple counter-strategies to persist and survive inside host-cells. By manipulating host effector mechanisms, including phagosome maturation, vacuolar escape, autophagy, antigen-presentation and metabolic pathways, pathogenic mycobacteria are able to establish long-lasting infection. Counteracting these mycobacteria-induced host modifying mechanisms can be accomplished by host-directed therapeutic (HDT) strategies. HDTs offer several major advantages compared to conventional antibiotics: 1) HDTs can be effective against both drug-resistant and drug-susceptible bacteria, as well as potentially dormant mycobacteria; 2) HDTs are less likely to induce bacterial drug-resistance; and 3) HDTs could synergize with, or shorten antibiotic treatment by targeting different pathways. In this review, we will explore host-pathogen interactions that have been identified for *Mtb* for which potential HDTs impacting both innate and adaptive immunity are available, and outline those worthy of future research. We will also discuss possibilities to target NTM-infection by HDT, although current knowledge regarding host-pathogen interactions for NTM is limited compared to *Mtb*. Finally, we speculate that combinatorial HDT-strategies can potentially synergize to achieve optimal mycobacterial host immune control.

1. Introduction

Tuberculosis (TB), caused by *Mycobacterium tuberculosis* (*Mtb*), remains a major health problem. With an estimated 10 million disease cases and 1.4 million deaths in 2019, *Mtb* is the deadliest infectious agent worldwide and TB is one of the top-10 leading causes of deaths globally (1). Approximately a quarter of the world's population is infected with *Mtb* and in most cases, progression towards TB-disease is prevented by an efficient host immune response, often resulting in a latent TB infection (LTBI).(1) Five to fifteen percent of LTBI individuals will develop TB-disease during their life-time, often concomitant with host immunocompromising conditions, including HIV-infection and use of immunosuppressive medication. Treatment of patients with active TB has largely remained unchanged for over 30 years (1), and due to its lengthiness (6-24 months) and considerable side-effects, treatment-adherence is low fueling development of multi-drug and extensive-drug resistance (MDR and XDR). The large TB-disease burden and the increasing incidence of drug-resistance make alternative treatment solutions imperative.

While the number of TB-cases is slowly declining, a trend that may well be broken as a result of the COVID-19 pandemic (2), the prevalence of infections known to be caused by nontuberculous mycobacteria (NTM) is increasing at an alarming rate, currently reaching 0.2-9.8 per 100.000 individuals (3). NTM represent a group of opportunistic mycobacterial pathogens that mostly cause pulmonary diseases (PD), predominantly in vulnerable populations due to immunodeficiencies and/or pre-existing lung conditions. *Mycobacterium avium* (*Mav*) complex (MAC) and Mycobacterium abscessus (Mab) account for the large majority of reported cases (3). Despite extended treatment regimens, clinical outcome is poor, with cure-rates of approximately 50-88% among MAC-PD patients and 25-58% among Mab-infected individuals (3), urging the development of novel treatment modalities.

Mycobacteria are well known for their capability to manipulate intracellular signaling pathways to escape from host-defense mechanisms in human cells. *Mtb* is best studied in this regard, but NTM have also been shown to modulate host immune responses, including preventing phagosome acidification and maturation or escaping from phagosomes into the nutrient-rich cytosol. Counteracting pathogen-induced immune modulation by host-directed therapy (HDT) is a promising adjunct therapy to antibiotic therapy to combat intracellular mycobacterial infections, with several major advantages over current antibiotics. First, HDT can also be effective against MDR/XDR mycobacteria that are insensitive to current standard antibiotics. Second, because there is no direct selection pressure on mycobacteria, host-targeting compounds are less likely to result in drug resistance. Third, host-targeting compounds have the potential to target metabolically-inactive, non-replicating bacilli during LTBI, which are tolerant or resistant to conventional therapies. Fourth, HDT may allow shortening of current lengthy TB/NTM-treatment regimens, thereby increasing compliance. Fifth, HDT may permit dose-lowering of standard antibiotics, thus reducing toxicity without impacting efficacy. Finally, as HDT and mycobacterium-targeting compounds (i.e. antibiotics) by definition act on different pathways, combinatorial regimens would be expected to synergize. In this review, we will provide a comprehensive overview of host-pathogen interactions that have been identified in *Mtb* infections and that are amenable to targeting by HDTs (summarized in **Fig. 1 and Table 1**). Furthermore, despite a limited

number of reports, we will also discuss NTM-mediated host-modulation and speculate whether HDTs could also be of interest to combat these mycobacterial infections. Finally, we will discuss the possibility of combinatorial HDTs that target distinct host signaling pathways to promote possible synergistic treatment effects.

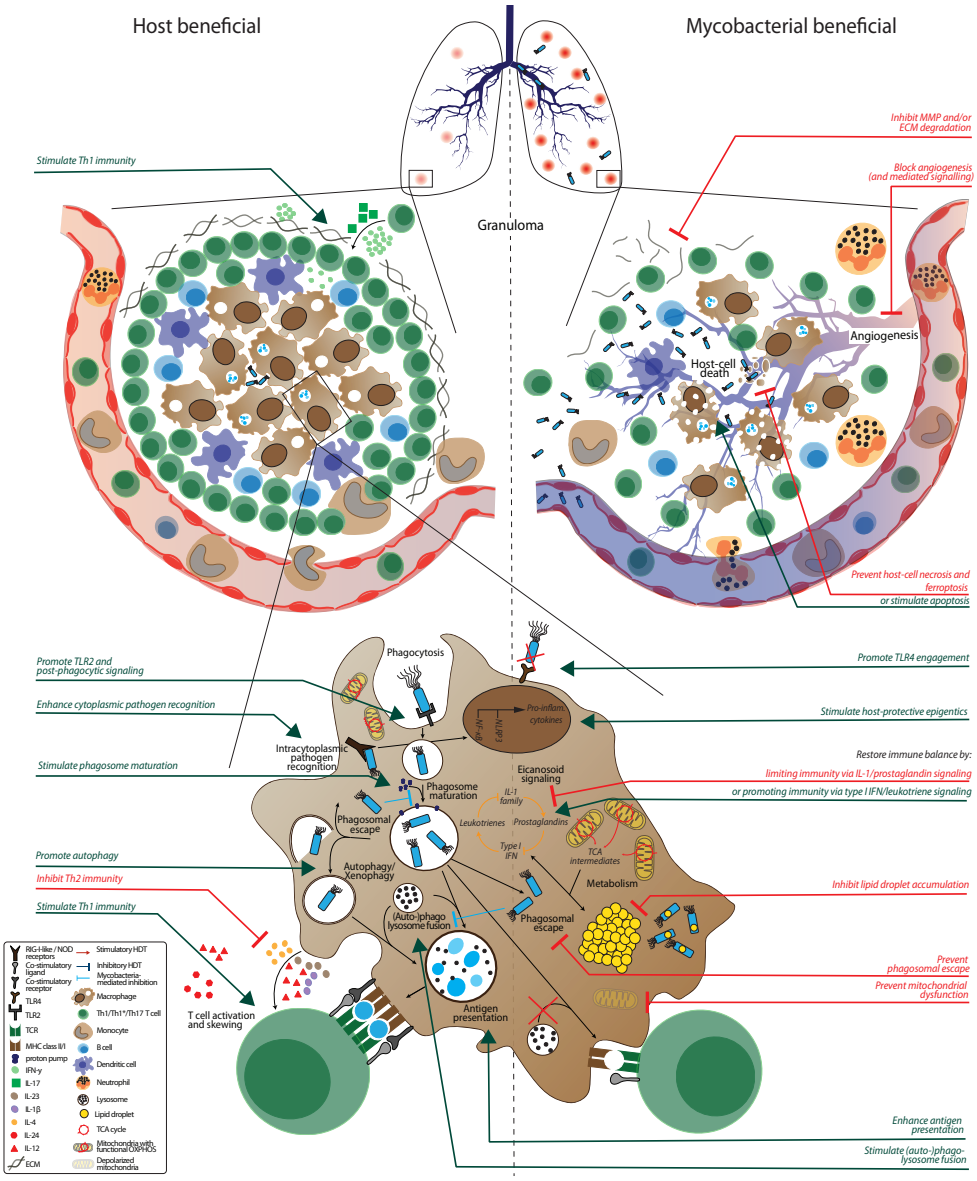

Figure 1. Host-pathogen interactions and potential host directed therapies (HDT). Granulomas are characteristic for tuberculosis and mycobacterial infections in general. Pathologic granulomas are poorly vascularized due to ineffective angiogenesis, leading to hypoxia and concomitant host-cell necrosis and bacterial dissemination. Blocking angiogenesis, preventing host-cell necrosis (or stimulating apoptosis) or inhibiting extracellular matrix (ECM)

degradation improves granuloma structure and concomitant disease outcome. Macrophages, key cells in the antimycobacterial response, initiate phagocytosis after toll-like receptor (TLR) recognition, which is prevented and/or modulated by mycobacteria. Promoting TLR4 engagement, TLR2 signaling and post-phagocytic signaling via receptor tyrosine kinase are all potential targets for HDT to improve host immunity during mycobacterial infection. After internalization, mycobacteria are located to phagosomes that slowly mature and ultimately fuse with lysosomes, which are all inhibited by mycobacteria. Alternatively, mycobacteria escape to the cytosol where they can be recognized by cytoplasmic pathogen recognition receptor (PRR) and 'recaptured' using autophagy, which again is inhibited by mycobacteria. HDTs that 1) prevent phagosomal escape, 2) alleviate blockage of (auto-)phagosome maturation, 3) promote autophagy and/or 4) stimulate (auto-)phago-lysosome fusion all enhance mycobacterial killing. HDT that enhance cytoplasmic recognition of mycobacteria also improve the anti-mycobacterial immune response. Mycobacteria that remain in the cytosol impair host metabolic pathways by stimulating tricarboxylic acid (TCA) cycle intermediates from mitochondria to be expelled into the cytosol to form lipid droplets and induce mitochondrial membrane depolarization. HDTs that 1) impair lipid droplet accumulation, 2) prevent mitochondrial membrane depolarization and/or 3) stimulate TCA cycle intermediates being allocated in eicosanoid signaling, maintain macrophage functionality which leads to better mycobacterial control. Finally, mycobacteria prevent the host from mounting an effective adaptive immune response by inhibiting antigen presentation and impairing T-cell skewing. HDTs that promote adaptive immunity by enhancing antigen presentation, stimulating Th1 skewing or inhibiting Th2/Treg immunity all improve disease outcome. Compounds that can correct the above processes are represented in red for inhibitory/blocking therapies and in green for stimulatory therapies and summarized in *Table 1*, ordered per physiological process.

2. HDT modulating innate immune cell function

2.1 Phagocytosis and phagosome maturation

The first potential target for HDT to interfere with host-pathogen interactions is to modulate mycobacterial host-cell entry. Mycobacteria infect host-cells, predominantly alveolar macrophages and epithelial cells, in the lower respiratory tract, following inhalation of small bacteria-containing aerosols. Mycobacteria express pathogen-associated molecular patterns (PAMPs) that are recognized by pattern recognition receptors (PRRs), such as Toll-like receptors (TLRs), C-type lectin receptors and other scavenger receptors expressed on the surface of host-cells to initiate phagocytosis (4). Especially TLR2, which forms heterodimers with TLR1 and TLR6 to recognize lipoproteins or lipopeptides (e.g. lipomannan), and TLR4, which recognizes cell wall lipids, glycoproteins, and secreted proteins, are known to mediate *Mtb*-induced cellular activation (4). Mice lacking TLR2 are more susceptible to infections with virulent *Mtb* and *Mav* strains (5-7). NTM, including *Mav* and Mab, express a class of glycolipids known as glycopeptidolipids (GPLs) which mask underlying cell wall phosphatidyl-myo-inositol mannosides, thereby limiting interactions with TLR2 (8, 9). Moreover, the acetylation state of lipomannan modulates TLR2-mediated macrophage activation, and subversion of the TLR2-MyD88 pathway has been linked to phagolysosome escape of virulent *Mtb* to the cytosol (10, 11), indicating a crucial role for TLR-signaling pathways in the control of intracellular mycobacteria. Several PRR agonists, including TLR2 agonist Pam2Cys, have been identified that activate both innate and adaptive immune responses against *Mtb*, positioning PPRs as potential HDT-targets to combat mycobacterial infections (12-16). Furthermore, also downstream PRR-signaling might be modulated by HDT. TLR2-dependent expression of miRNA-125 hampered autophagy in murine macrophages (17, 18). TLR2-MyD88 signaling in *Mtb*-infected murine macrophages was also repressed by

upregulation of miRNA-23a-5p, restricting *Mtb*-infection-induced autophagy and thus increasing intracellular *Mtb* survival (19). Inhibition of miRNA-125 (17, 18) or miRNA-23a (19) both reduced *Mtb* survival, identifying miRNA-125 and miRNA-23a as potential targets for HDTs.

After phagocytosis, mycobacteria become localized in phagosomes that are initially non-degradative, but slowly mature into increasingly hostile organelles. This so-called phagosome maturation hinges upon fusion with lysosomes that contain antimicrobial peptides and induce intravesicular acidification enhancing lysosomal enzyme activity. (20) While initially thought to be simply transport vehicles, phagosomes have appeared to be highly dynamic structures that are regulated by several membrane markers, such as PI3P, acidifying proton adenosine triphosphatases (ATPases) and Rab-GTPases (20, 21). As GTPases are also involved in autophagy induction, these enzymes could be interesting targets for HDT, but as of yet have not been investigated in this context. To prevent (auto)phagosome maturation, *Mtb* secretes proteins such as SapM and PknG, which inhibit PI3P-phosphorylation, dissociation of early endosomal protein Rab5 and acquisition of late endosomal protein Rab7 (22). In addition, *Mtb* prevents recruitment of the proton pumping enzyme vacuolar-type H^+-ATPase (v-ATPase) by phagosomes, thus further arresting phagosome acidification (23). Several receptor tyrosine kinases (RKTs) that are activated upon internalization of *Mtb* and NTM are involved in both bacterial uptake and intracellular trafficking, and could be exploited as targets for HDT (24). Abelson tyrosine kinase (Abl), involved in bacterial uptake by regulating cytoskeletal dynamics in host-cells, can be chemically inhibited by imatinib (23), and indeed, imatinib treatment impaired internalization of *Mtb* by human macrophages (25). Furthermore, Abl also modulates the expression of v-ATPase, and inhibiting RTKs with imatinib induced expression of several v-ATPase pump-subunits and their colocalization with *Mtb*-containing phagosomes, promoting phagosomal acidification and enhancing bacterial killing in human macrophages (26). In line with this, imatinib treatment of mice infected with *Mtb* or *Mycobacterium marinum* (*Mm*) decreased mycobacterial load and combining imatinib with first-line anti-TB drug rifampicin synergistically reduced mycobacterial load in mice and in a murine macrophage-like cell line (24-26). The potential of inhibiting host tyrosine kinases to impair intracellular mycobacterial survival is further highlighted with AZD0530 treatment, a Src-inhibitor, that lowered disease burden in *Mtb*-infected guinea pigs by promoting phagosomal acidification (27). Moreover, Korbee et al. showed that inhibiting RTK-signaling with the repurposed drugs AT9283, ENMD-2076 and dovitinib significantly reduced intracellular *Mtb* in primary human macrophages (28). Being repurposed, these compounds are already FDA approved or in phase II and III clinical trials, thus accelerating potential clinical application as adjunct therapy in treating (MDR)-TB and treatment of refractory NTM infections.

Formation and subsequent acidification of phagolysosomes is also inhibited by *Mtb*-secreted protein 1-tuberculosinyladenosineantacid (1-TbAd) (29). Accumulation of 1-TbAd in acidic intracellular compartments resulted in swelling and ultimately bursting of phagosomes, permitting mycobacterial escape into the cytosol. To further impair phagosome integrity, *Mtb* permeabilizes phagosomal membranes using the bacterial ESX-1 secretion system (i.e. ESAT-6) (30), which leads to leakage of phagosomal cargo

Table 1. HDT compounds and their biological activity against mycobacterial infections.

Compound	Biological activity	Model	Pathogen	Ref.
Phagocytosis and phagosome maturation				
PRR agonists	↑ PRR-signaling	*in vitro*	*Mtb*	13-17
miRNA-125 inhib.*	↑ TLR2-signaling	*in vitro*	*Mtb*	19
miRNA-23a-5p inhib.*	↑ TLR2-signaling	*in vitro*	*Mtb*	20
Imatinib*	↑ Phagosomal acidification ↓ Phagocytosis	*in vitro*, *in vivo*, (R)CT	*Mtb, Mm*	26,27
AZD0530	↑ Phagosomal acidification	*in vivo*	*Mtb*	28
AT9283	Unknown	*in vitro*	*Mtb*	29
ENMD-2076	Unknown	*in vitro*	*Mtb*	29
Dovitinib	Unknown	*in vitro*	*Mtb*	29
Nitazoxanide	↑ Cytoplasmic pathogen recognition	*in vitro*, (R)CT	*Mtb*	33,34
Metformin*	↑ Phagosome maturation	*in vitro*, *in vivo*, (R)CT	*Mtb*	71-77
Gefitinib*	↑ Lysosomal biogenesis	*in vitro*, *in vivo*	*Mtb*	78
Bedaquilline*	↑ (Auto)-phagolysosome fusion	*in vitro*, *in vivo*, (R)CT	*Mtb*	84,222-224
2062*	↑ (Auto)-phagolysosome fusion	*in vitro*, *in vivo*	*Mtb*	85
GM-CSF*	↑ Phagocytosis ↑ (Auto)-phagolysosome fusion	*in vitro*, *in vivo*, CR	*Mtb, Mav*	86-92
Resveratrol*	↑ (Auto)-phagolysosome fusion	*in vitro*	*Mtb*	70
SRT1720*	↑ (auto)-phagolysosome fusion	*in vitro*, *in vivo*	*Mtb*	70
Celecoxib*	↑ Phagocytosis	*in vivo*, (R)CT	*Mtb*	187
Statins*	↑ Phagosome maturation	*in vitro*, *in vivo*, (R)CT	*Mtb*	181,184-186
Autophagy				
Imatinib*	↑ Autophagy	*in vitro*	*Mtb*	26,27
Vitamin-D	↑ Autophagy	*in vitro*, (R)CT	*Mtb*	40-47,51,52
PBA	↑ Autophagy	*in vitro*, (R)CT	*Mtb*	49-53
Vitamin-A (± Zn^{2+})	↑ Autophagy	*in vitro*, *in vivo*, (R)CT	*Mtb*	55-62

Compound	Biological activity	Model	Pathogen	Ref.
Antigen presentation and priming				
MiRNA-106b inhib.	↑ Antigen presentation	*in vitro*	*Mtb*	121
AGK2	↑ Antigen presentation	*ex vivo*, *in vivo*	*Mtb*	116
G1-4A	↑ Th1 immunity (TLR4-signaling)	*in vitro*, *in vivo*	*Mtb*	122
LPS+CD40 agonist	↑ Th1 immunity (TLR4-signaling)	*in vitro*, *in vivo*	*Mtb*	13
Bergenin	↑ Th1 immunity	*ex vivo*, *in vivo*	*Mtb*	124
D-1MT*	↑ Th1 immunity	*ex vivo*, *in vivo*	*Mtb*	129
Skewing of T-cells				
IFN-γ	↑ Th1 immunity	*in vitro*, (R)CT	*Mtb, Mav*	133,134,137-140
IL-12	↑ Th1 immunity	*in vivo*	*Mtb*	141
IL-24	↑ Th1 immunity	*in vivo*	*Mtb*	142
FPS-ZM1	↓ Immune response	*in vivo*	*Mtb*	145
Blocking IL-4	↓ Th2 immunity	*in vitro*	*Mtb*	131
IL-2	↑ Th1 immunity	*in vivo*, (R)CT	*Mtb, Mav*	146-149
IL-2+HMBPP	↑ Th1 immunity	*in vivo*	*Mtb*	151
PBMCs + cytokines	↑ Th1 immunity	CR	*Mtb*	152
Prednisolone	↓ Immune response	(R)CT	*Mtb*	158-160
(Programmed) cell death				
Mcl-1 inhib.	↑ Apoptosis	*in vitro*	*Mtb*	155
Nicotinamide	↓ Necrosis	*in vitro*	*Mtb*	99
SQ22536	↑ TNF-α	*in vitro*	*Mtb*	161
H-89	↑ TNF-α	*in vitro*	*Mtb*	161
Dexamethasone	↓ Necrosis ↓ Immune response	*in vitro*, *in vivo*, R(CT)	*Mtb*	157-160,188,191
Doramapimod	↓ Necrosis	*in vitro*	*Mtb*	157

Compound	Biological activity	Model	Pathogen	Ref.
MiRNA-27a antagomir	↑ Autophagy	*in vivo*	*Mtb*	66
Everolimus	↑ Autophagy	*in vitro*, (R)CT	*Mtb*	68
Ibrutinib	↑ Autophagy	*in vitro*, *ex vivo*	*Mtb*	69
Metformin*	↑ Autophagy ↓ Mitochondrial dysfunction	*in vitro*, *in vivo*, (R)CT	*Mtb*	71-77
Gefitinib*	↑ Autophagy	*in vitro*, *in vivo*	*Mtb*	78
Bazedoxifene*	↑ Autophagy	*in vitro*	*Mtb*	79
Loperamide	↑ Autophagy	*in vitro*, *ex vivo*	*Mtb*	80
Bedaquilline*	↑ Autophagy	*in vitro*, *in vivo*, (R)CT	*Mtb*	84,222-224
2062*	↑ Autophagy	*in vitro*, *in vivo*	*Mtb*	
Resveratrol*	↑ Autophagy	*in vitro*	*Mtb*	70
SRT1720*	↑ Autophagy	*in vitro*, *in vivo*	*Mtb*	70
miRNA-125 inhib.*	↑ Autophagy	*in vitro*	*Mtb*	19
miRNA-23a-5p inhib.*	↑ Autophagy	*in vitro*	*Mtb*	20
Statins*	↑ Autophagy	*in vitro*, *in vivo*, (R)CT	*Mtb*	181,184-186
Intracellular killing mechanisms				
CD157	↑ Reactive oxygen species	*in vitro*	*Mtb*	95,97
N-acetyl-cysteine	↓ Reactive oxygen species	*in vitro*, *in vivo*, (R)CT	*Mtb*	99-101
L-arginine	↑ Reactive nitrogen species	(R)CT	*Mtb*	107-109
Bazedoxifene*	↑ Reactive oxygen species	*in vitro*	*Mtb*	79
Metformin*	↑ Reactive oxygen species	*in vitro*, *in vivo*, (R)CT	*Mtb*	71-77
Celecoxib*	↑ Reactive oxygen species	*in vivo*, (R)CT	*Mtb*	187
Epigenetic regulation				
TMP195	↑ Host-protective epigenetics	*in vitro*, *in vivo*	*Mtb, Mm*	115
TMP269	↑ Host-protective epigenetics	*in vitro*, *in vivo*	*Mtb, Mm*	115

Compound	Biological activity	Model	Pathogen	Ref.
Alisporivir	↓ Necrosis ↓ TNF-α	*in vivo*	*Mm*	163
Desiparamine	↓ Necrosis	*in vivo*	*Mm*	163
Cilostazol	↓ TNF-α	*in vivo*	*Mtb*	164,165
Sildenafil	↓ TNF-α	*in vivo*	*Mtb*	164,165
Ferrostatin 1	↓ Ferroptosis	*in vitro*, *in vivo*	*Mtb*	171
D-1MT*	↑ Apoptosis	*ex vivo*, *in vivo*	*Mtb*	129
ATP administration*	↑ Apoptosis	*in vitro*	*Mtb, Mav*	176,177
Carbohydrate and lipids				
2-DG	↓ Glycolysis	*in vitro*	*Mtb*	174
FX11	↓ Glycolysis	*in vivo*	*Mtb*	175
ATP administration*	↑ Iron chelation	*in vitro*	*Mtb, Mav*	176,177
Clemastine	↑ Immune response?	*in vivo*	*Mm*	
M1	↓ Mitochondrial dysfunction	*in vitro*	*Mtb*	180
Ezetimibe	↓ Lipid droplet accumulation	*in vitro*	*Mtb*	179
Statins*	↓ Membranal cholesterol incorporation	*in vitro*, *in vivo*, (R)CT	*Mtb*	181,184-186
Eicosanoids				
PGE2 and/or Zileuton	↑ IL-1β/prostaglandin signaling	*in vivo*	*Mtb*	189,190
Celecoxib*	↓ IL-1β/prostaglandin signaling	*in vivo*, (R)CT	*Mtb*	187
LTB_4	↑ IL-1β/prostaglandin signaling	*in vivo*	*Mtb*	187
Ibuprofen	↓ IL-1β/prostaglandin signaling	*in vivo*, (R)CT	*Mtb*	192,193
Aspirin	↓ IL-1β/prostaglandin signaling	*in vivo*, (R)CT	*Mtb*	193-198
Granuloma: formation, angiogenesis and hypoxia				
Cipemastat	↓ MMP/ECM degradation	*in vivo*	*Mtb*	208
MMP-9 inhib.	↓ MMP/ECM degradation	*in vivo*	*Mm*	25

Compound	Biological activity	Model	Pathogen	Ref.	Compound	Biological activity	Model	Pathogen	Ref.
Trichostatin A	↑ Host-protective epigenetics	*in vitro*, *in vivo*	*Mtb, Mm*	[115]	Sb-3ct	↓ MMP/ECM degradation	*in vitro*, *in vivo*	*Mtb*	[212,213]
Resveratrol*	↑ Host-protective epigenetics	*in vitro*	*Mtb*	[70]	AB0046	↓ MMP/ECM degradation	*in vivo*	*Mtb*	[166]
SRT1720*	↑ Host-protective epigenetics	*in vitro*, *in vivo*	*Mtb*	[70]	Doxycycline	↓ MMP/ECM degradation	*in vitro*, *in vivo*, (R)CT	*Mtb*	[210,214]
Valproic acid	↑ Host-protective epigenetics	*in vitro*	*Mtb*	[117]	Marimastat	↓ MMP/ECM degradation	*in vitro*, *in vivo*	*Mtb*	[203,205]
SAHA	↑ Host-protective epigenetics	*in vitro*	*Mtb*	[117]	Batimastat	↓ MMP/ECM degradation	*in vivo*	*Mtb*	[205]
					MMP-9 inhib.	↓ MMP/ECM degradation	*in vivo*	*Mtb*	[205]
					Bevacizumab	↓ Angiogenesis	*in vivo*	*Mtb*	[217]
					SU5416	↓ Angiogenesis	*in vivo*	*Mm*	[218]
					Pazopanib	↓ Angiogenesis	*in vivo*	*Mm*	[218]
					AKB-9785	↓ Angiogenesis	*in vivo*	*Mm*	[219]

*Compounds targeting distinct host intracellular pathways are categorized under multiple sections. *Mtb, Mycobacterium tuberculosis*; *Mav, Mycobacterium avium*; *Mm, Mycobacterium marinum*; (R)CT, (randomized) clinical trial; CR, case report; PRR, pathogen recognition receptor; inhib., inhibitor; GM-CSF, granulocyte-macrophage colony-stimulating factor; PBA, phenylbutyrate; SAHA, suberoylanilide hydroxamic acid; IFN-γ, interferon-γ; IL, interleukin; TNF-α, tumor necrosis factor-α; HMBPP, (E)-4-hydroxy-3-methyl-but-2-enyl pyrophosphate; PBMCs, peripheral blood mononuclear cells; 2-DG, 2-deoxy-D-glucose; ATP, adenosine triphosphatases; LTB_4, leukotriene-B4; MMP, matrix metalloprotease.

into the cytosol, allowing phagosomal escape of mycobacteria. Although the cytosol contains an abundance of nutrients to support bacterial growth, translocation into the cytosol also activates DNA- and RNA-sensing pathways via intracellular recognition of PAMPs and danger-associated molecular patterns (DAMPs) to induce anti-mycobacterial host effector mechanisms. Retinoid acid-inducible gene I (RIG-I)-like receptors are cytosolic PRRs recognizing single- and double-stranded RNA and upon ligation induce the type-I IFN pathway, amongst others (31). Nucleotide-binding oligomerization domain (NOD)-like receptors are intracellular sensors for several DAMPs and PAMPs, including bacterial RNA, that can induce both type-I IFN and IL-1 responses (31). Enhancing expression levels of RIG-I-like receptors using nitazoxanide treatment during mycobacterial infection increased IFN-β levels and concomitantly reduced mycobacterial loads in an *in vitro* TB model (32), but did not show efficacy in TB-patients, possibly due to negligible concentrations at the site of infection (33).

2.2 Autophagy

Autophagy is a mechanism mediating self-maintenance and cellular homeostasis and is induced under stress such as hypoxia, starvation but also microbial infection (34). Autophagy is crucial during *Mtb* and NTM infections and inhibition of autophagy using azithromycin increased susceptibility of cystic fibrosis patients to NTM infection (35)

Autophagy is initiated by formation of a double-membraned phagophore that, under stringent control of ubiquitin-like protein conjugation systems, expands around the intracytoplasmic cargo to form autophagosomes, which ultimately fuse with lysosomes to mediate degradation. Two autophagic pathways are important for mycobacterial degradation: LC3-associated phagocytosis (LAP) and the STING-dependent cytosolic pathway (36). LAP is initiated by downstream signaling of numerous receptors, including TLRs (36), after which the phagosome becomes decorated with PI3P produced by the PI3KC3 complex, that includes Beclin-1 and Rubicon. PI3P and Rubicon are required for the generation of reactive oxygen species (ROS) and conjugation of lipidated LC3-II to the membrane to enhance phagosomal maturation (36). The STING-dependent pathway is triggered by mycobacterial DNA released into the cytosol through the bacterial ESX-1 system. When mycobacterial DNA is sensed by a STING-dependent DNA sensor, cytosolic *Mtb* is ubiquitinated by the ubiquitin-ligating (E3) ligase, bound to autophagic receptors including p62/sequestosome 1, NDP52 protein and TBK1, and subsequently delivered to autophagosomes by engagement of membrane-associated LC3 (31).

Numerous drugs have been identified that promote autophagy by targeting different components of the autophagic pathways. Beclin-1 is induced by human antimicrobial peptide (AMP) LL-37, also known as cathelicidin (37). Cathelicidin is able to suppress *Mtb* growth and can be induced by pathogens after TLR2/TLR1 ligation, and also by vitamin-D (38). *In vitro* experiments identified calcitriol, the bioactive metabolite of vitamin-D, to exert antimicrobial activity by mediating intracellular killing of *Mtb* through cathelicidin (39). Calcitriol has also been linked to nitric oxide (NO) production and suppression of matrix metalloproteases (MMPs) which may further protect the host from TB immunopathology (40, 41). The efficacy of vitamin-D as HDT during TB-disease has been investigated in multiple randomized controlled trials (RCTs).

Vitamin-D administration corrected any vitamin-D deficiencies and was safe in use but did not show consistent beneficial outcomes during mycobacterial infections in meta-analyses (42-44). Acceleration of *Mtb* clearance from sputum was mainly observed in MDR-TB-cases or patients with a specific genotype, such as polymorphisms in the vitamin-D receptor-gene (45, 46). Furthermore, low levels of vitamin-D have been linked to a higher susceptibility to develop TB-disease (47). Some studies combined vitamin-D therapy with Phenylbutyrate (PBA), which stimulates cathelicidin-induced autophagy and also inhibits bacterial growth directly (48, 49). Combining vitamin-D and PBA treatment further increased expression of cathelicidin in healthy volunteers, but the augmented expression level was constrained to a defined dose-range of PBA (50). The narrow therapeutic window of PBA might clarify why certain RCTs failed to detect accelerated sputum-smear conversion by co-administering vitamin-D and PBA (51) and only showed accelerated sputum-smear conversion at week 4 following combined treatment, but not at week 8 in vitamin-D-deficient patients (52). Due to these inconsistencies, progression of vitamin-D as potential HDT in TB treatment regimens has not been successful.

Vitamin-A-deficiency has also been correlated with an increased risk to develop TB-disease (53). STING-dependent autophagy can be targeted by the active metabolite of vitamin-A, i.e. all-trans retinoic acid (ATRA), which promotes TBK1-mediated enhancement of autophagy which reduces *Mtb* survival in human macrophages (54). ATRA is also known to increase CD1d receptor expression on innate immune cells (55). and treatment with non-mycobacterial CD1d ligand α-galactosylceramide (α-GalCer) reduced mycobacterial load and improved survival of mice with TB (56), and while α-GalCer combined with ATRA and vitamin-D did not clear the infection in mice, it improved containment of the infection (57). In patients, vitamin-A supplementation combined with Zn^{2+} or vitamin-D gave inconsistent results (58-61). Thus, although vitamin-A reduced *Mtb* loads *in vitro* and *in vivo*, evidence for its efficacy in patients is inconsistent. An additional regulator of the selective STING-dependent autophagy pathway is DNA-damage regulated autophagy-modulator protein 1 (DRAM1). DRAM1 was found to trigger autophagy in both *Mtb*-infected human macrophages and *Mm*-infected zebrafish larvae, whereas DRAM1-deficiency resulted in host-detrimental cell death, underscoring DRAM1 as an interesting target for HDT (62, 63).

In addition to Beclin-1 and TBK1, other components of the autophagic pathways have also been targeted to promote mycobacterial clearance. Ca^{2+}-signaling is pivotal in inducing autophagy by activating the Ca^{2+}/calmodulin-dependent serine/threonine-kinase (CaMKK2)/ULK1 complex.(64) CaMKK2-mediated autophagy and killing of intracellular *Mtb* requires Ca^{2+} transporter CACNA2D3 which is, however, suppressed by *Mtb*-induced miRNA27a (65). Intracellular survival of *Mtb* could be impaired by inhibiting miRNA-27, providing a new HDT target.

Another important negative regulator of autophagy is the PI3K-Akt-mTOR signaling pathway, which is robustly activated by *Mtb* to facilitate its intracellular survival (66). Everolimus, an improved analog of mTOR inhibitor rapamycin, was able to reduce *Mtb* burden in a human granuloma model and these effects were additive to first-line TB drugs, possibly by HDT activity and/or by inhibiting mycobacterial growth directly (67). Inhibition of protein-kinase C-beta (PKC-B), another important regulator of

the PI3K-Akt-mTOR pathway, by ibrutinib also enhanced autophagy and restricted intracellular growth of *Mtb* in macrophages and mice in the spleen, although not in the lungs (68). Alleviating the *Mtb*-mediated suppression of sirtuin-1, a class-III histone deacetylase that also modulates autophagy via 5'AMP-activated protein-kinase (AMPK), using resveratrol restricted intracellular *Mtb* growth by stimulating autophagy and phagosome-lysosome fusion (69). Metformin, a well-established stimulator of AMPK-mediated inhibition of mTOR-signaling, is widely used for the treatment of type-2 diabetes, but also induces ROS-production, phagosome maturation and autophagy *in vitro* and prevents mitochondrial membrane depolarization (70-72). In non-diabetic healthy volunteers, metformin treatment downregulated genes involved in *Mtb*-mediated modulation of autophagy, as well as type-I IFN signaling, while upregulating genes involved in phagocytosis and ROS-production (73). Several clinical trials have shown that metformin treatment reduces the risk of latent TB reactivation and TB-mortality, and in patients with cavitary TB, improves sputum culture conversion (74-76).

Like metformin, repurposing of drugs that are clinically approved in the context of other diseases have been shown to enhance autophagy and to reduce intracellular bacterial growth, suggesting these drugs may be considered as HDT-candidates. The anti-cancer drug gefitinib, an inhibitor of epidermal growth factor receptor (EGFR), promotes intracellular *Mtb* killing by alleviating the STAT3-dependent repression of effective immune responses in *Mtb*-infected mice and by enhancing lysosomal biogenesis and targeting of mycobacteria to lysosomes in *Mtb*-infected macrophages (77). Gefitinib also induced autophagy (77), but since no specific targeting of mycobacteria to the autophagic pathway was observed, this activity has not been formally linked to restricting intracellular *Mtb* survival. Bazedoxifene, a selective estrogen receptor modulator (SERM) used for breast cancer treatment, was also shown to inhibit intracellular *Mtb* growth in macrophages through enhanced ROS-dependent autophagy (78), and to inhibit *Mtb* growth in liquid culture. Furthermore, one study showed that loperamide, an anti-diarrheal drug, promoted autophagy as indicated by p62 degradation and decreased mycobacterial burden *in vitro* and ex vivo in murine macrophages (79).

Mtb not only inhibits the initiation of autophagy, but also fusion of autophagosomes with lysosomes via protein P2-PGRS47 (22, 80). Furthermore, the *Mtb* secretion-factor SapM inhibits Rab7-recruitment to prevent autophagosome-lysosome fusion (81). *Mtb*-expressed mannosylated lipoarabinomannan (ManLAM) also inhibits maturation of autophagosomes, by blocking LC3-translocation to autophagosome membranes (31, 82). Releasing such blockades in autophagosome-lysosome fusion could represent potential HDT strategies. Bedaquilline, a novel antibiotic now in use for MDR-TB, has also been shown to induce phagosome-lysosome fusion and autophagy via activation of TFEB, possibly contributing to it successful application as a new TB-drug (83). In line with this, a small molecule called 2062 improved autophagy and lysosomal pathway activity via activation of TFEB when administered with suboptimal doses of rifampicin (84).

Although autophagy-targeting HDTs have been investigated mainly in the context of *Mtb* infections, several case reports have been published for (disseminated) *Mav* infections in patients who received granulocyte-macrophage colony-stimulating factor (GM-CSF) or IFN-γ. GM-CSF treatment during *Mtb* infection reduced bacterial burden by

promoting phagosome-lysosome fusion and increased expression of TNF-α, IFN-γ and inducible nitric oxide synthase (iNOS) (85-87). GM-CSF treatment during *Mav* infection increased phagocytosis and impaired bacterial growth *in vitro* in human macrophages and in *Mav*-infected patients with or without HIV infection (partially) improved clinical outcome (88-91). Thus autophagy likely plays an important role also in NTM immunity, and could represent an attractive target for HDT in severe NTM infections.

2.3 Intracellular killing mechanisms: reactive oxygen and nitrogen species

To eliminate mycobacteria during infection, host-cells trigger the production of reactive oxygen species (ROS) and reactive nitrogen species (RNS), via NADPH oxidase 2 (NOX2) (92) and inducible nitric oxide synthase 2 (iNOS), respectively. iNOS catalyzes production of nitric oxide (NO) by converting L-arginine into L-citrulline, which is subsequently converted into RNS (93). Once expressed, both ROS and RNS interact with the phagosome to destroy bacterial components (94). Mycobacterium-induced ROS-production occurs via the TLR(2)-MyD88 signaling axis and impairments in this pathway increase susceptibility to *Mtb* infection (6, 95). Recently, TLR2-dependent ROS-production and bactericidal activity was found to be impaired in CD157-deficient murine macrophages which could be rescued by administration of soluble CD157 (94, 96). Moreover, expression levels of CD157, an enzyme important for leukocyte migration and involved in nicotinamide-adenine-dinucleotide (NAD^+) metabolism, are elevated in patients with active TB compared to LTBI and lowered when patients are treated with TB chemotherapy, indicating an important role of CD157 in host immunity, biomarker profiling and also providing a potential HDT (96).

Although ROS-production is important for host resistance against mycobacterial infection, modulating ROS as HDT strategy requires careful monitoring as excess ROS leads to oxidative stress and concomitant necrosis.(97) Corroborating this view, reducing ROS accumulation in *Mtb*-infected macrophages with ROS scavenger N-acetyl-cysteine in fact restricted *Mtb* replication and restored macrophage cell viability (98), and in a guinea pig *Mtb*-infection model N-acetyl-cysteine administration was also shown to be efficacious (99). Moreover, N-acetyl-cysteine was found to be safe in a cohort of TB-HIV co-infected individuals (100), although its impact on culture conversion remains to be determined (100). Nevertheless, ROS-production is important for the bactericidal activity of macrophages (101) and the critical balance in ROS-production and its regulation is important in restricting intracellular mycobacterial growth without harming the host.

Multiple studies in mice and humans have shown antimicrobial effects of NO, but the exact underlying mechanisms remain unclear (102, 103). Macrophages from LTBI patients were shown to control *Mtb* growth via NO-production, and human macrophages required iNOS for intracellular killing of *Mtb* (104). Moreover, compared to wildtype murine macrophages, protein-kinase R (PKR)-deficient-macrophages induced higher levels of iNOS during *Mtb* infection (105), and PKR-deficient mice had lower *Mtb* loads and less severe lung pathology compared to infected wildtype mice, highlighting the potential of PKR as HDT target. Despite its importance as substrate for NO-production, supplementing L-arginine did not consistently improve clinical outcomes such as cure rate or (sputum) smear conversion in several clinical trials (106-108).

Several *Mtb*-associated proteins have been identified that protect *Mtb* from RNS, but *Mav* naturally tolerates intracellular NO levels and may even benefit from host NO (109-111). Mice that cannot produce NO were more resistant to *Mav* infections, while being more prone to *Mtb* infections (112). In agreement with this, compared to wildtype mice, NOS2-deficient mice showed higher IFN-γ responses during *Mav* infection and increased accumulation of especially $CD4^+$ T-cells (113). Enhancing NO-production can thus be beneficial in combatting mycobacterial infections such as *Mtb*, but not *Mav*.

2.4 Epigenetic regulation

Macrophage polarization is an important mechanism of the immune system to respond adequately to the plethora of pathogens, which is partly mediated by epigenetic regulation of gene expression using histone acetylation. The level of histone acetylation is regulated by the balanced activity of histone acetyltransferases (HATs) and histone deacetylases (HDACs). HDACs are divided into four classes, three of which are Zn^{2+}-dependent (class I, IIa/IIb and IV), while class-III is NAD^+-dependent (114). *Mtb* infection actively modulates the acetylation status of host histones by 1) suppressing expression of class-II HDACs (i.e. HDAC 3, 5, 7, and 10) in macrophages, with anti-inflammatory M2 macrophages being more affected than pro-inflammatory M1 macrophages (114), 2) inhibiting the expression of class-III HDAC sirtuin-1 both *in vitro* and in human tissues from TB-patients (69), and 3) upregulating expression of sirtuin-2, another class-III HDAC that regulates cell cycle and metabolism (115). Type IIa-specific HDAC inhibitors (HDACi) TMP195 or TMP269 reduced bacterial loads in M2, but not M1 macrophages, while broad spectrum HDACi trichostatin A reduced bacterial loads in both M1 and M2 macrophages. Interestingly, combining HDACi with AKT1 kinase inhibitor H-89 resulted in cumulative reduction in bacterial loads. Importantly, in a *Mm* zebrafish infection model, both class-IIa and pan-HDAC inhibition reduced bacterial loads, confirming the *in vivo* potential of HDAC inhibition as HDT to treat TB (114). Sirtuin-1, a class-III HDAC important during (viral) infections, regulates stress responses and cellular metabolism. Resveratrol or SRT1720, a natural and synthetic activator of sirtuin-1, enhanced clearance of drug-sensitive and drug-resistant *Mtb* (69). Both compounds stimulate autophagy and phagolysosome fusion in THP-1 cells, which likely accounts for the enhanced bacterial killing, while reducing pathology in a TB mouse model, possibly by inhibiting expression of IL-1β, IL-6, MCP-1 and TNF-α (69).

The *Mtb* genome encodes Rv1151c, a sirtuin-like NAD-dependent deacetylase, allowing *Mtb* to produce acetyl coenzyme A (acetyl-CoA) synthetase, a critical enzyme in energy metabolism of both host-cells and bacteria. Targeting this pathway using HDACi valproic acid directly inhibited bacterial growth, likely by inhibiting acetyl-CoA production by *Mtb* itself, while co-treatment of valproic acid and rifampicin/isoniazid therapy resulted in cumulative effects (116). By contrast, FDA-approved HDACi suberoylanilide hydroxamic acid (SAHA) had no direct effect on *Mtb* growth, but it reduced mycobacterial growth via host-directed mechanisms and synergized with rifampicin/isoniazid therapy (116). As Rv1151c is well conserved across different mycobacterial species including *Mav* (117), the above therapies may also be efficacious against NTM.

3. HDT modulating adaptive immune responses

3.1 Antigen presentation and priming

Upon phagocytosis, pathogens are processed and degraded, such that pathogen-derived peptides can be loaded and presented in MHC-class I and II molecules to initiate adaptive T-cell responses. One strategy of mycobacteria to evade host adaptive immune responses is to impair presentation of mycobacterial peptides by evading phagosomal degradation. Improving mycobacterial degradation by promoting phagosomal maturation and/or autophagy induction as discussed above, likely both enhance antigen-presentation and concomitant adaptive immunity. Another strategy of mycobacteria to evade host adaptive immune responses is to predominantly infect macrophages instead of dendritic cells, the former requiring stronger activation before being able to efficiently process and present antigens for priming naïve T-cells (118). Macrophage activation is required to induce expression of CIITA, a major positive regulator of MHC-class II. By actively engaging TLR2 rather than other TLRs, *Mtb* (and to a lesser extent M. smegmatis) minimizes upregulation of CIITA and concomitant MHC-class II expression. In addition, TLR2 (among all TLRs), most potently induces an innate (IL-6) response (119), leading to upregulation of suppressor-of-cytokine-signaling-1 (SOCS1) that in turn inhibits signal-transducer-and-activator-of-transcription 1 (STAT1) phosphorylation and antigen-presentation, further impairing the adaptive host immune response (22). MiR106b, which degrades mRNA encoding cathepsin S, a protein that modulates MHC-class II molecules to allow peptide loading, is significantly upregulated during *Mtb* infection (120). Inhibition of miR106b using miRIDIAN hairpin inhibitors upregulated expression of both cathepsin S and HLA-DR and enhanced subsequent CD4 T-cell proliferation (120). Alternatively, inhibition of sirtuin-2 activity in macrophages using AGK2 modulated gene expression-promoted antigen-presentation (115). AGK2 treatment of mice resulted in upregulation of MHC-class II expression but also of co-stimulatory molecules and markers of activation, leading to enhanced priming of T-cells and improved *Mtb* killing (115).

Since *Mtb* limits activation of antigen-presenting cells (APCs), which precludes the host from mounting an effective adaptive immune response, proper activation of APCs could be an interesting HDT. A possible strategy for HDT could be administration of G1-4A, a polysaccharide from Tinospora cordifolia that presumably signals via TLR4, or TLR4 ligand LPS combined with a CD40 agonistic antibody (12, 121). Both treatments induced vast cytokine production (IFN-γ/IL-12, TNF-α, IL-6) and upregulation of co-stimulatory molecules by dendritic cells *in vitro* (121). Furthermore, both treatments reduced bacterial loads in murine TB infection models which was, at least in part, T-cell-mediated (121). However, systemic administration of TLR ligands is known to cause significant side effects (122), and may only be applicable via local administration. Bergenin, a phytochemical extracted from tender leaves, enhanced macrophage activation, as evidenced by enhanced CD11b expression as well as augmented NO, TNF-α and IL-12 production, through activating the MAPK/ERK pathway. The resulting increased IL-12 production induced a robust Th1 response with concomitant IFN-γ production by T-cells. Bergenin therapy reduced bacterial loads as well as lung pathology in a murine TB infection model (123). Of note, vaccination could also be an interesting HDT approach to activate APCs or reprogram an effective adaptive immune response. This, however, falls outside the scope of this review and is excellently

reviewed elsewhere (124).

Due to the chronic immune stimulation during persisting mycobacterial infections, including LTBI, T-cells and APCs upregulate inhibitory receptors such as PD-1/PD-L1, which can impair T-cell effector functions (22), and may be interesting targets for HDT. Expression of exhaustion-associated markers by T-cells during active disease however, is rather ambiguous: despite successes in anti-cancer therapies by inhibiting immune checkpoint molecules with anti-PD-1/PD-L1 antibodies, PD1/PDL1-directed experimental therapies in *in vitro* and *in vivo* TB models resulted in impaired intracellular control of *Mtb* and TB exacerbation rather than improved resolution (125, 126), suggesting PD-1 may be a T-cell activation rather than exhaustion marker during TB. Moreover, reports of LTBI-reactivation in cancer patients treated with anti-PD-1/PD-L1 (127), warrants a cautionary note against this therapy in TB.

Indoleamine 2,3-dioxygenase (IDO) expression is actively induced by mycobacteria in animal (macaques and mice) models of acute TB, but not LTBI, and IDO levels correlated with bacterial burden. IDO catabolizes tryptophan into kynurenine, which in turn suppresses IFN-γ production by CD4 T-cells, a cytokine pivotal in the anti-TB response, identifying IDO as potential target for HDT. *In vivo* inhibition of IDO activity using D-1MT one week after mycobacterial infection enhanced T-cell proliferation and differentiation in effector and memory cells while apoptosis was enhanced (128). Furthermore, D-1MT treatment improved penetration of T-cells into granulomas, likely allowing protective T-cell-mediated granuloma reorganization, and reduced bacterial loads and lung pathology (128).

3.2 Skewing of T-cells

Th1-responses, characterized by high IFN-γ secretion, are crucial in effective anti-*Mtb* immune responses (129-131). Nevertheless, *Mav* and *Mtb* reduce cellular responses to IFN-γ and deficiencies in the IL-12/IL-23/IFN-γ-axis increase susceptibility to *Mav* infections (132, 133). In several patients suffering from pulmonary TB, direct administration of IFN-γ accelerated sputum smear conversion and improved chest radiograph (134, 135). Administration of IFN-γ also reduced *Mav* growth in murine macrophages (136), and improved clinical outcome (i.e. decreased respiratory symptoms and mortality) in several but not all *Mav*-infected individuals (137-139), suggesting potential of IFN-γ as HDT in both *Mtb* and *Mav* infections. *In vivo* administration of IL-12, a key cytokine that drives Th1 skewing, enhanced IFN-γ and TNF-α responses and significantly reduced bacterial burden in an acute mouse TB model (140). Similarly, restoring IL-24 expression in a mouse TB model enhanced Th1-responses and IFN-γ production, with concomitant improved survival and reduced bacterial loads (141). A large proportion of human *Mtb*-specific CD4 Th1-cells expresses CCR6 and co-produces IFN-γ/IL-17, often depicted as Th1* or Th1-17 cells, and being associated with LTBI suggest their importance in protection against active TB (142). However, IL-17 responses during TB need to be carefully regulated to prevent neutrophil-driven lung pathology, which is mediated by regulatory T-cells as well as so-called regulatory CD4 Th17-cells that co-produce IL-17 and IL-10 (143). In case of disbalanced Th17 responses with concomitant excessive neutrophil recruitment, RAGE receptor inhibition may be an interesting HDT. RAGE receptor is upregulated during active TB-disease and after ligation with S100A8/A9 mediates neutrophil recruitment (144). In a TB model, mice

deficient in S100A8/A9 had reduced bacterial loads, neutrophil influx and pathology compared to wildtype. Moreover, inhibition of the RAGE receptor using FPS-ZM1 improved outcome comparably as S100A8/A9-deficiency (144).

Th2-responses have been associated with active cavitary TB-disease or TB-treatment failure (129, 130), and administration of IL-4, a hallmark Th2-cytokine, impaired mycobacterial control by human macrophages and enhanced the proportion of regulatory T-cells *in vitro* (130). Blocking IL-4 completely alleviated these effects and improved bacterial control (130), suggesting Th skewing could be an interesting target for HDT.

Alternatively, administration of IL-2, which stimulates T-cell proliferation while inhibiting T-cell anergy, in patients infected with drug-resistant *Mtb* has been investigated in five RCTs and compared in a meta-analysis (145). While CD4 T-cell numbers increased and time to culture conversion improved, radiographic changes were not observed compared to standard chemotherapy (145). In mice infected with *Mav*, IL-2 therapy resulted in decreased bacterial burden (146), whereas mixed results were described in case reports (147, 148). The limited effect of IL-2 therapy may be due to immune suppression caused by expansion of regulatory T-cells and myeloid-derived suppressor cells (MDSC), both expressing elevated levels of the high affinity IL-2 receptor, as depletion of these suppressor cells improved outcome in a mouse TB model (149). Combining IL-2 therapy with mycobacterial phosphoantigen (E)-4-hydroxy-3-methyl-but-2-enyl pyrophosphate (HMBPP) in non-human primates induced significant expansion of Vg2Vd2 T-cells that migrated to the lungs, evoking a Th1-response that significantly reduced mycobacterial burden as well as lung pathology (150). Rather than systemic administration of cytokines, which frequently results in systemic side effects, ex vivo stimulation of autologous peripheral blood mononuclear cells (PBMCs) with a cocktail of IFN-γ, IL-2, IL-1α and anti-CD3 before reinfusion, yielded positive results with minimal side-effects in a case report with MDR-TB (151). This, however, requires further clinical investigation.

4. (Programmed) cell death

Several types of cell death can follow mycobacterial infection of macrophages: apoptosis, necrosis and ferroptosis (31). During apoptosis, bacteria remain encapsulated, which facilitates bacterial clearance; however, pathogenic mycobacteria have developed strategies to limit apoptosis (152). Activation of transcriptional regulator peroxisome proliferator-activated receptor gamma (PPARγ) by ManLAM, stimulating mannose receptors, upregulated (pro-host-cell survival) Mcl-1 and repressed (pro-apoptotic) Bax without Bak and improved host-cell survival (153, 154). In agreement with the PPARγ-dependent inhibition of host-cell apoptosis and concomitant anti-mycobacterial immunity, direct pharmacological inhibition of Mcl-1 resulted in reduced intracellular *Mtb* growth in human macrophages (154).

Besides inhibiting apoptosis, virulent *Mtb* stimulates host-cell necrosis, which allows infection to disseminate to neighboring cells (31). *Mtb* can induce necrosis via the virulence factor tuberculosis necrotizing toxin (TNT), which is secreted into the cytosol where its NAD^+ glycohydrolase activity depletes the host-cell from NAD^+ (155), leading to permeabilization of mitochondrial membranes, decreasing ATP-production and

activating necrosis. Nicotinamide-based HDT alleviated necrosis-induced host-cell cytotoxicity in *Mtb*-infected cells by replenishing NAD^+ (98). *Mtb* can furthermore induce necrosis mediated by mitochondrial membrane permeability transition via p38-MAPK phosphorylation, which can be inhibited by corticosteroids dexamethasone and doramapimod (156). In addition, corticosteroids dexamethasone and prednisolone, both well-known general immunosuppressants, have also been investigated as HDT during mycobacterial infections. With some reports of improved survival (157, 158), likely by limiting secretion of pro-inflammatory cytokines, meta-analysis failed to show a significant improvement in clinical outcome after corticosteroid therapy in patients with TB (159). Interestingly, while promoting pro-inflammatory cytokine levels of TNF-α by adenylate cyclase inhibitor (SQ22536) or a PKA inhibitor (H-89) has been shown to improve control of infection by stimulating mitochondrial ROS-production (160), excess TNF-α lead to membrane disruption and ATP-depletion via mitochondrial enzyme cyclophilin D, which together with lysosomal enzyme acid sphingomyelinase induced necrosis (161, 162). Alisporivir and desiparamine, two clinically approved drugs that inhibit cyclophilin D and acid sphingomyelinase, respectively, prevented TNF-α-induced necrosis without compromising TNF-α-induced ROS-dependent mycobacterial killing (162). Correspondingly, upregulation of cAMP levels by phosphodiesterase (PDE) inhibitors cilostazol and sildenafil decreased TNF-α levels, resulting in reduced immunopathology and fastened bacterial clearance in *Mtb*-infected mice (163, 164). Blocking TNF-α, which facilitates necrotizing granulomas during active TB, displayed promising results in preclinical animal models (165, 166). However, blocking TNF-α also leads to disease reactivation and concomitant dissemination in LTBI patients and in the absence of standard TB chemotherapy exacerbated disease severity (167-169), precluding clinical application of TNF-α inhibition as HDT in TB. The balance between TNF-α-mediated beneficial and detrimental effects on host control of TB and likely other mycobacterial infections including NTM is thus delicate. Taken together, these data indicate that *Mtb*-induced host-cell necrosis favors mycobacterial survival and this can be effectively counteracted by HDT, while the double-edge sword of modulating TNF-α levels currently prohibit clinical application.

Ferroptosis is a type of necrosis characterized by accumulation of free iron and toxic lipid peroxides (170). In *Mtb*-infected cells expression of glutathione peroxidase-4 (GPX4) is reduced, leading to failure of glutathione-dependent antioxidant defenses and cell death (171). Inhibiting ferroptosis by ferrostatin 1 reduced bacterial burden both *in vitro* in human macrophages and *in vivo* in *Mtb*-infected mice (170). Furthermore, ferroptosis could also be inhibited by increasing GPX4 levels with selenium, a protein involved in GPX4 catalysis (172), showing that targeting this host pathway is a potential HDT strategy.

5. Metabolism

5.1 Carbohydrate and lipids

Mtb has developed numerous strategies to modulate host metabolic pathways, which are broadly divided into glycolysis, oxidative phosphorylation (OXPHOS) and lipid metabolism. Glycolysis conditions an environment favoring *Mtb* growth, and inhibition of glycolysis using 2-deoxy-D-glucose (2-DG) reduced *Mtb* viability in one study, and as a result of ATP depletion induced macrophage apoptosis (173). An important enzyme during glycolysis, lactate dehydrogenase (LDH), which converts pyruvate into lactate,

is significantly upregulated during *Mtb* infection (174). Although the pathophysiology of LDH upregulation remains to be addressed, pharmacological inhibition of LDH using FX11 reduced bacterial load and development of necrotic lesions in granulomas in a murine TB model, suggesting a significant role of LDH in driving disease and a potential target for HDT (174). Interestingly, while ATP depletion can induce macrophage apoptosis (considered host protective), exogenous ATP activates macrophages via the $P2RX_7$/$P2X_7$ receptor and also directly inhibits growth of mycobacteria, including *Mtb* and *Mav*, due to chelation of iron (175, 176). ATP treatment has already been shown to synergize with standard *Mav* antibiotic treatment, making ATP an interesting adjunctive HDT-molecule to enhance chemotherapeutic efficacy against mycobacterial infections (176). In addition, an FDA-approved potentiator of $P2RX_7$/$P2X_7$, clemastine, enhanced mycobacterial killing in a zebrafish model (177). This may provide a potentially attractive avenue to explore synergistic effects between ATP and clemastine treatment in future studies.

Conversion of pyruvate into acetyl-coenzyme A (Ac-CoA) initiates the tricarboxylic acid (TCA) cycle which produces energy using OXPHOS. During *Mtb* infection, several enzymes important in the TCA cycle are downregulated and TCA cycle intermediates, such as citrate, are translocated from mitochondria into the cytosol. Typically, citrate is converted into itaconate which dampens tissue hyperinflammation by suppressing both ROS-production and production of pro-inflammatory cytokines such as IL-1β, IL-6 and IL-12 (173). In the cytosol, however, citrate is cleaved into Ac-CoA, which is either converted into arachidonic acid or into mevalonate and malonyl-CoA. This leads to synthesis of eicosanoids, cholesterol and free fatty acids, respectively, of which the latter two are stored intracellularly in lipid droplets (173). Hypercholesterolemia results in spontaneous formation of lipid droplets in macrophages. Further accumulation of intracellular lipid droplets is actively stimulated by *Mtb* (173, 178) and enhanced by both IL-6 and TNF-α signaling, while IL-17 and IFN-γ limit intracellular lipid accumulation (173). Lipid-loaded macrophages are impaired in killing intracellular mycobacteria (i.e. *Mtb*, *Mav*, and BCG) (179) and ultimately transform into foamy macrophages, which are associated with necrotic granulomas and tissue pathology (173). The impaired functionality of lipid-loaded macrophages involves mitochondrial dysfunction and could be restored using small molecule mitochondrial fusion promoter M1, which also restored macrophage bactericidal activity (179). In addition, ezetimibe, a cholesterol absorption inhibitor, prevented intracellular lipid accumulation and concomitantly reduced intracellular growth in *Mtb*-infected macrophages (178). The effects of standard antibiotic treatment improved and perhaps even synergized with ezetimibe treatment (178), and investigating the *in vivo* efficacy of ezetimibe as well as M1 could be promising.

Statins, currently clinically used to reduce cholesterol levels, could be interesting drugs to prevent lipid accumulation in macrophages. Comparing eight different statins, simvastatin, pravastatin and fluvastatin were most efficacious in enhancing mycobacterial killing without affecting cell viability *in vitro* (180). Mechanistically, while (simva)statin inhibits phagosomal acidification and degradation (180), cholesterol incorporation in (auto-)phagosomal membranes is prevented. The presence of cholesterol in phagosomal membranes facilitates prolonged survival of *Mtb* and *Mav* within host-cells due to blockage of phago-lysosome fusion by mechanisms not fully

understood (181-183). Preventing phagosomal escape ultimately enhances delivery of mycobacteria to (auto-)phagolysosomes and thereby bacterial degradation (184, 185). *In vivo* treatment with either pravastatin or simvastatin in a mouse TB model reduced mycobacterial loads both as a single therapy (180, 184) or combined with standard antibiotic treatment (180, 183).

5.2 Eicosanoids

Eicosanoids are lipid mediators involved in regulating inflammatory responses and are categorized into prostaglandins (PG), leukotrienes (LT), thromboxanes, lipoxins and hydroxy eicosatetraenoic acids, all of which are produced from arachidonic acid by a competing network of enzymes, including cyclooxygenases (COX) and lipoxygenases (186, 187). During *Mtb* infection, the expression of eicosanoids is significantly altered, with prostaglandin-E2 (PGE2) and leukotriene-B4 (LTB_4) mostly upregulated (186). Being an immune suppressor and immune stimulator, respectively, the balance between these eicosanoids is highly important in regulating immunity to clear the infection, without causing tissue pathology due to excessive inflammation. Important in this regulation are IL-1β- and type-I IFN-signaling. IL-1β signaling stimulates production of prostaglandin-E2, which is necessary to dampen the inflammation mediated by pro-inflammatory leukotrienes A_4 and B_4 (LTA_4 is the precursor of LTB_4) that are induced upon type-I IFN signaling. In severe TB, the PGE2/LTA_4 ratio is reduced, suggesting potential benefit of enhancing PGE2 signaling. Indeed, both increasing PGE2 levels using administration of exogenous PGE2 or reducing LTA_4/LTB_4 production with zileuton improved host survival, while reducing bacterial loads and necrotic lung pathology in *Mtb*-infected mice (188). Moreover, combinatory therapy of zileuton with PGE2 further restricted *Mtb* replication (189).

A single nucleotide polymorphism in the promotor of the gene encoding LTA_4-hydrolase (rs17525495), the enzyme that converts LTA_4 into LTB_4, has been shown to affect expression of LTA_4 hydrolase, with homozygous individuals having a high (T/T) or low (C/C) expression (187, 190). Both homozygous genotypes have poorer survival compared to heterozygous individuals, showing the delicateness of the immune balance during mycobacterial infection (187). Depending on the genotype, different treatment regimens will be required, as general immune suppression using dexamethasone favored outcome in T/T individuals, while being detrimental in C/C individuals (187, 190), suggesting the necessity of personalized HDT-based medicine targeting eicosanoid metabolism. Mice deficient in 5-lipoxygenase, an enzyme that stimulates production of LTA_4 and thus LTB_4 (thereby being a model for C/C individuals), were impaired in controlling mycobacterial infection due to absence of LTB_4. Treatment with celecoxib, a COX inhibitor that prevents PGE2 production and thereby stimulates LTB_4 production, or directly supplementing LTB_4, restored mycobacterial control (186). Furthermore, COX inhibitors ibuprofen and aspirin administered as single therapy or combined with conventional TB antibiotics were shown to limit bacterial burden in *Mtb*-infected mice (191-193), and low-dose aspirin treatment also reduced bacterial loads in a *Mm* zebrafish infection model (194). Aspirin treatment of TB or TB meningitis patients improved survival (195, 196), but may impair conventional treatment regimens by reducing efficacy of isoniazid (197), but not pyrazinamide (192). Both ibuprofen and aspirin are currently tested in clinical trials as adjunct therapy for treating (drug-resistant) TB (189).

6. Granuloma: formation, angiogenesis and hypoxia

One hallmark of TB is the extensive formation of granulomas. Granulomas are highly heterogenous and dynamic structures which differ significantly in the level of hypoxia and available nutrients. Granuloma formation is actively initiated by *Mtb* to stimulate matrix-metalloprotease 9 (MMP9) production. Granulomas are also induced during NTM infections, including *Mav* (198, 199) and *Mm* (200). During initial granuloma formation non-activated macrophages are recruited to the site of infection and serve as feeder cells for the granuloma (24, 201). In addition to MMP9, upregulation of several other MMPs has been observed in lung samples from individuals infected with *Mtb*, and other mycobacteria including *Mav*, which may suggest that similar mechanisms are involved (201-205). MMPs are enzymes that degrade and modulate extracellular matrix and are therefore key in the development of granulomas (203). Their expression and activity has multiple layers of regulation. Many MMPs require Zn^{2+} for their activation, potent MMPs require activation by other MMPs, and their activation is inhibited by tissue inhibitors of metalloproteinases (TIMPs). Expression of MMPs is stimulated by pro-inflammatory cytokines, including IFN-γ, TNF-α, IL-12, and IL-17 and because enhanced MMP-activity is associated with extensive tissue damage during TB (202), MMPs are promising targets for HDTs.

MMP1, a collagenase that degrades collagen in the extracellular matrix, is upregulated after TLR2-ligation and due to its high potency may drive granuloma formation during TB (206). In transgenic mice expressing human MMP1, *Mtb* infection promoted alveolar destruction and collagen breakdown in lung granulomas, identifying MMP1 as a therapeutic target to limit immunopathology (206). MMP7, which is highly expressed in the cavitary wall and hypoxic granulomas, stimulates epithelial proliferation and promotes activity of other MMPs. Inhibition of MMP7 and MMP1 using cipemastat, a drug originally registered to prevent lung fibrosis, surprisingly increased cavitation, immunopathology and mortality in mice (207), suggesting either a protective role of MMP1 or MMP7 during TB or off-target effects of the drug. The role of MMP8 is more controversial with high interindividual variation (202, 208, 209), which may relate to the presence of neutrophils in granulomas. MMP8 is more readily detectable in HIV-associated TB (209), suggesting that neutrophils are recruited preferentially in settings of impaired adaptive immunity. Mice deficient in MMP9 have less granuloma formation and reduced bacterial loads (210), suggesting a prominent role of MMP9 in driving disease pathology. Indeed, inhibition of MMP9 expression using morpholinos reduced granuloma formation and bacterial growth in a zebrafish *Mm*-model (24). In agreement with this concept, treatment with Sb-3ct, a specific MMP2 and MMP9 inhibitor, combined with frontline TB antibiotics potentiated bacterial clearance both *in vitro* and *in vivo* in a TB meningitis mouse model (211, 212). Blocking MMP9 using monoclonal antibody AB0046 did not affect bacterial burden, but the rate of relapse was reduced in a necrotic granuloma TB mouse model, by mechanisms not yet fully clarified (165). Using an *in vitro* model for extracellular matrix degradation, treatment with doxycycline, an FDA-approved antibiotic that non-selectively inhibits human MMPs, strongly abolished *Mtb*-induced matrix degradation (209). In addition, doxycycline reduced granuloma formation in a guinea pig model, likely resulting from abolishing *Mtb*-enhanced promotor activity of MMP1 and by directly inhibiting bacterial growth (213). Pan-MMP inhibitor marimastat (BB-2516), a collagen-peptidomimetic binding

the active Zn^{2+} site contained in many MMPs, reduced granuloma size and bacterial burden during *Mtb* infection in lung tissue models (202). Interestingly, treatment of *Mtb*-infected mice with a panel of MMP inhibitors, including marimastat, as solo therapy was not effective, while all 4 small molecules enhanced *in vivo* potency of frontline TB drugs isoniazide and rifampicin, likely by blocking MMP-mediated cleavage of collagen and by improving vascular integrity, resulting in enhanced delivery of isoniazide and rifampicin to the lungs. The finding that batimastat (a pan-MMP inhibitor), Sb-3ct (a MMP2 and MMP9 inhibitor) and MMP9 inhibitor-I yielded similar results, highlights the importance of MMP9 in driving these effects (204). Augmenting TIMP1 activity to inhibit activity of multiple MMPs may also be an interesting HDT target. To our knowledge, however, modulating the activity of TIMPs has not been investigated yet in the context of HDT.

Central hypoxia in granulomas may initially favor host immunity as low oxygen tension increases granulysin expression in T-cells and NK-cells, enhancing bacterial killing in an *in vitro* co-culture system of *Mtb*-specific T-cells and macrophages (214). However, due to poor vasculature within granulomas and hyperactive IFN-γ or possible superimposed IL-4/IL-13 released by activated T-cells, full blown central necrosis leads to cavity formation and concomitant bacterial dissemination within the host (201, 210, 214). Due to the hypoxic, acidic and nutrient-poor conditions in granulomas, mycobacterial dormancy is promoted (24), and while this effectively inhibits bacterial replication, eradication of mycobacteria is greatly hampered because most antibiotics only affect replicating and metabolically active bacteria. Furthermore, poor vascularization hampers drug delivery in granulomas, which is further impaired due to fibrosis and scarring of lung tissue caused by the disease (24). Trehalose dimycolate, a mycolic acid expressed on mycobacterial cell walls, directly induces vascular endothelial growth factor (VEGF) expression in host-cells to stimulate angiogenesis (215). Although angiogenesis could potentially increase host-cell viability, the net effect likely favors bacterial replication and dissemination. Blocking angiogenesis may therefore be an interesting HDT. Indeed, inhibition of VEGF using FDA-approved bevacizumab in *Mtb*-infected rabbits, reduced the total number of vessels but improved both structurally and functionally the remaining vessels, leading to enhanced drug targeting to granulomatous lesions and diminished hypoxia (216). Corroborating these findings, treatment of *Mm*-infected zebrafish with VEGF pathway inhibitors SU5416, a tyrosine kinase inhibitor, or pazopanib, a VEGF receptor inhibitor, reduced bacterial loads and dissemination. Both drugs also synergized with first-line antimycobacterial drugs rifampicin and metronidazole, a drug that targets hypoxic bacteria (217). Inhibiting vascular leakage rather than angiogenesis may be equally efficacious to limit nutrient supply to mycobacteria. During *Mm* infection, angiopoietin-2 (ANG2) is robustly induced in granulomatous lesions. ANG2 antagonizes ANG1, which promotes vessel stability while limiting angiogenesis and vascular leakage. Indeed, AKB-9785, a molecule that mimics functions of ANG1, reduced vascular leakage and bacterial burden in a *Mm* zebrafish infection model (218). Thus, inhibition of angiogenesis is an interesting target for HDT to enhance drug delivery to the site of infection and combined with other therapies is likely to be even more potent.

7. Personalized and combinatorial HDT

Although HDT could be considered as stand-alone therapy, e.g. in patients suffering from

total drug-resistant TB, HDT is primarily envisaged as adjunct therapy in combination with classical antibiotics. HDT might be co-administered for a limited duration at the initiation of the standard of care regimens to shorten treatment length and reduce dosage of antibiotics to minimize side-effects, or towards the end of treatment to boost host immunity to prevent potential relapse. Consequently, investigating the interactions between HDT and conventional chemotherapy is pivotal, but has only been reported for a limited number of HDTs. Furthermore, in case of undesired interactions between TB drugs and drugs for TB-comorbidities (e.g. between rifampicin and anti-HIV therapy or anti-diabetic drugs) (219), HDT might be used to shorten current treatment regimens or possibly partially replace components of the conventional chemotherapy cocktail. In line with this, interactions between HDT and drugs used to treat TB-comorbidities should also be investigated thoroughly.

Rather than targeting one specific aspect of the inflammatory response during mycobacterial infections, we hypothesize that correcting the overall immunological disbalance likely is most promising. Type-I IFN and IL-1β signaling, regulating levels of anti-inflammatory prostaglandins and pro-inflammatory leukotrienes, respectively, play an important role in regulating the immune balance during mycobacterial infections (188). At the time of writing, multiple randomized controlled trials investigate targeting of (one of) these pathways by HDTs. As some TB-patients suffer from overactive type-I IFN/leukotriene signaling while others are characterized by overactive IL-1/prostaglandin activity, we postulate that in this context personalized HDT would be safest and most efficacious. However, this will increase therapeutic costs, which could make such therapy stratifications less attractive and feasible in lower resourced settings. To be able to predict whether patients would benefit from a certain HDT, biomarkers monitoring the (immunological) status of patients may need to be identified and developed. This, however, may not be required for all HDTs as some HDT may improve anti-mycobacterial immunity in all patients. As mycobacteria modulate host immunity via many different pathways, a multi-targeted approach could be necessary to fully counteract mycobacteria-mediated host modulation. To our knowledge, however, only two combinations of HDT treatments have been published; combining vitamin-D with PBA did not mediate additive effects compared to solo-therapy (50-52), likely because both compounds target the same pathway, while in another *in vitro* study combining protein-kinase A/B inhibitors H-89 or 97i with HDAC inhibitors revealed additive effects *in vitro* in reducing bacterial load in primary human macrophages (114).

Modulating (auto-)phagosome maturation using receptor tyrosine kinase inhibitors including imatinib (24), AZD0530 (27), and multiple repurposed drugs recently identified in our own group (28) has been shown to improve mycobacterial clearance by human macrophages *in vitro*. Importantly, releasing the mycobacteria-mediated arrest in (auto-)phagosome maturation likely benefits both patients with active disease as well as individuals with latent infection. Above, we have reviewed multiple HDT candidates that enhance autophagy-mediated bacterial clearance. Which of these will be most efficacious against mycobacteria should ideally be determined in head-to-head comparisons. Metformin, being the most frequently investigated, has already been shown to reduce TB recurrence and bacterial loads in patients (74-76), and in addition to its effects on autophagy, also enhances mitochondrial membrane polarization (220), which could further enhance its efficacy.

As discussed above, host-cell death pathways are actively exploited by mycobacteria to promote their survival and dissemination and have been shown to be a potential target for HDT in multiple *in vitro* and animal studies. Active clinical modulation of (programmed) cell death in patients, however, could lead to significant adverse effects given the complex time- and context-dependency of this mechanism during mycobacterial infection.

Targeting metabolic pathways has been shown to be feasible and represents an attractive target for HDT. While most metabolic pathways are also necessary for host-cell energy production, intracellular lipid accumulation in lipid droplets seems to mainly benefit the intracellular survival of mycobacteria. Preventing or reducing lipid droplet formation in macrophages and concomitant impaired immunity can be mediated by 1) limiting oxidative phosphorylation by e.g. stimulating polarization of macrophages towards pro-inflammatory M1-macrophages (173), 2) improving/maintaining mitochondrial membrane potential using small molecule M1 (179) or NAD (155) and/or 3) blocking cellular cholesterol uptake using e.g. ezetimibe (178), which also inhibits phagosomal escape by mycobacteria. Targeting metabolism with HDT may also help correcting the balance between prostaglandins and thromboxanes, as lipid droplets and cytosolic TCA intermediates are the most important sources of eicosanoids.

Irrespective of what causes defective mycobacterial clearance, improving drug delivery to the site of infection likely benefits all TB-patients. Angiogenesis in granulomas is significantly impaired and further enhances hypoxia and nutrient-limitation. Targeting angiogenesis during TB by 1) inhibiting VEGF (bevacizumab) (216), 2) inhibiting VEGF-mediated signaling (SU5416 or pazopanib) (217)) or 3) antagonizing pro-angiogenesis growth factor ANG2 (AKB-9785) (218), have all been shown to enhance both drug delivery as well as oxygenation within granulomas in animal models of TB, and may be promising HDTs in combination with other therapies. Despite being most frequently investigated in combination with antibiotics, efflux pump inhibitors could also improve drug delivery of HDTs. To our knowledge, however, this has not been investigated so far but verapamil, known to enhance the efficacy of rifampicin and bedaquiline against different mycobacterial infections, both *in vitro* and in mice (221-223), and also chloroquine (224) and piperine (225) are interesting molecules for combinatorial HDT.

Given their central and important role in orchestrating a functional antimycobacterial immune response, restoring (CD4 Th1/17) T-cell immunity has been pursued in many investigations. In addition to enhancing activation of antigen presenting cells, HDTs that promote phagosomal bacterial degradation (i.e. stimulating autophagy, enhancing phagosome maturation and promoting (auto-)phago-lysosome fusion) are all expected to enhance presentation of bacterial-derived peptides and thereby improve adaptive immunity. Modulating T-cell responses to restore immunity can be mediated by vaccination or T-cell cytokine therapies. Administration of IL-12 (140) or IL-24 (141), or blocking Th2 cytokine IL-4 (130) promotes Th1 responses with lasting IFN-γ production that may be preferred over IFN-γ administration. Which of these strategies is (most) efficacious and which patients benefit most from this therapy remains to be addressed.

While most of the evidence available for host-pathogen interactions and HDT are from TB studies, the limited number of NTM experimental models investigating host modulation

and/or HDT emphasizes the need and urgency to understand NTM pathogenesis as well as identify potentially relevant host targets. Together, these studies will help assess the safety and efficacy of HDT, paving the way for the introduction of HDT against a wide range of mycobacteria.

Search strategy and selection criteria

We searched PubMed (MEDLINE) for all relevant studies published from Jan 1, 2000 until Oct 1, 2020. The medical subject headings used were "host directed", "HDT", "adjunctive", "immunotherapeutic" or "immunomodulation" combined with "mycobacterium", "mycobacteria", "tuberculosis", "nontuberculous" or "NTM". All relevant abstracts were screened independently by two researchers. The final reference list was generated based on relevance to the topics covered in this review. Only papers published in English were included.

Data availability statement

Data sharing not applicable to this article as no datasets were generated or analysed during the current study.

Acknowledgments

This work was supported by grants from the Netherlands Organisation for Scientific Research (NWO-TTW) within the Novel Antibacterial Compounds and Therapies Antagonising Resistance (NACTAR) program (grant N° 16444), European Union's Horizon 2020 research and innovation programme (SMA-TB grant N° 847762) and the Innovative Medicines Initiative 2 Joint Undertaking (IMI2 JU) under the RespiriNTM (grant N° 853932) and RespiriTB (grant N° 853903) projects within the IMI AntiMicrobial Resistance (AMR) Accelerator program. The funders had no role in study design, data collection and analysis, decision to publish, or preparation of the manuscript.

Conflict of interest

All authors declare no competing or conflicting interests.

References

1. World Health Organization. Tuberculosis (https://www.who.int/news-room/fact-sheets/detail/tuberculosis) https://www.who.int/news-room/fact-sheets/detail/tuberculosis2020 [
2. Cilloni L, Fu H, Vesga JF, Dowdy D, Pretorius C, Ahmedov S, et al. The potential impact of the COVID-19 pandemic on the tuberculosis epidemic a modelling analysis. EClinicalMedicine. 2020;28:100603.
3. Wu ML, Aziz DB, Dartois V, Dick T. NTM drug discovery: status, gaps and the way forward. Drug Discov Today. 2018;23(8):1502-19.
4. Kawai T, Akira S. TLR signaling. Cell Death Differ. 2006;13(5):816-25.
5. Gomes MS, Florido M, Cordeiro JV, Teixeira CM, Takeuchi O, Akira S, et al. Limited role of the Toll-like receptor-2 in resistance to Mycobacterium avium. Immunology. 2004;111(2):179-85.
6. Drennan MB, Nicolle D, Quesniaux VJ, Jacobs M, Allie N, Mpagi J, et al. Toll-like receptor 2-deficient mice succumb to Mycobacterium tuberculosis infection. Am J Pathol. 2004;164(1):49-57.
7. Orme IM, Ordway DJ. Host response to nontuberculous mycobacterial infections of current clinical importance. Infect Immun. 2014;82(9):3516-22.
8. Bhatnagar S, Schorey JS. Elevated mitogen-activated protein kinase signalling and increased macrophage activation in cells infected with a glycopeptidolipid-deficient Mycobacterium avium. Cell Microbiol. 2006;8(1):85-96.
9. Rhoades ER, Archambault AS, Greendyke R, Hsu FF, Streeter C, Byrd TF. Mycobacterium abscessus Glycopeptidolipids mask underlying cell wall phosphatidyl-myo-inositol mannosides blocking induction of human macrophage TNF-alpha by preventing interaction with TLR2. J Immunol. 2009;183(3):1997-

2007.
10. Rahman A, Sobia P, Gupta N, Kaer LV, Das G. Mycobacterium tuberculosis subverts the TLR-2-MyD88 pathway to facilitate its translocation into the cytosol. PLoS One. 2014;9(1):e86886.
11. Gilleron M, Nigou J, Nicolle D, Quesniaux V, Puzo G. The acylation state of mycobacterial lipomannans modulates innate immunity response through toll-like receptor 2. Chem Biol. 2006;13(1):39-47.
12. Khan N, Pahari S, Vidyarthi A, Aqdas M, Agrewala JN. Stimulation through CD40 and TLR-4 Is an Effective Host Directed Therapy against Mycobacterium tuberculosis. Front Immunol. 2016;7:386.
13. Khan N, Pahari S, Vidyarthi A, Aqdas M, Agrewala JN. NOD-2 and TLR-4 Signaling Reinforces the Efficacy of Dendritic Cells and Reduces the Dose of TB Drugs against Mycobacterium tuberculosis. J Innate Immun. 2016;8(3):228-42.
14. Gowthaman U, Singh V, Zeng W, Jain S, Siddiqui KF, Chodisetti SB, et al. Promiscuous peptide of 16 kDa antigen linked to Pam2Cys protects against Mycobacterium tuberculosis by evoking enduring memory T-cell response. J Infect Dis. 2011;204(9):1328-38.
15. Chodisetti SB, Gowthaman U, Rai PK, Vidyarthi A, Khan N, Agrewala JN. Triggering through Toll-like receptor 2 limits chronically stimulated T-helper type 1 cells from undergoing exhaustion. J Infect Dis. 2015;211(3):486-96.
16. Pahari S, Negi S, Aqdas M, Arnett E, Schlesinger LS, Agrewala JN. Induction of autophagy through CLEC4E in combination with TLR4: an innovative strategy to restrict the survival of Mycobacterium tuberculosis. Autophagy. 2020;16(6):1021-43.
17. Harding CV, Boom WH. Regulation of antigen presentation by Mycobacterium tuberculosis: a role for Toll-like receptors. Nat Rev Microbiol. 2010;8(4):296-307.
18. Kim JK, Yuk JM, Kim SY, Kim TS, Jin HS, Yang CS, et al. MicroRNA-125a Inhibits Autophagy Activation and Antimicrobial Responses during Mycobacterial Infection. J Immunol. 2015;194(11):5355-65.
19. Gu X, Gao Y, Mu DG, Fu EQ. MiR-23a-5p modulates mycobacterial survival and autophagy during mycobacterium tuberculosis infection through TLR2/MyD88/NF-kappaB pathway by targeting TLR2. Exp Cell Res. 2017;354(2):71-7.
20. Jefferies KC, Cipriano DJ, Forgac M. Function, structure and regulation of the vacuolar (H+)-ATPases. Arch Biochem Biophys. 2008;476(1):33-42.
21. Lawrence RE, Zoncu R. The lysosome as a cellular centre for signalling, metabolism and quality control. Nat Cell Biol. 2019;21(2):133-42.
22. Ankley L, Thomas S, Olive AJ. Fighting Persistence: How Chronic Infections with Mycobacterium tuberculosis Evade T Cell-Mediated Clearance and New Strategies To Defeat Them. Infect Immun. 2020;88(7): e00916-19.
23. Wong D, Bach H, Sun J, Hmama Z, Av-Gay Y. Mycobacterium tuberculosis protein tyrosine phosphatase (PtpA) excludes host vacuolar-H+-ATPase to inhibit phagosome acidification. Proc Natl Acad Sci U S A. 2011;108(48):19371-6.
24. Hawn TR, Matheson AI, Maley SN, Vandal O. Host-directed therapeutics for tuberculosis: can we harness the host? Microbiol Mol Biol Rev. 2013;77(4):608-27.
25. Napier RJ, Rafi W, Cheruvu M, Powell KR, Zaunbrecher MA, Bornmann W, et al. Imatinib-sensitive tyrosine kinases regulate mycobacterial pathogenesis and represent therapeutic targets against tuberculosis. Cell Host Microbe. 2011;10(5):475-85.
26. Bruns H, Stegelmann F, Fabri M, Dohner K, van Zandbergen G, Wagner M, et al. Abelson tyrosine kinase controls phagosomal acidification required for killing of Mycobacterium tuberculosis in human macrophages. J Immunol. 2012;189(8):4069-78.
27. Chandra P, Rajmani RS, Verma G, Bhavesh NS, Kumar D, Stallings CL. Targeting Drug-Sensitive and -Resistant Strains of Mycobacterium tuberculosis by Inhibition of Src Family Kinases Lowers Disease Burden and Pathology. mSphere. 2016;1(2):e00043-15.
28. Korbee CJ, Heemskerk MT, Kocev D, van Strijen E, Rabiee O, Franken K, et al. Combined chemical genetics and data-driven bioinformatics approach identifies receptor tyrosine kinase inhibitors as host-directed antimicrobials. Nat Commun. 2018;9(1):358.
29. Buter J, Cheng TY, Ghanem M, Grootemaat AE, Raman S, Feng X, et al. Mycobacterium tuberculosis releases an antacid that remodels phagosomes. Nat Chem Biol. 2019;15(9):889-99.
30. Houben D, Demangel C, van Ingen J, Perez J, Baldeon L, Abdallah AM, et al. ESX-1-mediated translocation to the cytosol controls virulence of mycobacteria. Cell Microbiol. 2012;14(8):1287-98.
31. Chai Q, Wang L, Liu CH, Ge B. New insights into the evasion of host innate immunity by Mycobacterium tuberculosis. Cell Mol Immunol. 2020;17(9):901-13.
32. Ranjbar S, Haridas V, Nambu A, Jasenosky LD, Sadhukhan S, Ebert TS, et al. Cytoplasmic RNA Sensor Pathways and Nitazoxanide Broadly Inhibit Intracellular Mycobacterium tuberculosis Growth. iScience. 2019;22:299-313.

33. Walsh KF, McAulay K, Lee MH, Vilbrun SC, Mathurin L, Jean Francois D, et al. Early Bactericidal Activity Trial of Nitazoxanide for Pulmonary Tuberculosis. Antimicrob Agents Chemother. 2020;64(5):e01956-19.
34. Levine B, Mizushima N, Virgin HW. Autophagy in immunity and inflammation. Nature. 2011;469(7330):323-35.
35. Renna M, Schaffner C, Brown K, Shang SB, Tamayo MH, Hegyi K, et al. Azithromycin blocks autophagy and may predispose cystic fibrosis patients to mycobacterial infection. Journal of Clinical Investigation. 2011;121(9):3554-63.
36. Paik S, Kim JK, Chung C, Jo EK. Autophagy: A new strategy for host-directed therapy of tuberculosis. Virulence. 2019;10(1):448-59.
37. Yuk JM, Shin DM, Lee HM, Yang CS, Jin HS, Kim KK, et al. Vitamin D3 Induces Autophagy in Human Monocytes/Macrophages via Cathelicidin. Cell Host & Microbe. 2009;6(3):231-43.
38. Liu PT, Stenger S, Li HY, Wenzel L, Tan BH, Krutzik SR, et al. Toll-like receptor triggering of a vitamin D-mediated human antimicrobial response. Science. 2006;311(5768):1770-3.
39. Liu PT, Stenger S, Tang DH, Modlin RL. Cutting edge: Vitamin D-mediated human antimicrobial activity against Mycobacterium tuberculosis is dependent on the induction of cathelicidin. Journal of Immunology. 2007;179(4):2060-3.
40. Rockett KA, Brookes R, Udalova I, Vidal V, Hill AV, Kwiatkowski D. 1,25-Dihydroxyvitamin D3 induces nitric oxide synthase and suppresses growth of Mycobacterium tuberculosis in a human macrophage-like cell line. Infect Immun. 1998;66(11):5314-21.
41. Coussens A, Timms PM, Boucher BJ, Venton TR, Ashcroft AT, Skolimowska KH, et al. 1alpha,25-dihydroxyvitamin D3 inhibits matrix metalloproteinases induced by Mycobacterium tuberculosis infection. Immunology. 2009;127(4):539-48.
42. Jolliffe DA, Ganmaa D, Wejse C, Raqib R, Haq MA, Salahuddin N, et al. Adjunctive vitamin D in tuberculosis treatment: meta-analysis of individual participant data. Eur Respir J. 2019;53(3):1802003.
43. Tang XZ, Huang T, Ma Y, Fu XY, Qian K, Yi YL, et al. [Meta-analysis of efficacy and safety of vitamin D supplementation in the treatment of pulmonary tuberculosis]. Zhonghua Yi Xue Za Zhi. 2020;100(32):2525-31.
44. Wu HX, Xiong XF, Zhu M, Wei J, Zhuo KQ, Cheng DY. Effects of vitamin D supplementation on the outcomes of patients with pulmonary tuberculosis: a systematic review and meta-analysis. Bmc Pulm Med. 2018;18(1):108.
45. Tukvadze N, Sanikidze E, Kipiani M, Hebbar G, Easley KA, Shenvi N, et al. High-dose vitamin D3 in adults with pulmonary tuberculosis: a double-blind randomized controlled trial. Am J Clin Nutr. 2015;102(5):1059-69.
46. Ganmaa D, Munkhsul B, Bromage S, Buyankhishig B, Martineau AR. High-Dose Vitamin D3 during Intensive Phase Treatment of Pulmonary Tuberculosis in Mongolia: A Double-Blind Randomised Controlled Trial. Thorax. 2016;71:A67-A8.
47. Huang SJ, Wang XH, Liu ZD, Cao WL, Han Y, Ma AG, et al. Vitamin D deficiency and the risk of tuberculosis: a meta-analysis. Drug Des Dev Ther. 2017;11:91-102.
48. Coussens AK, Wilkinson RJ, Martineau AR. Phenylbutyrate Is Bacteriostatic against Mycobacterium tuberculosis and Regulates the Macrophage Response to Infection, Synergistically with 25-Hydroxy-Vitamin D3. PLoS Pathog. 2015;11(7):e1005007.
49. Rekha RS, Muvva SSVJR, Wan M, Raqib R, Bergman P, Brighenti S, et al. Phenylbutyrate induces LL-37-dependent autophagy and intracellular killing of Mycobacterium tuberculosis in human macrophages. Autophagy. 2015;11(9):1688-99.
50. Mily A, Rekha RS, Kamal SMM, Akhtar E, Sarker P, Rahim Z, et al. Oral intake of phenylbutyrate with or without vitamin D-3 upregulates the cathelicidin LL-37 in human macrophages: a dose finding study for treatment of tuberculosis. Bmc Pulm Med. 2013;13:23.
51. Bekele A, Gebreselassie N, Ashenafi S, Kassa E, Aseffa G, Amogne W, et al. Daily adjunctive therapy with vitamin D3 and phenylbutyrate supports clinical recovery from pulmonary tuberculosis: a randomized controlled trial in Ethiopia. Journal of Internal Medicine. 2018;284(3):292-306.
52. Mily A, Rekha RS, Kamal SM, Arifuzzaman AS, Rahim Z, Khan L, et al. Significant Effects of Oral Phenylbutyrate and Vitamin D3 Adjunctive Therapy in Pulmonary Tuberculosis: A Randomized Controlled Trial. PLoS One. 2015;10(9):e0138340.
53. Tenforde MW, Yadav A, Dowdy DW, Gupte N, Shivakoti R, Yang WT, et al. Vitamin A and D Deficiencies Associated With Incident Tuberculosis in HIV-Infected Patients Initiating Antiretroviral Therapy in Multinational Case-Cohort Study. Jaids-J Acq Imm Def. 2017;75(3):E71-E9.
54. Coleman MM, Basdeo SA, Coleman AM, Cheallaigh CN, Peral de Castro C, McLaughlin AM, et al. All-trans Retinoic Acid Augments Autophagy during Intracellular Bacterial Infection. Am J Respir Cell

Mol Biol. 2018;59(5):548-56.
55. Chen QY, Mosovsky KL, Ross AC. Retinoic acid and alpha-galactosylceramide regulate the expression of costimulatory receptors and transcription factors responsible for B cell activation and differentiation. Immunobiology. 2013;218(12):1477-87.
56. Sada-Ovalle I, Skold M, Tian T, Besra GS, Behar SM. alpha-Galactosylceramide as a Therapeutic Agent for Pulmonary Mycobacterium tuberculosis Infection. Am J Resp Crit Care. 2010;182(6):841-7.
57. Mourik BC, Leenen PJ, de Knegt GJ, Huizinga R, van der Eerden BC, Wang J, et al. Immunotherapy Added to Antibiotic Treatment Reduces Relapse of Disease in a Mouse Model of Tuberculosis. Am J Respir Cell Mol Biol. 2017;56(2):233-41.
58. Karyadi E, West CE, Schultink W, Nelwan RHH, Gross R, Amin Z, et al. A double-blind, placebo-controlled study of vitamin A and zinc supplementation in persons with tuberculosis in Indonesia: effects on clinical response and nutritional status. Am J Clin Nutr. 2002;75(4):720-7.
59. Visser ME, Grewal HM, Swart EC, Dhansay MA, Walzl G, Swanevelder S, et al. The effect of vitamin A and zinc supplementation on treatment outcomes in pulmonary tuberculosis: a randomized controlled trial. Am J Clin Nutr. 2011;93(1):93-100.
60. Wang J, Xiong K, Wang Q, Zhao S, Liu Y, Ma A. Adjunctive vitamin A and D during pulmonary tuberculosis treatment: a randomized controlled trial with a 2 × 2 factorial design. Food & Function. 2020;11(5):4672-81.
61. Lawson L, Thacher TD, Yassin MA, Onuoha NA, Usman A, Emenyonu NE, et al. Randomized controlled trial of zinc and vitamin A as co-adjuvants for the treatment of pulmonary tuberculosis. Trop Med Int Health. 2010;15(12):1481-90.
62. van der Vaart M, Korbee CJ, Lamers GE, Tengeler AC, Hosseini R, Haks MC, et al. The DNA damage-regulated autophagy modulator DRAM1 links mycobacterial recognition via TLR-MYD88 to autophagic defense. Cell Host Microbe. 2014;15(6):753-67.
63. Zhang R, Varela M, Forn-Cuni G, Torraca V, van der Vaart M, Meijer AH. Deficiency in the autophagy modulator Dram1 exacerbates pyroptotic cell death of Mycobacteria-infected macrophages. Cell Death Dis. 2020;11(4):277.
64. Racioppi L, Means AR. Calcium/Calmodulin-dependent Protein Kinase Kinase 2: Roles in Signaling and Pathophysiology. Journal of Biological Chemistry. 2012;287(38):31658-65.
65. Liu F, Chen J, Wang P, Li H, Zhou Y, Liu H, et al. MicroRNA-27a controls the intracellular survival of Mycobacterium tuberculosis by regulating calcium-associated autophagy. Nat Commun. 2018;9(1):4295.
66. Singh P, Subbian S. Harnessing the mTOR Pathway for Tuberculosis Treatment. Front Microbiol. 2018;9:70.
67. Ashley D, Hernandez J, Cao R, To K, Yegiazaryan A, Abrahem R, et al. Antimycobacterial Effects of Everolimus in a Human Granuloma Model. J Clin Med. 2020;9(7):2043.
68. Hu Y, Wen Z, Liu S, Cai Y, Guo J, Xu Y, et al. Ibrutinib suppresses intracellular mycobacterium tuberculosis growth by inducing macrophage autophagy. J Infect. 2020;80(6):e19-e26.
69. Cheng CY, Gutierrez NM, Marzuki MB, Lu XH, Foreman TW, Paleja B, et al. Host sirtuin 1 regulates mycobacterial immunopathogenesis and represents a therapeutic target against tuberculosis. Sci Immunol. 2017;2(9):eaaj1789.
70. Singhal A, Jie L, Kumar P, Hong GS, Leow MKS, Paleja B, et al. Metformin as adjunct antituberculosis therapy. Sci Transl Med. 2014;6(263):263ra159.
71. Wallis RS, Hafner R. Advancing host-directed therapy for tuberculosis. Nat Rev Immunol. 2015;15(4):255-63.
72. Russell SL, Lamprecht DA, Mandizvo T, Jones TT, Naidoo V, Addicott KW, et al. Compromised Metabolic Reprogramming Is an Early Indicator of CD8(+) T Cell Dysfunction during Chronic Mycobacterium tuberculosis Infection. Cell Reports. 2019;29(11):3564-79.
73. Lachmandas E, Eckold C, Bohme J, Koeken V, Marzuki MB, Blok B, et al. Metformin Alters Human Host Responses to Mycobacterium tuberculosis in Healthy Subjects. J Infect Dis. 2019;220(1):139-50.
74. Degner NR, Wang JY, Golub JE, Karakousis PC. Metformin Use Reverses the Increased Mortality Associated With Diabetes Mellitus During Tuberculosis Treatment. Clin Infect Dis. 2018;66(2):198-205.
75. Lee MC, Chiang CY, Lee CH, Ho CM, Chang CH, Wang JY, et al. Metformin use is associated with a low risk of tuberculosis among newly diagnosed diabetes mellitus patients with normal renal function: A nationwide cohort study with validated diagnostic criteria. PLoS One. 2018;13(10):e0205807.
76. Lee YJ, Han SK, Park JH, Lee JK, Kim DK, Chung HS, et al. The effect of metformin on culture conversion in tuberculosis patients with diabetes mellitus. Korean J Intern Med. 2018;33(5):933-40.
77. Sogi KM, Lien KA, Johnson JR, Krogan NJ, Stanley SA. The Tyrosine Kinase Inhibitor Gefitinib

Restricts Mycobacterium tuberculosis Growth through Increased Lysosomal Biogenesis and Modulation of Cytokine Signaling. ACS Infect Dis. 2017;3(8):564-74.
78. Ouyang Q, Zhang K, Lin D, Feng CG, Cai Y, Chen X. Bazedoxifene Suppresses Intracellular Mycobacterium tuberculosis Growth by Enhancing Autophagy. mSphere. 2020;5(2):e00124-20.
79. Juarez E, Carranza C, Sanchez G, Gonzalez M, Chavez J, Sarabia C, et al. Loperamide Restricts Intracellular Growth of Mycobacterium tuberculosis in Lung Macrophages. Am J Respir Cell Mol Biol. 2016;55(6):837-47.
80. Saini NK, Baena A, Ng TW, Venkataswamy MM, Kennedy SC, Kunnath-Velayudhan S, et al. Suppression of autophagy and antigen presentation by Mycobacterium tuberculosis PE_PGRS47. Nat Microbiol. 2016;1(9):16133.
81. Chandra P, Ghanwat S, Matta SK, Yadav SS, Mehta M, Siddiqui Z, et al. Mycobacterium tuberculosis Inhibits RAB7 Recruitment to Selectively Modulate Autophagy Flux in Macrophages. Sci Rep. 2015;5:16320.
82. Shui W, Petzold CJ, Redding A, Liu J, Pitcher A, Sheu L, et al. Organelle membrane proteomics reveals differential influence of mycobacterial lipoglycans on macrophage phagosome maturation and autophagosome accumulation. J Proteome Res. 2011;10(1):339-48.
83. Giraud-Gatineau A, Coya JM, Maure A, Biton A, Thomson M, Bernard EM, et al. The antibiotic bedaquiline activates host macrophage innate immune resistance to bacterial infection. eLife. 2020;9:e55692.
84. Bryk R, Mundhra S, Jiang X, Wood M, Pfau D, Weber E, et al. Potentiation of rifampin activity in a mouse model of tuberculosis by activation of host transcription factor EB. PLoS Pathog. 2020;16(6):e1008567.
85. Francisco-Cruz A, Mata-Espinosa D, Estrada-Parra S, Xing Z, Hernandez-Pando R. Immunotherapeutic effects of recombinant adenovirus encoding granulocyte-macrophage colony-stimulating factor in experimental pulmonary tuberculosis. Clin Exp Immunol. 2013;171(3):283-97.
86. Pasula R, Azad AK, Gardner JC, Schlesinger LS, McCormack FX. Keratinocyte growth factor administration attenuates murine pulmonary mycobacterium tuberculosis infection through granulocyte-macrophage colony-stimulating factor (GM-CSF)-dependent macrophage activation and phagolysosome fusion. J Biol Chem. 2015;290(11):7151-9.
87. Benmerzoug S, Marinho FV, Rose S, Mackowiak C, Gosset D, Sedda D, et al. GM-CSF targeted immunomodulation affects host response to M. tuberculosis infection. Scientific Reports. 2018;8(1):8652.
88. Hariadi NI, Blackwood RA. Disseminated Mycobacterium Avium Complex in an Adolescent with Perinatally-Acquired HIV Infection. Infect Dis Rep. 2017;9(2):6884.
89. Nannini EC, Keating M, Binstock P, Samonis G, Kontoyiannis DP. Successful treatment of refractory disseminated Mycobacterium avium complex infection with the addition of linezolid and mefloquine. J Infect. 2002;44(3):201-3.
90. de Silva TI, Cope A, Goepel J, Greig JM. The use of adjuvant granulocyte-macrophage colony-stimulating factor in HIV-related disseminated atypical mycobacterial infection. J Infect. 2007;54(4):e207-10.
91. Kedzierska K, Mak J, Mijch A, Cooke I, Rainbird M, Roberts S, et al. Granulocyte-macrophage colony-stimulating factor augments phagocytosis of Mycobacterium avium complex by human immunodeficiency virus type 1-infected monocytes/macrophages *in vitro* and *in vivo*. J Infect Dis. 2000;181(1):390-4.
92. Nathan C. Specificity of a third kind: reactive oxygen and nitrogen intermediates in cell signaling. J Clin Invest. 2003;111(6):769-78.
93. Bogdan C, Rollinghoff M, Diefenbach A. The role of nitric oxide in innate immunity. Immunol Rev. 2000;173:17-26.
94. Awuh JA, Flo TH. Molecular basis of mycobacterial survival in macrophages. Cell Mol Life Sci. 2017;74(9):1625-48.
95. Fremond CM, Yeremeev V, Nicolle DM, Jacobs M, Quesniaux VF, Ryffel B. Fatal Mycobacterium tuberculosis infection despite adaptive immune response in the absence of MyD88. J Clin Invest. 2004;114(12):1790-9.
96. Yang Q, Liao M, Wang W, Zhang M, Chen Q, Guo J, et al. CD157 Confers Host Resistance to Mycobacterium tuberculosis via TLR2-CD157-PKCzeta-Induced Reactive Oxygen Species Production. mBio. 2019;10(4):e01949-19.
97. Zhang Y, Su SS, Zhao S, Yang Z, Zhong CQ, Chen X, et al. RIP1 autophosphorylation is promoted by mitochondrial ROS and is essential for RIP3 recruitment into necrosome. Nat Commun. 2017;8:14329.
98. Pajuelo D, Gonzalez-Juarbe N, Niederweis M. NAD hydrolysis by the tuberculosis necrotizing toxin induces lethal oxidative stress in macrophages. Cell Microbiol. 2020;22(1):e13115.

99. Palanisamy GS, Kirk NM, Ackart DF, Shanley CA, Orme IM, Basaraba RJ. Evidence for oxidative stress and defective antioxidant response in guinea pigs with tuberculosis. PLoS One. 2011;6(10):e26254.
100. Safe IP, Lacerda MVG, Printes VS, Praia Marins AF, Rebelo Rabelo AL, Costa AA, et al. Safety and efficacy of N-acetylcysteine in hospitalized patients with HIV-associated tuberculosis: An open-label, randomized, phase II trial (RIPENACTB Study). PLoS One. 2020;15(6):e0235381.
101. Yang CS, Shin DM, Kim KH, Lee ZW, Lee CH, Park SG, et al. NADPH oxidase 2 interaction with TLR2 is required for efficient innate immune responses to mycobacteria via cathelicidin expression. J Immunol. 2009;182(6):3696-705.
102. Chan ED, Chan J, Schluger NW. What is the role of nitric oxide in murine and human host defense against tuberculosis? Current knowledge. Am J Resp Cell Mol. 2001;25(5):606-12.
103. Pearl JE, Torrado E, Tighe M, Fountain JJ, Solache A, Strutt T, et al. Nitric oxide inhibits the accumulation of CD4+CD44hiTbet+CD69lo T cells in mycobacterial infection. Eur J Immunol. 2012;42(12):3267-79.
104. Yang CS, Yuk JM, Jo EK. The role of nitric oxide in mycobacterial infections. Immune Netw. 2009;9(2):46-52.
105. Wu K, Koo J, Jiang X, Chen R, Cohen SN, Nathan C. Improved control of tuberculosis and activation of macrophages in mice lacking protein kinase R. PLoS One. 2012;7(2):e30512.
106. Schon T, Elias D, Moges F, Melese E, Tessema T, Stendahl O, et al. Arginine as an adjuvant to chemotherapy improves clinical outcome in active tuberculosis. Eur Respir J. 2003;21(3):483-8.
107. Ralph AP, Waramori G, Pontororing GJ, Kenangalem E, Wiguna A, Tjitra E, et al. L-arginine and vitamin D adjunctive therapies in pulmonary tuberculosis: a randomised, double-blind, placebo-controlled trial. PLoS One. 2013;8(8):e70032.
108. Schon T, Idh J, Westman A, Elias D, Abate E, Diro E, et al. Effects of a food supplement rich in arginine in patients with smear positive pulmonary tuberculosis--a randomised trial. Tuberculosis (Edinb). 2011;91(5):370-7.
109. Ruan J, St John G, Ehrt S, Riley L, Nathan C. noxR3, a novel gene from Mycobacterium tuberculosis, protects Salmonella typhimurium from nitrosative and oxidative stress. Infect Immun. 1999;67(7):3276-83.
110. Chen L, Xie QW, Nathan C. Alkyl hydroperoxide reductase subunit C (AhpC) protects bacterial and human cells against reactive nitrogen intermediates. Mol Cell. 1998;1(6):795-805.
111. McGarvey J, Bermudez LE. Pathogenesis of nontuberculous mycobacteria infections. Clin Chest Med. 2002;23(3):569-83.
112. Gomes MS, Florido M, Pais TF, Appelberg R. Improved clearance of Mycobacterium avium upon disruption of the inducible nitric oxide synthase gene. J Immunol. 1999;162(11):6734-9.
113. Pearl JE, Torrado E, Tighe M, Fountain JJ, Solache A, Strutt T, et al. Nitric oxide inhibits the accumulation of CD4+CD44hiTbet+CD69loT cells in mycobacterial infection. European Journal of Immunology. 2012;42(12):3267-79.
114. Moreira JD, Koch BEV, van Veen S, Walburg KV, Vrieling F, Mara Pinto Dabes Guimaraes T, et al. Functional Inhibition of Host Histone Deacetylases (HDACs) Enhances *in vitro* and *in vivo* Anti-mycobacterial Activity in Human Macrophages and in Zebrafish. Front Immunol. 2020;11:36.
115. Bhaskar A, Kumar S, Khan MZ, Singh A, Dwivedi VP, Nandicoori VK. Host sirtuin 2 as an immunotherapeutic target against tuberculosis. eLife. 2020;9:e55415.
116. Rao M, Valentini D, Zumla A, Maeurer M. Evaluation of the efficacy of valproic acid and suberoylanilide hydroxamic acid (vorinostat) in enhancing the effects of first-line tuberculosis drugs against intracellular Mycobacterium tuberculosis. Int J Infect Dis. 2018;69:78-84.
117. Hegde SR. Computational Identification of the Proteins Associated With Quorum Sensing and Biofilm Formation in Mycobacterium tuberculosis. Front Microbiol. 2019;10:3011.
118. Cohen SB, Gern BH, Delahaye JL, Adams KN, Plumlee CR, Winkler JK, et al. Alveolar Macrophages Provide an Early Mycobacterium tuberculosis Niche and Initiate Dissemination. Cell Host Microbe. 2018;24(3):439-46 e4.
119. Flynn CM, Garbers Y, Lokau J, Wesch D, Schulte DM, Laudes M, et al. Activation of Toll-like Receptor 2 (TLR2) induces Interleukin-6 trans-signaling. Sci Rep. 2019;9(1):7306.
120. Pires D, Bernard EM, Pombo JP, Carmo N, Fialho C, Gutierrez MG, et al. Mycobacterium tuberculosis Modulates miR-106b-5p to Control Cathepsin S Expression Resulting in Higher Pathogen Survival and Poor T-Cell Activation. Front Immunol. 2017;8:1819.
121. Gupta PK, Chakraborty P, Kumar S, Singh PK, Rajan MG, Sainis KB, et al. G1-4A, a Polysaccharide from Tinospora cordifolia Inhibits the Survival of Mycobacterium tuberculosis by Modulating Host Immune Responses in TLR4 Dependent Manner. PLoS One. 2016;11(5):e0154725.
122. Anwar MA, Shah M, Kim J, Choi S. Recent clinical trends in Toll-like receptor targeting therapeu-

tics. Med Res Rev. 2019;39(3):1053-90.
123. Dwivedi VP, Bhattacharya D, Yadav V, Singh DK, Kumar S, Singh M, et al. The Phytochemical Bergenin Enhances T Helper 1 Responses and Anti-Mycobacterial Immunity by Activating the MAP Kinase Pathway in Macrophages. Front Cell Infect Microbiol. 2017;7:149.
124. Ottenhoff TH, Kaufmann SH. Vaccines against tuberculosis: where are we and where do we need to go? PLoS Pathog. 2012;8(5):e1002607.
125. Khan N, Vidyarthi A, Amir M, Mushtaq K, Agrewala JN. T-cell exhaustion in tuberculosis: pitfalls and prospects. Crit Rev Microbiol. 2017;43(2):133-41.
126. Tezera LB, Bielecka MK, Ogongo P, Walker NF, Ellis M, Garay-Baquero DJ, et al. Anti-PD-1 immunotherapy leads to tuberculosis reactivation via dysregulation of TNF-alpha. eLife. 2020;9:e52668.
127. Anastasopoulou A, Ziogas DC, Samarkos M, Kirkwood JM, Gogas H. Reactivation of tuberculosis in cancer patients following administration of immune checkpoint inhibitors: current evidence and clinical practice recommendations. J Immunother Cancer. 2019;7(1):239.
128. Gautam US, Foreman TW, Bucsan AN, Veatch AV, Alvarez X, Adekambi T, et al. *In vivo* inhibition of tryptophan catabolism reorganizes the tuberculoma and augments immune-mediated control of Mycobacterium tuberculosis. Proc Natl Acad Sci U S A. 2018;115(1):E62-E71.
129. Marchant A, Amedei A, Azzurri A, Vekemans J, Benagiano M, Tamburini C, et al. Polarization of PPD-specific T-cell response of patients with tuberculosis from Th0 to Th1 profile after successful antimycobacterial therapy or *in vitro* conditioning with interferon-alpha or interleukin-12. Am J Respir Cell Mol Biol. 2001;24(2):187-94.
130. Pooran A, Davids M, Nel A, Shoko A, Blackburn J, Dheda K. IL-4 subverts mycobacterial containment in Mycobacterium tuberculosis-infected human macrophages. Eur Respir J. 2019;54(2):1802242.
131. Esmail H, Riou C, Bruyn ED, Lai RP, Harley YXR, Meintjes G, et al. The Immune Response to Mycobacterium tuberculosis in HIV-1-Coinfected Persons. Annu Rev Immunol. 2018;36:603-38.
132. Vazquez N, Greenwell-Wild T, Rekka S, Orenstein JM, Wahl SM. Mycobacterium avium-induced SOCS contributes to resistance to IFN-gamma-mediated mycobactericidal activity in human macrophages. J Leukoc Biol. 2006;80(5):1136-44.
133. Ottenhoff TH, Verreck FA, Lichtenauer-Kaligis EG, Hoeve MA, Sanal O, van Dissel JT. Genetics, cytokines and human infectious disease: lessons from weakly pathogenic mycobacteria and salmonellae. Nat Genet. 2002;32(1):97-105.
134. Dawson R, Condos R, Tse D, Huie ML, Ress S, Tseng CH, et al. Immunomodulation with recombinant interferon-gamma1b in pulmonary tuberculosis. PLoS One. 2009;4(9):e6984.
135. Gao XF, Yang ZW, Li J. Adjunctive therapy with interferon-gamma for the treatment of pulmonary tuberculosis: a systematic review. Int J Infect Dis. 2011;15(9):e594-600.
136. Appelberg R, Orme IM. Effector mechanisms involved in cytokine-mediated bacteriostasis of Mycobacterium avium infections in murine macrophages. Immunology. 1993;80(3):352-9.
137. Holland SM, Eisenstein EM, Kuhns DB, Turner ML, Fleisher TA, Strober W, et al. Treatment of refractory disseminated nontuberculous mycobacterial infection with interferon gamma. A preliminary report. N Engl J Med. 1994;330(19):1348-55.
138. Milanes-Virelles MT, Garcia-Garcia I, Santos-Herrera Y, Valdes-Quintana M, Valenzuela-Silva CM, Jimenez-Madrigal G, et al. Adjuvant interferon gamma in patients with pulmonary atypical Mycobacteriosis: a randomized, double-blind, placebo-controlled study. BMC Infect Dis. 2008;8:17.
139. Lauw FN, van Der Meer JT, de Metz J, Danner SA, van Der Poll T. No beneficial effect of interferon-gamma treatment in 2 human immunodeficiency virus-infected patients with Mycobacterium avium complex infection. Clin Infect Dis. 2001;32(4):e81-2.
140. Mata-Espinosa D, Francisco-Cruz A, Marquina-Castillo B, Barrios-Payan J, Ramos-Espinosa O, Bini EI, et al. Immunotherapeutic effects of recombinant adenovirus encoding interleukin 12 in experimental pulmonary tuberculosis. Scandinavian Journal of Immunology. 2018;89:e12743.
141. Ma Y, Chen HD, Wang Y, Wang Q, Li Y, Zhao Y, et al. Interleukin 24 as a novel potential cytokine immunotherapy for the treatment of Mycobacterium tuberculosis infection. Microbes Infect. 2011;13(12-13):1099-110.
142. Lindestam Arlehamn CS, Gerasimova A, Mele F, Henderson R, Swann J, Greenbaum JA, et al. Memory T cells in latent Mycobacterium tuberculosis infection are directed against three antigenic islands and largely contained in a CXCR3+CCR6+ Th1 subset. PLoS Pathog. 2013;9(1):e1003130.
143. Rakshit S, Hingankar N, Alampalli SV, Adiga V, Sundararaj BK, Sahoo PN, et al. HIV Skews a Balanced *Mtb*-Specific Th17 Response in Latent Tuberculosis Subjects to a Pro-inflammatory Profile Independent of Viral Load. Cell Rep. 2020;33(9):108451.
144. Scott NR, Swanson RV, Al-Hammadi N, Domingo-Gonzalez R, Rangel-Moreno J, Kriel BA, et al. S100A8/A9 regulates CD11b expression and neutrophil recruitment during chronic tuberculosis. J Clin

Invest. 2020;130(6):3098-112.
145. Zhang R, Xi X, Wang C, Pan Y, Ge C, Zhang L, et al. Therapeutic effects of recombinant human interleukin 2 as adjunctive immunotherapy against tuberculosis: A systematic review and meta-analysis. PLoS One. 2018;13(7):e0201025.
146. Bermudez LE, Stevens P, Kolonoski P, Wu M, Young LS. Treatment of experimental disseminated Mycobacterium avium complex infection in mice with recombinant IL-2 and tumor necrosis factor. J Immunol. 1989;143(9):2996-3000.
147. Sekiguchi Y, Yasui K, Yamazaki T, Agematsu K, Kobayashi N, Koike K. Effective combination therapy using interferon-gamma and interleukin-2 for disseminated Mycobacterium avium complex infection in a pediatric patient with AIDS. Clin Infect Dis. 2005;41(11):e104-6.
148. Trojan T, Collins R, Khan DA. Safety and efficacy of treatment using interleukin-2 in a patient with idiopathic CD4(+) lymphopenia and Mycobacterium avium-intracellulare. Clin Exp Immunol. 2009;156(3):440-5.
149. Gupta S, Cheung L, Pokkali S, Winglee K, Guo H, Murphy JR, et al. Suppressor Cell-Depleting Immunotherapy With Denileukin Diftitox is an Effective Host-Directed Therapy for Tuberculosis. J Infect Dis. 2017;215(12):1883-7.
150. Chen CY, Yao S, Huang D, Wei H, Sicard H, Zeng G, et al. Phosphoantigen/IL2 expansion and differentiation of Vgamma2Vdelta2 T cells increase resistance to tuberculosis in nonhuman primates. PLoS Pathog. 2013;9(8):e1003501.
151. Xu P, Pang Y, Xu J, Chen H, Tang P, Wu M. Cytokine-induced killer cell therapy as a promising adjunctive immunotherapy for multidrug-resistant pulmonary TB: a case report. Immunotherapy. 2018;10(10):827-30.
152. Mohareer K, Asalla S, Banerjee S. Cell death at the cross roads of host-pathogen interaction in Mycobacterium tuberculosis infection. Tuberculosis. 2018;113:99-121.
153. Rajaram MV, Brooks MN, Morris JD, Torrelles JB, Azad AK, Schlesinger LS. Mycobacterium tuberculosis activates human macrophage peroxisome proliferator-activated receptor gamma linking mannose receptor recognition to regulation of immune responses. J Immunol. 2010;185(2):929-42.
154. Arnett E, Weaver AM, Woodyard KC, Montoya MJ, Li M, Hoang KV, et al. PPARgamma is critical for Mycobacterium tuberculosis induction of Mcl-1 and limitation of human macrophage apoptosis. PLoS Pathog. 2018;14(6):e1007100.
155. Pajuelo D, Gonzalez-Juarbe N, Tak U, Sun J, Orihuela CJ, Niederweis M. NAD(+) Depletion Triggers Macrophage Necroptosis, a Cell Death Pathway Exploited by Mycobacterium tuberculosis. Cell Rep. 2018;24(2):429-40.
156. Grab J, Suarez I, van Gumpel E, Winter S, Schreiber F, Esser A, et al. Corticosteroids inhibit Mycobacterium tuberculosis-induced necrotic host cell death by abrogating mitochondrial membrane permeability transition. Nat Commun. 2019;10(1):688.
157. Kim YJ, Pack KM, Jeong E, Na JO, Oh YM, Lee SD, et al. Pulmonary tuberculosis with acute respiratory failure. Eur Respir J. 2008;32(6):1625-30.
158. Malhotra HS, Garg RK, Singh MK, Agarwal A, Verma R. Corticosteroids (dexamethasone versus intravenous methylprednisolone) in patients with tuberculous meningitis. Ann Trop Med Parasitol. 2009;103(7):625-34.
159. Critchley JA, Orton LC, Pearson F. Adjunctive steroid therapy for managing pulmonary tuberculosis. Cochrane Database Syst Rev. 2014(11):CD011370.
160. Kalamidas SA, Kuehnel MP, Peyron P, Rybin V, Rauch S, Kotoulas OB, et al. cAMP synthesis and degradation by phagosomes regulate actin assembly and fusion events: consequences for mycobacteria. J Cell Sci. 2006;119(Pt 17):3686-94.
161. Roca FJ, Whitworth LJ, Redmond S, Jones AA, Ramakrishnan L. TNF Induces Pathogenic Programmed Macrophage Necrosis in Tuberculosis through a Mitochondrial-Lysosomal-Endoplasmic Reticulum Circuit. Cell. 2019;178(6):1344-61 e11.
162. Roca FJ, Ramakrishnan L. TNF dually mediates resistance and susceptibility to mycobacteria via mitochondrial reactive oxygen species. Cell. 2013;153(3):521-34.
163. Maiga M, Agarwal N, Ammerman NC, Gupta R, Guo H, Maiga MC, et al. Successful shortening of tuberculosis treatment using adjuvant host-directed therapy with FDA-approved phosphodiesterase inhibitors in the mouse model. PLoS One. 2012;7(2):e30749.
164. Maiga M, Ammerman NC, Maiga MC, Tounkara A, Siddiqui S, Polis M, et al. Adjuvant host-directed therapy with types 3 and 5 but not type 4 phosphodiesterase inhibitors shortens the duration of tuberculosis treatment. J Infect Dis. 2013;208(3):512-9.
165. Ordonez AA, Pokkali S, Kim S, Carr B, Klunk MH, Tong L, et al. Adjunct antibody administration with standard treatment reduces relapse rates in a murine tuberculosis model of necrotic granulomas.

PLoS One. 2018;13(5):e0197474.
166. Skerry C, Harper J, Klunk M, Bishai WR, Jain SK. Adjunctive TNF inhibition with standard treatment enhances bacterial clearance in a murine model of necrotic TB granulomas. PLoS One. 2012;7(6):e39680.
167. Kolloli A, Subbian S. Host-Directed Therapeutic Strategies for Tuberculosis. Front Med (Lausanne). 2017;4:171.
168. Zhang Z, Fan W, Yang G, Xu Z, Wang J, Cheng Q, et al. Risk of tuberculosis in patients treated with TNF-alpha antagonists: a systematic review and meta-analysis of randomised controlled trials. BMJ Open. 2017;7(3):e012567.
169. Danko JR, Gilliland WR, Miller RS, Decker CF. Disseminated Mycobacterium marinum infection in a patient with rheumatoid arthritis receiving infliximab therapy. Scand J Infect Dis. 2009;41(4):252-5.
170. Amaral EP, Costa DL, Namasivayam S, Riteau N, Kamenyeva O, Mittereder L, et al. A major role for ferroptosis in Mycobacterium tuberculosis-induced cell death and tissue necrosis. J Exp Med. 2019;216(3):556-70.
171. Conrad M, Kagan VE, Bayir H, Pagnussat GC, Head B, Traber MG, et al. Regulation of lipid peroxidation and ferroptosis in diverse species. Genes Dev. 2018;32(9-10):602-19.
172. Ingold I, Berndt C, Schmitt S, Doll S, Poschmann G, Buday K, et al. Selenium Utilization by GPX4 Is Required to Prevent Hydroperoxide-Induced Ferroptosis. Cell. 2018;172(3):409-22 e21.
173. Howard NC, Khader SA. Immunometabolism during Mycobacterium tuberculosis Infection. Trends Microbiol. 2020;28(10):832-50.
174. Krishnamoorthy G, Kaiser P, Abu Abed U, Weiner J, 3rd, Moura-Alves P, Brinkmann V, et al. FX11 limits Mycobacterium tuberculosis growth and potentiates bactericidal activity of isoniazid through host-directed activity. Dis Model Mech. 2020;13(3):dmm041954.
175. Tatano Y, Kanehiro Y, Sano C, Shimizu T, Tomioka H. ATP exhibits antimicrobial action by inhibiting bacterial utilization of ferric ions. Sci Rep. 2015;5:8610.
176. Tatano Y, Yamabe S, Sano C, Tomioka H. Anti-Mycobacterium avium complex activity of clarithromycin, rifampin, rifabutin, and ethambutol in combination with adenosine 5'-triphosphate. Diagn Microbiol Infect Dis. 2017;88(3):241-6.
177. Matty MA, Knudsen DR, Walton EM, Beerman RW, Cronan MR, Pyle CJ, et al. Potentiation of P2RX7 as a host-directed strategy for control of mycobacterial infection. Elife. 2019;8.
178. Tsai IF, Kuo CP, Lin AB, Chien MN, Ho HT, Wei TY, et al. Potential effect of ezetimibe against Mycobacterium tuberculosis infection in type II diabetes. Respirology. 2017;22(3):559-66.
179. Asalla S, Mohareer K, Banerjee S. Small Molecule Mediated Restoration of Mitochondrial Function Augments Anti-Mycobacterial Activity of Human Macrophages Subjected to Cholesterol Induced Asymptomatic Dyslipidemia. Front Cell Infect Microbiol. 2017;7:439.
180. Dutta NK, Bruiners N, Zimmerman MD, Tan S, Dartois V, Gennaro ML, et al. Adjunctive Host-Directed Therapy With Statins Improves Tuberculosis-Related Outcomes in Mice. J Infect Dis. 2020;221(7):1079-87.
181. Pieters J. Mycobacterium tuberculosis and the macrophage: maintaining a balance. Cell Host Microbe. 2008;3(6):399-407.
182. de Chastellier C, Thilo L. Cholesterol depletion in Mycobacterium avium-infected macrophages overcomes the block in phagosome maturation and leads to the reversible sequestration of viable mycobacteria in phagolysosome-derived autophagic vacuoles. Cell Microbiol. 2006;8(2):242-56.
183. Dutta NK, Bruiners N, Pinn ML, Zimmerman MD, Prideaux B, Dartois V, et al. Statin adjunctive therapy shortens the duration of TB treatment in mice. J Antimicrob Chemother. 2016;71(6):1570-7.
184. Parihar SP, Guler R, Khutlang R, Lang DM, Hurdayal R, Mhlanga MM, et al. Statin therapy reduces the mycobacterium tuberculosis burden in human macrophages and in mice by enhancing autophagy and phagosome maturation. J Infect Dis. 2014;209(5):754-63.
185. Guerra-De-Blas PDC, Bobadilla-Del-Valle M, Sada-Ovalle I, Estrada-Garcia I, Torres-Gonzalez P, Lopez-Saavedra A, et al. Simvastatin Enhances the Immune Response Against Mycobacterium tuberculosis. Front Microbiol. 2019;10:2097.
186. Sorgi CA, Soares EM, Rosada RS, Bitencourt CS, Zoccal KF, Pereira PAT, et al. Eicosanoid pathway on host resistance and inflammation during Mycobacterium tuberculosis infection is comprised by LTB4 reduction but not PGE2 increment. Biochim Biophys Acta Mol Basis Dis. 2020;1866(3):165574.
187. Tobin DM, Roca FJ, Oh SF, McFarland R, Vickery TW, Ray JP, et al. Host genotype-specific therapies can optimize the inflammatory response to mycobacterial infections. Cell. 2012;148(3):434-46.
188. Mayer-Barber KD, Andrade BB, Oland SD, Amaral EP, Barber DL, Gonzales J, et al. Host-directed therapy of tuberculosis based on interleukin-1 and type I interferon crosstalk. Nature. 2014;511(7507):99-103.

189. Kaufmann SHE, Dorhoi A, Hotchkiss RS, Bartenschlager R. Host-directed therapies for bacterial and viral infections. Nat Rev Drug Discov. 2018;17(1):35-56.
190. Thuong NTT, Heemskerk D, Tram TTB, Thao LTP, Ramakrishnan L, Ha VTN, et al. Leukotriene A4 Hydrolase Genotype and HIV Infection Influence Intracerebral Inflammation and Survival From Tuberculous Meningitis. J Infect Dis. 2017;215(7):1020-8.
191. Vilaplana C, Marzo E, Tapia G, Diaz J, Garcia V, Cardona PJ. Ibuprofen Therapy Resulted in Significantly Decreased Tissue Bacillary Loads and Increased Survival in a New Murine Experimental Model of Active Tuberculosis. Journal of Infectious Diseases. 2013;208(2):199-202.
192. Byrne ST, Denkin SM, Zhang Y. Aspirin and ibuprofen enhance pyrazinamide treatment of murine tuberculosis. J Antimicrob Chemother. 2007;59(2):313-6.
193. Kroesen VM, Rodriguez-Martinez P, Garcia E, Rosales Y, Diaz J, Martin-Cespedes M, et al. A Beneficial Effect of Low-Dose Aspirin in a Murine Model of Active Tuberculosis. Front Immunol. 2018;9:798.
194. Hortle E, Johnson KE, Johansen MD, Nguyen T, Shavit JA, Britton WJ, et al. Thrombocyte Inhibition Restores Protective Immunity to Mycobacterial Infection in Zebrafish. J Infect Dis. 2019;220(3):524-34.
195. Lee MR, Lee MC, Chang CH, Liu CJ, Chang LY, Zhang JF, et al. Use of Antiplatelet Agents and Survival of Tuberculosis Patients: A Population-Based Cohort Study. J Clin Med. 2019;8(7):923.
196. Misra UK, Kalita J, Nair PP. Role of aspirin in tuberculous meningitis: a randomized open label placebo controlled trial. J Neurol Sci. 2010;293(1-2):12-7.
197. Byrne ST, Denkin SM, Zhang Y. Aspirin antagonism in isoniazid treatment of tuberculosis in mice. Antimicrob Agents Chemother. 2007;51(2):794-5.
198. Smith D, H. H, G. B, Ehlers S. T-cell-independent granuloma formation in response to Mycobacterium avium: role of tumour necrosis factor-alpha and interferon-gamma. Immunology. 1997;92(4):413-21.
199. Hänsch HC, Smith DA, Mielke ME, Hahn H, Bancroft GJ, Ehlers S. Mechanisms of granuloma formation in murine Mycobacterium avium infection: the contribution of CD4+ T cells. Int Immunol. 1996;8(8):299-310.
200. Streit M, Bregenzer T, Heinzer I. Cutaneous infections due to atypical mycobacteria. Hautarzt. 2008;59(1):59-70.
201. Ehlers S, Schaible UE. The granuloma in tuberculosis: dynamics of a host-pathogen collusion. Front Immunol. 2012;3:411.
202. Parasa VR, Muvva JR, Rose JF, Braian C, Brighenti S, Lerm M. Inhibition of Tissue Matrix Metalloproteinases Interferes with Mycobacterium tuberculosis-Induced Granuloma Formation and Reduces Bacterial Load in a Human Lung Tissue Model. Front Microbiol. 2017;8:2370.
203. Sabir N, Hussain T, Mangi MH, Zhao D, Zhou X. Matrix metalloproteinases: Expression, regulation and role in the immunopathology of tuberculosis. Cell Prolif. 2019;52(4):e12649.
204. Xu Y, Wang L, Zimmerman MD, Chen KY, Huang L, Fu DJ, et al. Matrix metalloproteinase inhibitors enhance the efficacy of frontline drugs against Mycobacterium tuberculosis. PLoS Pathog. 2018;14(4):e1006974.
205. Singh S, Kubler A, Singh UK, Singh A, Gardiner H, Prasad R, et al. Antimycobacterial drugs modulate immunopathogenic matrix metalloproteinases in a cellular model of pulmonary tuberculosis. Antimicrob Agents Chemother. 2014;58(8):4657-65.
206. Elkington P, Shiomi T, Breen R, Nuttall RK, Ugarte-Gil CA, Walker NF, et al. MMP-1 drives immunopathology in human tuberculosis and transgenic mice. J Clin Invest. 2011;121(5):1827-33.
207. Ordonez AA, Pokkali S, Sanchez-Bautista J, Klunk MH, Urbanowski ME, Kubler A, et al. Matrix Metalloproteinase Inhibition in a Murine Model of Cavitary Tuberculosis Paradoxically Worsens Pathology. J Infect Dis. 2019;219(4):633-6.
208. Ong CW, Elkington PT, Brilha S, Ugarte-Gil C, Tome-Esteban MT, Tezera LB, et al. Neutrophil-Derived MMP-8 Drives AMPK-Dependent Matrix Destruction in Human Pulmonary Tuberculosis. PLoS Pathog. 2015;11(5):e1004917.
209. Walker NF, Wilkinson KA, Meintjes G, Tezera LB, Goliath R, Peyper JM, et al. Matrix Degradation in Human Immunodeficiency Virus Type 1-Associated Tuberculosis and Tuberculosis Immune Reconstitution Inflammatory Syndrome: A Prospective Observational Study. Clin Infect Dis. 2017;65(1):121-32.
210. Machelart A, Song OR, Hoffmann E, Brodin P. Host-directed therapies offer novel opportunities for the fight against tuberculosis. Drug Discov Today. 2017;22(8):1250-7.
211. Majeed S, Singh P, Sharma N, Sharma S. Title: role of matrix metalloproteinase -9 in progression of tuberculous meningitis: a pilot study in patients at different stages of the disease. BMC Infect Dis. 2016;16(1):722.
212. Majeed S, Radotra BD, Sharma S. Adjunctive role of MMP-9 inhibition along with conventional

anti-tubercular drugs against experimental tuberculous meningitis. Int J Exp Pathol. 2016;97(3):230-7.
213. Walker NF, Clark SO, Oni T, Andreu N, Tezera L, Singh S, et al. Doxycycline and HIV infection suppress tuberculosis-induced matrix metalloproteinases. Am J Respir Crit Care Med. 2012;185(9):989-97.
214. Zenk SF, Vollmer M, Schercher E, Kallert S, Kubis J, Stenger S. Hypoxia promotes Mycobacterium tuberculosis-specific up-regulation of granulysin in human T cells. Med Microbiol Immunol. 2016;205(3):219-29.
215. Walton EM, Cronan MR, Cambier CJ, Rossi A, Marass M, Foglia MD, et al. Cyclopropane Modification of Trehalose Dimycolate Drives Granuloma Angiogenesis and Mycobacterial Growth through Vegf Signaling. Cell Host Microbe. 2018;24(4):514-25 e6.
216. Datta M, Via LE, Kamoun WS, Liu C, Chen W, Seano G, et al. Anti-vascular endothelial growth factor treatment normalizes tuberculosis granuloma vasculature and improves small molecule delivery. Proc Natl Acad Sci U S A. 2015;112(6):1827-32.
217. Oehlers SH, Cronan MR, Scott NR, Thomas MI, Okuda KS, Walton EM, et al. Interception of host angiogenic signalling limits mycobacterial growth. Nature. 2015;517(7536):612-5.
218. Oehlers SH, Cronan MR, Beerman RW, Johnson MG, Huang J, Kontos CD, et al. Infection-Induced Vascular Permeability Aids Mycobacterial Growth. J Infect Dis. 2017;215(5):813-7.
219. Niemi M, Backman JT, Fromm MF, Neuvonen PJ, Kivisto KT. Pharmacokinetic interactions with rifampicin : clinical relevance. Clin Pharmacokinet. 2003;42(9):819-50.
220. Russell SL, Lamprecht DA, Mandizvo T, Jones TT, Naidoo V, Addicott KW, et al. Compromised Metabolic Reprogramming Is an Early Indicator of CD8(+) T Cell Dysfunction during Chronic Mycobacterium tuberculosis Infection. Cell Rep. 2019;29(11):3564-79 e5.
221. Gupta S, Tyagi S, Bishai WR. Verapamil increases the bactericidal activity of bedaquiline against Mycobacterium tuberculosis in a mouse model. Antimicrob Agents Chemother. 2015;59(1):673-6.
222. Martin A, Bouyakoub Y, Soumillion K, Mantu EON, Colmant A, Rodriguez-Villalobos H. Targeting bedaquiline mycobacterial efflux pump to potentially enhance therapy in Mycobacterium abscessus. Int J Mycobacteriol. 2020;9(1):71-5.
223. Viljoen A, Raynaud C, Johansen MD, Roquet-Baneres F, Herrmann JL, Daher W, et al. Verapamil Improves the Activity of Bedaquiline against Mycobacterium abscessus *In vitro* and in Macrophages. Antimicrob Agents Chemother. 2019;63(9):e00705-19.
224. Matt U, Selchow P, Dal Molin M, Strommer S, Sharif O, Schilcher K, et al. Chloroquine enhances the antimycobacterial activity of isoniazid and pyrazinamide by reversing inflammation-induced macrophage efflux. Int J Antimicrob Agents. 2017;50(1):55-62.
225. Hegeto LA, Caleffi-Ferracioli KR, Nakamura-Vasconcelos SS, Almeida AL, Baldin VP, Nakamura CV, et al. *In vitro* combinatory activity of piperine and anti-tuberculosis drugs in Mycobacterium tuberculosis. Tuberculosis (Edinb). 2018;111:35-40.

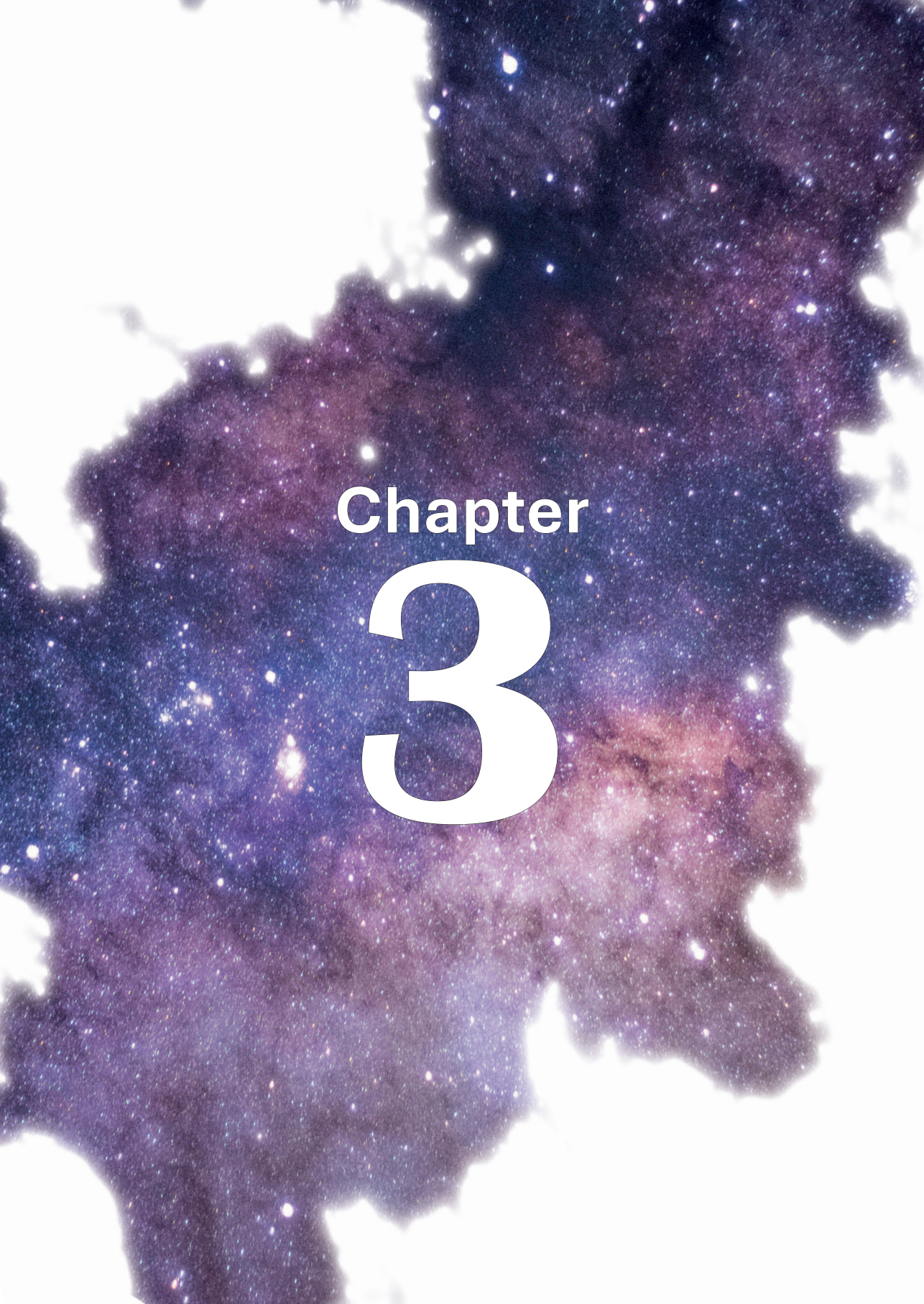
Chapter
3

Development of human cell-based *in vitro* infection models to determine the intracellular survival of *Mycobacterium avium*

Gül Kilinç[1], Kimberley V. Walburg[1], Kees L. M. C. Franken[1], Merel L. Valkenburg[1], Alexandra Aubry[2], Mariëlle C. Haks[1], Anno Saris[1] and Tom H. M. Ottenhoff[1]

[1] Department of Infectious Diseases, Leiden University Medical Center, Leiden, The Netherlands
[2] Sorbonne Université, INSERM, Centre d'Immunologie et des Maladies Infectieuses, U1135, AP-HP, Hôpital Pitié-Salpêtrière, Centre National de Référence des Mycobactéries et de la Résistance des Mycobactéries aux Antituberculeux, Paris, France

Front Cell Infect Microbiol. 2022 Jun 24:12:872361

Abstract

Mycobacterium avium (*Mav*) complex accounts for more than 80% of all pulmonary diseases caused by non-tuberculous mycobacteria (NTM) infections, which have an alarming increase in prevalence and vary in different regions, currently reaching 0.3-9.8 per 100.000 individuals. Poor clinical outcomes, as a result of increasing microbial drug-resistance and low treatment adherence due to drug-toxicities, emphasize the need for more effective treatments. Identification of more effective treatments, however, appears to be difficult, which may be due to the intracellular life of NTM and concomitant altered drug-sensitivity that is not taken into account using traditional drug susceptibility testing screenings. We therefore developed human cell-based *in vitro Mav* infection models using the human MelJuSo cell line as well as primary human macrophages and a fluorescently labeled *Mav* strain. By testing a range of multiplicity of infection (MOI) and using flow cytometry and colony-forming unit (CFU) analysis, we found that an MOI of 10 was the most suitable for *Mav* infection in primary human macrophages, whereas an MOI of 50 was required to achieve similar results in MelJuSo cells. Moreover, by monitoring intracellular bacterial loads over time, the macrophages were shown to be capable of controlling the infection, while MelJuSo cells failed to do so. When comparing the MGIT system with the classical CFU counting assay to determine intracellular bacterial loads, MGIT appeared as a less labor-intensive, more precise and more objective alternative. Next, using our macrophage-*Mav* infection models, drug efficacy of first-line drug rifampicin and more recently discovered bedaquiline on intracellular bacteria was compared to activity on extracellular bacteria. The efficacy of the antibiotics inhibiting bacterial growth was significantly lower against intracellular bacteria compared to extracellular bacteria. This finding emphasizes the crucial role of the host cell during infection and drug-susceptibility and highlights the usefulness of the models. Taken together, the human cell-based *Mav* infection models are reliable tools to determine intracellular loads of *Mav*, which will enable to investigate host-pathogen interactions and to evaluate the efficacy of (host-directed) therapeutic strategies against *Mav*.

Introduction

Mycobacterium avium (*Mav*), a pathogen widely distributed in the environment, is a member of non-tuberculous mycobacteria (NTM). NTM infections predominantly manifest as chronic lung disease (NTM-LD), of which the prevalence has been rising over the last 30 years, being more prevalent than tuberculosis in some regions (1, 2). The vast majority (80%) of these NTM-LD cases are caused by the *Mav* complex (3), and the higher occurrence of *Mav*-LD is mainly observed in immunocompromised patients with structural lung conditions or immunologic and genetic disorders (4-7). However, despite its rarity in immunocompetent individuals (<10 cases per 100.000 people below the age of 50 years), *Mav* also causes LD without predisposing conditions, especially in elderly women (5, 8, 9).

The treatment for *Mav* infection consists of a multidrug antibiotic regimen, including a macrolide (usually clarithromycin or azithromycin), ethambutol and a rifamycin (rifampicin or rifabutin) (10, 11), and in severe cases also an aminoglycoside (12, 13). Despite a lengthy treatment that should be maintained at least 12 months after negative sputum culture conversion, approximately 60% of treatments are unsuccessful (14). The high failure rate is largely due to drug resistance and low treatment adherence as a result of lengthiness of treatment and concomitant adverse reactions, but also because of limited treatment responses and patient relapses (9, 12, 15, 16). Hence, the development of new treatments to eradicate *Mav* infections is highly desired.

A promising alternative or adjunctive therapy for mycobacterial infection is host-directed therapy (HDT). HDT stimulates host cells to eliminate invading pathogens and/or counteract pathogen-induced mechanisms that prevent or impair bacterial clearance. As mycobacteria are predominantly intracellular pathogens, with many host-pathogen interactions, HDT is an appealing adjunctive therapy. By targeting infected host cells, HDT offers several advantages over antibiotics: (1) HDT has a low probability of evoking de novo drug resistance as the drugs do not target the pathogen; (2) HDT will most likely be effective against drug-resistant mycobacterial strains; (3) HDT could also be effective against metabolically inactive and/or non-replicating bacteria; and (4) HDT and classical antibiotic could act synergistically as both target different processes, such that antibiotic treatment duration and/or dosage (and concomitant adverse effects) might be significantly reduced. Host-pathogen interactions and HDT are extensively investigated with regard to Mycobacterium tuberculosis (*Mtb*), and although it is known that NTM are able to modulate host immune responses, including inhibition of phagosome maturation or host epigenetic features (17-19), the limited knowledge on the host-pathogen interactions during *Mav* infections still hampers the identification of targets for HDT (20).

To gain further insight into host-pathogen interactions and to identify new therapeutic molecules against intracellular *Mav*, robust *in vitro* infection models in human cells are required. We previously described *in vitro* infection models for (multi-drug resistant) *Mtb* that allow accurate determination of mycobacterial loads and proved suitable to identify HDTs for *Mtb* infections (17, 18, 21). In the present study, we adapted and modified these models to NTM, by generating fluorescently labeled *Mav* and establishing suitable infection conditions in a human cell line as well as primary macrophages. In addition, an automated liquid culture method known as the BACTEC Mycobacteria

Growth Indicator Tube (MGIT) 960 system was validated here to accurately determine intracellular bacterial loads of *Mav* (22). The models described here can be used to identify antimicrobial and HDT compounds and to investigate what host signaling pathways and regulatory networks control *Mav* infection.

Materials and methods

Cell cultures

The MelJuSo human melanoma cell line (kindly provided by Jacques Neefjes, Leiden University Medical Center, Leiden, the Netherlands) was maintained in Gibco Iscove's Modified Dulbecco's Medium (IMDM) (Life Technologies, Bleiswijk, the Netherlands) supplemented with 10% fetal bovine serum (FBS, Greiner Bio-One, Alphen a/d Rijn, the Netherlands), 100 units/mL penicillin and 100 µg/mL streptomycin (Life Technologies) at 37 °C/5% CO_2. Peripheral blood mononuclear cells were isolated from anonymized healthy donor buffy coats obtained after written informed consent (Sanquin Blood Bank, Amsterdam, the Netherlands) by density gradient centrifugation over Ficoll Amidotrizoate (Pharmacy, LUMC, the Netherlands). This was approved by the Sanquin Ethical Advisory Board, in accordance with the declaration of Helsinki and according to Dutch regulations. CD14+ monocytes were isolated by magnetic cell sorting using anti-CD14-coated microbeads (Miltenyi Biotec, Bergisch Gladsbach, Germany) and differentiated for 6 days into pro-inflammatory (M1) or anti-inflammatory (M2) macrophages with 5 ng/mL of granulocyte-macrophage colony-stimulating factor (GM-CSF; Miltenyi Biotec) or 50 ng/mL macrophage-CSF (M-CSF; R&D Systems, Abingdon, UK), respectively, as previously reported (23). Monocytes and macrophages were cultured in Gibco Dutch modified Roswell Park Memorial Institute (RPMI) 1640 medium (Life Technologies) supplemented with 10% FBS, 2 mM L-alanyl-L-glutamine (PAA, Linz, Austria) and during differentiation with 100 units/ml penicillin and 100 µg/mL streptomycin at 37 °C/5% CO_2.

Bacterial cultures

Mav laboratory strain 101 (700898, ATCC, Virginia, the United States) and three clinical isolates denoted as *Mav* 100 (amikacin-resistant), (drug-susceptible) 568 and (clarithromycin-resistant) 918 strains (the clinical isolates were isolated from pulmonary infections and displayed different susceptibility profiles to antibiotics as indicated, according to the French guidelines (Comité de l'Antibiograme de la SFM V.1.0 Avril 2021, European Committee on Antimicrobial Susceptibility Testing)) were cultured in Difco Middlebrook 7H9 broth (Becton Dickinson, Breda, the Netherlands), containing 0.2% glycerol (Merck Life Science, Amsterdam, the Netherlands), 0.05% Tween-80 (Merck Life Science) and 10% Middlebrook albumin, dextrose and catalase (ADC) enrichment (Becton Dickinson), which was supplemented with 100 µg/mL Hygromycin B (Life Technologies) for culturing the green fluorescently-labeled *Mav* Wasabi strain.

Growth of *Mav* Wasabi in suspension at 37 °C was evaluated by measuring the absorbance at optical density of 600 nm (OD_{600}) using the OD_{600} Ultrospec 10 Cell density meter (Amersham Biosciences). In parallel, growth was evaluated by enumerating bacterial colonies by agar plate assay to determine the OD factor (defined as CFU/mL in a culture with an OD_{600} of 1.0) for *Mav* Wasabi. Bacterial suspensions were therefore prepared using the estimated OD factor and plated on 7H10 square agar

plates, containing Difco Middlebrook 7H10 broth (Becton Dickinson) supplemented with 10% Middlebrook oleic, albumin, dextrose and catalase (OADC) enrichment (Becton Dickinson) and 0.5% glycerol for a standard colony-forming unit (CFU) assay. Afterwards, the estimated OD factor was adjusted to the colonies counted to achieve the final OD factor. The doubling-time (the time required for a population of bacteria to double in number), was calculated by first determining the doubling factor (i.e. the number of times the bacteria have doubled in numbers) by determining how many times the bacteria have doubled in numbers (c in the below equation) from early log-phase (OD600=0.25; b in the equation) until late log-phase culture (OD>3; a in the equation).

Doubling-factor = (LOG(a)-LOG(b))/LOG(c)

(As an example: Doubling-factor = (LOG(3,9)-LOG(0,25))/LOG(2) = 3,96. This number indicates how many times the bacteria have doubled in numbers. When this doubling factor is corrected for the amount of time that was used, say 96 h, the doubling time of the bacteria is determined: the doubling-time = time required for doubling-factor/ doubling-factor = 3,96/96 = 24,22 h. This number indicates the time required for one generation round.

Electroporation with and expression of Wasabi construct in *Mav* 101

Electroporation of *Mav* 101 was performed using the pSMT3-Wasabi construct. The Wasabi gene, amplified from the pTEC15 plasmid (Addgene plasmid #30174) by PCR, was kindly provided by Herman Spaink (Leiden University, Leiden, the Netherlands) and cloned into the mycobacterial expression vector pSMT3 (24). In this vector, expression of Wasabi is constitutive and controlled by the hygromycin resistance gene-containing hsp60 promoter. First, electrocompetent *Mav* was freshly prepared from a 50 mL log-phase culture by incubation with 1.5% glycine (Life Technologies) for 18 h at 37 °C. Subsequently, bacteria were centrifuged at 1,934 rcf for 20 min and washed three times with 37°C deionized H_2O supplemented with 10% glycerol and 0.5 M sucrose (electroporation solution) followed by centrifugation at 2,120 rcf for 10 min. Electrocompetent bacteria were concentrated 100× in electroporation solution and 100 µL of bacteria was electroporated at room temperature with 5 µg plasmid DNA using 0.2 cm gap Gene Pulser electroporation cuvettes and the Gene Pulser Xcell Electroporation System (Bio-Rad) with the following settings: 1,000 Ω, 25 µF, 1.25 kV and 2.5 V. Transformed bacteria were incubated overnight in 7H9 broth at 37 °C in a shaking incubator, transferred to 7H10 agar plates under 100 µg/mL hygromycin selection and incubated at 37 °C/5% CO_2 for 7-10 days. Expression of the Wasabi green fluorescent protein in individual clones of *Mav* Wasabi was analyzed by fixating samples in Falcon Round-Bottom Polystyrene Tubes with 1% paraformaldehyde at 4 °C for at least 45 min before measuring samples at wavelength 518-548 nm on the BD Accuri C6 Plus flow cytometer (BD Biosciences). FlowJo v10 Software (BD Biosciences) was used for analysis. Resistance to hygromycin was validated by mixing early log-phase *Mav* Wasabi culture with either 100 µg/mL or 200 µg/mL hygromycin, 20 µg/mL rifampicin (Sigma-Aldrich, Zwijndrecht, the Netherlands) as positive control or DMSO (Merck Life Science) as negative control. Plates were incubated at 37 °C/5% CO_2 for 10 days. Once every 2 days, the wells were resuspended and the absorbance at 600 nm was measured using the EnVision Multimode Plate Reader (Perkin Elmer). Outgrowth of bacteria in the hygromycin condition was compared to the controls.

***Mav* infection of human cells**

One day prior to infection, cultures of *Mav* Wasabi and the three clinical isolates of *Mav* were diluted to a density corresponding with early log-phase growth (OD_{600} of 0.4). On day of infection, bacterial suspensions were diluted in appropriate cell culture medium without antibiotics to reach the indicated multiplicity of infection (MOI). MOI of the inoculum was verified by preparing tenfold serial dilutions in 7H9 medium and plating 10-µL drops of each dilution on 7H10 agar plates. For experiments using the MGIT system, 125 µL of each dilution was transferred into MGIT tubes that contain a fluorescence-quenching oxygen sensor and prepared according to manufacturer's protocol. Subsequently, the inoculated tubes were incubated at 37°C in a BACTEC MGIT 960 instrument and were monitored automatically for oxygen utilization, which results in an increase in fluorescence. The number of days from inoculation until cultures reached a fluorescent intensity threshold was recorded as time to positivity (TTP). The TTP measurements were plotted against plate-counted log10 CFU using linear regression to be able to calculate bacterial loads (**Supplementary Figure 1**).MelJuSo cells or primary human macrophages, seeded in flat bottom 96-well plates at a density of 20,000 cells (2×10^5 cells/mL) or 30,000 cells (3×10^5 cells/mL) per well respectively in MelJuSo or macrophage culture medium without antibiotics 1 day before infection, were inoculated in triplicate or indicated otherwise with 100 µL of the bacterial suspension). Plates were centrifuged for 3 min at 129 rcf and incubated for 1 h at 37 °C/5% CO_2. In order to monitor only intracellular bacteria following infection, cells were washed with culture medium containing 30 µg/mL gentamicin (Merck Life Science), which blocks extracellular *Mav* growth (**Supplementary Figure 2**). Afterwards, cells were treated with fresh cell culture medium containing 5 µg/mL gentamicin and if applicable compounds of interest. Plates were incubated at 37 °C/5% CO_2 until readout by flow cytometry, CFU or MGIT, as indicated.

Quantification of infection

Cells were infected as described above and infection rates were determined by washing cells with PBS and subsequently trypsinized with Gibco 0.05% Trypsin-EDTA (Life Technologies). After trypsinization, appropriate cell culture medium containing FBS was added to the wells to inactivate Trypsin and the monolayers were scraped. Harvested cells were centrifuged in Falcon Round-Bottom Polystyrene Tubes at 453 rcf for 5 min to remove the supernatant. Cells were fixated with 1% paraformaldehyde prior to measurement and analysis as described above.

To determine numbers of bacteria taken up during infection and the subsequent survival of bacteria after prolonged incubation, infected MelJuSo cells were lysed at 0 and 24 h and primary human macrophages also at 48, 72 and 144 h post-infection using 100 µL lysis buffer (H_2O + 0.05% SDS). Cell lysates were serially diluted in multiple steps in 7H9 medium and 10 µL droplets were plated on 7H10 agar plates. After 7-10 days of incubation at 37 °C/5% CO_2, plates were photographically scanned, and bacterial colonies were counted. CFU counts were averaged and corrected for dilution factors to give CFU count per sample.

The ability of the MGIT system to accurately predict CFU of *Mav* was determined by evaluating intracellular bacterial loads of experimental cell lysates obtained in the same way as for the CFU analysis. Of each cell lysate, 125 µL was transferred to MGIT tubes.

The obtained TTP measurements were then converted into CFU counts by using linear regression and compared with the plate-counted values. The percentage of bacterial survival was defined as the fraction of CFU measured during prolonged incubation of the total CFU measured at uptake (=100%). As part of the validation of the MGIT assay, primary human macrophages exposed to *Mav* Wasabi (10:1) were treated for 24 h with 20 µg/mL rifampicin or 0.1% DMSO as negative control. After incubation, supernatant was removed, and cells were lysed with 100 µL lysis buffer. Number of bacteria per cell lysate was measured by both agar plate assay and MGIT assay. The activity of the antibiotic was determined by calculating the fraction of bacteria observed in the rifampicin condition of the total CFU measured in control (=100%).

Application of the MGIT system to assess the susceptibility to antibiotics of intracellular bacteria, compared with extracellular bacteria

To determine efficacy of antibiotics on extracellular bacteria, early log-phase *Mav* Wasabi culture was mixed in round-bottom 96-wells plates in duplicate with 1.29 µg/mL rifampicin, 1.74 µg/mL bedaquiline (kindly provided by Dirk Lamprecht, Janssen, Beerse, Belgium) or control (0.1% DMSO). These concentrations indicate the minimal inhibitory concentration (MIC) determined for each antibiotic by testing twofold serial drug dilutions against *Mav* Wasabi in liquid broth cultures (**Supplementary Figure 3**). Plates were incubated at 37 °C/5% CO_2 for 2 weeks. Once every 2 days, the wells were resuspended and absorbance at 600 nm was measured using the Envision Multimode Plate Reader (Perkin Elmer). For the determination of intracellular activity, primary human macrophages exposed to *Mav* Wasabi (10:1) in duplicate were treated for 24 h with 1.29 µg/mL rifampicin, 1.74 µg/mL bedaquiline or control (0.1% DMSO). After treatment, supernatant was removed, and cells were lysed with 100 µL lysis buffer. Cell lysates were further evaluated by the MGIT assay as described above. The activity of the antibiotics on bacteria was determined by calculating the fraction of bacteria observed in the rifampicin or bedaquiline conditions of the total CFU measured in control (=100%).

Statistical analysis

Normality of data was assessed using the Shapiro-Wilk test. For normally distributed paired datasets of more than two groups, we used repeated measures one-way ANOVA if data were determined by one independent variable, and repeated measures two-way ANOVA if two independent variables were involved. Paired and unpaired t-tests were used to evaluate differences in normally distributed datasets between two groups, whereas the Wilcoxon matched-pairs signed rank test was used for non-normally distributed paired data. To determine the strength of association between non-normally distributed datasets, the Spearman rank correlation test was used. Analyses were performed using GraphPad Prism 9.0 (GraphPad Software, San Diego, CA, USA), with p-values < 0.05 considered as significant.

Results

Generation of fluorescently labeled *Mav* strain 101

The first step in developing the human cell-based *in vitro* infection models was the generation of a green fluorescent protein-expressing *Mav* strain. This was achieved by electroporating a hygromycin resistance conferring plasmid, pSMT3-Wasabi, into wild-type laboratory strain *Mav* 101. Successful transfection was confirmed by expression

of the Wasabi fluorescent protein using flow cytometry (**Figure 1A**), and resistance to hygromycin by observing outgrowth (**Figure 1B**).

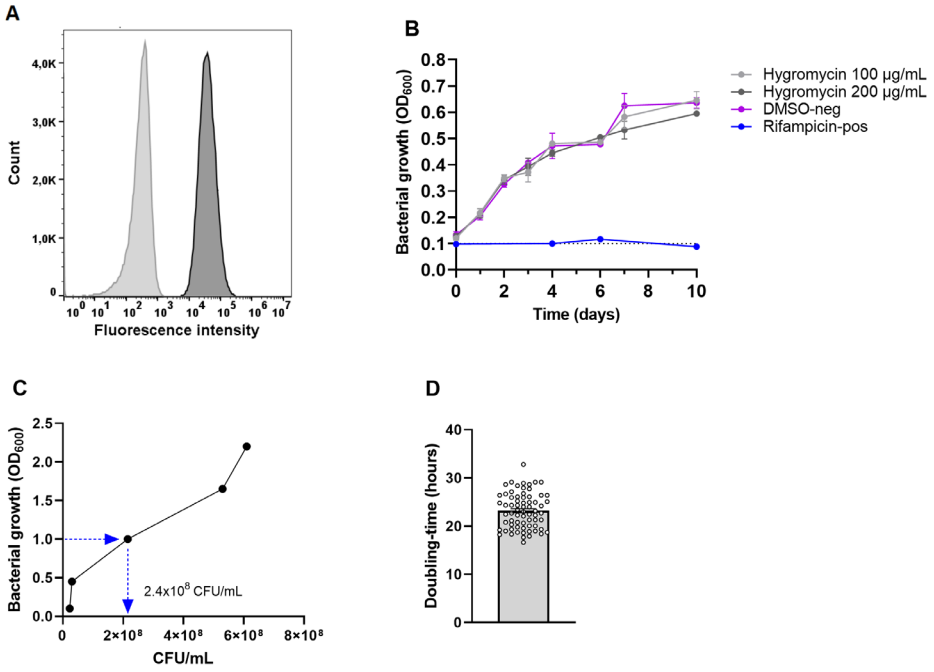

Figure 1. Confirmation of the generation of the green-fluorescent *Mav* Wasabi strain and its OD factor and doubling-time. *Mav* was electroporated with pSMT3-Wasabi plasmid to generate a green fluorescent *Mav* strain and its fluorescence (dark grey) is presented relative to non-fluorescent *Mav* (light grey) **(A)**. *Mav* Wasabi growth in presence of hygromycin in the indicated concentrations, DMSO (negative control) or 20 µg/mL rifampicin (positive control) was monitored by absorbance measurements at 600 nm, performed in n=3 with error bars depicting SEM between experiments **(B)**. Growth kinetics of *Mav* Wasabi was monitored by measuring OD_{600} values once every 24 hours, while CFU were quantified using CFU agar plate counting at same timepoints. After 48 hours, the bacterial density was measured to be OD_{600} of 1.0 **(C)**. The doubling-time was determined as the amount of time required for the multiple generations that occurred in the *Mav* Wasabi bacterial population **(D)**. The bar and whiskers represent mean±SEM.

Growth kinetics of *Mav* Wasabi

The OD factor of *Mav* (the number of colony forming units per mL (CFU/mL) in a culture with an OD_{600} value of 1.0) was determined to be able to prepare bacterial suspensions and infect cells with standardized MOI. To this end, growth kinetics of *Mav* were determined by measuring the optical density (OD_{600}) and enumerating CFU of *Mav* Wasabi cultures at 0, 24, 48, 72, and 96 h after the start of the culture (**Figure 1C**). Starting in early log-phase (OD_{600}=0.1), the bacterial culture reached an OD_{600} value of 1.0 after 48 h. At the same time point, the number of CFU/mL was obtained and verified in multiple inocula to obtain the definitive OD factor of 2.4×10^8 CFU/mL.

Ultimately, the bacteria grew to an OD_{600} value of 2.2 within 96 h (**Figure 1C**). The doubling-time was calculated for multiple *Mav* cultures and was determined to be 23 h on average (range: 17-33 h) (**Figure 1D**), which is in line the slow replication rate

reported in literature (25).

***In vitro Mav* infection models using human MeJuSo cells and human PBMC-derived primary macrophages**

In order to investigate NTM infections at the intracellular bacterial level, we developed human-cell based infection models for *Mav*, adapted from our previously reported infection models for *Mtb* (17, 21). First, we evaluated the capacity of MeJuSo cells to engulf *Mav* and optimized the level of infection by adjusting the MOI to reach an infection percentage comparable to what we observed previously in our MeJuSo-*Mtb* infection model (17). In *Mav*-infected MeJuSo cells, an MOI-dependent increase in infection was observed, as reflected by an increase in infection rate (% of infected cells) and intracellular bacterial loads directly after infection as determined by flow cytometry and CFU analysis, respectively (**Figures 2A, B**). By infecting cells for 1 h with an MOI of 10, 8% of the cells were infected as determined by flow cytometry, reflected in intracellular *Mav* counts of $1.2 \times 10^4 \pm 2 \times 10^3$ CFU. In contrast, *Mtb*-MeJuSo cells reached an infection rate of near 30% at an MOI of 10 (**Figure 2A**) (17). Cells exposed to an MOI of 20, 50 or 100 of *Mav* showed a mean infection rate of 11, 18 or 22% and CFU counts of $2.5 \times 10^4 \pm 8 \times 10^3$, $5.3 \times 10^4 \pm 2 \times 10^4$, or $1.1 \times 10^5 \pm 3 \times 10^4$, respectively. After 24 h incubation, intracellular bacterial loads were similar to bacterial loads directly after infection (**Figure 2B**), suggesting a steady state infection during the first 24 h.

In addition to the MeJuSo-*Mav* infection model, we also developed a *Mav*-infection model using primary monocyte-derived human macrophages, differentiated into two diametrically opposed subsets, namely GM-CSF driven classically activated pro-inflammatory macrophages (M1), and M-CSF driven alternatively activated anti-inflammatory macrophages (M2), which represent the two main phenotypes of human alveolar macrophages (26, 27). A clear MOI-associated increase in infection was observed for both M1 and M2 (**Figure 2C**); using an MOI of 1, 10 and 100, M1 showed infection percentages of 6, 22 and 60%, respectively, while 7, 64 and 93% of M2 were infected. Using a similar model, the infection rates for MOI 10 *Mtb*-infected macrophages were reported to be 41% and 67% for M1 and M2, respectively (**Figure 2C**) (17). No differences were observed in flow-cytometry based infection levels between M1 and M2, and also no consistent significant differences in numbers of CFU were observed between these cells (**Figure 2D**). In addition to the laboratory *Mav* strain, we also evaluated the phagocytosis capacity of the macrophages for the three *Mav* clinical isolates 100, 568 and 918. The uptake by M1 and M2 of these clinical isolates during infection at MOI 10 was in the same magnitude ($3.3 \times 10^4 \pm 5 \times 10^3$, $2.4 \times 10^4 \pm 4 \times 10^3$ and $3.5 \times 10^4 \pm 1 \times 10^3$ CFU) as observed for the laboratory strain (**Figure 2E**).

The above results show that primary macrophages are more readily infected with *Mav* compared to MeJuSo cells. Using an MOI of 10 in the macrophage *Mav* model or an MOI of 50 in MeJuSo model will allow detection of at least a 3-log reduction (i.e., bacterial survival from 100% down to 0.1%), in intracellular bacterial load, which will be sufficient to identify efficacious (HDT) compounds, while at the same time not overloading the cells with bacteria.

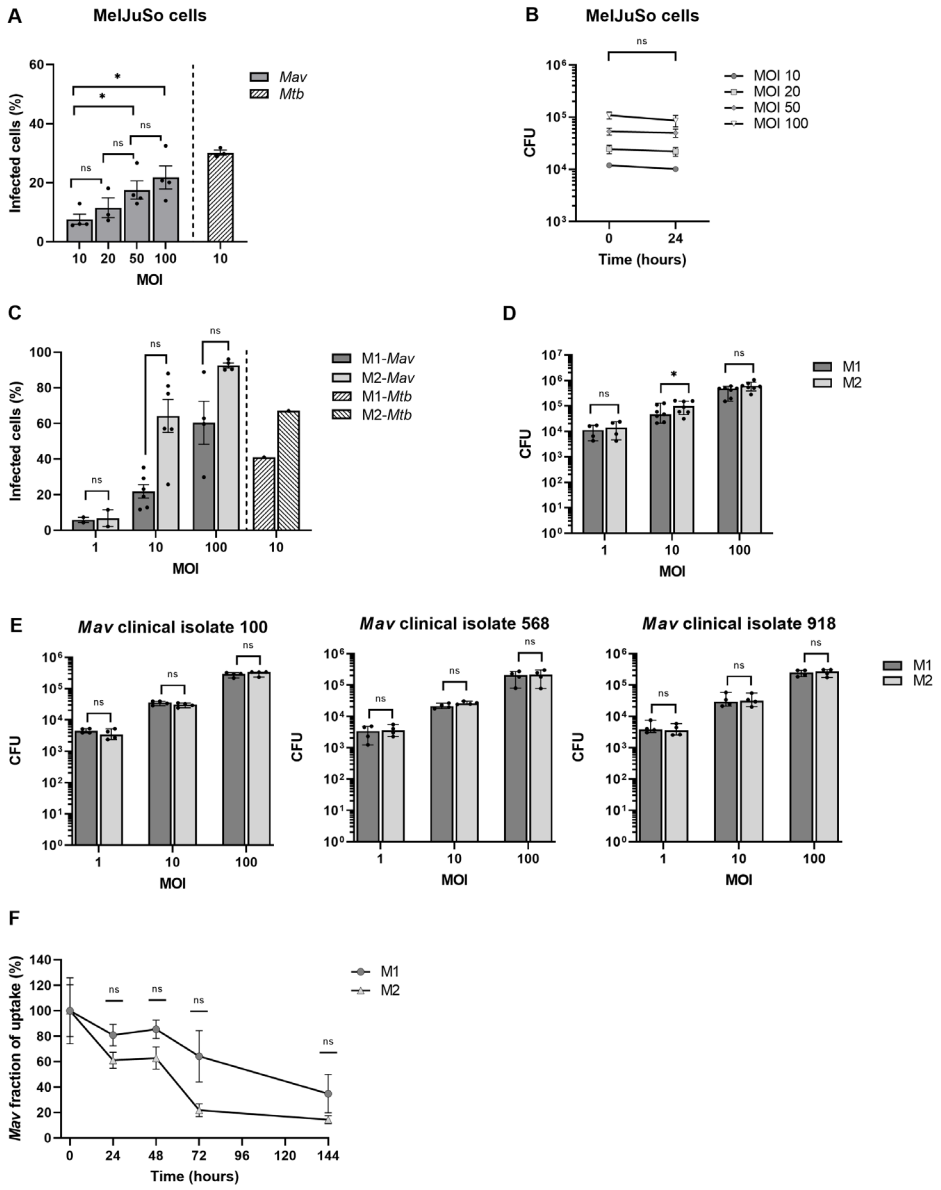

Figure 2. Quantification of infection with and eradication of intracellular *Mav* Wasabi and/or clinical isolates by flow cytometry and/or CFU enumeration in MeJuSo cells and primary human macrophages. MeJuSo cells were infected with a multiplicity of infection (MOI) range of *Mav* Wasabi for 1 h. Directly after infection (0 h post-infection), the percentage of infected cells was determined by flow cytometry **(A)** and intracellular bacterial load was quantified using a CFU assay **(B)**. Bacterial elimination was monitored by lysing cells for CFU analysis 24 h post-infection **(B)**. The bars and whiskers represent the mean±SEM of four different experiments. Differences were tested for statistical significant using one-way ANOVA with Tukey's multiple comparison testing for infection rates between indicated MOI **(A)** or two-way ANOVA with Bonferroni's multiple comparison testing for CFU between time points for each MOI **(B)**. Monocyte-derived human

macrophages differentiated into pro-inflammatory macrophages (M1) or anti-inflammatory macrophages (M2) were infected with a multiplicity of infection (MOI) range **(C, D)** or MOI of 10 **(F)** of *Mav* Wasabi for 1 h. M1 and M2 macrophages were also exposed to an MOI range of three *Mav* clinical isolate strains 100, 568 and 918 **(E)**. Directly after infection (0 h post-infection), the percentage of infected cells was determined by flow cytometry **(C)** and intracellular bacterial load was quantified using a CFU assay **(D, E)**. In *Mav* Wasabi-infected macrophages, eradication of bacteria was monitored over time by lysing cells for CFU analysis at indicated time points post-infection **(F)**. Primary human macrophages were obtained from 4-7 different donors. The bars/symbols and whiskers/error bars represent the mean±SEM **(C, F)** or median±range **(D, E)**. Dark and light bars represent M1 and M2, respectively. Hatched bars represent previously reported infection rates in *Mtb*-infected cells (10:1). Relevance of observed differences in infection rate and intracellular bacteria between M1 and M2 at each MOI was tested using Wilcoxon matched-pairs signed rank tests with Holm-Sidak multiple comparison testing **(C, D, E)**, whereas two-way ANOVA with Bonferroni's multiple comparison testing was used for CFU between time points **(F)** *: $p<0.05$, ns: non-significant.

Primary macrophages are able to control intracellular *Mav* early after infection

To determine how effective macrophages are in controlling *Mav* infection, clearance of *Mav* Wasabi by M1 and M2 exposed to MOI 10 was assessed 24, 48, 72 and 144 h post-infection (**Figure 2F**). Numbers of CFU decreased in both M1 and M2, with M2 seemingly better in controlling the infection. At the last time point, 144 h post-infection, 65±20% and 86±12% of intracellular bacteria were eliminated in M1 and M2, respectively (**Figure 2F**).

Additionally, we compared the intracellular elimination of *Mav* by macrophages with *Mtb* over time. We previously described kinetic analysis of intracellular *Mtb* survival in a similar M2 model, which showed a rapid reduction in *Mtb* bacterial load (21). These cells eliminated *Mtb* by at least 85% after 24 h, implying that *Mtb* is instantly controlled after infection, while this was less profound for *Mav* (39±17%, **Figure 2F**). *Mav* was, however, controlled to a similar extent as *Mtb* eventually (86±12% and 97.8% elimination, respectively).

MGIT as alternative to quantify intracellular bacteria

To increase throughput and to enhance objectivity (since CFU agar plate assays are known to result in inter-observer variation when enumerating colonies), the BACTEC MGIT 960 system was used to quantify bacteria by measuring bacterial metabolic activity as a surrogate for bacterial loads.

Intracellular bacterial loads of *Mav*-infected macrophages estimated by the MGIT significantly correlated with the CFU counted from plates (Spearman r: 0.78; p-value = 0.011) and intra-assay variation for data obtained with the MGIT seemed to be smaller (coefficient of variation: 36% compared to 51% for plate-counted CFU analysis; p-value = 0.109) (**Figure 3A**).

To obtain further insight into the usefulness of our infection model, we compared the MGIT system to determine the activity of first-line antibiotic rifampicin on intracellular *Mav* to the classical CFU assay (**Figure 3B**). Rifampicin-induced effects determined by MGIT are in concordance with the classical CFU assay for both M1 and M2. This indicates that the MGIT system, which showed a trend of higher CFU numbers possibly due to liquid medium as inherent characteristic, was able to observe compound-induced effect.

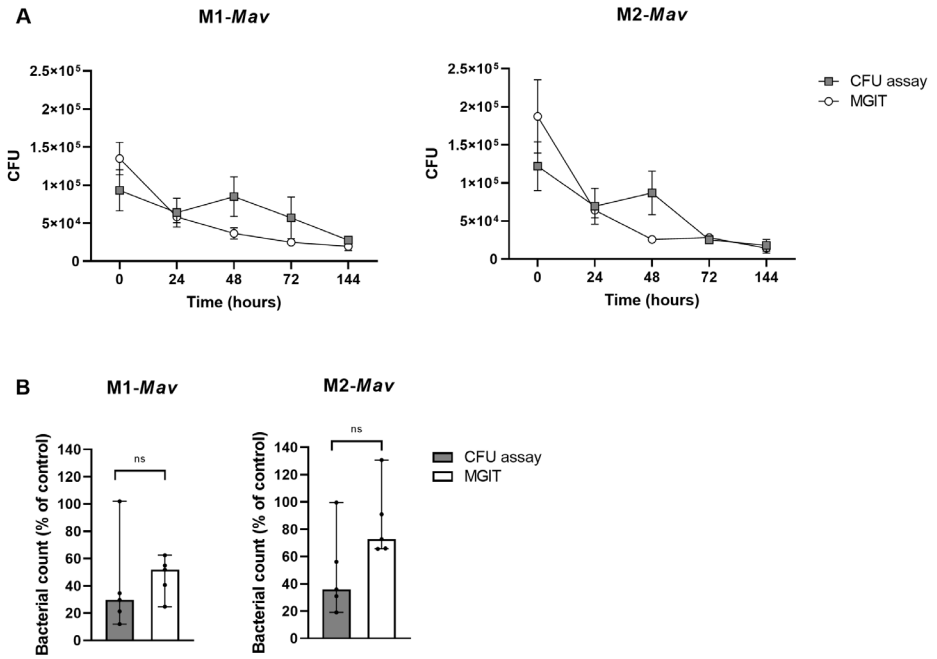

Figure 3. Quantification and comparison of infection with and eradication of intracellular *Mav* Wasabi by CFU enumeration based on agar plate assay and the MGIT system in primary human macrophages (A). Validation of the MGIT system to determine antibiotic efficacy in primary human macrophages infected with *Mav* Wasabi **(B)**. To assess the MGIT system as a valid enumeration technique of intracellular bacteria, pro-inflammatory macrophages (M1) or anti-inflammatory macrophages (M2) were infected with a MOI 10 of *Mav* Wasabi for 1 h. After infection and during prolonged incubation, intracellular bacterial loads were quantified using the classical CFU assay and the MGIT system **(A)**. The MGIT system was validated for its use for drug testing by treating *Mav*-infected M1 and M2 (10:1) with rifampicin (20 µg/mL) or control (DMSO) for 24 hours **(B)**. After treatment, cells were lysed and CFU numbers in lysates were determined by using the classical CFU assay and the MGIT assay. The symbols and whiskers represent the mean±SEM of counted (grey boxes) and MGIT-based (open circles) CFU numbers (n=3) **(A)**, whereas the bars and error bars represent the median±range (n=5) **(B)**. CFU numbers determined by either the CFU assay or MGIT were significantly correlated (Spearman r: 0.78; p-value=0.011) **(A)** and Wilcoxon matched-pairs signed rank tests with Holm-Sidak multiple comparison testing was used to compare compound-induced effects between both methods **(B)**. Ns: non-significant.

Additionally, the intra-assay variation in MGIT seemed to be smaller compared to classical CFU assay (coefficient of variation: 32% versus 78%, respectively; p-value: 0.170), as observed in **Figure 3A**. Based on these data, we considered the MGIT system as a viable alternative to plate-counting CFU analysis for the determination of intracellular bacterial loads.

Currently, the gold standard to evaluate antibacterial activity of chemical compounds is by monitoring the growth of bacteria in the extracellular space (i.e., broth microdilutions) (28). Also identified in this way was the first new tuberculosis drug in several decades, bedaquiline, which showed bactericidal activity against (multi-drug resistant) *Mtb* but has also shown promising results against extracellular *Mav* and other NTM *in vitro* (29-

32). Interestingly, cases of bedaquiline-resistance have also been reported (33-35). Here, we applied the MGIT system to drug susceptibility testing by determining the susceptibility to both rifampicin and bedaquiline of intracellular *Mav* (within M1) in comparison to extracellular bacteria (in liquid broth).

While a concentration of 1.29 µg/mL rifampicin significantly impaired growth of extracellular bacteria (97% as compared to untreated controls), only a 31% reduction was observed in intracellular bacteria (**Figure 4A**). In line, bedaquiline treatment (1.74 µg/mL) impaired extracellular bacterial growth completely, while intracellular bacteria were only reduced by 17% as compared to untreated controls (**Figure 4B**). These findings show the higher susceptibility of extracellular bacteria to antibiotics, indicating that extracellular drug testing might overestimate bacterial susceptibility to treatments during the course of intracellular infection *in vivo*. Taken together, our *Mav*-macrophage model facilitates screening of antibacterial agents against intracellular *Mav* and emphasizes the importance of measuring the intracellular compartment on antibiotic-susceptibility.

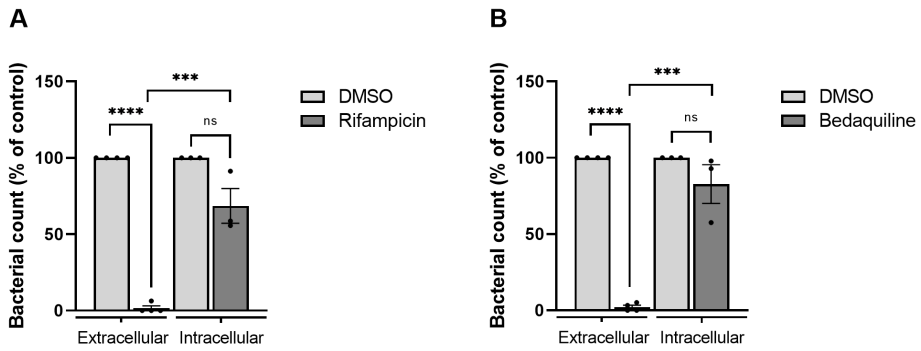

Figure 4. Evaluation of drug susceptibility of *Mav* Wasabi extracellularly in liquid broth versus intracellularly in primary human macrophages. To determine differential susceptibility of intracellular versus extracellular *Mav* to antibiotics, *Mav* Wasabi in liquid broth was cultured with a range of concentrations of rifampicin **(A)**, bedaquiline **(B)** or control (DMSO). Bacterial outgrowth was monitored by absorbance measurements at 600 nm. After 14 days incubation, the minimum concentration in which rifampicin **(A)** and bedaquiline **(B)** was assessed to be 1.29 µg/mL and 1.74 µg/mL, respectively, and used for intracellular activity evaluation. Pro-inflammatory macrophages (M1) were infected with a MOI 10 of *Mav* Wasabi for 1 h. After infection, cells were treated with rifampicin (1.29 µg/mL), bedaquiline (1.74 µg/mL) or control (DMSO) for 24 hours. After treatment, cells were lysed, and intracellular bacterial loads were determined by the MGIT system. The bar and whiskers represent the mean±SEM of extracellular (n=4) or intracellular (n=3) experiments. Statistics were performed using paired t-tests to compare activity of antibiotic to control within each type of experiment and unpaired t-tests were used to determine differences between potency of antibiotic against extracellular versus intracellular bacteria. ***:$p < 0.001$, ****:$p < 0.0001$, ns: non-significant.

Discussion

The incidence of *Mav* pulmonary disease is increasing rapidly (36, 37), whose therapy, despite being long and comprising multiple drugs, still has poor efficacy, as illustrated by the estimated poor cure rate of about 39% (14). The limited treatment success may be due to the fact that development of new drugs is routinely tested using DST (36), that

is on extracellular bacteria, while *Mav* is an intracellular pathogen whose drug sensitivity may be vastly different intracellularly as compared to extracellularly. We therefore aimed to set up a model to determine intracellular numbers of *Mav* and the two present models, one using a human phagocytic (melanoma derived) cell line and one with primary human macrophages. In these models, viability of intracellular bacteria could be monitored and quantified over time using a classical CFU assay as well as the MGIT assay. Our models identified that the activity of first-line drug rifampicin and new class antibiotic bedaquiline was 3.1-fold and 5.7-fold less potent on intracellular bacteria as compared to extracellular bacteria, which may be caused by altered bacterial biology within host cells that affects drug susceptibility and/or limited exposure to antibiotics. The latter is at least partially involved as intracellular drug concentrations of rifampicin and bedaquiline have been shown to be lower than drug treatment concentrations (38, 39). Hence, our findings emphasize the importance of taking the intracellular efficacy of an antibiotic regimen into account, for which the models presented can be exploited.

Macrophages are known to play an essential role in *Mav* infections and many host-pathogen interactions occur, of which the exact mechanisms remain to be elucidated (40-42). Macrophages are known to play an essential role in *Mav* infections and many host-pathogen interactions occur, of which the exact mechanisms remain to be elucidated (20, 40-42). To decipher these mechanisms in the natural niche of *Mav*, we developed a model that uses primary human monocyte-derived macrophages that can be used to study infections up to at least 6 days post infection. Although using primary cells is physiologically more relevant, limits on numbers of available cells and particularly inter-donor-variation restrict its use in high- and medium-throughput screenings. In literature, models using cell lines THP-1 and U937 (43-46) have been used. These however, require PMA stimulation, which largely disrupts and/or interferes with intracellular signaling pathways and is thereby unsuitable to identify novel HDTs (47, 48). To circumvent this limitation, we have adapted a model using MelJuSo cells, which we have previously used to study *Mtb* infections and which do not require such pre-stimulation (17). The MelJuSo cell line is derived from human melanocytes, and the latter have been shown to share several important characteristics with professional phagocytes like macrophages: (1) Melanocytes have acidic and hydrolyse-containing vesicles, melanosomes, which very likely can function as lysosomes present in primary macrophages (49); (2) Melanocytes can also produce superoxides, which are one of the important antibacterial molecules produced by macrophages; and (3) Human melanocytes also have shown to process and present mycobacterial antigens to human T cells (50-52). The functional immune characteristics shared between melanocytes and macrophages are indirectly supported by Korbee et al. (17), who showed that the activity of published as well as newly discovered host-directed compounds in MelJuSo cells could be validated in human macrophages. Thus, whereas the MelJuSo model allows medium-throughput HDT compound screenings, relevant hits can be validated in the low-throughput primary macrophage model.

During mycobacterial infections, many host-pathogen interactions are at play that modulate both innate and adaptive immune responses to a large extent and are exploited by mycobacteria to facilitate bacterial survival. Consequently, modulating these interactions in favor of the host using so-called HDTs are appealing to improve the outcome. The presented model system is most suitable to study HDTs that target

intracellular processes within macrophages, but cannot assess the effects of HDTs acting systemically, including promoting adaptive immune responses. However, the impact of HDTs on macrophage-mediated antigen presentation can be assessed in our new model. While for *Mtb* many potent effector functions of macrophages have been shown to be manipulated as part of *Mtb*'s strategy to survive intracellularly, our understanding of host-pathogen interactions of *Mav* is limited (20, 41, 53, 54). To improve our understanding of these processes, the models presented in this paper are ideally suitable and can furthermore be exploited to identify HDTs to improve treatment of *Mav*.

Quantification of mycobacteria is traditionally done using CFU assays, despite being labor-intensive, time-consuming and prone to inter-individual variation. To improve objectivity and robustness, we validated the BACTEC MGIT 960 system, a liquid culture system with fully automated detection to monitor intracellular bacteria over time, by showing strong correlation with the CFU assay, but with seemingly less variation. The MGIT has already been shown to be a robust, objective and valid system for direct and indirect DST against *Mtb* (55-58), which is in line with previously identified concordance between MGIT measurements and CFU counting on solid media (59, 60). The MGIT system, however, measures metabolic activity in a liquid culture while CFU assays rely on growth on solid media, which might be differently affected by certain treatments. It has been shown that liquid medium offers a higher mycobacterial recovery rate, likely due to a wider range of mycobacterial populations being able to outgrow in liquid, but not in solid cultures and liquid broth thereby enables growth of mycobacterial populations which can also be present *in vivo* (61, 62). In line with this, rifampicin treatment appeared to be more effective in the conventional CFU assay, as compared to MGIT, which likely is merely a reflection of bacterial colonies that are unable to grow on solid agar after rifampicin treatment than being a real effect. Consequently, enumeration of CFU on solid media could underestimate the residual mycobacterial populations after anti-*Mav* treatment and MGIT may be a better indicator of mycobacterial survival, and therefore physiologically more relevant.

Here, by establishing the optimal infection conditions, we developed *in vitro* human cell-based infection models for *Mav*. Both the MelJuSo cell line and primary human macrophages were capable of phagocytosing *Mav* and intracellular survival of *Mav* within primary macrophages could be evaluated by using the MGIT system as an alternative to the classical CFU assay. The relevance and importance of such *Mav*-infection models is highlighted by our finding that antibiotics were unable to eradicate intracellular *Mav*, while extracellular bacteria exposed to the same drug concentration were eliminated. Taken together, the models described here can be used to improve *Mav* therapy by also taking into account intracellular bacteria, and furthermore to advance our understanding of host-pathogen interactions and ultimately develop (host-directed) therapies to combat *Mav* infections.

Data availability statement

The raw data supporting the conclusions of this article will be made available by the authors, without undue reservation.

Author contributions

GK designed and performed the experiments, analyzed the data and drafted the figures. Construction of the pSMT3 construct was done by KF, whereas KW performed the electroporation. MV supported in performing experiments. GK, MH, TO and AS contributed to the interpretation of the results. AA isolated and provided the clinical isolates. GK wrote the manuscript. MH, AS and TO supervised the project and together with AA provided critical revision of the manuscript. All authors Contributed to the article and approved the submitted version.

Funding

This project has received funding from the Innovative Medicines Initiative 2 Joint Undertaking (IMI2 JU) (www.imi.europa.eu) under the RespiriNTM (grant N° 853932) project within the IMI AntiMicrobial Resistance (AMR) Accelerator program. The JU receives support from the European Union's Horizon 2020 research and innovation programme and EFPIA. The funders had no role in study design, data collection and analysis, decision to publish, or preparation of the manuscript. All claims expressed in this article reflect solely the authors' view and do not necessarily represent those of the JU. The JU is not responsible for any use that may be made of the information it contains. The authors would like to thank Jacques Neefjes for providing the MelJuSo cell line, Herman Spaink for providing the pTEC15-Wasabi plasmid and Dirk Lamprecht for providing bedaquiline.

Acknowledgments

The authors would like to thank Jacques Neefjes for providing the MelJuSo cell line, Herman Spaink for providing the pTEC15-Wasabi plasmid, and Dirk Lamprecht for providing bedaquiline.

Conflict of interest

The authors declare that the research was conducted in the absence of any commercial or financial relationships that could be construed as a potential conflict of interest.

References

1. Adjemian J, Olivier KN, Seitz AE, Holland SM, Prevots DR. Prevalence of nontuberculous mycobacterial lung disease in U.S. Medicare beneficiaries. Am J Respir Crit Care Med. 2012;185(8):881-6.
2. Marras TK, Chedore P, Ying AM, Jamieson F. Isolation prevalence of pulmonary non-tuberculous mycobacteria in Ontario, 1997 2003. Thorax. 2007;62(8):661-6.
3. Rindi L, Garzelli C. Genetic diversity and phylogeny of Mycobacterium avium. Infect Genet Evol. 2014;21:375-83.
4. Olivier KN, Weber DJ, Wallace RJ, Jr., Faiz AR, Lee JH, Zhang Y, et al. Nontuberculous mycobacteria. I: multicenter prevalence study in cystic fibrosis. Am J Respir Crit Care Med. 2003;167(6):828-34.
5. Daley CL. Mycobacterium avium Complex Disease. Microbiol Spectr. 2017;5(2).
6. Corti M, Palmero D. Mycobacterium avium complex infection in HIV/AIDS patients. Expert Rev Anti-Infe. 2008;6(3):351-63.
7. Ottenhoff TH, Verreck FA, Lichtenauer-Kaligis EG, Hoeve MA, Sanal O, van Dissel JT. Genetics, cytokines and human infectious disease: lessons from weakly pathogenic mycobacteria and salmonellae. Nat Genet. 2002;32(1):97-105.
8. Inderlied CB, Kemper CA, Bermudez LE. The Mycobacterium avium complex. Clin Microbiol Rev. 1993;6(3):266-310.
9. Field SK, Fisher D, Cowie RL. Mycobacterium avium complex pulmonary disease in patients without HIV infection. Chest. 2004;126(2):566-81.
10. Arend SM, van Soolingen D, Ottenhoff TH. Diagnosis and treatment of lung infection with nontuberculous mycobacteria. Curr Opin Pulm Med. 2009;15(3):201-8.

11. Daley CL, Iaccarino JM, Lange C, Cambau E, Wallace RJ, Jr., Andrejak C, et al. Treatment of nontuberculous mycobacterial pulmonary disease: an official ATS/ERS/ESCMID/IDSA clinical practice guideline. Eur Respir J. 2020;56(1).
12. Kwon YS, Koh WJ, Daley CL. Treatment of Mycobacterium avium Complex Pulmonary Disease. Tuberc Respir Dis (Seoul). 2019;82(1):15-26.
13. van Ingen J, Boeree MJ, van Soolingen D, Mouton JW. Resistance mechanisms and drug susceptibility testing of nontuberculous mycobacteria. Drug Resist Updat. 2012;15(3):149-61.
14. Xu HB, Jiang RH, Li L. Treatment outcomes for Mycobacterium avium complex: a systematic review and meta-analysis. Eur J Clin Microbiol Infect Dis. 2014;33(3):347-58.
15. Koh WJ, Hong G, Kim SY, Jeong BH, Park HY, Jeon K, et al. Treatment of Refractory Mycobacterium avium Complex Lung Disease with a Moxifloxacin-Containing Regimen. Antimicrobial Agents and Chemotherapy. 2013;57(5):2281-5.
16. Veziris N, Andrejak C, Bouee S, Emery C, Obradovic M, Chiron R. Non-tuberculous mycobacterial pulmonary diseases in France: an 8 years nationwide study. BMC Infect Dis. 2021;21(1):1165.
17. Korbee CJ, Heemskerk MT, Kocev D, van Strijen E, Rabiee O, Franken K, et al. Combined chemical genetics and data-driven bioinformatics approach identifies receptor tyrosine kinase inhibitors as host-directed antimicrobials. Nat Commun. 2018;9(1):358.
18. Moreira JD, Koch BEV, van Veen S, Walburg KV, Vrieling F, Mara Pinto Dabes Guimaraes T, et al. Functional Inhibition of Host Histone Deacetylases (HDACs) Enhances *in vitro* and *in vivo* Anti-mycobacterial Activity in Human Macrophages and in Zebrafish. Front Immunol. 2020;11:36.
19. Early J, Fischer K, Bermudez LE. Mycobacterium avium uses apoptotic macrophages as tools for spreading. Microb Pathogenesis. 2011;50(2):132-9.
20. Kilinc G, Saris A, Ottenhoff THM, Haks MC. Host-directed therapy to combat mycobacterial infections. Immunol Rev. 2021;301(1):62-83.
21. Vrieling F, Wilson L, Rensen PCN, Walzl G, Ottenhoff THM, Joosten SA. Oxidized low-density lipoprotein (oxLDL) supports Mycobacterium tuberculosis survival in macrophages by inducing lysosomal dysfunction. PLoS Pathog. 2019;15(4):e1007724.
22. Tortoli E, Cichero P, Piersimoni C, Simonetti MT, Gesu G, Nista D. Use of BACTEC MGIT 960 for recovery of mycobacteria from clinical specimens: multicenter study. J Clin Microbiol. 1999;37(11):3578-82.
23. Verreck FA, de Boer T, Langenberg DM, van der Zanden L, Ottenhoff TH. Phenotypic and functional profiling of human proinflammatory type-1 and anti-inflammatory type-2 macrophages in response to microbial antigens and IFN-gamma- and CD40L-mediated costimulation. J Leukoc Biol. 2006;79(2):285-93.
24. Gaora PO. Expression of genes in mycobacteria. Methods Mol Biol. 1998;101:261-73.
25. Ratnatunga CN, Lutzky VP, Kupz A, Doolan DL, Reid DW, Field M, et al. The Rise of Non-Tuberculosis Mycobacterial Lung Disease. Front Immunol. 2020;11:303.
26. Hu G, Christman JW. Editorial: Alveolar Macrophages in Lung Inflammation and Resolution. Front Immunol. 2019;10:2275.
27. Mitsi E, Kamng'ona R, Rylance J, Solorzano C, Jesus Reine J, Mwandumba HC, et al. Human alveolar macrophages predominately express combined classical M1 and M2 surface markers in steady state. Respir Res. 2018;19(1):66.
28. Brown-Elliott BA, Nash KA, Wallace RJ, Jr. Antimicrobial susceptibility testing, drug resistance mechanisms, and therapy of infections with nontuberculous mycobacteria. Clin Microbiol Rev. 2012;25(3):545-82.
29. Brown-Elliott BA, Philley JV, Griffith DE, Thakkar F, Wallace RJ, Jr. *In vitro* Susceptibility Testing of Bedaquiline against Mycobacterium avium Complex. Antimicrob Agents Chemother. 2017;61(2).
30. Aguilar-Ayala DA, Cnockaert M, Andre E, Andries K, Gonzalez YMJA, Vandamme P, et al. *In vitro* activity of bedaquiline against rapidly growing nontuberculous mycobacteria. J Med Microbiol. 2017;66(8):1140-3.
31. Mahajan R. Bedaquiline: First FDA-approved tuberculosis drug in 40 years. Int J Appl Basic Med Res. 2013;3(1):1-2.
32. Vesenbeckh S, Schonfeld N, Roth A, Bettermann G, Krieger D, Bauer TT, et al. Bedaquiline as a potential agent in the treatment of Mycobacterium abscessus infections. Eur Respir J. 2017;49(5).
33. Philley JV, Wallace RJ, Benwill JL, Taskar V, Brown-Elliott BA, Thakkar F, et al. Preliminary Results of Bedaquiline as Salvage Therapy for Patients With Nontuberculous Mycobacterial Lung Disease. Chest. 2015;148(2):499-506.
34. Alexander DC, Vasireddy R, Vasireddy S, Philley JV, Brown-Elliott BA, Perry BJ, et al. Emergence of mmpT5 Variants during Bedaquiline Treatment of Mycobacterium intracellulare Lung Disease. J Clin Microbiol. 2017;55(2):574-84.
35. Veziris N, Bernard C, Guglielmetti L, Le Du D, Marigot-Outtandy D, Jaspard M, et al. Rapid emer-

gence of Mycobacterium tuberculosis bedaquiline resistance: lessons to avoid repeating past errors. Eur Respir J. 2017;49(3).
36. Griffith DE, Aksamit T, Brown-Elliott BA, Catanzaro A, Daley C, Gordin F, et al. An official ATS/IDSA statement: Diagnosis, treatment, and prevention of nontuberculous mycobacterial diseases. Am J Resp Crit Care. 2007;175(4):367-416.
37. Kendall BA, Winthrop KL. Update on the Epidemiology of Pulmonary Nontuberculous Mycobacterial Infections Preface. Semin Resp Crit Care. 2013;34(1):87-94.
38. Kumar PV, Asthana A, Dutta T, Jain NK. Intracellular macrophage uptake of rifampicin loaded mannosylated dendrimers. J Drug Target. 2006;14(8):546-56.
39. Tanner L, Mashabela GT, Omollo CC, de Wet TJ, Parkinson CJ, Warner DF, et al. Intracellular Accumulation of Novel and Clinically Used TB Drugs Potentiates Intracellular Synergy. Microbiol Spectr. 2021;9(2):e0043421.
40. de Chastellier C, Thilo L. Pathogenic Mycobacterium avium remodels the phagosome membrane in macrophages within days after infection. Eur J Cell Biol. 2002;81(1):17-25.
41. Rocco JM, Irani VR. Mycobacterium avium and modulation of the host macrophage immune mechanisms. Int J Tuberc Lung Dis. 2011;15(4):447-52.
42. McGarvey J, Bermudez LE. Pathogenesis of nontuberculous mycobacteria infections. Clin Chest Med. 2002;23(3):569-83.
43. Danelishvili L, Poort MJ, Bermudez LE. Identification of Mycobacterium avium genes up-regulated in cultured macrophages and in mice. FEMS Microbiol Lett. 2004;239(1):41-9.
44. Garcia RC, Banfi E, Pittis MG. Infection of macrophage-like THP-1 cells with Mycobacterium avium results in a decrease in their ability to phosphorylate nucleolin. Infect Immun. 2000;68(6):3121-8.
45. Ichimura N, Sato M, Yoshimoto A, Yano K, Ohkawa R, Kasama T, et al. High-Density Lipoprotein Binds to Mycobacterium avium and Affects the Infection of THP-1 Macrophages. J Lipids. 2016;2016:4353620.
46. Orme IM, Roberts AD, Furney SK, Skinner PS. Animal and Cell-Culture Models for the Study of Mycobacterial Infections and Treatment. Eur J Clin Microbiol. 1994;13(11):994-9.
47. Liu WS, Heckman CA. The sevenfold way of PKC regulation. Cell Signal. 1998;10(8):529-42.
48. Wu-Zhang AX, Newton AC. Protein kinase C pharmacology: refining the toolbox. Biochem J. 2013;452(2):195-209.
49. Le Poole IC, van den Wijngaard RM, Westerhof W, Verkruisen RP, Dutrieux RP, Dingemans KP, et al. Phagocytosis by normal human melanocytes *in vitro*. Exp Cell Res. 1993;205(2):388-95.
50. Le Poole IC, Mutis T, van den Wijngaard RM, Westerhof W, Ottenhoff T, de Vries RR, et al. A novel, antigen-presenting function of melanocytes and its possible relationship to hypopigmentary disorders. J Immunol. 1993;151(12):7284-92.
51. van Ham M, van Lith M, Lillemeier B, Tjin E, Gruneberg U, Rahman D, et al. Modulation of the major histocompatibility complex class II-associated peptide repertoire by human histocompatibility leukocyte antigen (HLA)-DO. Journal of Experimental Medicine. 2000;191(7):1127-35.
52. van Ham SM, Tjin EP, Lillemeier BF, Gruneberg U, van Meijgaarden KE, Pastoors L, et al. HLA-DO is a negative modulator of HLA-DM-mediated MHC class II peptide loading. Curr Biol. 1997;7(12):950-7.
53. Abreu R, Giri P, Quinn F. Host-Pathogen Interaction as a Novel Target for Host-Directed Therapies in Tuberculosis. Front Immunol. 2020;11:1553.
54. Upadhyay S, Mittal E, Philips JA. Tuberculosis and the art of macrophage manipulation. Pathog Dis. 2018;76(4).
55. Huang TS, Lee SSJ, Tu HZ, Huang WK, Chen YS, Huang CK, et al. Use of MGIT 960 for rapid quantitative measurement of the susceptibility of Mycobacterium tuberculosis complex to ciprofloxacin and ethionamide. J Antimicrob Chemoth. 2004;53(4):600-3.
56. Jhamb SS, Goyal A, Singh PP. Determination of the activity of standard anti-tuberculosis drugs against intramacrophage Mycobacterium tuberculosis, *in vitro*: MGIT 960 as a viable alternative for BACTEC 460. Braz J Infect Dis. 2014;18(3):336-40.
57. Kolibab K, Yang A, Parra M, Derrick SC, Morris SL. Time to Detection of Mycobacterium tuberculosis Using the MGIT 320 System Correlates with Colony Counting in Preclinical Testing of New Vaccines. Clin Vaccine Immunol. 2014;21(3):453-5.
58. Shin SJ, Han JH, Manning EJB, Collins MT. Rapid and reliable method for quantification of Mycobacterium paratuberculosis by use of the BACTEC MGIT 960 system. Journal of Clinical Microbiology. 2007;45(6):1941-8.
59. Diacon AH, Maritz JS, Venter A, van Helden PD, Andries K, McNeeley DF, et al. Time to detection of the growth of Mycobacterium tuberculosis in MGIT 960 for determining the early bactericidal activity of antituberculosis agents. Eur J Clin Microbiol. 2010;29(12):1561-5.
60. Pheiffer C, Carroll NM, Beyers N, Donald P, Duncan K, Uys P, et al. Time to detection of Myco-

bacterium tuberculosis in BACTEC systems as a viable alternative to colony counting. Int J Tuberc Lung D. 2008;12(7):792-8.
61. Dhillon J, Lowrie DB, Mitchison DA. Mycobacterium tuberculosis from chronic murine infections that grows in liquid but not on solid medium. BMC Infect Dis. 2004;4:51.
62. Mitchison DA, Coates AR. Predictive *in vitro* models of the sterilizing activity of anti-tuberculosis drugs. Curr Pharm Des. 2004;10(26):3285-95.

Supplementary material

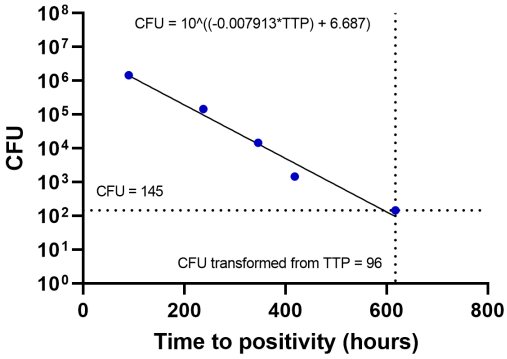

Supplementary Figure 1. Example of relationship between plate-counted CFU and TTP values, with equation used to convert TTP values into CFU numbers. For each MGIT experiment, the inoculum was serially diluted and CFU counts were determined by both the MGIT system and agar-plate counting. The plate-counted CFU and TTP measurements obtained for each dilution were plotted and linear regressed. The dotted lines represent the limit of detection for enumeration by classical CFU assay and the MGIT system. The equation derived from the linear regression was used to calculate CFU numbers from TTP values.

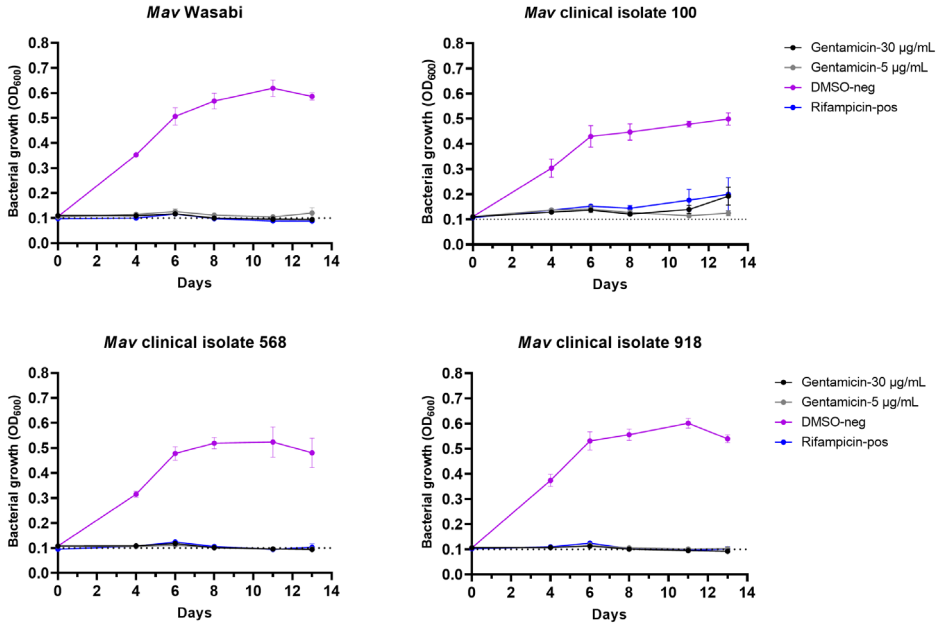

Supplementary Figure 2. Susceptibility of *Mav* strains to gentamicin and the validity for gentamicin-use to kill extracellular bacteria in infection protocols. Susceptibility to gentamicin, which was used to kill extracellular bacteria in infection protocols, was determined for the four *Mav* strains. Liquid cultures of *Mav* were exposed to 5 µg/mL or 30 µg/mL gentamicin,

DMSO (negative control) or rifampicin (positive control) and bacterial growth was monitored by absorbance measurements at 600 nm. Symbols and error bars represent the mean±SEM (n=4).

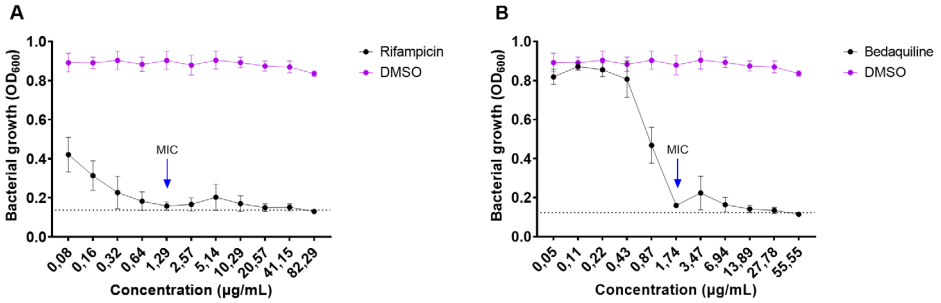

Supplementary Figure 3. Determination of the MIC of rifampicin and bedaquiline for *Mav* Wasabi using the broth microdilution method. The minimal inhibitory concentration (MIC) of rifampicin and bedaquiline was determined for *Mav* Wasabi, by exposing the bacteria in liquid broth to two-fold serial dilution of the antibiotics or control (DMSO). Bacterial growth was monitored by absorbance measurements at 600 nm. The arrow indicates the determined MIC. Symbols and error bars represent the mean±SEM (n=2).

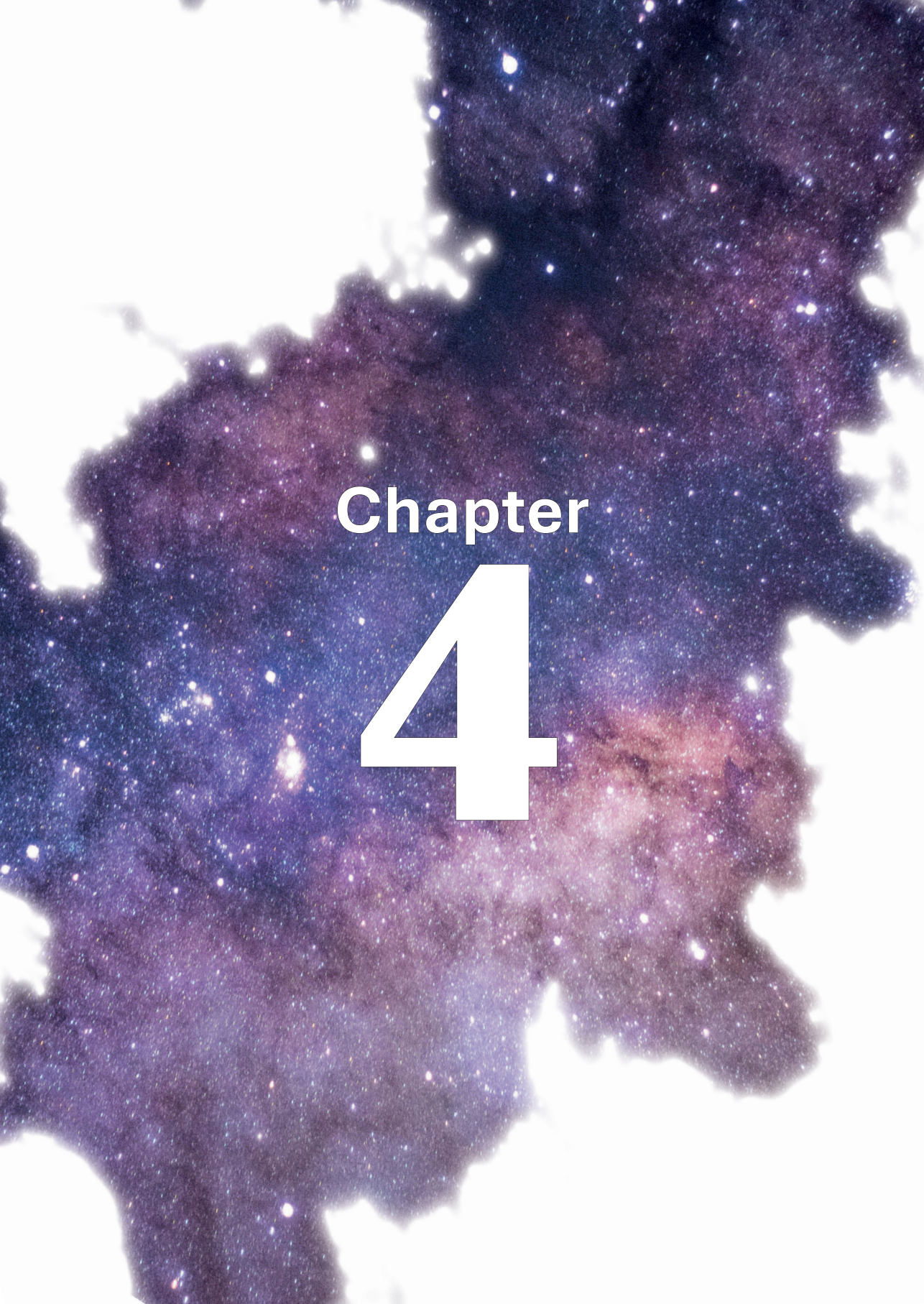
Chapter
4

Host-directed therapy with amiodarone in preclinical models restricts mycobacterial infection and enhances autophagy

Gül Kilinç[#,1], Ralf Boland[#,2], Matthias T. Heemskerk[1], Herman P. Spaink[2], Mariëlle C. Haks[1], Michiel van der Vaart[2], Tom H. M. Ottenhoff[1], Annemarie H. Meijer[#,2] and Anno Saris[#,1]

[1] Department of Infectious Diseases, Leiden University Medical Center, Leiden, The Netherlands
[2] Institute of Biology Leiden, Leiden University, Leiden, The Netherlands
[#] These authors contributed equally to this work

Microbiol Spectr. 2024 Aug 6;12(8):e0016724

Abstract
Mycobacterium tuberculosis (*Mtb*) as well as nontuberculous mycobacteria are intracellular pathogens whose treatment is extensive and increasingly impaired due to the rise of mycobacterial drug resistance. The loss of antibiotic efficacy has raised interest in the identification of host-directed therapeutics (HDT) to develop novel treatment strategies for mycobacterial infections. In this study, we identified amiodarone as a potential HDT candidate that inhibited both intracellular *Mtb* and *Mycobacterium avium* in primary human macrophages without directly impairing bacterial growth, thereby confirming that amiodarone acts in a host-mediated manner. Moreover, amiodarone induced the formation of (auto)phagosomes and enhanced autophagic targeting of mycobacteria in macrophages. The induction of autophagy by amiodarone is likely due to enhanced transcriptional regulation, as the nuclear intensity of the transcription factor EB, the master regulator of autophagy and lysosomal biogenesis, was strongly increased. Furthermore, blocking lysosomal degradation with bafilomycin impaired the host-beneficial effect of amiodarone. Finally, amiodarone induced autophagy and reduced bacterial burden in a zebrafish embryo model of tuberculosis, thereby confirming the HDT activity of amiodarone *in vivo*. In conclusion, we have identified amiodarone as an autophagy-inducing antimycobacterial HDT that improves host control of mycobacterial infections.

Introduction

In 2022, *Mycobacterium tuberculosis* (*Mtb*) infection affected an estimated 10.6 million people with tuberculosis (TB), of whom 1.3 million died, making TB one of the top 10 leading causes of death globally (1). TB is difficult to treat with classical antibiotics due to the presence of metabolically inactive, i.e., dormant, bacteria inside TB granulomas, the pathological hallmark of TB (2). These dormant bacteria are far less susceptible to antibiotics (3, 4). The occurrence of multidrug-resistant (MDR) and extensively drug-resistant (XDR) *Mtb* strains further complicates the treatment of TB. While the number of TB cases has been slowly declining in the last decades, a trend that may well be broken as a result of the COVID-19 pandemic (5), the prevalence of infections caused by nontuberculous mycobacteria (NTM) is increasing (1, 6, 7). NTM represent a group of opportunistic mycobacterial pathogens that mostly cause pulmonary diseases (PD), predominantly in populations vulnerable due to immunodeficiencies and/or pre-existing lung conditions. *Mycobacterium avium* (*Mav*) complex accounts for over 80% of the reported NTM-PD cases (8). Despite extensive antibiotic regimens of at least 12 months after negative sputum culture conversion, clinical outcome is poor. Furthermore, *Mav* and several other NTM species display a high level of natural resistance to antibiotics (9). Thus, both for TB and NTM diseases, the development of novel treatment modalities is highly desired.

A promising alternative or adjunctive therapy for mycobacterial infection is host-directed therapy (HDT) (10–14). HDT promotes the host's ability to eliminate invading pathogens either by stimulating host defense mechanisms or alleviating pathogen-induced manipulations of host cellular functions. By targeting host cells, HDT offers several advantages compared to conventional antibiotics: (i) HDT is less likely to result in drug resistance as the pathogen is not directly targeted; (ii) HDT is also effective against MDR/XDR mycobacteria that are insensitive to current standard antibiotics; (iii) HDT has the potential to be effective against dormant bacteria; and (iv) as HDT and antibiotics target different processes, they are expected to act synergistically, which could significantly reduce antibiotic treatment duration and/or dosage, thereby increasing compliance and reducing toxicity. To identify and develop HDT for mycobacterial infection, it is important to understand the host-pathogen interactions (11).

Mycobacteria are predominantly intracellular pathogens and macrophages are the main innate immune cell type wherein they survive and replicate. Macrophages attempt to eliminate mycobacteria in a process whereby mycobacteria are internalized and introduced in mycobacteria-containing phagosomes that mature and ultimately fuse with lysosomes (11, 15, 16). This process should result in the degradation of the content of the formed phagolysosomes by lysosomal hydrolytic enzymes (17). However, mycobacteria are well known for their capability to modulate signaling pathways to escape from host-defense mechanisms: both *Mtb* and *Mav* can arrest phagosome maturation and potentially escape into the cytosol (11, 17–19). Host cells try to capture and subsequently degrade cytosolic bacteria using the autophagy pathway (20, 21). Studies have already shown that induction of (non)-canonical autophagy in *Mtb*- and *Mav*-infected macrophages restricts intracellular bacterial growth, which supports further research into autophagy as a potential target for HDT (20, 22–24).

A previous drug repurposing screen of a library composed of autophagy-modulating compounds revealed that several antipsychotic drugs as well as the antiarrhythmic drug amiodarone reduce the bacterial burden of *Mtb* in a human cell line (25, 26). Amiodarone functions by blocking calcium, sodium, and potassium channels as well as inhibiting alpha- and beta-adrenergic receptors. Furthermore, amiodarone has been shown to induce autophagy (27–31), and by accumulating in acidic organelles, amiodarone may also interact with other intracellular degradation processes, like the endocytic pathway (32). Whether amiodarone improves host control of mycobacteria, however, has not been established. Here, we aimed to assess the efficacy of amiodarone in reducing mycobacterial burden, both in primary cells and *in vivo,* and to elucidate via which mechanism amiodarone acts as an HDT. To do so, both classically activated pro-inflammatory (M1) macrophages and alternatively activated anti-inflammatory (M2) macrophages were used as surrogates for the polar ends of the human macrophage differentiation spectrum *in vivo* (33). Furthermore, we used the zebrafish (*Danio rerio*) embryo model for TB, in which zebrafish embryos are infected with their natural pathogen *Mycobacterium marinum* (*Mmar*) (34–37), an NTM that shares major virulence factors with *Mtb* and is frequently used as a surrogate model for TB (37–40). The formation of granulomatous aggregates of leukocytes is recapitulated in the zebrafish TB model (2, 37, 38, 41). Moreover, the zebrafish model has been used to study the role of autophagy in mycobacterial infection, showing that autophagy contributes to host defense *in vivo* (40, 42–44). This makes the zebrafish embryo model for TB a highly suitable model to investigate the role of autophagy in the antimycobacterial effect of amiodarone.

In this study, we aimed to investigate amiodarone as HDT against multiple mycobacterial species in primary human macrophages. Moreover, to understand the mechanism of action of amiodarone, we evaluated the effect of amiodarone on autophagy and the role of autophagy during infection control by amiodarone. Finally, we assessed the efficacy of amiodarone in a zebrafish TB model to determine the *in vivo* translatability.

Results

In vitro identification of amiodarone as a novel HDT against intracellular mycobacteria

To identify new drugs with host-directed therapeutic activity against intracellular *Mtb,* we have previously screened the Screen-Well autophagy library of clinically approved molecules by treating *Mtb*-infected human cells for 24 hours (25). A promising candidate from this screen was amiodarone (**Fig. 1A**). To validate the antimycobacterial effect of amiodarone in a physiologically more relevant model, we used a primary human macrophage infection model (26). Classical colony-forming unit (CFU) assays were used to determine the reduction of intracellular *Mtb* load after 24 hours of treatment with 10 μM amiodarone. Amiodarone treatment significantly impaired intracellular bacterial survival in both M1 and M2 macrophages (**Fig. 1B; Fig. S1A**). To exclude direct antibacterial effects, *Mtb* in liquid broth was exposed to amiodarone at the same concentration, which did not show any effect of amiodarone (**Fig. 1C**), thereby confirming amiodarone acts in a host-directed manner during *Mtb* infection.

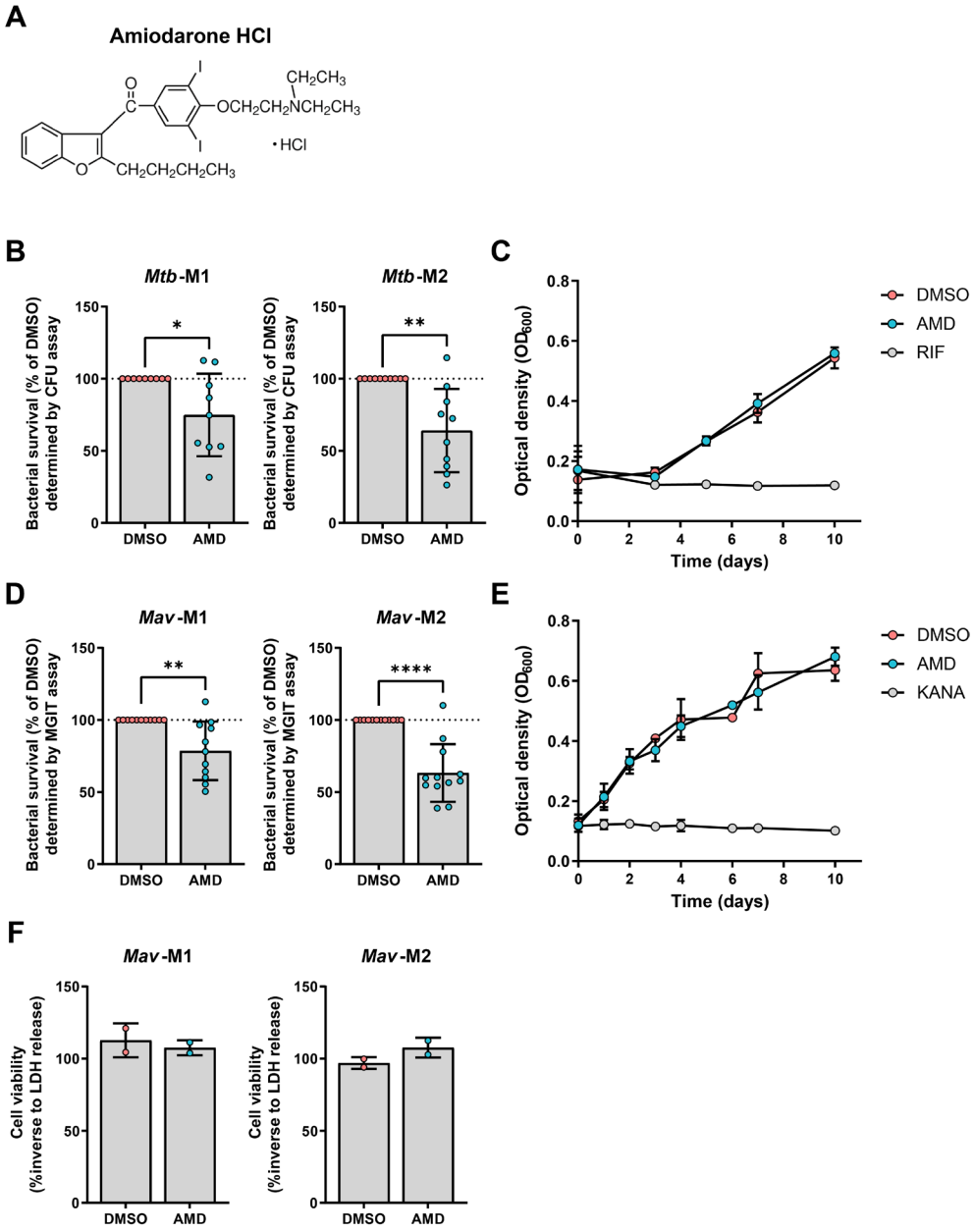

Figure 1. Identification of amiodarone as host-directed therapeutic for mycobacterial infections in primary human macrophages.
Identification of amiodarone as host-directed therapeutic for mycobacterial infections in primary human macrophages. **(A)** Chemical structure of amiodarone HCl (AMD). **(B)** *Mtb* H37Rv-infected M1 and M2 macrophages were treated for 24 hours with 10 μM amiodarone or an equal volume of vehicle control dimethyl sulfoxide (DMSO). Cells were subsequently lysed and bacterial survival was determined by CFU assay. Bacterial survival data represent the mean ± standard deviation (SD) from different donors (*n* = 9 or 10). Dots represent the mean from triplicate wells of a single

donor. Bacterial survival is expressed as the percentage of vehicle control DMSO (=100%, indicated with the dotted line) per donor. Statistical significance was tested using a paired *t*-test. **(C)** Growth of *Mtb* H37Rv in liquid broth was monitored for 10 days after exposure to positive control 20 µg/mL rifampicin (RIF), 10 µM amiodarone, or vehicle control DMSO. Data represent the mean ± SD of triplicate wells from three independent experiments. **(D)** Bacterial survival of *Mav* within M1 and M2 macrophages after treatment for 24 hours with 10 µM amiodarone or an equal volume of vehicle control DMSO. Cells were subsequently lysed and bacterial survival was determined by mycobacteria growth indicator tube (MGIT) assay. Data represent the mean ± SD from different donors (n = 11 or 12). Dots represent the mean from triplicate wells of a single donor. Bacterial survival is expressed as the percentage of vehicle control DMSO (=100%, indicated with the dotted line) per donor. Statistical significance was tested using a paired *t*-test. **(E)** Growth of *Mav* in liquid broth was monitored for 10 days after exposure to positive control 100 µg/mL kanamycin (KANA), 10 µM amiodarone, or vehicle control DMSO. Data represent the mean ± SD of triplicate wells from three independent experiments. **(F)** Percentage of viable M1 and M2 macrophages [based on lactate dehydrogenase (LDH) release] after 24 hours of treatment with 10 µM amiodarone or an equal volume of vehicle control DMSO (0.1%, vol/vol). Data represent the mean ± SD from different donors (n = 2). *P < 0.05, **P < 0.01, and ****P < 0.0001.

To determine whether amiodarone is exclusive for *Mtb* or may also act against other intracellular pathogenic mycobacteria, the activity of amiodarone was also tested in our M1 and M2 macrophage model infected with the NTM *Mycobacterium avium* (45). Intracellular bacterial survival in primary macrophages, as determined by the mycobacteria growth indicator tube (MGIT) assay, was impaired after amiodarone treatment (**Fig. 1D; Fig. S1B**). To confirm amiodarone's HDT activity against *Mav*, bacteria were treated with amiodarone in the absence of macrophages. No direct inhibition of bacterial growth was observed (**Fig. 1E**). Due to our experimental setup, i.e., gentamicin-protection assay, macrophage cell death also results in reduced intracellular bacterial burden. To exclude the involvement of such false-positive results, the effect of amiodarone on cellular viability was determined using the lactate dehydrogenase (LDH) release assay in *Mav*-infected macrophages. There were no indications that amiodarone affected the viability of *Mav*-infected macrophages (**Fig. 1F**). Taken together, amiodarone was identified as a potential HDT candidate, which impaired the survival of both *Mtb* and *Mav* in primary human pro-inflammatory and anti-inflammatory macrophages.

Amiodarone enhances the autophagy response to mycobacterial infection

Since amiodarone is known to induce autophagy (28, 29), we assessed this as the potential mechanism of action against mycobacteria. Considering that amiodarone showed the most consistent effect in *Mav*- versus *Mtb*-infected macrophages (standard deviation of 20.1 compared to 28.7, respectively) and that M2 macrophages better resemble alveolar macrophages, which are the primary cells involved during mycobacterial infections (33, 46), we focused on *Mav*-infected M2 macrophages. First, we measured the effect of amiodarone on total protein levels of LC3-II, which is the lipidated form of LC3 that is attached to the (auto)phagosome membrane. These experiments were performed both in the absence and presence of bafilomycin A1 (Baf), a vacuolar-type ATPase inhibitor that impairs lysosomal acidification and thereby blocks the degradation of (auto)phagosomes, allowing the quantification of total autophagic flux. Amiodarone treatment significantly increased LC3-II protein levels in *Mav*-infected macrophages (**Fig. 2A and B; Fig. S2**), which persisted in the presence of bafilomycin, indicating that amiodarone promotes both the formation of (auto)phagosomes and the

autophagic flux. To further investigate the induction of (auto)phagosomes, we assessed the area of LC3-II puncta in macrophages infected with Wasabi-expressing *Mav* using confocal microscopy (**Fig. 2D**). Amiodarone treatment resulted in increased LC3-II area in infected macrophages (**Fig. 2E**). Additionally, colocalization of bacteria and LC3-II-positive vesicles was determined, which showed that amiodarone treatment increased the percentage of bacteria localized in (auto)phagosomes (**Fig. 2F**). Thus, amiodarone promotes (auto)phagosome formation and flux, which results in enhanced targeting of bacteria to autophagic compartments.

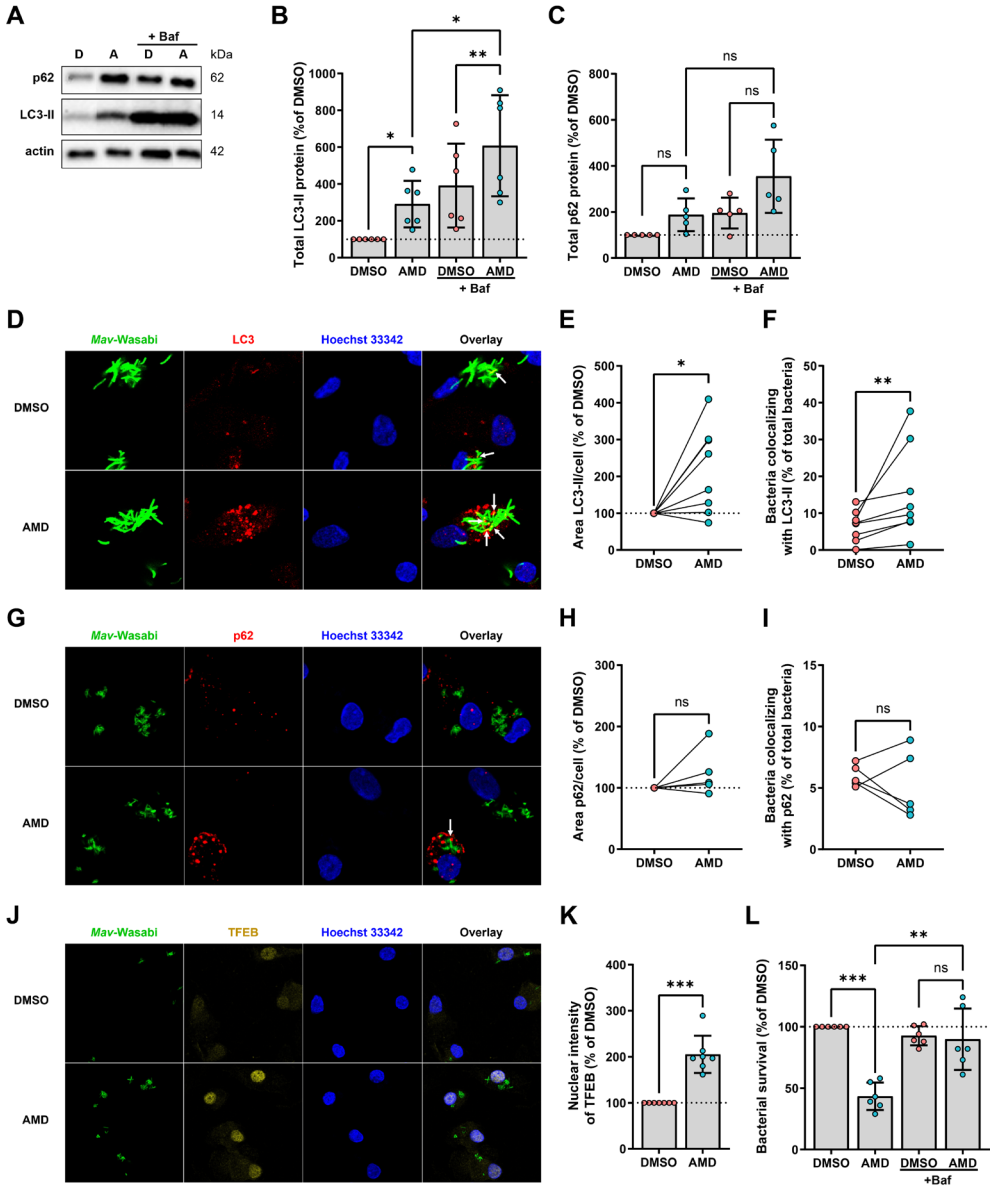

Figure 2. Amiodarone controls *Mav* infection in primary human macrophages, by promoting

antimycobacterial autophagy and activating master autophagy regulator TFEB.
(A) Western blot analysis of autophagy markers in M2 macrophages treated for 24 hours with 10 μM amiodarone or an equal volume of vehicle control dimethyl sulfoxide (DMSO) (0.1%, vol/vol) in the presence or absence of bafilomycin A1 (Baf) (10 nM) during *Mav* infection. Shown are blots from one representative donor out of six donors tested. The image depicts the boxed lanes from the unprocessed original images (Fig. S2). **(B)** Quantification of LC3-II (+Baf) protein levels from panel A. Protein levels were first normalized to actin and subsequently compared to DMSO control (=100%, indicated with the dotted line) per donor. Data represent the mean ± SD from different donors (n = 6). Statistical significance was tested using a repeated-measures one-way ANOVA with Bonferroni's multiple comparison correction. **(C)** Quantification of p62 (+Baf) protein levels from panel A. Protein levels were first normalized to actin and subsequently compared to DMSO control (=100%, indicated with the dotted line) per donor. Data represent the mean ± SD from different donors (n = 5). Statistical significance was tested using a repeated-measures one-way ANOVA with Bonferroni's multiple comparison correction. **(D)** M2 macrophages were treated for 24 hours with 10 μM amiodarone or an equal volume of vehicle control DMSO (0.1%, vol/vol) after infection with Wasabi-expressing *Mav* (green). Cells were subsequently stained with LC3-II (red) and Hoechst 33342 (blue) and analyzed by confocal microscopy. Images shown are of one representative donor out of eight donors tested. Arrows indicate colocalization of *Mav*-Wasabi with LC3-II puncta. **(E)** Quantification of the LC3-II area per cell count. Dots represent the mean from three wells (three images/well) per condition of a single donor (n = 8). Data are expressed as the percentage of vehicle control DMSO (=100%, indicated with the dotted line) per donor. Statistical significance was tested using a Wilcoxon matched-pairs test. **(F)** The percentage colocalization (indicated by white arrows in panel D) of intracellular mycobacteria with LC3-II puncta was determined. Dots represent the mean from three wells (three images/well) per condition of a single donor (n = 8). Statistical significance was tested using a Wilcoxon matched-pairs test. **(G)** M2 macrophages were treated for 4 hours with 10 μM amiodarone or an equal volume of vehicle control DMSO (0.1%, vol/vol) in the presence or absence of 10 nM Baf after infection with Wasabi-expressing *Mav* (green). Cells were subsequently stained with p62 (red) and Hoechst 33342 (blue) and analyzed by confocal microscopy. Images shown are of one representative donor out of five donors tested. Arrows indicate colocalization of *Mav*-Wasabi with p62. **(H)** Quantification of the p62 area per cell count. Dots represent the mean from three wells (three images/well) per condition of a single donor (n = 5). Data are expressed as the percentage of vehicle control DMSO (=100%, indicated with the dotted line) per donor. Statistical significance was tested using a Wilcoxon matched-pairs test. **(I)** The percentage colocalization (indicated by white arrows in panel G) of intracellular mycobacteria with p62 was determined. Dots represent the mean from three wells (three images/well) per condition of a single donor (n = 5). Data are expressed as the percentage of vehicle control DMSO. Statistical significance was tested using a Wilcoxon matched-pairs test. **(J)** Confocal microscopy of Wasabi-expressing (green) *Mav*-infected M2 macrophages treated with 10 μM amiodarone or an equal volume of vehicle control DMSO for 4 hours. Cells were subsequently stained for TFEB (yellow) and Hoechst 33342 (blue). Shown are images of one representative donor out of seven donors tested. **(K)** Quantification of the total intensity of TFEB within the mark of the cell nucleus. Data represent the mean ± SD from different donors (n = 7). Dots represent the mean from three wells (three images/well) per condition of a single donor. Data are expressed as the percentage of vehicle control DMSO (=100%, indicated with the dotted line) per donor. Statistical significance was tested using a paired t-test. **(L)** Bacterial survival of *Mav* within M2 macrophages after treatment for 24 hours with 10 μM amiodarone or an equal volume of vehicle control DMSO in the absence or presence of 10 nM Baf. Cells were subsequently lysed and bacterial survival was determined by MGIT assay. Data represent the mean ± SD from different donors (n = 6). Dots represent the mean from triplicate wells of a single donor. Bacterial survival is expressed as the percentage of vehicle control DMSO (=100%, indicated with the dotted line) per donor. Statistical significance was tested using a repeated-measures one-way ANOVA with Bonferroni's multiple comparison correction. ns, non-significant; *P < 0.05; **P < 0.01; and ***P < 0.001.

The autophagy response to intracellular pathogens often occurs as a receptor-mediated process (selective autophagy or xenophagy). Therefore, we examined p62, which acts as

a cargo receptor that targets ubiquitinated cytoplasmic material (including intracellular bacteria) to (auto)phagosomes for degradation (47, 48). Quantification of total p62-protein levels by western blot showed that treatment of *Mav*-infected macrophages with amiodarone alone did not significantly affect p62 levels (**Fig. 2C**). In the presence of bafilomycin, a mild, albeit not statistically significant, accumulation of p62 was induced. Moreover, the p62 area and colocalization of Wasabi-expressing *Mav* with p62-positive puncta showed no major alterations upon treatment with amiodarone (**Fig. 2G-I)**. These results suggest that amiodarone might stimulate non-selective (bulk) autophagy, as also occurs during starvation, and the effect on selective autophagy, or a non-canonical autophagy process, remains inconclusive (49).

Amiodarone increases the activation of the major autophagy regulator TFEB and requires autophagy to eliminate intracellular bacteria

To further investigate the observed effects of amiodarone on infection control and autophagy induction, we focused on transcription factor EB (TFEB), a master regulator of autophagy and lysosomal biogenesis (30, 50–53). Once activated, TFEB enters the nucleus and promotes the expression of autophagy-related genes as well as the coordinated lysosomal expression and regulation gene network (52, 54). Therefore, nuclear intensity of TFEB was assessed in *Mav*-infected M2 macrophages after amiodarone treatment. Compared to untreated controls, a significant increase in nuclear intensity of TFEB was observed in amiodarone-treated cells (**Fig. 2J and K**).

To establish whether the enhanced autophagic response after amiodarone treatment is required for the reduction of intracellular bacteria, autophagic flux was blocked using bafilomycin in amiodarone-treated *Mav*-infected M2 macrophages. Amiodarone treatment clearly reduced bacterial loads compared to untreated control, but this phenotype was abrogated after blocking (auto)phagosomal lysosomal degradation with bafilomycin (**Fig. 2L**). Taken together, although we cannot discriminate between bacterial killing or restriction of replication, host-directed therapy with amiodarone controls *Mav* infection in primary human macrophages by promoting antimycobacterial autophagy, which correlates with activation of the master transcriptional regulator TFEB.

Amiodarone reduces bacterial burden *in vivo*

To validate the activity of amiodarone *in vivo*, we used the zebrafish embryo TB model based on infection with *Mycobacterium marinum*. Before employing this model, we wished to exclude that amiodarone might affect the development or migration properties of zebrafish leukocytes, which would confound the results of infection experiments. Therefore, we used an established injury-based migration assay, the tail amputation assay (55, 56), in a double transgenic neutrophil and macrophage marker line. No alterations in the numbers of neutrophils and macrophages that accumulated at the site of inflammation were observed after treatment with 5 μM amiodarone (**Fig. S3**). Therefore, we proceeded to assess the effect of amiodarone on infection. Zebrafish embryos were infected 1-day post-fertilization (dpf) with Wasabi-expressing *Mmar*, and treatment was initiated 1-hour post-infection (hpi) with amiodarone in increasing doses (5, 10, and 20 μM). At 4 days post-infection (dpi), the bacterial burden was determined by quantifying the bacterial fluorescent signal using confocal microscopy (**Fig. 3A**).

Amiodarone reduced bacterial burden in a dose-dependent manner at 5 and 10 µM (**Fig. 3B; Fig. S4A**), without showing any signs of toxicity in zebrafish embryos. The highest dose tested (i.e., 20 µM) induced developmental toxicity (e.g., edema and lethality), and bacterial loads were therefore not quantified. When tested on *in vitro* bacterial cultures, 5 µM amiodarone did not affect *Mmar* growth, while the growth of cultures exposed for 48 h to 10 µM amiodarone was inhibited (**Fig. S5**). Therefore, in subsequent experiments, the dosage of 5 µM amiodarone was used to ensure looking at host-mediated effects. To determine the infection dynamics, bacterial loads were quantified daily from 1 up to 4 dpi. In both the control and treatment groups, bacterial burden increased over time (**Fig. 3C; Fig. S4B**). Amiodarone treatment, however, significantly impaired the progression of infection, which at 4 dpi resulted in almost a twofold lower bacterial load compared to the control treatment. These results confirm that host-directed therapy with amiodarone reduces mycobacterial loads in a relevant *in vivo* model of TB using zebrafish embryos.

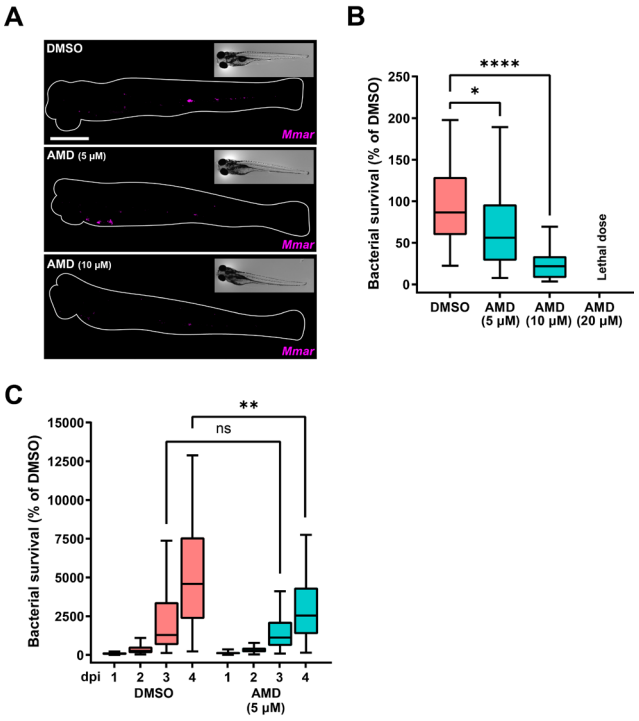

Figure 3. Amiodarone restricts *Mmar* infection in a host-directed manner.
(A) Bacterial burden assay of mWasabi-expressing *Mmar*-infected zebrafish larvae treated with increasing doses of amiodarone (5, 10, and 20 µM) or vehicle control dimethyl sulfoxide (DMSO). Treatment was started at 1 hpi. and larvae were anesthetized at 4 dpi for imaging. Representative stereo fluorescent images of whole larvae infected with mWasabi-expressing *Mmar*. Magenta shows *Mmar*. Scale bar annotates 1 mm. **(B)** Quantification of bacterial burden shown in panel A. Bacterial burden was normalized to the mean of the control. Data from two independent experiments were combined (n = 39–42 per group). Boxplots with 95% confidence intervals are shown, and the black line in the boxplots indicates the group median. Statistical significance was tested using a Kruskal-Wallis with Dunn's multiple comparisons test. **(C)** Bacterial burden

assay of mWasabi-expressing *Mmar*-infected zebrafish larvae treated with 5 µM of amiodarone or vehicle control DMSO. Treatment was started at 1 hpi, and larvae were anesthetized at 1, 2, 3, and 4 dpi for imaging. Bacterial burden was normalized to the control (DMSO at 1 dpi), and data from two experimental repeats were combined (n = 65–70 per group). Boxplots with 95% confidence intervals are shown, and the black line in the boxplots indicates the group median. Statistical significance was tested using a Kruskal-Wallis with Dunn's multiple comparisons test. ns, non-significant; *P < 0.05; **P < 0.01; and ****P < 0.0001.

Amiodarone enhances the formation of (auto)phagosomes *in vivo*

To confirm that the reduced bacterial burden in zebrafish after amiodarone treatment is related to enhanced autophagic activity, as observed in human macrophages, we used a fluorescent zebrafish reporter line for LC3 (GFP-LC3) (57). Embryos at 3 dpf were treated with amiodarone for 24 hours, and GFP-LC3-positive structures were quantified in the tail fin using confocal microscopy (**Fig. 4A**) (58). Compared to controls, the number of GFP-LC3 structures was significantly increased after amiodarone treatment (**Fig. 4B**). Subsequently, zebrafish embryos (1 dpf) were infected with mCherry-expressing *Mmar* to investigate whether the increased number of autophagic vesicles after amiodarone treatment colocalized with bacteria. At 2 dpi, embryos were imaged using confocal microscopy in the caudal hematopoietic tissue (CHT) region, the location where infected macrophages are known to aggregate, as an initial step of granuloma formation (38). Both in control and amiodarone-treated embryos, bacterial clusters colocalized with GFP-LC3 clusters, without detectable differences between both groups (**Fig. 4C and E**). Furthermore, in both groups, an overall increase in the percentage of *Mmar* clusters colocalizing with GFP-LC3 signal was observed, when autophagy flux was blocked with bafilomycin (**Fig. 4D and E**). In conclusion, while no differences in GFP-LC3-positive *Mmar* clusters were detected, amiodarone showed a marked effect on total GFP-LC3 levels in the zebrafish model, in agreement with our observations in primary human macrophages.

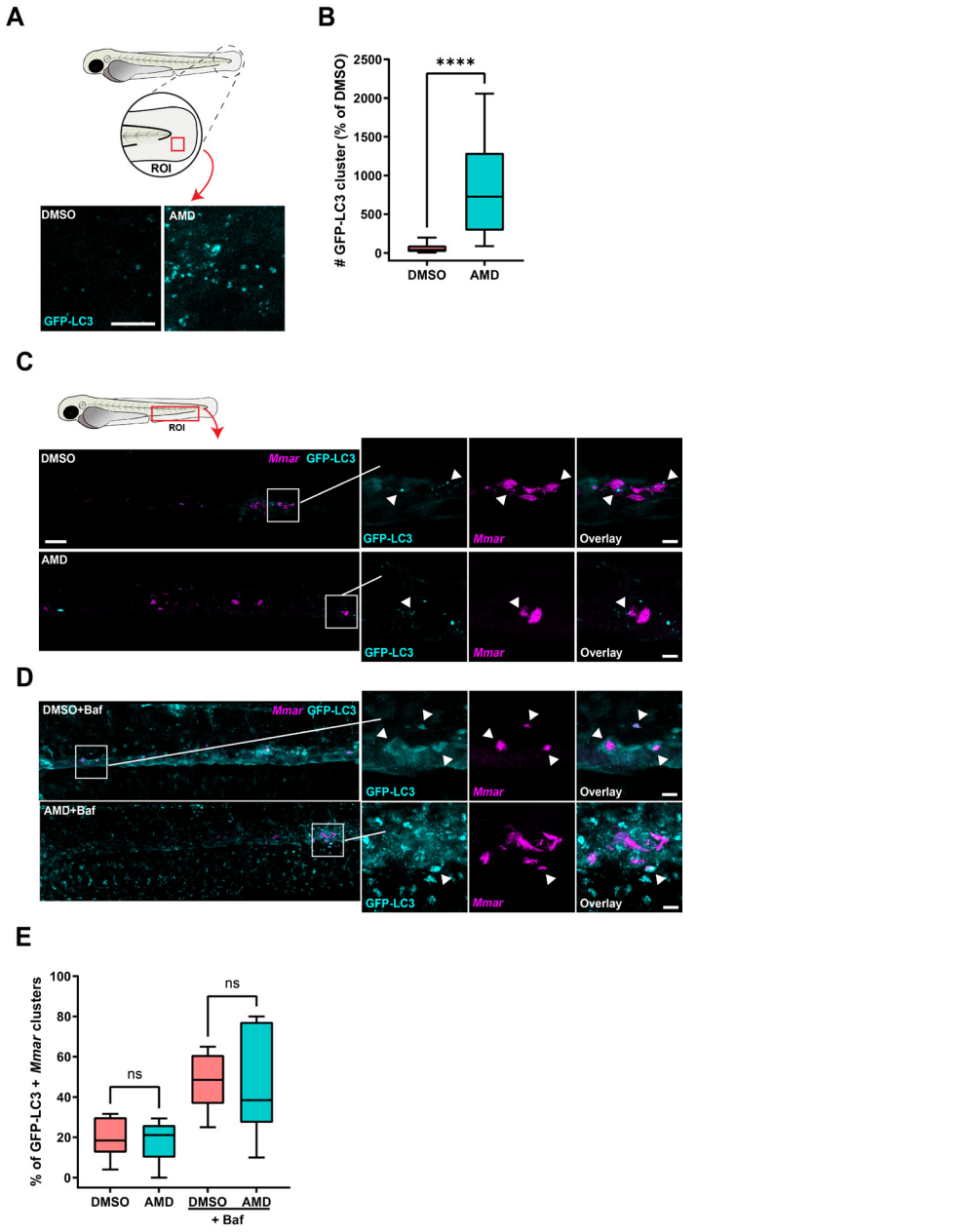

Figure 4. Amiodarone induces an increase in (auto)phagosomes, without affecting autophagic targeting of *Mmar* clusters.
Amiodarone induces an increase in (auto)phagosomes, without affecting autophagic targeting of *Mmar* clusters. **(A)** Confocal microscopy max projection of transgenic GFP-LC3 zebrafish larvae treated with 5 µM of amiodarone or vehicle control dimethyl sulfoxide (DMSO). Treatment was started at 3 dpf and larvae were fixed with 4% paraformaldehyde at 4 dpf for imaging. Representative max projection images of GFP-LC3-positive vesicles in the indicated region of imaging (ROI) in the tail fin are shown. Cyan shows GFP-LC3-positive vesicles. Scale bar annotates 10 µm. **(B)** Quantification of GFP-LC3 structures is shown in panel A. Data were normalized to

the control, and data from two independent experiments were combined (n = 16–17 per group). Boxplots with 95% confidence intervals are shown, and the black line in the boxplots indicates the group median. Statistical significance was tested using a Mann-Whitney test. **(C)** Confocal microscopy max projection of mCherry-expressing *Mmar*-infected transgenic GFP-LC3 zebrafish larvae treated with 5 µM of amiodarone or vehicle control DMSO. Treatment was started at 1 hpi, and at 2 dpi, larvae were fixed with 4% paraformaldehyde for imaging. Representative max projection images of the ROI in the CHT region are shown. Cyan shows GFP-LC3-positive vesicles and magenta shows *Mmar*. Scale bar annotates 50 µm. Enlargement of areas indicated in panel C: cyan shows GFP-LC3-positive vesicles and magenta shows *Mmar*. Arrowheads indicate GFP-LC3-positive *Mmar* clusters. Scale bar in the left panel annotates 50 µm and in the right panel 10 µm. **(D)** Confocal microscopy max projection of mCherry-expressing *Mmar*-infected transgenic GFP-Lc3 zebrafish larvae treated with 5 µM of amiodarone and 160 nm of bafilomycin or vehicle control DMSO. Treatment was started at 1 hpi, and at 2 dpi, larvae were fixed with 4% paraformaldehyde for imaging. Representative max projection images of the ROI in the CHT region are shown. Cyan shows GFP-Lc3-positive vesicles and magenta shows *Mmar*. Scale bar annotates 50 µm. Enlargement of areas indicated in panel D: cyan shows GFP-LC3-positive vesicles and magenta shows *Mmar*. Arrowheads indicate GFP-LC3-positive *Mmar* clusters. Scale bar in the left panel annotates 50 µm and in the right panel 10 µm. **(E)** Quantification of GFP-LC3-positive *Mmar* clusters in the CHT region shown in panels A and D normalized to the control (n = 8 per group). Boxplots with 95% confidence intervals are shown, and the black line in the boxplots indicates the group median. Statistical analysis was performed using a Kruskal-Wallis with Dunn's multiple comparisons test. ns, non-significant and ****P < 0.0001.

Discussion

Antibiotic resistance is emerging as one of the principal global health problems for bacterial infections, which impairs the treatment of TB and other difficult-to-treat intracellular bacterial infections, including NTM. Stimulating host defense mechanisms and/or counteracting pathogen-induced immune modulation by host-directed therapy is a promising alternative strategy to combat intracellular mycobacterial infections. Here, we report that amiodarone enhances the antimicrobial response of primary human macrophages infected with *Mtb* and *Mav*, paralleled with a significant reduction in mycobacterial burden of *Mmar*-infected zebrafish embryos. Importantly, amiodarone is shown to promote the activity of transcriptional regulator TFEB and induce the formation of (auto)phagosomes and autophagy flux. Inhibition of autophagic flux by blocking lysosomal degradative activity effectively impaired the protective effect of amiodarone, supporting that activation of the host (auto)phagolysosomal pathway is causally involved in the mechanism of action of amiodarone.

This study has identified the host-directed activity of amiodarone both *in vitro* and *in vivo* against both nontuberculous and tuberculosis mycobacteria. Amiodarone is known to induce autophagy and modulate endocytic pathways (28, 29, 32), which may be beneficial during mycobacterial infections as both pathways are crucial processes in the intracellular defense against infections with *Mtb* and *Mmar* (20, 40, 42, 59), and has furthermore been suggested for *Mav* (60, 61). Amiodarone increased autophagic flux both *in vitro* in primary human macrophages and *in vivo*. In primary human macrophages, we could additionally demonstrate that amiodarone promoted autophagic targeting of intracellular *Mav*. Targeting bacteria to autophagosomes for degradation is a specific form of canonical autophagy called xenophagy (48). LC3, however, is not a specific autophagosome marker since LC3 can also be lipidated to phagosomes in a non-canonical autophagy process such as LC3-associated phagocytosis (62), which uses components of the canonical autophagy machinery but selects cargo extracellularly

(62). Conversely, bacterial control during xenophagy is dependent on the ability of bacteria to escape the phagosome into the cytosol. Phagosomal escape is known as one of the virulence mechanisms of *Mtb* and *Mmar* (17–19, 63, 64), but whether *Mav* also escapes phagosomes remains unknown. Amiodarone treatment of *Mav*-infected macrophages did not significantly modify the levels of p62 (e.g., SQSTM1), one of the most well-known receptors targeting ubiquitinated cytosolic cargo to the autophagosome. Moreover, colocalization of bacteria with p62 was not increased upon amiodarone treatment. Although the involvement of other cargo receptors including NDP52 and Optineurin cannot be excluded (42, 48, 65), our data are supported by others who showed that amiodarone induced non-canonical autophagy independently of the canonical autophagy pathway (28).

Amiodarone is able to induce autophagy via mTOR-independent and -dependent pathways. Amiodarone can induce mTOR-independent autophagy by blocking calcium-mediated production of calpains (66). Calpains stimulate the production of cAMP, which inhibits autophagy via the cyclical mTOR-independent pathway (67, 68) and are suggested to cleave Atg5, which is required for the formation of autophagosomes (69). When sufficient cellular nutrients are available, mTORC1 inhibits autophagy by interacting directly with ULK1, an important enzyme for the initiation of autophagosome biogenesis (21). In addition, mTORC1 impairs the nuclear translocation and activation of TFEB by promoting its phosphorylation (70–72). When mTOR is inhibited, by starvation or lysosomal dysfunction (e.g., phospholipidosis), dephosphorylated TFEB translocates to the nucleus where it coordinates the transcriptional program to increase lysosomal biogenesis and autophagy (30, 51, 73). Our finding that co-treatment with lysosomal activity inhibitor bafilomycin abrogated the antimycobacterial effect of amiodarone shows that lysosomal degradation is operational and instrumental for the host-protective effect of amiodarone. Amiodarone furthermore enhanced the nuclear intensity of TFEB in *Mav*-infected macrophages, likely by inhibition of mTOR (66). In agreement, overexpression of TFEB was previously shown to potentiate autophagy (30). By potentially interacting with multiple players from the autophagy machinery, amiodarone might prove to be a robust activator for autophagy in varying conditions, including during mycobacterial infection.

In addition to its effects on autophagy pathways, amiodarone has been reported to impair the function of certain lysosomal enzymes and induce phospholipidosis (30, 74). Phospholipidosis is a phospholipid storage disorder, characterized by the accumulation of phospholipids within lysosomes, which cells try to overcome by promoting autophagy (30, 75). Thus, the effect of amiodarone may depend on the phospholipidosis-mediated induction of autophagy during TFEB overexpression. For SARS-CoV-2, the *in vitro* activity of phospholipidosis-inducing drugs failed to translate *in vivo,* which hampers drug discovery (76). Regardless, amiodarone has been shown to induce phospholipidosis in rodents (77–79). In our study, the host-directed effect of amiodarone was reproducible in zebrafish, suggesting that the activity of drugs that may act by inducing phospholipidosis can be translated *in vivo* for mycobacterial infections. To control mycobacterial infections in our study, amiodarone was used in concentrations of 5 and 10 μM. In patients treated with amiodarone, peak serum concentrations are reported to range from 1 to 5.1 μM and can increase up to

11 μM shortly after intravenous administration (80, 81). Nevertheless, amiodarone has a number of well-known and occasional serious side effects upon chronic usage including lung toxicity, which are more common in patients with plasma levels exceeding 3.9 μM (82–84). As the amiodarone concentrations required to mediate a protective host-directed effect during mycobacterial infections are on the high end of patient serum concentrations, complicating the clinical applicability of amiodarone, identifying autophagy-inducing compounds with a more favorable safety profile is highly desirable to aid clinical translation. For *Mtb*, the relevance of promoting autophagy is currently being investigated in clinical trials (85, 86), and our study underlines that promoting autophagy may also be beneficial in patients infected with nontuberculous mycobacteria.

Our study might have several limitations. First, although we identified the HDT activity of amiodarone against multiple mycobacterial species, the role of autophagy in infection control by amiodarone was only shown during *Mav* infection. If mycobacteria differ in their intracellular behavior and the way they are degraded, our findings regarding autophagy during *Mav* infection might not apply to *Mtb* or *Mmar*. Second, we showed that induction of autophagy by amiodarone is required for infection control and that TFEB activation upon amiodarone treatment is enhanced. However, our study lacks evidence that TFEB activation is promoting the autophagy-mediated HDT activity of amiodarone. Third, we did not evaluate the efficacy of amiodarone in combination with standard-of-care antibiotics to detect any cumulative or synergistic effects. Clinical application of HDT, however, will most likely be considered as an adjunctive therapy to standard of care used to treat mycobacterial infections (11). Despite these limitations, we support the possible clinical applicability of amiodarone by showing that amiodarone improved host control of mycobacterial infections both *in vitro* and *in vivo*. Furthermore, our study presents a new autophagy-inducing compound suitable for drug repurposing. Drug repurposing as HDT has various advantages, including the known safety profile of drugs and the faster facilitation of the identification of HDT to treat mycobacterial infections.

Taken together, amiodarone acts as a host-directed therapeutic in primary human macrophages and in zebrafish against nontuberculous and tuberculous mycobacterial strains. Amiodarone induces autophagy, most likely by promoting the nuclear translocation of TFEB and concomitant upregulation of proteins involved in autophagy, and activation of the (auto)phagolysosomal pathway by amiodarone interferes with the ability of mycobacteria to survive intracellularly. While our study shows the feasibility of exploiting autophagy as a target for HDT during *Mtb* as well as NTM infections, further understanding of the molecular mechanisms of how autophagy is regulated and controls mycobacterial infection will enable the development of autophagy-modulating HDT with a more favorable therapeutic index.

Materials and methods

Reagents and antibodies

Anti-human CD163-PE, CD14-PE-Cy7, and CD1a-Alexa Fluor 647 (1:20) were obtained from Biolegend (Amsterdam, the Netherlands) and anti-human CD11b-BB515 (1:20)

from BD Biosciences. For confocal microscopy, the following antibodies were used: rabbit anti-human LC3A/B (1:200) and rabbit anti-human TFEB (1:200) from Cell Signaling Technology (Leiden, the Netherlands), mouse anti-human SQSTM1/p62 (1:200) from Santa Cruz Biotechnology (Heidelberg, Germany), and donkey anti-rabbit IgG (H + L)-Alexa Fluor 555 (1:200) and goat anti-mouse IgG (H + L)-Alexa Fluor 647 (1:200) from Abcam (Amsterdam, the Netherlands). Hoechst 33342 (1:2,000) was purchased from Sigma-Aldrich (Zwijndrecht, the Netherlands). For western blot, rabbit anti-human LC3B (1:500) from Novus Biologicals/Bio-Techne (Abingdon, UK), mouse anti-human SQSTM1/p62 (1:500) from Santa Cruz Biotechnology (Heidelberg, Germany), and mouse anti-human β-actin (1:1,000) from Sigma-Aldrich were used. Horseradish peroxidase-conjugated goat anti-rabbit IgG (H + L) and goat anti-mouse IgG (H + L) (1:5,000) were purchased from Invitrogen, ThermoFisher Scientific.

Dimethyl sulfoxide (DMSO), amiodarone HCl, bafilomycin A1, rifampicin, and kanamycin sulfate were purchased from Sigma-Aldrich.

Cell culture

Buffy coats were obtained from healthy anonymous donors (Dutch adults) after written informed consent (Sanquin Blood Bank, Amsterdam, the Netherlands). Primary human macrophages were obtained as described previously (45). In short, CD14+ monocytes were isolated from peripheral blood mononuclear cells by density gradient centrifugation over Ficoll (Pharmacy, LUMC, the Netherlands) and by magnetic-activated cell sorting using anti-CD14-coated microbeads (Miltenyi Biotec, Auburn, CA, USA). Purified CD14+ monocytes were cultured for 6 days at 37°C/5% CO_2 in Gibco Dutch modified Roswell Park Memorial Institute (RPMI) 1640 medium (ThermoFisher Scientific, Landsmeer, the Netherlands) supplemented with 10% fetal calf serum, 2 mM L-glutamine (PAA, Linz, Austria), 100 units/nL penicillin, 100 µg/mL streptomycin, and either 5 ng/mL granulocyte-macrophage colony-stimulating factor (ThermoFisher Scientific) or 50 ng/mL macrophage colony-stimulating factor (R&D Systems, Abingdon, UK) to promote pro-inflammatory M1 or anti-inflammatory M2 macrophage differentiation, respectively. Cytokines were refreshed on day 3 of differentiation. One day prior to experimental procedures, macrophages were harvested by trypsinization with 0.05% Trypsin-EDTA (ThermoFisher Scientific) and scraping and seeded into flat-bottom 96-well plates (30,000 cells/well) if not indicated otherwise. The M1 and M2 macrophage differentiation was validated based on cell surface marker expression (CD11b, CD1a, CD14, and CD163) as determined by flow cytometry and quantification of cytokine production (IL-10 and IL-12) using ELISA following 24 hours of stimulation of cells with 100 ng/mL lipopolysaccharide (InvivoGen, San Diego, USA).

Bacterial cultures

Mav laboratory strain 101 (700898, ATCC, VA, USA), *Mtb* (wild-type H37Rv), and mCherry-expressing *Mmar* M-strain were cultured as described previously (25, 45, 87). Bacterial concentrations were determined by measuring the optical density of planktonic cultures at 600 nm (OD_{600}).

Cell-free bacterial growth assay

Mtb, Mav, and Mmar cultures were diluted to an OD_{600} of 0.1 in Difco Middlebrook 7H9

broth (Becton Dickinson, Breda, the Netherlands), containing 0.2% glycerol (Merck Life Science, Amsterdam, the Netherlands), 0.05% Tween-80 (Merck Life Science), 10% Middlebrook albumin, dextrose, and catalase enrichment (Becton Dickinson), and 100 µg/mL Hygromycin B (Life Technologies-Invitrogen, Bleiswijk, the Netherlands), of which 50 µL per flat-bottom 96 well of *Mtb* and *Mav* and 5 mL of *Mmar* were incubated with 50 µL of chemical compounds or DMSO (0.1%, vol/vol) at indicated concentration at 37°C/5% CO_2. Bacterial growth of *Mtb* and *Mav* was monitored until 10–14 days of incubation, and *Mmar* growth was measured during 2 days of incubation at 28.5°C. Absorbance at a 600 nm wavelength was measured directly after plating and at indicated time points following resuspension of wells on the Envision Multimode Plate Reader (Perkin Elmer).

Bacterial infection and treatment of cells

One day prior to infection, *Mtb* or *Mav* was diluted to a density corresponding with early log-phase growth (OD_{600} of 0.25) to reach the log phase during infection. On the day of infection, bacterial suspensions were diluted in a cell culture medium without antibiotics to infect macrophages with a multiplicity of infection (MOI) of 10. The accuracy of the MOI was verified by a standard CFU (45).

After the addition of bacteria to the cells, plates were centrifuged for 3 minutes at 130 rcf and incubated for 1 hour at 37°C/5% CO_2. Extracellular bacteria were removed, and cells were treated with fresh RPMI 1640 containing 30 µg/mL gentamicin for 10 minutes to eradicate residual extracellular bacteria. Cells were subsequently incubated at 37°C/5% CO_2 in RPMI 1640 medium supplemented with 5 µg/mL gentamicin and, if indicated, compounds at indicated concentration or vehicle control (DMSO 0.1%, vol/vol) until readout. Following the treatment of cells, the supernatant was removed, and the cells were either lysed using 100 or 125 µL of lysis buffer (H_2O + 0.05% SDS) for the determination of intracellular bacterial burden using a CFU assay or the MGIT system (45), or processed for western blot or confocal microscopy analysis. The activity of amiodarone on the elimination of bacteria was determined by calculating the fraction of intracellular bacteria measured after treatment compared to the control.

Lactate dehydrogenase release assay

Cells (30,000 cells/well) were infected and treated as described above and centrifuged for 3 minutes at 130 rcf. Supernatants were transferred to a new plate and reacted with substrate mix from the Cytotoxicity Detection kit (LDH) (Merck Life Science) for 30 minutes at room temperature in the dark. Absorbance at OD_{485} and OD_{690} was measured using an Envision Plate Reader. Toxicity was calculated using the absorbance values and the formula (experimental sample – untreated sample)/(positive control sample – untreated sample), where the positive control indicates cells lysed using 2% Triton X-100 (Sigma-Aldrich). Cell viability was determined as the inverse value of toxicity, where 100% indicates the cell viability of the untreated sample.

Western blot analysis

Cell lysates (300,000 cells/well in 24-well plates) were prepared and protein concentrations were measured as described previously (88). Cell lysates were loaded on a 15-well 4%–20% Mini-PROTEAN TGX Precast Protein Gel (Bio-Rad Laboratories,

Veenendaal, the Netherlands), and Amersham ECL Full-Range Rainbow Molecular Weight Marker (Sigma-Aldrich) was added as a reference. Proteins were transferred to ethanol-activated Immun-Blot PVDF membranes (Bio-Rad) in Tris-glycine buffer (25 mM Tris, 192 mM glycine, and 20% methanol). Subsequently, membranes were blocked for 45 minutes in PBS with 5% non-fat dry milk (PBS/5% milk) (Campina, Amersfoort, the Netherlands) and probed with the indicated antibodies in PBS/5% milk for 90 minutes at RT. Membranes were washed and incubated two times for 5 minutes with PBS + 0.75% Tween-20 (PBST) and stained with secondary antibodies in PBS/5% milk for 45 minutes at RT. Membranes were washed and incubated two times for 5 minutes with PBST before revelation using enhanced chemiluminescence SuperSignal West Dura extended duration substrate (ThermoFisher Scientific). Imaging was performed on an iBright Imaging System (Invitrogen, Breda, the Netherlands). Protein bands were quantified using ImageJ/Fiji software (NIH, Bethesda, MD, USA) and normalized to actin.

Confocal microscopy of cells

For confocal microscopy, cells (30,000 cells/well) were cultured in pre-washed poly-d-lysine-coated glass-bottom 96-well plates (no. 1.5, MatTek Corporation, Ashland, MA, USA). Following infection and treatment, cells were fixed with 1% (wt/vol) formaldehyde (ThermoFisher Scientific) for 1 hour at RT, washed twice, and Fc receptors were blocked with 5% human serum diluted in PBS (PBS/5% HS) for 45 minutes at RT. Next, cells were stained with indicated antibodies in PBS/5% HS for 30 minutes at RT, washed twice with PBS/5% HS, and incubated with secondary antibodies for 30 minutes at RT in the dark. Cells were incubated with 5 µg/mL Hoechst 33342 for 10 minutes at RT in the dark and mounted overnight using ProLong Glass Antifade Mountant (Invitrogen, ThermoFisher Scientific, Landsmeer, the Netherlands). Plates were imaged by taking three images per well, using a Leica SP8WLL Confocal microscope (Leica, Amsterdam, the Netherlands) equipped with a 63× oil immersion objective.

Image analysis was performed as follows: LC3 and p62 channels were background subtracted in ImageJ/Fiji software with rolling ball algorithm using a 20-pixel radius (89). CellProfiler 3.0.0. was used for the segmentation of both the fluorescent bacteria and the markers of interest with global manual thresholding (bacteria) and adaptive two or three-class Otsu thresholding (LC3 and p62, respectively) (90). The area of each fluorescent marker was specified for each image and was normalized to cell count based on Hoechst 33342 staining. The percentage of overlap, i.e., colocalization, of *Mav* with LC3 and p62 was calculated for each image, and the average colocalization was determined for each treatment condition. The integrated/mean intensity of TFEB per single nucleus was used to determine the nuclear presence of TFEB.

Zebrafish culture

Zebrafish lines (Table S1) were maintained according to standard protocols (www.zfin.org). Zebrafish eggs were obtained by natural spawning of single crosses to achieve synchronized developmental timing. Eggs from at least five couples were combined to achieve heterogeneous groups. Eggs and embryos were kept in egg water (60 µg/mL sea salt, Sera Marin, Heinsberg, Germany) at ~28.5°C after harvesting and in embryo medium after infection and/or treatment (E2, buffered medium, composition: 15 mM

NaCl, 0.5 mM KCl, 1 mM MgSO4, 150 µM KH_2PO_4, 1 mM $CaCl_2$, and 0.7 mM $NaHCO_3$) at ~28.5°C for the duration of experiments.

Bacterial infection and treatment of zebrafish embryos

Zebrafish embryos were infected with *Mmar* inoculum resuspended in PBS containing 2% (wt/vol) polyvinylpyrrolidone (PVP40). The injection dose was determined by optical density measurement (OD_{600} of 1 corresponds to ~100 CFU/nL). Infection experiments were conducted according to previously described procedures (35, 87). In brief, microinjections were performed using borosilicate glass microcapillary injection needles (Harvard Apparatus, 300038, 1 mm O.D. × 0.78 mm I.D.) prepared using a micropipette puller device (Sutter Instruments Flaming/Brown P-97). Needles were mounted on a micromanipulator (Sutter Instruments MM-33R) positioned under a stereo microscope. Prior to injection, embryos were anesthetized using 200 µg/mL buffered 3-aminobenzoic acid ethyl ester (Tricaine, Sigma-Aldrich) in egg water. They were then positioned on a 1% agarose plate (in egg water) and injected with a 1-nL inoculum containing ~200 CFU *Mmar* at 30 hours post-fertilization in the blood island or at 3 dpf in the tail fin (58). Treatment of zebrafish embryos was performed by immersion. Stock concentrations were diluted to treatment doses in a complete embryo medium without antibiotics. As a solvent control treatment, DMSO was diluted to the same concentration (%, vol/vol) as amiodarone treatment.

For the assessment of bacterial burden, larvae were anesthetized using tricaine at 4 dpi, positioned on a 1% agarose (in egg water) plate, and imaged using a Leica M205 FA stereo fluorescence microscope equipped with a DFC345 FX monochrome camera. Bacterial burden was determined based on fluorescent pixel quantification (Stoop 2011). For confocal imaging, larvae were either fixed in 4% paraformaldehyde in PBS at 20°C for 2 hours or at 4°C or anesthetized using tricaine and embedded in 1.5% low melting point agarose (in egg water) before imaging (58). Time points of all confocal experiments are described in the figure legends.

Confocal microscopy of zebrafish

To visualize fixed 4-dpf uninfected or 1-dpi larvae, larvae were embedded in 1.5% low melting point agarose (weight per volume, in egg water) and imaged using a Leica TCS SPE confocal 63× oil immersion objective (HC PL APO CS2, NA 1.42) and a Leica TCS SP8 confocal microscope with a 40× water immersion objective (HCX APO L U-V-I, NA 0.8).

For the visualization of LC3 dynamics, Tg(CMV:EGFP-map1lc3b) larvae were embedded in 1.5% low melting point agarose (weight per volume, in egg water) and imaged using a Leica TCS SPE confocal microscope. Imaging was performed using a 63× oil immersion objective (HC PL APO CS2, NA 1.42) in a region of the tail fin to detect EGFP-map1lc3b, further referred to as GFP-LC3-positive vesicles. To determine colocalization between *Mmar* and GFP-LC3, larvae were embedded in 1.5% low melting agarose (in egg water) and imaged in the caudal hematopoietic tissue, using a Leica TCS SP8 confocal microscope with a 40× water immersion objective (HCX APO L U-V-I, NA 0.8). Images were obtained using Leica Las X software. For the quantification of GFP-LC3 levels, the find maxima algorithm with a noise tolerance of 50 was used in Fiji software

version 1.53c. To determine the association of GFP-LC3 with bacteria, manual counting was performed on the obtained confocal images using Leica Las X software.

Tail amputation assay
Embryos of a Tg(mpeg1:mcherryF)/Tg(mpx:gfp) double transgenic line were anesthetized using tricaine at 3 dpf, positioned on a 1% agarose (in egg water) plate, and the tails were partially amputated with a 1 mm sapphire blade (World Precision Instruments) under a Leica M165C stereomicroscope (91). After amputation, larvae were incubated in an embryo medium for 4 hours and fixed using 4% paraformaldehyde. After fixation, larvae were positioned on a 1% agarose (in egg water) plate and imaged using a Leica M205 FA stereo fluorescence microscope equipped with a DFC345 FX monochrome camera. Macrophages were detected based on the fluorescence of their mCherry label, and neutrophils were detected based on their GFP label. The number of leukocytes recruited to the wounded area was counted as described previously (91).

Statistical analysis
To evaluate the statistical relevance of observed differences for parametric paired data sets (normal distribution was determined using the Shapiro-Wilk normality test), a paired *t*-test when comparing two groups and repeated measures one-way ANOVA when comparing three or more groups were used. Nonparametric paired data sets were tested with the Wilcoxon matched-pairs test. In case of unpaired samples (i.e., zebrafish experiments), Mann-Whitney test or Kruskal-Wallis with Dunn's multiple comparisons test was applied when assessing the differences between two or more groups, respectively. Data were normalized to the mean of the control group and independent repeats were combined unless otherwise indicated. The number of experiments combined is indicated in the figure legend for each experiment.

Analyses and graphical representation were performed using GraphPad Prism 8.0 and 9.0 (GraphPad Software, San Diego, CA, USA), with P-values < 0.05 considered statistically significant.

Ethics statement
This study was approved by the Sanquin Ethical Advisory Board, in accordance with the Declaration of Helsinki and according to Dutch regulations.

Zebrafish were maintained and handled in compliance with the local animal welfare regulations as overseen by the Animal Welfare Body of Leiden University (license number: 10612). All practices involving zebrafish were performed in accordance with European laws, guidelines and policies for animal experimentation, housing, and care (European Directive 2010/63/EU on the protection of animals used for scientific purposes). The present study did not involve any procedures within the meaning of Article 3 of Directive 2010/63/EU and as such is not subject to authorization by an ethics committee.

Author contributions
G.K., R.B., M.T.H., H.P.S., M.C.H., M.v.d.V., T.H.M.O., A.H.M., and A.S. designed the experiments. G.K., R.B., and M.T.H. performed the experiments and processed the

experimental data. G.K., R.B., M.T.H., M.C.H, T.H.M.O., A.H.M., and A.S. contributed to the interpretation of the results. G.K. and R.B. designed the figures and wrote the original draft. G.K., R.B., M.T.H., M.C.H., M.v.d.V., T.H.M.O., A.H.M., and A.S. contributed to the final review and editing of the manuscript. M.C.H., M.v.d.V., T.H.M.O., A.H.M., and A.S. supervised the project. M.C.H., H.P.S., A.H.M., and T.H.M.O. secured funding. All authors reviewed the manuscript.

Funding

This project has received funding from the Innovative Medicines Initiative 2 Joint Undertaking (IMI2 JU) (www.imi.europa.eu) under the RespiriNTM (grant No. 853932) and the RespiriTB (grant No. 853903) project within the IMI AntiMicrobial Resistance (AMR) Accelerator program (the JU receives support from the European Union's Horizon 2020 research and innovation programme and EFPIA), NWO Domain Applied and Engineering Sciences (NWO-TTW grant 13259). The funders had no role in study design, data collection and analysis, decision to publish, or preparation of the manuscript.

Acknowledgments

We gratefully acknowledge Arthur Eibergen from the Department of Infectious Diseases, Leiden University Medical Center for his contribution to the validation of MGIT as an assay applicable for testing HDT, and Nils Olijhoek, Amy M. Barclay, Daniel C.M. van der Hoeven, and Elisa van der Sar from the Institute of Biology Leiden, Leiden University for their assistance in the experimental work that provided data used in this manuscript. We also gratefully acknowledge Gabriel Forn-Cuní from the Institute of Biology Leiden, Leiden University for the use of his raincloud plots application.

References

1. Global tuberculosis report 2023. Geneva: World Health Organization; 2023 Licence: CC BY-NC-SA 30 IGO. 2023.
2. Ramakrishnan L. Revisiting the role of the granuloma in tuberculosis. Nat Rev Immunol. 2012;12(5):352-66.
3. Boshoff HI, Barry CE, 3rd. Tuberculosis - metabolism and respiration in the absence of growth. Nat Rev Microbiol. 2005;3(1):70-80.
4. Friedrich N, Hagedorn M, Soldati-Favre D, Soldati T. Prison break: pathogens' strategies to egress from host cells. Microbiol Mol Biol Rev. 2012;76(4):707-20.
5. Cilloni L, Fu H, Vesga JF, Dowdy D, Pretorius C, Ahmedov S, et al. The potential impact of the COVID-19 pandemic on the tuberculosis epidemic a modelling analysis. (2589-5370 (Electronic)).
6. Brode SK, Daley CL, Marras TK. The epidemiologic relationship between tuberculosis and non-tuberculous mycobacterial disease: a systematic review. Int J Tuberc Lung Dis. 2014;18(11):1370-7.
7. Ratnatunga CN, Lutzky VP, Kupz A, Doolan DL, Reid DW, Field M, et al. The Rise of Non-Tuberculosis Mycobacterial Lung Disease. Front Immunol. 2020;11:303.
8. van Ingen J, Wagner D, Gallagher J, Morimoto K, Lange C, Haworth CS, et al. Poor adherence to management guidelines in nontuberculous mycobacterial pulmonary diseases. Eur Respir J. 2017;49(2).
9. Saxena S, Spaink HP, Forn-Cuni G. Drug Resistance in Nontuberculous Mycobacteria: Mechanisms and Models. Biology (Basel). 2021;10(2).
10. Hawn TR, Matheson AI, Maley SN, Vandal O. Host-directed therapeutics for tuberculosis: can we harness the host? Microbiol Mol Biol Rev. 2013;77(4):608-27.
11. Kilinc G, Saris A, Ottenhoff THM, Haks MC. Host-directed therapy to combat mycobacterial infections. Immunol Rev. 2021;301(1):62-83.
12. Tobin DM. Host-Directed Therapies for Tuberculosis. Cold Spring Harb Perspect Med. 2015;5(10).
13. Wallis RS, Hafner R. Advancing host-directed therapy for tuberculosis. Nat Rev Immunol. 2015;15(4):255-63.
14. Zumla A, Rao M, Dodoo E, Maeurer M. Potential of immunomodulatory agents as adjunct host-directed therapies for multidrug-resistant tuberculosis. BMC Med. 2016;14:89.

15. McGarvey J, Bermudez LE. Pathogenesis of nontuberculous mycobacteria infections. Clin Chest Med. 2002;23(3):569-83.
16. Rocco JM, Irani VR. Mycobacterium avium and modulation of the host macrophage immune mechanisms. Int J Tuberc Lung Dis. 2011;15(4):447-52.
17. Vergne I, Gilleron M, Nigou J. Manipulation of the endocytic pathway and phagocyte functions by Mycobacterium tuberculosis lipoarabinomannan. Front Cell Infect Microbiol. 2014;4:187.
18. Levitte S, Adams KN, Berg RD, Cosma CL, Urdahl KB, Ramakrishnan L. Mycobacterial Acid Tolerance Enables Phagolysosomal Survival and Establishment of Tuberculous Infection In Vivo. Cell Host Microbe. 2016;20(2):250-8.
19. Pires D, Marques J, Pombo JP, Carmo N, Bettencourt P, Neyrolles O, et al. Role of Cathepsins in Mycobacterium tuberculosis Survival in Human Macrophages. Sci Rep. 2016;6:32247.
20. Deretic V. Autophagy in inflammation, infection, and immunometabolism. Immunity. 2021;54(3):437-53.
21. Yang Z, Klionsky DJ. Mammalian autophagy: core molecular machinery and signaling regulation. Curr Opin Cell Biol. 2010;22(2):124-31.
22. Bradfute SB, Castillo EF, Arko-Mensah J, Chauhan S, Jiang S, Mandell M, et al. Autophagy as an immune effector against tuberculosis. Curr Opin Microbiol. 2013;16(3):355-65.
23. Gutierrez MG, Master SS, Singh SB, Taylor GA, Colombo MI, Deretic V. Autophagy is a defense mechanism inhibiting BCG and Mycobacterium tuberculosis survival in infected macrophages. Cell. 2004;119(6):753-66.
24. Wang Y, Chen C, Xu XD, Li H, Cheng MH, Liu J, et al. Levels of miR-125a-5p are altered in Mycobacterium avium-infected macrophages and associate with the triggering of an autophagic response. Microbes Infect. 2020;22(1):31-9.
25. Heemskerk MT, Korbee CJ, Esselink JJ, Dos Santos CC, van Veen S, Gordijn IF, et al. Repurposing diphenylbutylpiperidine-class antipsychotic drugs for host-directed therapy of Mycobacterium tuberculosis and Salmonella enterica infections. Sci Rep. 2021;11(1):19634.
26. Korbee CJ, Heemskerk MT, Kocev D, van Strijen E, Rabiee O, Franken K, et al. Combined chemical genetics and data-driven bioinformatics approach identifies receptor tyrosine kinase inhibitors as host-directed antimicrobials. Nat Commun. 2018;9(1):358.
27. Balgi AD, Fonseca BD, Donohue E, Tsang TC, Lajoie P, Proud CG, et al. Screen for chemical modulators of autophagy reveals novel therapeutic inhibitors of mTORC1 signaling. PLoS One. 2009;4(9):e7124.
28. Jacquin E, Leclerc-Mercier S, Judon C, Blanchard E, Fraitag S, Florey O. Pharmacological modulators of autophagy activate a parallel noncanonical pathway driving unconventional LC3 lipidation. Autophagy. 2017;13(5):854-67.
29. Zhang L, Yu J, Pan H, Hu P, Hao Y, Cai W, et al. Small molecule regulators of autophagy identified by an image-based high-throughput screen. Proc Natl Acad Sci U S A. 2007;104(48):19023-8.
30. Buratta S, Urbanelli L, Ferrara G, Sagini K, Goracci L, Emiliani C. A role for the autophagy regulator Transcription Factor EB in amiodarone-induced phospholipidosis. Biochem Pharmacol. 2015;95(3):201-9.
31. Mahavadi P, Knudsen L, Venkatesan S, Henneke I, Hegermann J, Wrede C, et al. Regulation of macroautophagy in amiodarone-induced pulmonary fibrosis. J Pathol Clin Res. 2015;1(4):252-63.
32. Stadler K, Ha HR, Ciminale V, Spirli C, Saletti G, Schiavon M, et al. Amiodarone alters late endosomes and inhibits SARS coronavirus infection at a post-endosomal level. Am J Respir Cell Mol Biol. 2008;39(2):142-9.
33. Verreck FA, de Boer T, Langenberg DM, van der Zanden L, Ottenhoff TH. Phenotypic and functional profiling of human proinflammatory type-1 and anti-inflammatory type-2 macrophages in response to microbial antigens and IFN-gamma- and CD40L-mediated costimulation. J Leukoc Biol. 2006;79(2):285-93.
34. Ramakrishnan L. The zebrafish guide to tuberculosis immunity and treatment. Cold Spring Harb Symp Quant Biol. 2013;78:179-92.
35. Benard EL, van der Sar AM, Ellett F, Lieschke GJ, Spaink HP, Meijer AH. Infection of zebrafish embryos with intracellular bacterial pathogens. J Vis Exp. 2012(61).
36. Lieschke GJ, Currie PD. Animal models of human disease: zebrafish swim into view. Nat Rev Genet. 2007;8(5):353-67.
37. Varela M, Meijer AH. A fresh look at mycobacterial pathogenicity with the zebrafish host model. Mol Microbiol. 2022;117(3):661-9.
38. Davis JM, Clay H, Lewis JL, Ghori N, Herbomel P, Ramakrishnan L. Real-time visualization of mycobacterium-macrophage interactions leading to initiation of granuloma formation in zebrafish embryos. Immunity. 2002;17(6):693-702.
39. Pagan AJ, Lee LJ, Edwards-Hicks J, Moens CB, Tobin DM, Busch-Nentwich EM, et al. mTOR-regulated mitochondrial metabolism limits mycobacterium-induced cytotoxicity. Cell. 2022;185(20):3720-38 e13.

40. van der Vaart M, Korbee CJ, Lamers GE, Tengeler AC, Hosseini R, Haks MC, et al. The DNA damage-regulated autophagy modulator DRAM1 links mycobacterial recognition via TLR-MYD88 to autophagic defense [corrected]. Cell Host Microbe. 2014;15(6):753-67.
41. Cronan MR, Hughes EJ, Brewer WJ, Viswanathan G, Hunt EG, Singh B, et al. A non-canonical type 2 immune response coordinates tuberculous granuloma formation and epithelialization. Cell. 2021;184(7):1757-74 e14.
42. Zhang R, Varela M, Vallentgoed W, Forn-Cuni G, van der Vaart M, Meijer AH. The selective autophagy receptors Optineurin and p62 are both required for zebrafish host resistance to mycobacterial infection. PLoS Pathog. 2019;15(2):e1007329.
43. Munoz-Sanchez S, van der Vaart M, Meijer AH. Autophagy and Lc3-Associated Phagocytosis in Zebrafish Models of Bacterial Infections. Cells. 2020;9(11).
44. Zhang R, Varela M, Forn-Cuni G, Torraca V, van der Vaart M, Meijer AH. Deficiency in the autophagy modulator Dram1 exacerbates pyroptotic cell death of Mycobacteria-infected macrophages. Cell Death Dis. 2020;11(4):277.
45. Kilinc G, Walburg KV, Franken K, Valkenburg ML, Aubry A, Haks MC, et al. Development of Human Cell-Based In Vitro Infection Models to Determine the Intracellular Survival of Mycobacterium avium. Front Cell Infect Microbiol. 2022;12:872361.
46. Verreck FA, de Boer T Fau - Langenberg DML, Langenberg Dm Fau - Hoeve MA, Hoeve Ma Fau - Kramer M, Kramer M Fau - Vaisberg E, Vaisberg E Fau - Kastelein R, et al. Human IL-23-producing type 1 macrophages promote but IL-10-producing type 2 macrophages subvert immunity to (myco)bacteria. (0027-8424 (Print)).
47. Verreck FA, de Boer T Fau - Langenberg DML, Langenberg Dm Fau - van der Zanden L, van der Zanden L Fau - Ottenhoff THM, Ottenhoff TH. Phenotypic and functional profiling of human proinflammatory type-1 and anti-inflammatory type-2 macrophages in response to microbial antigens and IFN-gamma- and CD40L-mediated costimulation. (0741-5400 (Print)).
48. Liu WJ, Ye L, Huang WF, Guo LJ, Xu ZG, Wu HL, et al. p62 links the autophagy pathway and the ubiqutin-proteasome system upon ubiquitinated protein degradation. Cell Mol Biol Lett. 2016;21:29.
49. Sharma V, Verma S, Seranova E, Sarkar S, Kumar D. Selective Autophagy and Xenophagy in Infection and Disease. Front Cell Dev Biol. 2018;6:147.
50. Mizushima N, Levine B, Cuervo AM, Klionsky DJ. Autophagy fights disease through cellular self-digestion. Nature. 2008;451(7182):1069-75.
51. Settembre C, Ballabio A. Lysosome: regulator of lipid degradation pathways. Trends Cell Biol. 2014;24(12):743-50.
52. Settembre C, Di Malta C, Polito VA, Garcia Arencibia M, Vetrini F, Erdin S, et al. TFEB links autophagy to lysosomal biogenesis. Science. 2011;332(6036):1429-33.
53. Song TT, Cai RS, Hu R, Xu YS, Qi BN, Xiong YA. The important role of TFEB in autophagy-lysosomal pathway and autophagy-related diseases: a systematic review. Eur Rev Med Pharmacol Sci. 2021;25(3):1641-9.
54. Zhu SY, Yao RQ, Li YX, Zhao PY, Ren C, Du XH, et al. The Role and Regulatory Mechanism of Transcription Factor EB in Health and Diseases. Front Cell Dev Biol. 2021;9:667750.
55. Settembre C, Medina DL. TFEB and the CLEAR network. Methods Cell Biol. 2015;126:45-62.
56. Renshaw SA, Loynes CA, Trushell DM, Elworthy S, Ingham PW, Whyte MK. A transgenic zebrafish model of neutrophilic inflammation. Blood. 2006;108(13):3976-8.
57. Xie Y, Meijer AH, Schaaf MJM. Modeling Inflammation in Zebrafish for the Development of Anti-inflammatory Drugs. Front Cell Dev Biol. 2020;8:620984.
58. He C, Bartholomew CR, Zhou W, Klionsky DJ. Assaying autophagic activity in transgenic GFP-Lc3 and GFP-Gabarap zebrafish embryos. Autophagy. 2009;5(4):520-6.
59. Hosseini R, Lamers GE, Hodzic Z, Meijer AH, Schaaf MJ, Spaink HP. Correlative light and electron microscopy imaging of autophagy in a zebrafish infection model. Autophagy. 2014;10(10):1844-57.
60. Gomes LC, Dikic I. Autophagy in antimicrobial immunity. Mol Cell. 2014;54(2):224-33.
61. Silwal P, Kim IS, Jo EK. Autophagy and Host Defense in Nontuberculous Mycobacterial Infection. Front Immunol. 2021;12:728742.
62. Zullo AJ, Jurcic Smith KL, Lee S. Mammalian target of Rapamycin inhibition and mycobacterial survival are uncoupled in murine macrophages. BMC Biochem. 2014;15:4.
63. Heckmann BL, Green DR. LC3-associated phagocytosis at a glance. J Cell Sci. 2019;132(5).
64. Houben D, Demangel C, van Ingen J, Perez J, Baldeon L, Abdallah AM, et al. ESX-1-mediated translocation to the cytosol controls virulence of mycobacteria. Cell Microbiol. 2012;14(8):1287-98.
65. Stamm LM, Morisaki JH, Gao LY, Jeng RL, McDonald KL, Roth R, et al. Mycobacterium marinum escapes from phagosomes and is propelled by actin-based motility. J Exp Med. 2003;198(9):1361-8.
66. Chai Q, Wang X, Qiang L, Zhang Y, Ge P, Lu Z, et al. A Mycobacterium tuberculosis surface protein recruits ubiquitin to trigger host xenophagy. Nat Commun. 2019;10(1):1973.

67. Fleming A, Noda T, Yoshimori T, Rubinsztein DC. Chemical modulators of autophagy as biological probes and potential therapeutics. Nat Chem Biol. 2011;7(1):9-17.
68. Noda T, Ohsumi Y. Tor, a phosphatidylinositol kinase homologue, controls autophagy in yeast. J Biol Chem. 1998;273(7):3963-6.
69. Sarkar S, Ravikumar B, Floto RA, Rubinsztein DC. Rapamycin and mTOR-independent autophagy inducers ameliorate toxicity of polyglutamine-expanded huntingtin and related proteinopathies. Cell Death Differ. 2009;16(1):46-56.
70. Mizushima N, Yamamoto A, Hatano M, Kobayashi Y, Kabeya Y, Suzuki K, et al. Dissection of autophagosome formation using Apg5-deficient mouse embryonic stem cells. J Cell Biol. 2001;152(4):657-68.
71. Martina JA, Chen Y, Gucek M, Puertollano R. MTORC1 functions as a transcriptional regulator of autophagy by preventing nuclear transport of TFEB. Autophagy. 2012;8(6):903-14.
72. Roczniak-Ferguson A, Petit CS, Froehlich F, Qian S, Ky J, Angarola B, et al. The transcription factor TFEB links mTORC1 signaling to transcriptional control of lysosome homeostasis. Sci Signal. 2012;5(228):ra42.
73. Settembre C, Zoncu R, Medina DL, Vetrini F, Erdin S, Erdin S, et al. A lysosome-to-nucleus signalling mechanism senses and regulates the lysosome via mTOR and TFEB. EMBO J. 2012;31(5):1095-108.
74. Palmieri M, Impey S, Kang H, di Ronza A, Pelz C, Sardiello M, et al. Characterization of the CLEAR network reveals an integrated control of cellular clearance pathways. Hum Mol Genet. 2011;20(19):3852-66.
75. de la Mata M, Cotan D, Villanueva-Paz M, de Lavera I, Alvarez-Cordoba M, Luzon-Hidalgo R, et al. Mitochondrial Dysfunction in Lysosomal Storage Disorders. Diseases. 2016;4(4).
76. Gefter WB, Epstein DM, Pietra GG, Miller WT. Lung disease caused by amiodarone, a new antiarrythmic agent. Radiology. 1983;147(2):339-44.
77. Tummino TA, Rezelj VV, Fischer B, Fischer A, O'Meara MJ, Monel B, et al. Drug-induced phospholipidosis confounds drug repurposing for SARS-CoV-2. Science. 2021;373(6554):541-7.
78. Blake TL, Reasor MJ. Pulmonary responses to amiodarone in hamsters: comparison of intratracheal and oral administrations. Toxicol Appl Pharmacol. 1995;131(2):325-31.
79. Mortuza GB, Neville WA, Delaney J, Waterfield CJ, Camilleri P. Characterisation of a potential biomarker of phospholipidosis from amiodarone-treated rats. Biochim Biophys Acta. 2003;1631(2):136-46.
80. Reasor MJ, Ogle CL, Miles PR. Response of rat lungs to amiodarone: preferential accumulation of amiodarone and desethylamiodarone in alveolar macrophages. Exp Lung Res. 1990;16(6):577-91.
81. Breitenstein A, Stampfli SF, Camici GG, Akhmedov A, Ha HR, Follath F, et al. Amiodarone inhibits arterial thrombus formation and tissue factor translation. Arterioscler Thromb Vasc Biol. 2008;28(12):2231-8.
82. Pollak PT, Bouillon T, Shafer SL. Population pharmacokinetics of long-term oral amiodarone therapy. Clin Pharmacol Ther. 2000;67(6):642-52.
83. Rotmensch HH, Belhassen B, Swanson BN, Shoshani D, Spielman SR, Greenspon AJ, et al. Steady-state serum amiodarone concentrations: relationships with antiarrhythmic efficacy and toxicity. Ann Intern Med. 1984;101(4):462-9.
84. Park HS, Kim YN. Adverse effects of long-term amiodarone therapy. Korean J Intern Med. 2014;29(5):571-3.
85. Papiris SA, Triantafillidou C, Kolilekas L, Markoulaki D, Manali ED. Amiodarone: review of pulmonary effects and toxicity. Drug Saf. 2010;33(7):539-58.
86. Lachmandas E, Eckold C, Bohme J, Koeken V, Marzuki MB, Blok B, et al. Metformin Alters Human Host Responses to Mycobacterium tuberculosis in Healthy Subjects. J Infect Dis. 2019;220(1):139-50.
87. Singhal A, Jie L, Kumar P, Hong GS, Leow MK, Paleja B, et al. Metformin as adjunct antituberculosis therapy. Sci Transl Med. 2014;6(263):263ra159.
88. Boland R, Heemskerk MT, Forn-Cuni G, Korbee CJ, Walburg KV, Esselink JJ, et al. Repurposing Tamoxifen as Potential Host-Directed Therapeutic for Tuberculosis. mBio. 2023;14(1):e0302422.
89. van Doorn CLR, Schouten GK, van Veen S, Walburg KV, Esselink JJ, Heemskerk MT, et al. Pyruvate Dehydrogenase Kinase Inhibitor Dichloroacetate Improves Host Control of Salmonella enterica Serovar Typhimurium Infection in Human Macrophages. Front Immunol. 2021;12:739938.
90. Schindelin J, Arganda-Carreras I, Frise E, Kaynig V, Longair M, Pietzsch T, et al. Fiji: an open-source platform for biological-image analysis. Nat Methods. 2012;9(7):676-82.
91. Carpenter AE, Jones TR, Lamprecht MR, Clarke C, Kang IH, Friman O, et al. CellProfiler: image analysis software for identifying and quantifying cell phenotypes. Genome Biol. 2006;7(10):R100.
92. Xie Y, Tolmeijer S, Oskam JM, Tonkens T, Meijer AH, Schaaf MJM. Glucocorticoids inhibit macrophage differentiation towards a pro-inflammatory phenotype upon wounding without affecting their migration. Dis Model Mech. 2019;12(5).

Supplementary material

Table S1: Zebrafish lines

Zebrafish lines		
Name	**Description**	**Reference**
AB/TL	Wild type strain	Zfin.org
Tg(CMV:EGFP-map1lc3b)^{zf155}	GFP-tagged zebrafish Lc3	He 2009
Tg(mpeg1:mCherryF)^{umsF001}	Macrophage marker	Bernut 2014
Tg(mpeg1:EGFP)^{gl22}	Macrophage marker	Ellett 2011
Tg(mpx:EGFP)^{i114}	Neutrophil marker	Renshaw 2006
Tg(mpeg1:mCherryF, mpx:EGFP)$^{umsF001, i114}$	Macrophage and neutrophil marker	Bernut 2014, Renshaw 2006

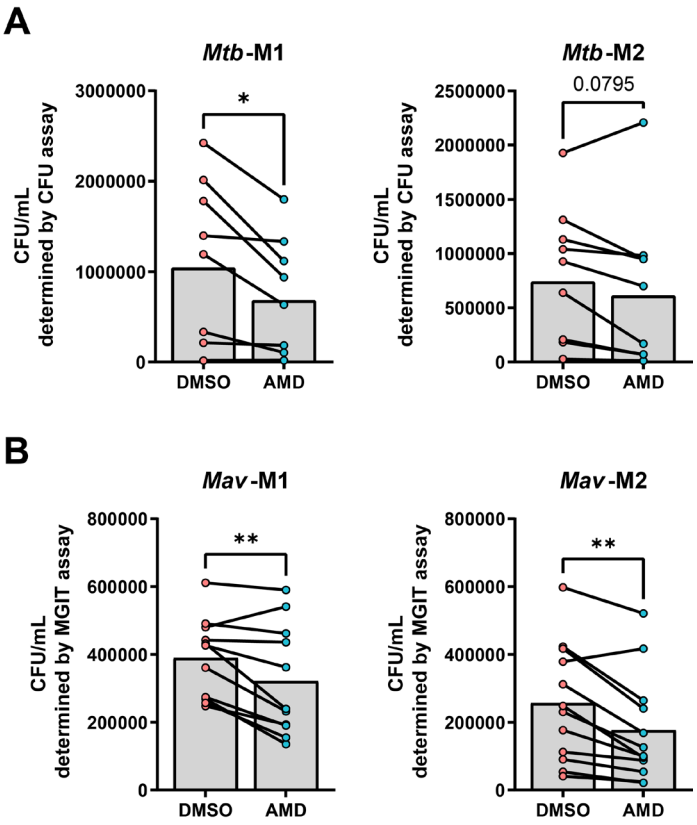

Figure S1. Identification of amiodarone as host-directed therapeutic for mycobacterial infections in primary human macrophages.
(A) *Mtb* H37Rv-infected M1 and M2 macrophages were treated 24 hours with 10 µM amiodarone or an equal volume of vehicle control DMSO. Cells were subsequently lysed and bacterial survival was determined by CFU assay. Data represent the mean from different donors (n=9 or

10). Dots represent the mean from triplicate wells of a single donor. Statistical significance was tested using a paired t-test. **(B)** Mav-infected M1 and M2 macrophages were treated 24 hours with 10 µM amiodarone or an equal volume of vehicle control DMSO. Cells were subsequently lysed and bacterial survival was determined by MGIT assay. Data represent the mean from different donors (n=11 or 12). Dots represent the mean from triplicate wells of a single donor. Statistical significance was tested using a paired t-test.
* = p<0.05 and ** = p<0.005.

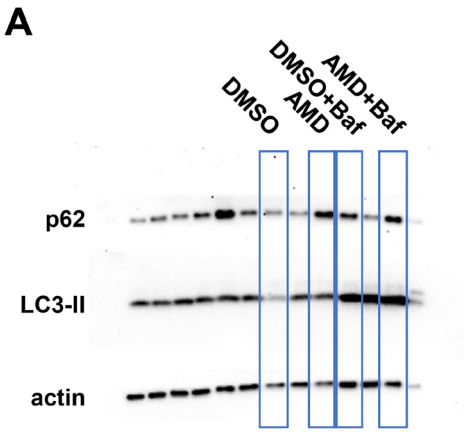

Figure S2. Protein levels of autophagy markers in primary human macrophages treated with amiodarone, in the absence or presence of bafilomycin.
(A) Western blot analysis of autophagy markers in M2 macrophages treated for 24 hours with 10 µM amiodarone or an equal volume of vehicle control DMSO (0.1% v/v) in the presence or absence of bafilomycin A1 (Baf) (10 nM) during *Mav* infection. Shown are blots for p62, LC3-II and actin from one representative donor out of six donors tested. The boxed lanes represent the lanes shown in Fig. 2A, whereas unboxed lanes contain samples that are not relevant for this study.

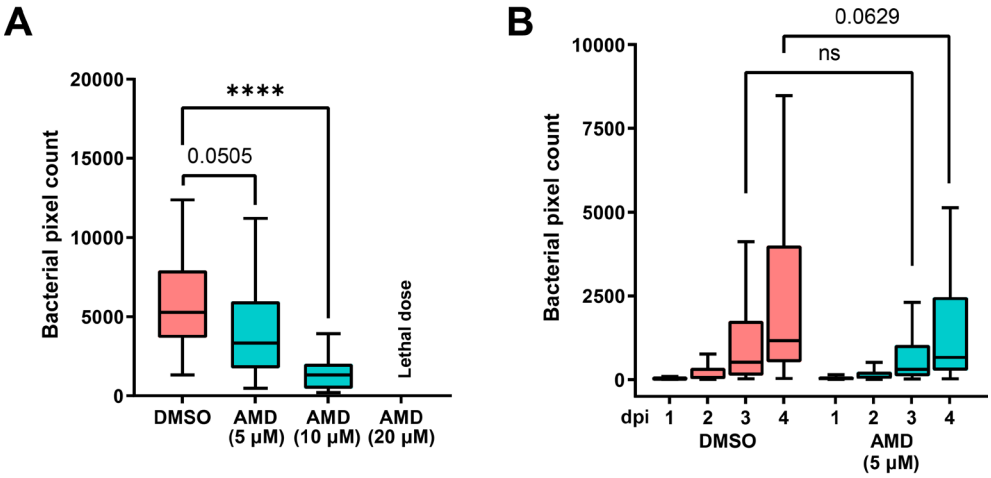

Figure S3. Amiodarone did not affect numbers of neutrophils and macrophages at the site of inflammation.

(A) Leukocyte migration assay of mpeg1:mcherryF/mpx:GFP double transgenic zebrafish larvae treated with 5 µM of Amiodarone or control (DMSO at equal v/v). Treatment was started at 1 dpf and larvae were anesthetized and leukocyte migration was induced by tail amputation at 3 dpf. Representative stereo fluorescence images of leukocyte migration towards the injury (4 hours post-amputation) are shown. Cyan shows neutrophils (mpx:GFP) and magenta shows macrophages (mpeg1:mCherryF). The region of interest (ROI) indicates the area for quantification of leukocyte migration. Scale bar annotates 220 µM. **(B-C)** Quantification of A, showing the number of migrated neutrophils **(B)** or macrophages **(C)**. Boxplots with 95% confidence intervals are shown and the black line in the boxplots indicates the group median. Statistical analysis was performed using a Mann-Whitney test.
Ns: non-significant.

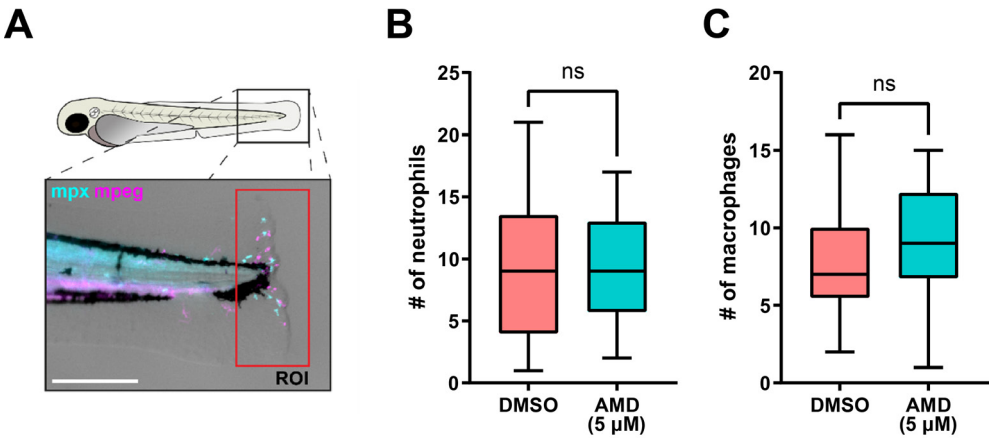

Figure S4. Amiodarone restricts *Mmar* infection in a host-directed manner.
(A) mWasabi-expressing *Mmar*-infected zebrafish larvae were treated with increasing doses of amiodarone (5, 10 and 20 µM) or vehicle control DMSO. Treatment was started at 1 hpi and bacterial pixel counts were quantified at 4 dpi. Data of 2 independent experiments were combined (n= 39-42 per group). Boxplots with 95% confidence intervals are shown and the black line in the boxplots indicates the group median. Statistical significance was tested using a Kruskal-Wallis with Dunn's multiple comparisons test. **(B)** mWasabi-expressing *Mmar*-infected zebrafish larvae were treated with 5 µM of amiodarone or vehicle control DMSO. Treatment was started at 1 hpi and larvae were anesthetized at 1, 2, 3 and 4 dpi for quantification of by imaging. Data of 2 experimental repeats were combined (n= 65-70 per group). Boxplots with 95% confidence intervals are shown and the black line in the boxplots indicates the group median. Statistical significance was tested using a Kruskal-Wallis with Dunn's multiple comparisons test.
Ns: non-significant and **** = p<0.0001.

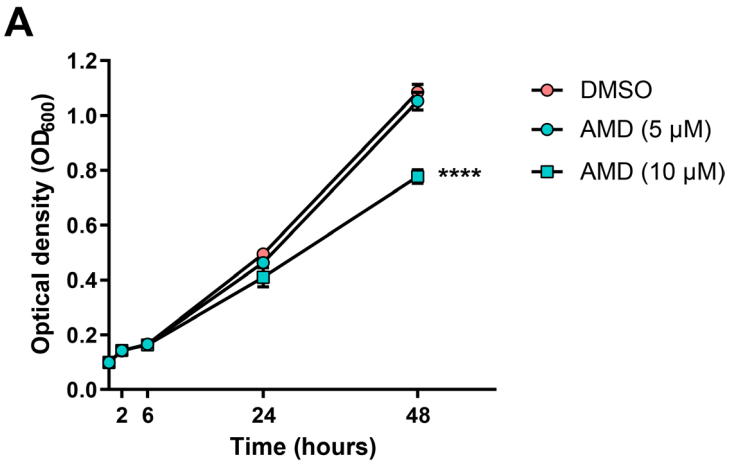

Figure S5. Growth of *Mmar* in liquid culture was not affected after exposure to 5 µM amiodarone.
(A) *Mmar* growth in liquid culture during treatment with 5 or 10 µM of amiodarone or control (DMSO at equal v/v) up to assay endpoint, day 2. Lines depict mean ± standard deviation of 2 experiments. Statistical significance of treatment versus control treatment was tested using a two-way ANOVA with Dunnett's multiple comparisons test.
**** = $p<0.0001$.

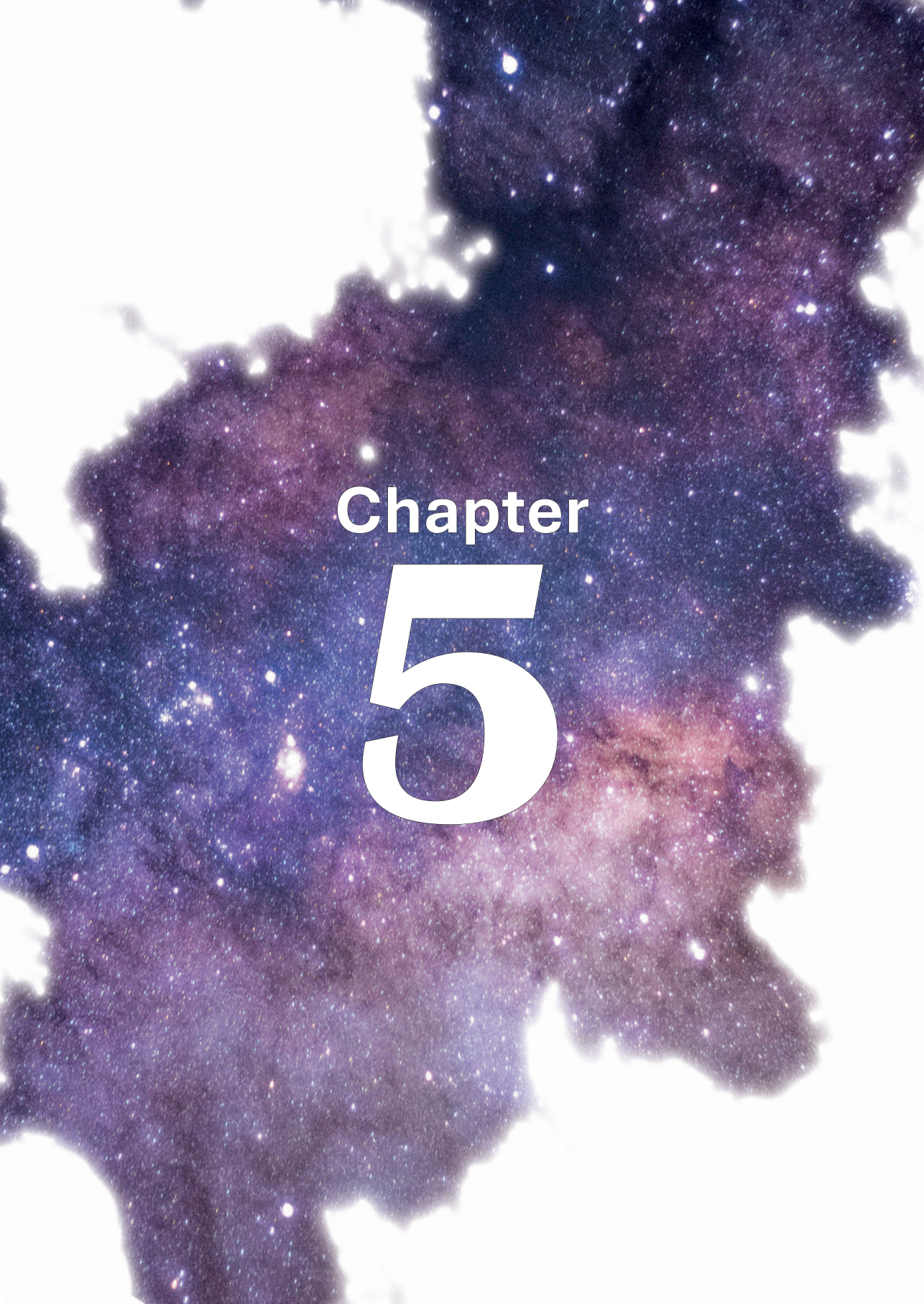
Chapter
5

Phenothiazines boost host control of *Mycobacterium avium* infection in primary human macrophages

Gül Kilinç[1], Tom H. M. Ottenhoff[1], and Anno Saris[1]

[1] Leiden University Center for Infectious Diseases, Leiden University Medical Center, Leiden, The Netherlands

Biomed Pharmacother. 2025 Feb 27:185:117941

Abstract

Mycobacterium avium (*Mav*) complex is the leading cause of pulmonary diseases associated with non-tuberculous mycobacterial (NTM) infections worldwide. The inherent and increasing acquired antibiotic resistance of *Mav* hampers the treatment of *Mav* infections and emphasizes the urgent need for alternative treatment strategies. A promising approach is host-directed therapy (HDT), which aims to boost the host's immune defenses to combat infections. In this study, we show that phenothiazines, particularly trifluoperazine (TFP) and chlorproethazine (CPE), restricted *Mav* survival in primary human macrophages. Notably, TFP and CPE did not directly inhibit mycobacterial growth at used concentrations, confirming these drugs function through host-dependent mechanisms. TFP and CPE induced a mild, albeit not statistically significant, increase in autophagic flux along with the nuclear intensity of transcription factor EB (TFEB), the master transcriptional regulator of autophagy. Inhibition of autophagic flux with bafilomycin, however, did not impair the improved host infection control by TFP and CPE, suggesting that the host (auto) phagolysosomal pathway is not causally involved in the mechanism of action of TFP and CPE. Additionally, TFP and CPE increased the production of both cellular and mitochondrial reactive oxygen species (ROS). Scavenging mitochondrial ROS did not impact, whereas inhibition of NADPH oxidase (NOX)-mediated ROS production partially impaired the HDT activity of TFP and CPE, indicating that oxidative burst may play a limited role in the improved host control of *Mav* infection by these drugs. Overall, our study demonstrates that phenothiazines are promising HDT candidates that enhance the antimicrobial response of macrophages against *Mav*, through mechanism(s) that were partially elucidated.

Graphical abstract

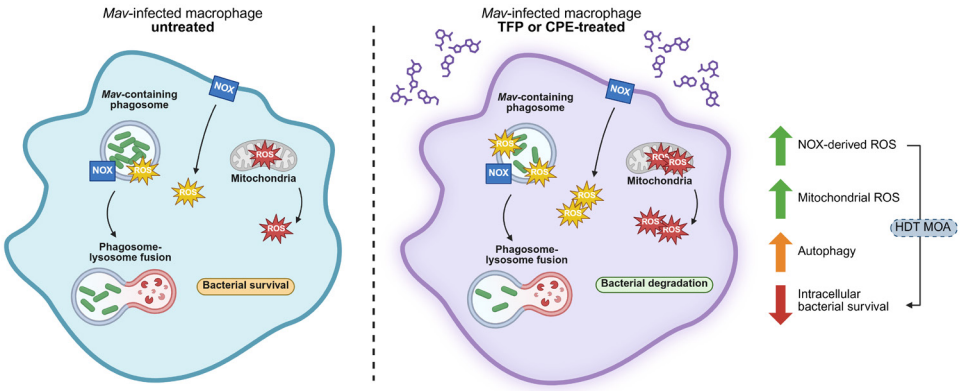

- TFP enhances host-directed control of *Mav* and *Mtb* in macrophages.
- TFP and CPE enhance macrophage control of *Mav* independently of autophagy.
- TFP and CPE strongly induce both NOX-derived and mitochondrial ROS production.
- NOX-derived ROS partially aids intracellular *Mav* infection control by TFP and CPE
- Phenothiazines are promising candidates for HDT against *Mav* infections.

1. Introduction

Nontuberculous mycobacteria (NTM), which comprise all mycobacterial species other than *Mycobacterium tuberculosis* (*Mtb*) and *Mycobacterium leprae*, are environmental microorganisms that have been isolated worldwide. The prevalence of diseases caused by NTM infections is increasing, exceeding that of tuberculosis (TB) in certain geographical regions (1-4). NTM most commonly cause lung disease, but can also lead to lymphadenitis, skin and soft tissue infections, and invasive disseminated disease (5). The *Mycobacterium avium* (*Mav*) complex is the most frequently causative pathogen of NTM infections in humans. Moreover, *Mav* is responsible for the majority of the chronic lung disease cases associated with NTM (6-8). Lung disease by *Mav* (*Mav*-LD) primarily occurs in individuals with predisposing (genetic) lung disorders (e.g. cystic fibrosis or chronic obstructive pulmonary disease) (9, 10), but *Mav*-LD also occurs in those without any known predisposing conditions (11).

The treatment of *Mav*-LD consists of a three-drug regimen comprising a macrolide, ethambutol, and a rifamycin that should be administered for at least 12 months after negative sputum conversion (5, 12). Despite this, the estimated pooled treatment success rate is only around 40% (13, 14). Furthermore, prolonged treatment duration with multiple drugs could cause adverse effects which hamper treatment adherence, contributing to the suboptimal treatment outcomes for *Mav*-LD (15). In addition, the resistance of mycobacteria to antibiotics, either intrinsic by their impermeable cell wall and localization in biofilms or cells or acquired due to suboptimal treatment further hampers successful treatment (16). Therefore, there is a pressing need for innovative approaches that improve the therapeutic response and shorten treatment duration, since this will reduce the probability of *de novo* drug resistance.

Innate immunity plays a critical role in the activation of the host response to mycobacterial infection. Upon inhalation, aerosols containing *Mav* reach the lower airways where alveolar macrophages provide the first line of defense (17, 18). Recognition of *Mav* by macrophage pattern recognition receptors, including Toll-like receptors (TLRs) and C-type lectins receptors, induces phagocytosis. Following phagocytosis, the early-forming *Mav*-containing phagosomes mature and fuse with lysosomes containing hydrolytic enzymes to form phagolysosomes capable of eliminating the mycobacteria (19, 20). In addition, TLR activation induces the production of bactericidal reactive oxygen species (ROS) (21, 22). However, mycobacteria are notorious for their capacity to impair host defense mechanisms, enabling them to persist in macrophages. For example, *Mav* protein MAV_2941 inhibits phagosome maturation, which thus prevents intracellular *Mav* killing (23, 24). In addition, predisposing host susceptibility factors, including inherited or acquired defects in the production and signaling of interleukin-12/interleukin-23/interferon-γ cascade (25), affect macrophage function, leading to an increased susceptibility to *Mav*-LD. Enhancing the antimycobacterial response of macrophages by host-directed therapy (HDT) may therefore improve the clinical outcome of *Mav* infection and is a promising adjunctive therapy to antibiotic therapy. By targeting host immunity, HDT may also help to eliminate non-replicating and drug-resistant bacteria that are tolerant or resistant to antibiotic therapy. In addition, adjunctive HDT confers the potential advantages of shortening the duration of current treatment regimens, which may reduce adverse drug effects, and reducing the likelihood of inducing mycobacterial

drug resistance since host rather than bacterial pathways are targeted. Although the development of HDT is an active area of investigation in the context of TB, this is largely lacking for *Mav* infections, and it remains unknown whether TB-directed HDT acts also on *Mav* infections.

An approach that has proved to be effective in relatively rapid identification of novel therapeutics against *Mtb* and other bacterial pathogens is drug repurposing (26, 27). Previous screening efforts with different FDA-approved drug libraries have identified several potential HDTs which could restrict intracellular mycobacterial growth (28, 29). A first step towards the identification of HDT candidates for *Mav* may be to employ the findings of the broad screening efforts for *Mtb*. Previously reported screenings of drugs on *Mtb*-infected human cells showed efficacy for several compounds annotated as autophagy-modulators, including trifluoperazine (TFP), in improving host control of infection (29). In this study, we aimed to assess the potential of TFP and related compounds as HDT against *Mav* and unravel the underlying host immune responses involved.

We identified phenothiazines as potential HDT candidates to control *Mav* bacteria in primary human macrophages. Importantly, these compounds did not show a direct antibacterial effect at the concentration in which they enhanced clearance of intracellular *Mav*, showing that phenothiazines must act via host signaling pathways. To unravel the mechanism of action, we investigated potential host antimicrobial mechanisms that have been associated with TFP.

2. Results

2.1 *In vitro i*dentification of phenothiazines as potential HDT for *Mav* infection

Based on previous screening efforts to identify new drugs with HDT activity against intracellular *Mtb*, trifluoperazine (TFP) was identified as a promising candidate (29). Before evaluating its potential to enhance clearance of intracellular *Mav* infection, the antimycobacterial effect of TFP on *Mtb* was first validated in a more physiologically relevant model. Screening of TFP decreased survival of *Mtb* in two polarized macrophages subsets, pro-inflammatory M1 and anti-inflammatory M2 macrophages (30), as determined by the MGIT system after treatment of 24 hours with 10 μM of the drug, identifying the phenothiazine-class of antipsychotic drugs as potential HDT candidates (**Fig. 1A-B**). To identify the most potent phenothiazine drug for *Mav*, we expanded the screening to include TFP and 15 additional (total 16) structurally related phenothiazines using the primary human macrophage model (31). The results showed a higher activity of phenothiazines in M1 compared to M2 macrophages (**Fig. 1C**). Five compounds showed significant impairment of bacterial survival in M1 macrophages: trifluoperazine (TFP), chlorproethazine (CPE), ZINC2187528 (ZINC), fluphenazine (FPZ) and chlorprothixene (CPT) (**Fig. 1C-D**). This effect was dose-dependent, as the drugs rapidly lost their ability to significantly impair intracellular bacteria at concentrations below 1 μM (**Supp Fig. 1**). In M2 macrophages, only CPE was able to significantly reduce the bacterial load (**Fig. 1C and 1E**). Importantly, treatment with TFP, CPE, ZINC, FPZ, and CPT did not affect the cell viability of *Mav*-infected M1 or M2 macrophages (**Fig. 1F-G**).

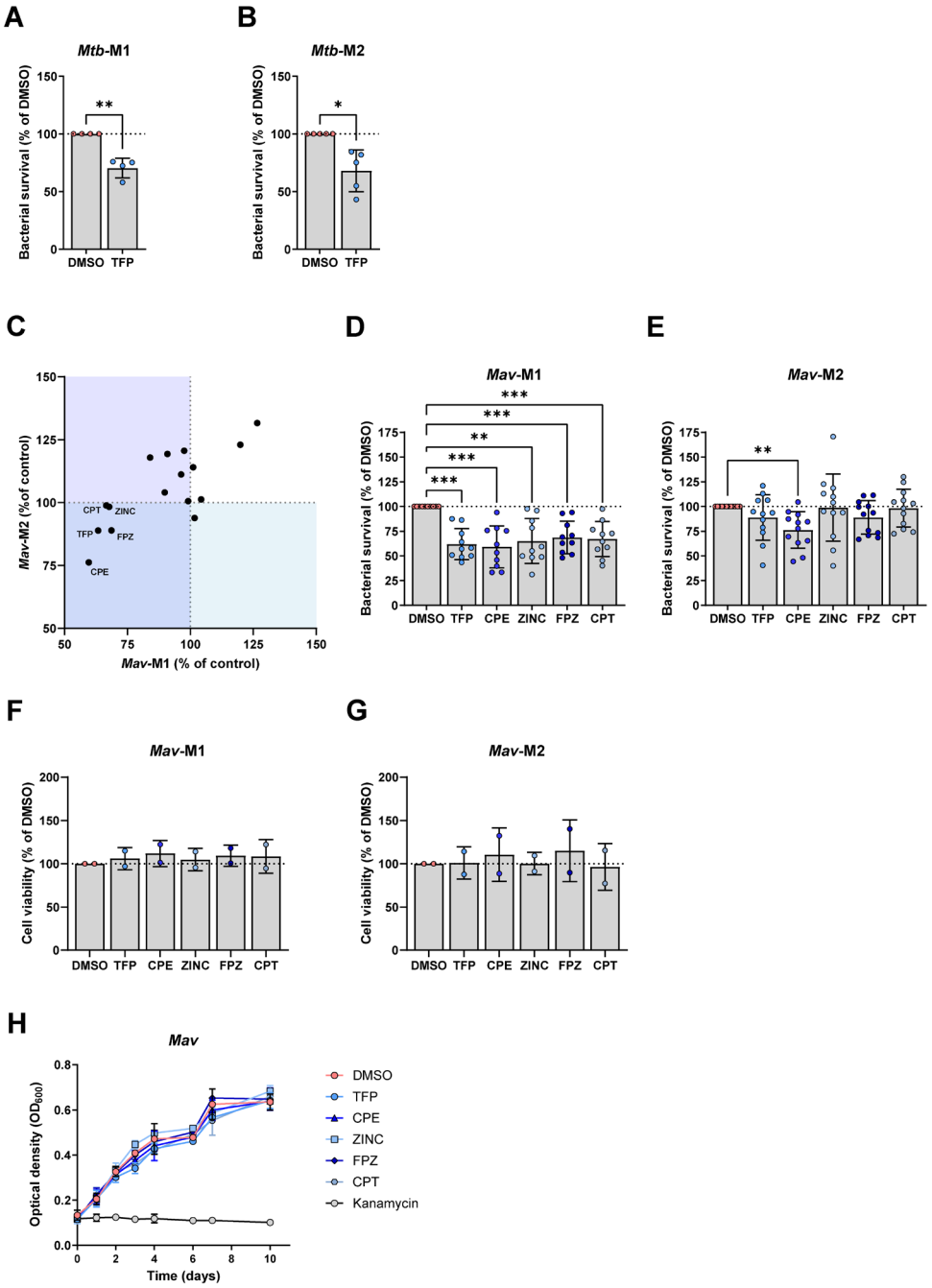

Figure 1. Identification of phenothiazines as host-directed therapeutics against *Mav* and *Mtb* in primary human macrophages. (A-B) Bacterial survival of *Mtb* within M1 and M2 macrophages after treatment with 10 µM TFP or DMSO for 24 hours, as determined by the MGIT assay (n = 4 or 5). Statistical significance was tested using a repeated-measures one-way ANOVA with Dunnett's multiple comparisons test. **(C)** Bacterial survival of *Mav* within

M1 and M2 macrophages after treatment with 10 µM of 16 phenothiazines or DMSO for 24 hours, as determined by the MGIT assay (n = 4). Dots indicated with name represent compounds that reduced intracellular bacterial survival in either M1 or M2 macrophages. **(D-E)** Bacterial survival of *Mav* within M1 and M2 macrophages after treatment with 10 µM of the five effective compounds from A or DMSO for 24 hours, as determined by the MGIT assay (n = 10 or 12). Statistical significance was tested using a repeated-measures one-way ANOVA with Dunnett's multiple comparisons test. **(F-G)** Percentage of viable *Mav*-infected M1 and M2 macrophages after treatment with 10 µM of the five effective phenothiazines or DMSO for 24 hours (n = 2). **(H)** Growth of *Mav* in liquid broth up to 10 days after exposure to positive control 100 µg/mL kanamycin, 10 µM of phenothiazines, or DMSO. Data represent the mean ± SD of triplicate wells from three independent experiments.
Dots represent the mean from triplicate wells of a single donor. Data represent the mean ± standard deviation (SD) from different donors and is expressed as a percentage of vehicle control DMSO (=100 %, indicated with the dotted line) per donor. TFP; trifluoperazine, CPE; chlorproethazine, ZINC; ZINC2187528, FPZ; fluphenazine, CPT; chlorprothixene. * = $p < 0.05$, ** = $p < 0.01$ and *** = $p < 0.001$.

To confirm that the TFP analogs reduced bacterial loads in a host-mediated manner, *Mav* in liquid medium was exposed to 10 µM of the drugs, the same concentration used as in the above *Mav* intracellular screenings. The TFP compounds did not affect the growth of *Mav*, whereas positive control kanamycin inhibited bacterial growth (**Fig. 1H**). Phenothiazine-derived molecules are cationic amphiphilic drugs (CADs), which have both lipophilic properties (logP > 1), enabling them to passively diffuse across cell and organelle membranes, and a weak base character (pKa > 8) that cause them to become positively charged under acidic conditions (**Supp Fig. 2A**) (32). These characteristics cause the drugs to become trapped within acidic compartments such as lysosomes, leading to increased intracellular drug concentrations. Therefore, we correlated the supposed ability of the drugs to reduce intracellular bacterial load with their tendency to accumulate intracellularly. After exposure of planktonic bacteria to 100 µM, growth (i.e., extracellular survival) was inhibited by the majority of phenothiazines whereas the ability of the compounds to impair intracellular bacteria, however, strongly varied between structural analogs (**Supp Fig. 2B**). The discrepancy between intra- and extracellular activity between compounds could not be explained by their tendency to accumulate intracellularly and direct inhibition of bacterial growth at higher concentrations (**Fig. 2A-B**). Thus, mere accumulation is an unlikely cause of the intracellular activity of phenothiazines, and host-directed mechanisms are more likely at play. Taken together, we identified host-directed therapy with phenothiazines that impaired the survival of intracellular *Mav* in M1 macrophages, and to a lesser extent in M2 macrophages.

To investigate the mechanism by which phenothiazines eliminated intracellular mycobacteria, we focused on TFP and CPE in M1 macrophages (in which more analogs were effective, **Fig. 1A-B**). The foremost function of phenothiazines is their antagonistic effect on D2 dopamine receptors (33, 34), receptors that are also expressed by macrophages (35). We, therefore, investigated if dopamine receptors were involved in the improved control of *Mav* infection by CPE. The addition of dopamine or quinpirole (D2 receptor agonist) did not affect bacterial survival in *Mav*-infected macrophages treated with CPE (**Supp Fig. 3A-B**). Of note, dopamine agonists in the absence of phenothiazines, in particular quinpirole, enhanced intracellular *Mav* killing,

suggesting that antagonism of dopamine D2 receptors by phenothiazines is unlikely the cause for the enhanced macrophage response to *Mav* infection. Consequently, we examined the contribution of additional intracellular host antibacterial pathways.

2.2 Improved host macrophage antimicrobial response by TFP and CPE is independent of autophagy induction

As described above, TFP and CPE are CADs, which are also known to induce phospholipidosis, a cellular phenotype caused by impaired degradation of phospholipids. To overcome phospholipidosis, cells can upregulate autophagy by enhancing the activation of transcription factor EB (TFEB), a major regulator of autophagy. Recently, CAD amiodarone was shown to impair the intracellular survival of mycobacteria by inducing autophagy via TFEB activation (36). We therefore determined whether TFP and CPE compounds induced the accumulation of phospholipids as well as activation of TFEB in *Mav*-infected macrophages. Macrophages treated with TFP or CPE showed increased accumulation of fluorescent phospholipid phosphatidylethanolamine (NBD-PE) (**Fig. 2A**). In addition, the nuclear intensity of TFEB was increased in macrophages treated with TFP or CPE, albeit not significant (p=0.051 or p=0.178, respectively) (**Fig. 2B-C**), supporting the notion that autophagy might be induced.

To further determine whether the induction of phospholipidosis could be associated with the induction of actual autophagy, the effect of TFP and CPE on autophagy markers during *Mav* infection was assessed by western blot (**Fig. 2D**). The levels of autophagosome component LC3-II were measured in the presence or absence of the (auto-)lysosomal inhibitor bafilomycin A1 (Baf); LC3-II levels indicate the formation of autophagosomes and the extent of LC3-II accumulation in presence of bafilomycin corresponds to autophagic flux. Both TFP and CPE treatment tended to increase protein levels of LC3-II, both in the absence and presence of bafilomycin (**Fig. 2E**). The autophagy response to intracellular pathogens can occur as a receptor-mediated process (selective autophagy or xenophagy) or more generally as a stress response (non-selective autophagy). To discriminate between these forms of autophagy, we examined p62, which selectively recruits polyubiquitinated cytoplasmic substrates to autophagosomes where p62 and the substrates are degraded (37, 38). Levels of p62 tended to be decreased in macrophages treated with TFP, while p62 flux remained unaffected by CPE (**Fig. 2F**). Furthermore, levels of lysosomal marker LAMP1 were not affected upon treatment with TFP and CPE (**Fig. 2G**). To determine whether the autophagy pathway was causally involved in the elimination of intracellular *Mav*, HDT activity of TFP and CPE was evaluated in *Mav*-infected macrophages whilst autophagy-mediated degradation was blocked using bafilomycin. Treatment with TFP and CPE reduced bacterial survival irrespective of inhibition of autophagy with bafilomycin (**Fig. 2H**). Collectively, these results show that while autophagy is affected by TFP and CPE treatment, the enhanced macrophage antimicrobial response upon treatment is independent of the induction of autophagy.

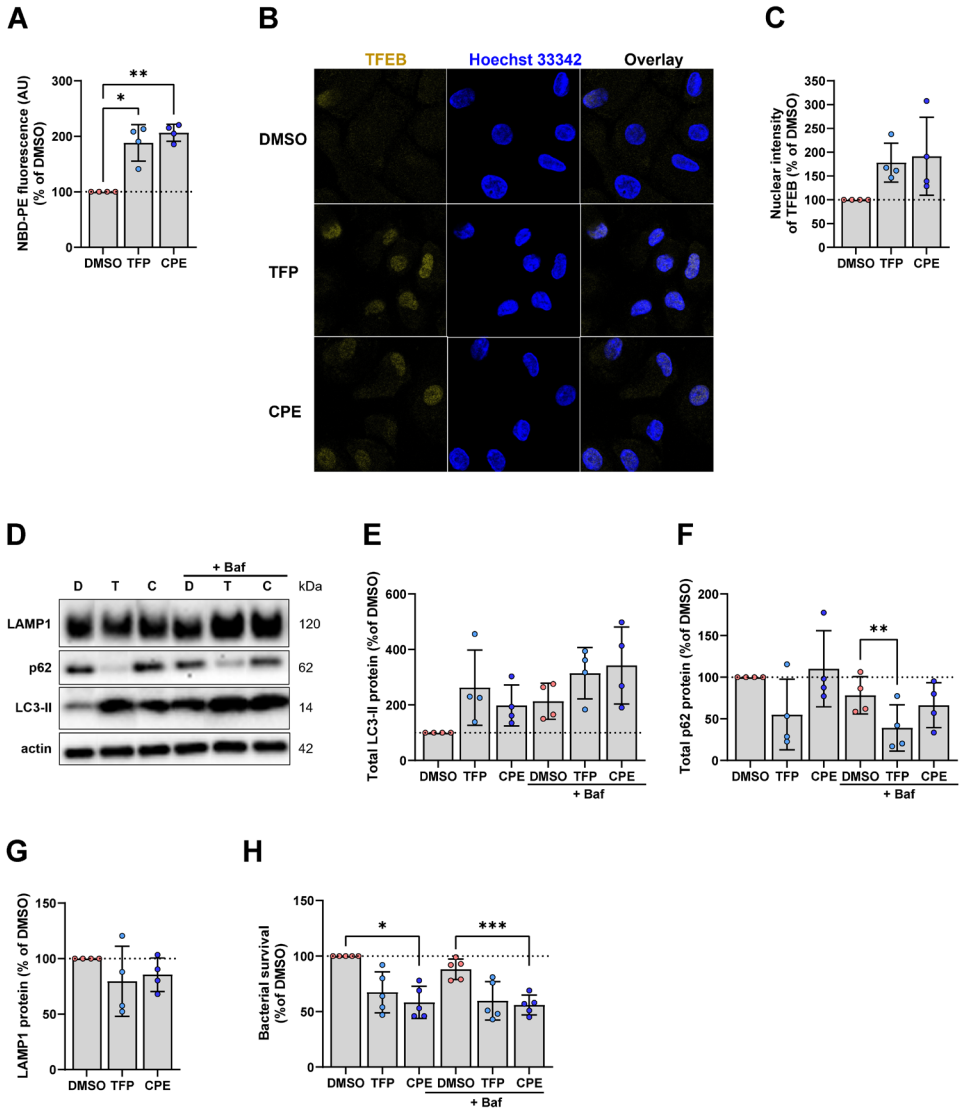

Figure 2. TFP and CPE do not require the host autophagy pathway to control *Mav* infection in primary human macrophages. (A) *Mav*-infected M1 macrophages were treated with 10 µM TFP, CPE, or DMSO and 5 µM NBD-PE for 24 hours to assess phospholipidosis induction (n = 4). Statistical significance was tested using a repeated-measures one-way ANOVA with Dunnett's multiple comparisons test. **(B)** Confocal microscopy of *Mav*-infected M1 macrophages treated with 10 µM TFP, CPE, or DMSO for 4 hours, stained for TFEB (yellow) and Hoechst 33342 (blue). Shown are images of one representative donor out of four donors tested. **(C)** Quantification of TFEB intensity within the mark of the cell nucleus. Dots represent the mean from three wells (three images/well) per condition of a single donor (n = 4). Statistical significance was tested using a repeated-measures one-way ANOVA with Dunnett's multiple comparisons test. **(D-G)** Western blot analysis of autophagy markers in M1 macrophages treated with 10 µM TFP, CPE DMSO with or without 10 nM bafilomycin A1 (Baf) for 4 hours during *Mav* infection. Shown are blots from one representative donor (D). Quantified protein levels of LC3-II (E), p62 (F), or LAMP1 (G) were normalized to actin (n = 4). Statistical significance was tested using a repeated-

measures one-way ANOVA with Bonferroni's (E-F) or Dunnett's (G) multiple comparisons test. **(H)** Bacterial survival of *Mav* within M1 macrophages treated with TFP, CPE or DMSO with or without 10 nM Baf for 24 hours, as determined by the MGIT assay (n = 5). Statistical significance was tested using a repeated-measures one-way ANOVA with Bonferroni's multiple comparisons test. Dots represent the mean from triplicate wells of a single donor. Data represent the mean ± standard deviation (SD) from different donors and is expressed as a percentage of vehicle control DMSO (=100 %, indicated with the dotted line) per donor. TFP; trifluoperazine, CPE; chlorproethazine. * = $p < 0.05$, ** = $p < 0.01$ and *** = $p < 0.001$.

2.3 NOX-derived ROS might play a limited role in TFP and CPE-enhanced host control of *Mav* infection

In addition to the autophagy pathway, the production of reactive oxygen species (ROS) has also been reported to be affected by TFP (39, 40). ROS represents another important host antimicrobial mechanism for the eradication of intracellular bacteria (41), leading us to investigate the role of ROS in the mechanism of action of both TFP and CPE. Two major sources of ROS are NADPH oxidases (NOX), located at the cell- or phagosomal- membrane, and complex I of the respiratory electron transport chain (ETC) of mitochondria (**Fig. 3A**). Using the fluorescent probe CellROX, total cellular ROS in *Mav*-infected macrophages treated with TFP or CPE was measured while the production of ROS by mitochondria was determined using the fluorescent probe MitoSOX. Both TFP and CPE significantly induced total ROS production (**Fig. 3B**). Also levels of mitochondrial ROS were significantly increased in *Mav*-infected macrophages after treatment with TFP or CPE (**Fig. 3C**). Even in the absence of infection, TFP and CPE enhanced both cellular and mitochondrial ROS in macrophages (**Supp Fig. 4A-B**). To determine whether the induction of (mitochondrial) ROS mediates TFP and CPE-enhanced host control of *Mav* infection, *Mav*-infected macrophages were treated with TFP or CPE in the presence of a variety of ROS scavengers. Known scavengers of cellular ROS, N-acetyl-cysteine (NAC) and reduced L-glutathione, failed to reduce ROS production during treatment with TFP and CPE and/or posed cell toxicity at concentrations used (**Supp Fig. 4C-F**) (42). While NAC is commonly depicted as a broad-spectrum ROS scavenger, NAC is unable to scavenge all types of ROS (43-45), and was unable to scavenge the types of ROS induced by TFP and CPE. Also MnTBAP (a superoxide dismutase mimic) did not inhibit cellular ROS production (**Supp Fig. 4G**) (46). In contrast, VAS2870, a pan-NOX inhibitor (47, 48), partially reduced cellular ROS production in control and induced by TFP and CPE (median percentage ROS induction compared to control reduced from 72% to 17% and from 134% to 72%, respectively) (**Fig. 3D**). Whilst these differences were not statistically significant, the addition of VAS2870 impaired the ability of TFP and CPE to reduce intracellular survival of *Mav* (inhibition of bacterial survival decreased from 21% to +12% and from 33% to 4%, respectively, compared to controls) (**Fig. 3E**). Thus, NOX-mediated ROS production is involved, at least to some extent, in the macrophage response to *Mav* improved by TFP and CPE.

To assess the role of mitochondrial ROS in the mode of action of TFP and CPE, MitoTEMPO (a mitochondria-targeted scavenger), rotenone (an inhibitor of complex I of the ETC) and MnTBAP were used. MitoTEMPO was ineffective in reducing TFP and CPE-induced mitochondrial ROS production (**Supp Fig. 5A-B**). If mitochondrial ROS

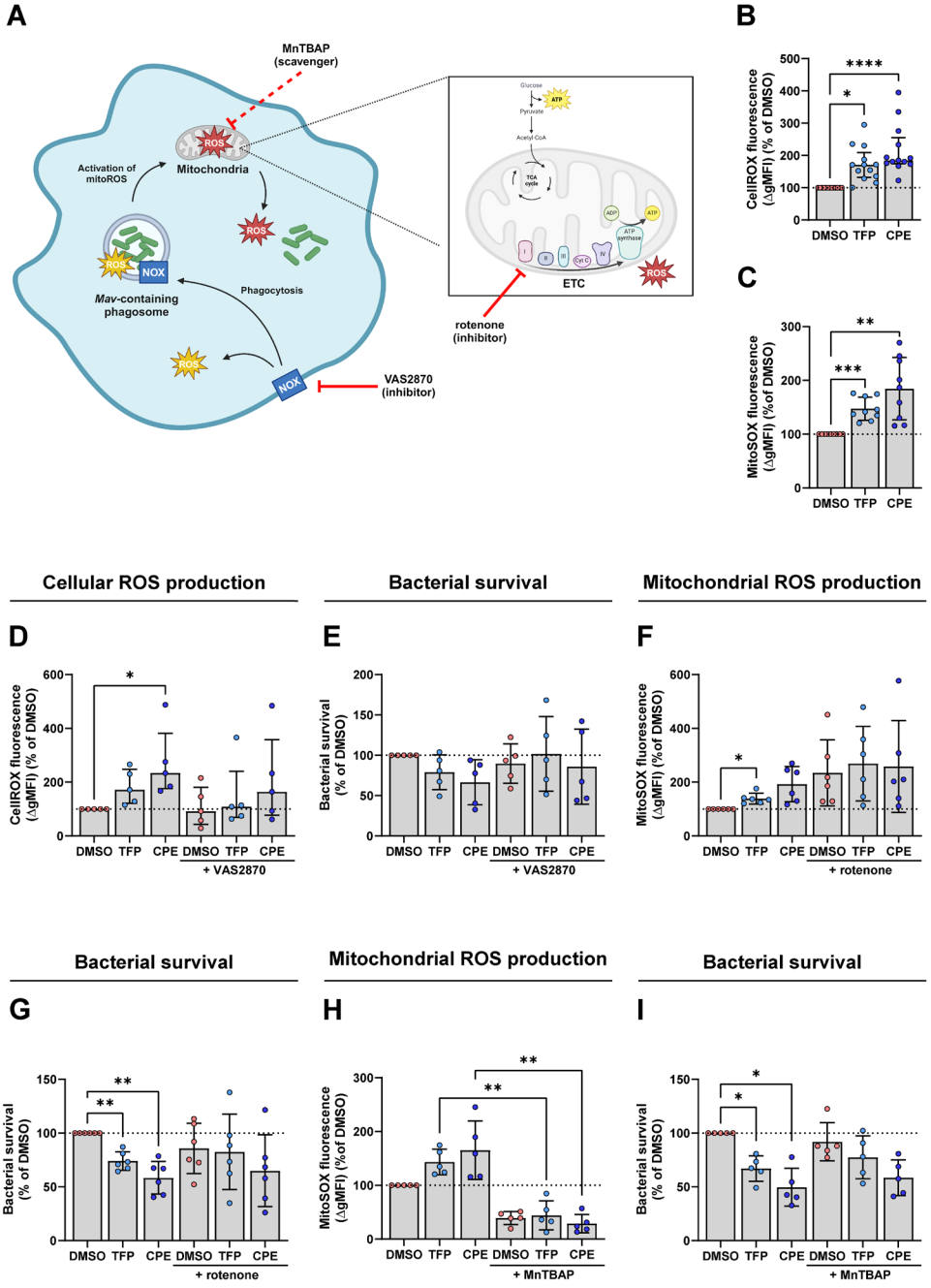

Figure 3. Induction of NOX-derived ROS by TFP and CPE might have a limited role in their enhanced macrophage response against *Mav*. (A) Schematic overview of the two major sources of ROS production in macrophages: NADPH oxidases (NOX) at (phagosomal) membranes and mitochondrial electron transport chain (ETC). Used ROS modulators: VAS2870 (NOX inhibitor), MnTBAP mitochondrial superoxide scavenger (dotted inhibition arrow), and

rotenone (ETC complex I inhibitor). **(B-C)** *Mav*-infected M1 macrophages were treated with 10 µM TFP, CPE or DMSO for 4 hours. Total cellular ROS production (B) or mitochondrial ROS (C) production was measured by flow cytometry. The geometric mean fluorescence intensity (ΔgMFI) was determined. Data represent the median ± interquartile range (B, n = 13) or mean ± SD from (C, n = 9). Statistical significance was tested using a Friedman test with Dunn's multiple comparisons test (B) or a repeated-measures one-way ANOVA with Dunnett's multiple comparisons test (C). **(D-E)** M1 macrophages were treated with 10 µM TFP, CPE, or DMSO with or without 10 µM VAS2870 for 4 (D) or 24 (E) hours after *Mav* infection. Total cellular ROS production was detected by flow cytometry. The geometric mean fluorescence intensity (ΔgMFI) (D) or bacterial survival by CFU assay (E) were determined. Data represent the median ± interquartile (D) or the mean ± SD (E) from different donors (n = 5). Statistical significance was tested using a Friedman test with Dunn's multiple comparisons test (D) or a repeated-measures one-way ANOVA with Bonferroni's multiple comparisons test (E). **(F-G)** M1 macrophages were treated with 10 µM TFP, CPE, or DMSO with or without 5 µM rotenone for 4 (F) or 24 (G) hours after *Mav* infection. Total mitochondrial ROS production was detected by flow cytometry. The geometric mean fluorescence intensity (ΔgMFI) (F) or bacterial survival by CFU assay (G) were determined. Data represent the mean ± SD from different donors (n = 6). Statistical significance was tested using a repeated-measures one-way ANOVA with Bonferroni's multiple comparisons test. **(H-I)** M1 macrophages were treated with 10 µM TFP, CPE, or DMSO with or without 100 µM MnTBAP for 4 (H) or 24 (I) hours after *Mav* infection. Total mitochondrial ROS production was detected by flow cytometry. The geometric mean fluorescence intensity (ΔgMFI) (H) or bacterial survival by CFU assay (I) were determined. Data represent the mean ± SD from different donors (n = 5). Statistical significance was tested using a repeated-measures one-way ANOVA with Bonferroni's multiple comparisons test. Dots represent the mean from duplicate wells of a single donor. Data is expressed as a percentage of vehicle control DMSO (=100 %, indicated with the dotted line) per donor. TFP; trifluoperazine, CPE; chlorproethazine. * = $p < 0.05$, ** = $p < 0.01$, *** = $p < 0.001$ and **** = $p < 0.0001$.

is produced by complex I of the ETC via the engagement of reverse electron transport (RET), rotenone will decrease ROS production, however if RET does not occur, rotenone will increase ROS production (49, 50). Here, rotenone mildly enhanced the induction of mitochondrial ROS, but did not affect the intracellular control of *Mav* by TFP and CPE (**Fig. 3F-G**). Moreover, MnTBAP significantly reduced levels of mitochondrial ROS induced by TFP or CPE in *Mav*-infected macrophages (mean percentage ROS induction compared to control reduced from 43% to 5% and from 65% to -11%, respectively) (**Fig. 3H**). Despite this substantial reduction in mitochondrial ROS, MnTBAP had a negligible effect on the intracellular control of *Mav* after TFP and CPE treatment (inhibition of bacterial survival decreased from 33% to 14% and from 50% to 33%, respectively, compared to controls) (**Fig. 3I**). Thus, while TFP and CPE induce mitochondrial ROS production, this is not causally involved in the reduced intracellular survival of *Mav*.

To exclude any false positive results caused by direct inhibition of bacterial growth by the ROS modulators, the effects of VAS2870, MnTBAP, and rotenone on bacterial growth were assessed in the absence of macrophages. Neither of the ROS modulators directly inhibited bacterial growth (**Supp Fig. 5C**). Moreover, cell death could also result in decreased intracellular bacterial load and falsely indicate that TFP and CPE act via HDT activity despite ROS modulation. VAS2870, MnTBAP, and rotenone, however, did not induce cell toxicity to *Mav*-infected macrophages (**Supp Fig. 4H and Supp Fig. 5D-E**). Taken together, these findings show that ROS production, particularly from NOX, seems to be involved in the improved host control of intracellular *Mav* induced by TFP and CPE.

3. Discussion

In this study, we identified phenothiazines, a class of antipsychotic drugs, as novel HDT candidates for the elimination of intracellular *Mav*. TFP, CPE, ZINC, FPZ, and CPT enhanced host control of *Mav* in primary human M1 macrophages at concentrations that did not directly impair bacterial growth, indicating that intracellular host rather than bacterial processes are modulated that resulted in reduced intracellular survival of *Mav*. To identify the mechanism of action, we evaluated two well-known host antibacterial pathways that are reported to be affected by TFP: autophagy and ROS production. While TFP and CPE treatments showed a trend toward induction of autophagy, this pathway was not mechanistically involved in the HDT effect of both compounds. In addition, TFP and CPE strongly induced the production of ROS without impairing cell viability. Reducing ROS production in mitochondria had no impact on bacterial survival, while inhibiting ROS from NOX partially restored the survival of intracellular *Mav* after TFP and CPE treatment. Hence, as reducing (NOX-mediated) ROS production did not fully restore the impaired bacterial survival after TFP and CPE treatment, we hypothesize that other mechanisms yet to be discovered are also at play.

Phenothiazines have been shown to have antimicrobial activity against a wide range of bacteria, including *Staphylococcus aureus* (51, 52), *Mtb* and *Mav* (53-59), by affecting multiple essential bacterial functions. At concentrations that effectively reduced intracellular *Mav* levels, both TFP and CPE did not have direct antimycobacterial activity, in line with previous observations that showed phenothiazines eradicated intracellular *Mtb* and *Mav* by macrophages (55, 60, 61), although the specific host cellular pathways involved were not addressed. Being CADs, which can accumulate intracellularly, the possibility remained that TFP and CPE might accumulate in acidic compartments in macrophages to reach antibacterial concentration levels. However, the ability of different phenothiazines to impair intracellular mycobacterial survival did not correlate with its antibiotic potency related to intracellular drug accumulation, suggesting that mere accumulation is unlikely the cause of the HDT effect and rather host-dependent mechanisms are at play. This finding aligns with previous research that shows that phenothiazine derivatives decrease bacterial burden within the host without directly affecting bacteria themselves, suggesting that these drugs modulate host cell pathways necessary to control infection (62-64).

Activation of the host autophagy pathway has been shown to reduce intracellular *Mav* burden (65), yet *Mav* has also evolved strategies to counteract this by interfering with phagosome-lysosome fusion to survive intracellularly (66, 67). Depending on the cell lines and drug concentrations used, phenothiazines have been shown to either suppress or induce autophagy (68). Suppression of autophagy may be the result of calmodulin inhibition by phenothiazines (69-71). Calmodulin is a cytosolic binding protein that is recruited and activated following increased cytosolic calcium levels in macrophages encountering mycobacteria (72, 73). The Ca^{2+}-Calmodulin complex promotes the maturation of phagosomes required for autophagy (73). In contrast, TFP is also described to promote autophagic flux in cells, including lung cell lines, and zebrafish (71, 74). Other phenothiazines than TFP promoted acidification of the phagolysosome, thereby improving intracellular killing of mycobacteria (61, 75). Previously, TFP was shown to induce autophagy in HeLa cells infected with *Salmonella*

Typhimurium and to improve clearance of intracellular infection, although it remains unclear whether these effects are causally linked (76). In the current study, TFP and CPE mildly enhanced autophagic flux and a noticeable trend in TFEB activation, in line with previous observations (77). Nevertheless, blocking autophagy and acidification did not impair the antimycobacterial HDT effect of TFP and CPE on intracellular bacteria, which indicates that lysosomal degradation is likely not essential for the host-protective effect of phenothiazines.

Another host pathway that is known to be fundamental for macrophages to kill invasive pathogens is ROS production (78). TFP has been shown to increase both cellular and mitochondrial ROS levels in our as well as other studies (39, 79). Two major sources of ROS are NADPH oxidases (NOX) and the mitochondrial electron transport chain (ETC) (41). NOX enzymes, primarily located on the plasma membrane, produce cytosolic ROS. During phagocytosis, the plasma membrane forms the interior wall of the phagocytic vesicle, releasing ROS into the vesicle to kill pathogens (78). ROS production induced by TFP and CPE was in part derived from NOX, as NOX inhibition only partially impaired ROS production. NOX-inhibition also restored bacterial survival after TFP and CPE treatment to a certain extent, suggesting that NOX plays a role in eliminating intracellular *Mav* by TFP and CPE. Furthermore, mitochondrial ROS, traditionally seen as a by-product of respiration and indicative of oxidative stress (41), is now also recognized as an important antibacterial response in innate immune cells (78, 80). In addition, mitochondrial ROS production via RET from complex II to complex I of the ETC was shown to promote intracellular killing of *Mav* (81). Our finding that TFP and CPE induced mitochondrial ROS production seemingly without involvement of RET, therefore, may explain why mitochondrial ROS is not involved in enhanced macrophage response induced by TFP and CPE against intracellular *Mav*. The discrepancy in the occurrence of RET within *Mav*-infected macrophages between this and the study by Røst et al. might be attributed to variations in the experimental setup (81), including the longer infection and shorter treatment duration until the readout of ROS in our study. Taken together, these findings suggest that while both NOX-mediated and mitochondrial ETC-mediated ROS production are induced, only the ROS production driven by NOX to a limited extent can account for the enhanced host control of *Mav* by TFP and CPE.

Phenothiazines are approved as drugs for the treatment of neurological disorders such as schizophrenia by inhibiting dopamine receptors (82, 83). While dopamine has been extensively studied for its role in the central nervous system, emerging evidence indicates its role as an immunomodulator in innate immunity (35). Treatment of macrophages with dopamine showed activation of NF-Kb leading to increased secretion of pro-inflammatory cytokines and chemokines (84-86), which are associated with macrophage activation and control of mycobacterial infections (87-89). Similarly, we show that dopamine receptor agonists improved control of intracellular *Mav* infection regardless of the presence of phenothiazines. Therefore, TFP and CPE, being dopamine receptor antagonists, reduce intracellular *Mav* loads likely by a mechanism independent of dopamine receptor antagonism. Moreover, TFP inhibits dopamine receptors at nanomolar concentrations (90), yet its host-directed effects against *Mav* were only evident at micromolar concentrations. The notion that TFP and CPE control *Mav* infection independent of dopamine receptors is supported

by the finding that structural modifications abolishing dopamine receptor binding did not affect phenothiazines' ability to inhibit intracellular *Mtb* growth (91). Hence, eliminating the dopamine receptor-dependent psychotropic effects of phenothiazines while maintaining their HDT activity against intracellular bacteria seems feasible.

Limitations of our study may be that, although HDT would likely be used as adjunctive therapy in clinical settings, the efficacy of phenothiazines in combination with conventional antibiotics was not assessed, as the primary focus was to discover the mechanism of action of phenothiazines. Future studies should explore drug interactions and effects on the efficacy of phenothiazines when combined with antibiotics, to design shorter, more effective, and safer drug regimens. In addition, when deciphering the mechanisms of phenothiazines, the focus was on M1 macrophages without examining the mechanistic effects on M2 macrophages. M1 macrophages are critical for immediate pathogen clearance, whereas M2 macrophages may involve different cellular pathways potentially linked to drug efficacy. Furthermore, while we investigated major sources of ROS production, the role of other ROS sources such as peroxisomes or cytochrome P450 enzymes was not explored (41). Although limited information exists on how these sources impact macrophage-mediated immunity, these minor ROS sources could play a role in the HDT activity of TFP and CPE which warrants further research. Moreover, although we suggest that TFP and CPE likely act independently of dopamine receptors, we cannot rule out receptor involvement entirely. Irrespectively, as these compounds are known to interact with dopamine receptors, concerns about (e.g., cognitive) side effects could limit their use for treating mycobacterial infections. Additionally, the effective concentration of TFP (and CPE) in our study exceeds the peak plasma levels (1.3-7.6 nM) following oral administration of a 5 mg TFP tablet (initial twice-daily dosing for the treatment of schizophrenia) (92). Ideally, phenothiazines will be chemically modified to reduce their binding to dopamine receptors while enhancing their antimycobacterial activity, which may improve the therapeutic window during clinical application. Another approach to address this issue may be alternative drug delivery strategies such as nanoencapsulation of TFP and CPE (93), which may limit systemic exposure and reduce toxicity risks while enabling localized drug delivery to infected macrophages. While we aimed to identify the mechanism of action, phenothiazines may improve host control of intracellular *Mav* by acting on multiple pathways. The pleiotropy of phenothiazines makes it extremely challenging to detect significant effects when only one pathway is analyzed at a time. Although the exact mechanisms of action of phenothiazines remain unidentified, our study rules out host autophagy and suggests that cellular ROS production plays a moderate role, thereby guiding the focus for future research. Given that *Mav* exploits various antioxidative strategies to evade host defenses (94-97), investigating by which mechanisms phenothiazines induce (NOX-derived) ROS production could provide valuable insights into how these bacterial defenses can be counteracted and how these drugs enhance macrophage activity against mycobacteria. By highlighting the potential of phenothiazines as novel HDT candidates, our study may contribute to the development of more effective therapeutic strategies to combat mycobacterial infection.

Our findings show that phenothiazines act via host-dependent mechanisms to promote the clearance of *Mav* within macrophages. Nevertheless, the precise

mechanisms underlying their therapeutic effects were only partially unraveled and require further investigation. Elucidating these mechanisms will not only deepen our understanding of host-pathogen interactions during *Mav* infection but will also facilitate the development of targeted therapeutic strategies utilizing phenothiazine-derived compounds as HDT for intracellular bacterial infections.

4. Materials and methods

4.1 Reagents and antibodies

Anti-human CD163-PE, CD14-PE-Cy7, and CD1a-Alexa Fluor 647 (1:20) were purchased from Biolegend (Amsterdam, the Netherlands), and anti-human CD11b-BB515 (1:20) from BD Biosciences. For confocal microscopy, rabbit anti-human TFEB (1:200) from Cell Signaling Technology (Leiden, the Netherlands), and donkey anti-rabbit IgG (H + L)-Alexa Fluor 555 (1:200) from Abcam (Amsterdam, the Netherlands) were used. Hoechst 33342 (1:2,000) was obtained from Sigma-Aldrich (Zwijndrecht, the Netherlands). For western blot, rabbit anti-human LC3B (1:500) from Novus Biologicals/Bio-Techne (Abingdon, UK), mouse anti-human SQSTM1/p62 (1:500) from Santa Cruz Biotechnology (Heidelberg, Germany), rabbit anti-human LAMP1 (1:500) from Abcam and mouse anti-human β-actin (1:1,000) from Sigma-Aldrich were used. Horseradish peroxidase-conjugated goat anti-rabbit IgG (H + L) and goat anti-mouse IgG (H + L) (1:5,000) were purchased from Invitrogen, ThermoFisher Scientific (Landsmeer, the Netherlands).

N-4-nitrobenzo-2-oxa-1,3-diazole-phosphatidylethanolamine (NBD-PE), CellROX, and MitoSOX probes were purchased from Invitrogen, ThermoFisher Scientific. Trifluoperazine dihydrochloride was obtained from Enzo Life Sciences (Brussels, Belgium), chlorproethazine hydrochloride from Toronto Research Chemical, chlorprothixene from Vitas-M Laboratory (Apeldoorn, the Netherlands), fluphenazine dihydrochloride from Sigma-Aldrich and ZINC218752 from Specs (Zoetermeer, the Netherlands). Dimethyl sulfoxide (DMSO), bafilomycin A1, kanamycin sulfate, dopamine hydrochloride, quinpirole hydrochloride, N-acetyl-L-cysteine, L-glutathione reduced, MitoTEMPO, MnTBAP, VAS2870, and rotenone were purchased from Sigma-Aldrich.

4.2 Cell culture

Buffy coats were collected from healthy anonymous Dutch adult donors who provided written informed consent (Sanquin Blood Bank, Amsterdam, the Netherlands), to isolate primary monocyte-derived macrophages as previously described (45). In summary, CD14+ monocytes were isolated from peripheral blood mononuclear cells using density gradient centrifugation with Ficoll (Pharmacy, LUMC, the Netherlands) and subsequently using magnetic-activated cell sorting with anti-CD14-coated microbeads (Miltenyi Biotec, Auburn, CA, USA). Purified CD14+ monocytes were cultured for 6 days at 37°C/5% CO_2 using Gibco Dutch modified Roswell Park Memorial Institute (RPMI) 1640 medium (ThermoFisher Scientific, Landsmeer, the Netherlands), which was supplemented with 10% fetal calf serum (FCS), 2 mM L-glutamine (PAA, Linz, Austria), 100 units/mL penicillin, 100 µg/mL streptomycin, and either 5 ng/mL granulocyte-macrophage colony-stimulating factor (GM-CSF, ThermoFisher Scientific) for pro-inflammatory M1 macrophage differentiation or 50 ng/mL macrophage colony-stimulating factor (M-CSF, R&D Systems, Abingdon, UK)

for anti-inflammatory M2 macrophage differentiation. One day prior to experiments, macrophages were harvested and seeded into flat-bottom 96-well plates (30,000 cells/well), if not indicated otherwise, in RPMI+10% FCS + 2 mM L-glutamine (without antibiotics or cytokines). Macrophage differentiation was quality controlled by quantifying cell surface marker expression (CD11b, CD1a, CD14, and CD163) using flow cytometry and secretion of cytokines (IL-10 and IL-12) following a 24-hour stimulation with 100 ng/mL lipopolysaccharide (InvivoGen, San Diego, USA).

4.3 Bacterial cultures

The *Mav* laboratory strain 101 (700898, ATCC, VA, USA) was transformed to express Wasabi, as previously described (31). Both *Mav* and *Mav*-Wasabi strains were cultured in Difco Middlebrook 7H9 broth, supplemented with 10% ADC (albumin, dextrose, and catalase) enrichment, (both from Becton Dickinson, Breda, the Netherlands), 0.2% glycerol (Merck Life Science, Amsterdam, the Netherlands), 0.05% Tween-80 (Merck Life Science), and in case of *Mav*-Wasabi, also with 100 µg/ml of Hygromycin B (Life Technologies). Bacteria were diluted twice weekly based on optical density at 600 nm (OD_{600}) measurements. Prior to experiments, bacterial concentrations were determined by measuring the OD_{600}. The Wasabi-expressing *Mav* strain was used for all experiments, except for the ROS production assays.

4.4 Cell-free bacterial growth assay

To determine any effect of compounds on bacterial growth, *Mav* cultures were diluted to OD_{600} =0.1. These cultures were mixed 1:1 with chemical compounds or DMSO control at indicated concentrations and subsequently incubated at 37°C/5% CO_2. Bacterial growth was monitored every other day, up to day 10 of incubation using OD_{600} measurements (Envision Multimode Plate Reader, Perkin Elmer).

4.5 Bacterial infection and treatment of cells

One day before infection, *Mav* culture was diluted to OD_{600}=0.25, corresponding to early log-phase growth. On the day of macrophage infection, bacteria were diluted in antibiotic-free cell culture medium to achieve a multiplicity of infection (MOI) of 10. The accuracy of the MOI was verified using a standard CFU assay (31). After adding bacteria to the cells, plates were centrifuged shortly (3 minutes at 130 rcf). After 1 hour of infection at 37°C/5% CO_2, the supernatant was removed, and cells were washed with RPMI 1640 medium containing 30 µg/mL gentamicin to inactivate the remaining extracellular bacteria. Cells were then treated with compounds at the indicated concentration or an equal volume of vehicle control (DMSO 0.1%, vol/vol), in the presence of 5 µg/mL gentamicin and incubated at 37°C/5% CO_2 until the experimental readout. After treatment, the supernatant was either harvested for lactate dehydrogenase (LDH) assay or discarded, and cells were lysed using either 100 or 125 µL of lysis buffer (H2O + 0.05% sodium dodecyl sulfate (SDS)) to assess the intracellular bacterial burden using a CFU assay or the MGIT system (31) respectively, or they were processed for further analysis. The activity of phenothiazines on the elimination of bacteria was determined by calculating the fraction of intracellular bacteria post-treatment in comparison to the control.

4.6 Lactate dehydrogenase (LDH) release assay

Cells (30,000 cells/well) were infected and treated as described for the appropriate

experiments. Supernatants were transferred to a new plate and used to quantify LDH release by reacting with the substrate mix from the Cytotoxicity Detection kit (LDH) (Merck Life Science) for 30 minutes at RT in the dark. LDH release was quantified by measuring the absorbance (A) at 485 nm using the SpectraMax i3x (Molecular Devices, San Jose, CA, USA). For the calculation of the cell viability, LDH release by samples treated with DMSO was used as the lower limit, and release by samples treated with 2% triton X-100 was used as the upper limit: $((1-(A_{sample}-A_{min}/A_{max}-A_{min}) *100\%$.

4.7 Western blot analysis

After infection and treatment, cells (300,000 cells/well in 24-well plates) were lysed with EBSB buffer (10% v/v glycerol, 3% SDS, 100 mM Tris-HCl, pH 6.8, supplemented with cOmplete™ EDTA-free protease inhibitor cocktail) (Sigma-Aldrich). Protein concentrations of cell lysates were measured using the Pierce™ BCA protein assay kit (ThermoFisher Scientific), as described previously (98). Protein levels of LC3-II, p62, or LAMP1 were assessed as described previously (99). In short, cell lysates were prepared and loaded on 15-well 4%–20% Mini-PROTEAN TGX Precast Protein Gel (Bio-Rad Laboratories, Veenendaal, the Netherlands). After transferring proteins to Immun-Blot PVDF membranes (Bio-Rad), the membranes were blocked with PBS containing 5% non-fat dry milk (PBS/5% milk) (Campina, Amersfoort, the Netherlands) for 45 minutes and incubated with primary antibodies for 90 minutes at RT. After two washing steps with PBS containing 0.75% Tween-20 (PBST), the membranes were incubated with secondary antibodies for 45 minutes at RT. Finally, the membranes underwent two washes with PBST before revelation using the enhanced chemiluminescence SuperSignal West Dura extended duration substrate (ThermoFisher Scientific). Protein bands were analyzed and quantified using ImageJ/Fiji software (NIH, Bethesda, MD, USA) and normalized against actin levels

4.8 Confocal microscopy

For confocal microscopy, poly-d-lysine-coated glass-bottom 96-well plates (no. 1.5, MatTek Corporation, Ashland, MA, USA) were washed using cell culture medium, after which macrophages (30,000 cells/well) were seeded one day prior to experiments. Following infection and treatment, cells were stained for TFEB as described before (99). In short, cells were fixed using 1% (wt/vol) formaldehyde for 1 hour, permeabilized using 0.1% Triton X-100 for 10 minutes, blocked with 5% human serum diluted in PBS (PBS/5% HS) for 45 minutes, and subsequently stained with primary antibodies for 30 minutes at RT. After two washing steps with PBS/5% HS, cells were incubated with secondary antibodies for 30 minutes at RT in the dark. Finally, cells were stained with Hoechst 33342 for 10 minutes at RT in the dark. Samples were cured overnight using ProLong Glass Antifade Mountant (Invitrogen, ThermoFisher Scientific). Each well was imaged with three images using a Leica SP8WLL Confocal microscope (Leica, Amsterdam, the Netherlands) equipped with a 63× oil immersion objective. CellProfiler 3.0.0. was used for the assessment of the integrated/mean intensity of TFEB per single nucleus, followed by the calculation of the median of the images per condition to determine the nuclear presence of TFEB.

4.9 Phospholipidosis induction assay

For the assessment of phospholipidosis induction, cells (30,000 cells/well) were cultured in black 96-well plates. Following infection, cells were treated with

compounds and 5 µM of the fluorescent phospholipid probe NBD-PE. Afterwards, cells were washed once with PBS and fluorescence was measured on the Envision Multimode Plate Reader.

4.10 ROS production assay

Cells (30,000 cells/well) were cultured in 96-well plates. Following infection, cells were treated for four hours until readout. Prior to readout, cells were incubated with 3 µM of CellROX or 5 µM MitoSOX probes for 30 minutes at 37°C/5% CO_2. Next, cells were washed thrice with PBS, trypsinized with 0.05% trypsin-EDTA, and scraped for collection. Fluorescence intensity was assessed by fixating samples with 1% paraformaldehyde before measuring samples at wavelength 533/30 nm (CellROX) or 585/40 nm (MitoSOX) on the BD Accuri C6 Plus flow cytometer (BD Biosciences). Fluorescence intensity was corrected for autofluorescence of cells. The analysis was performed using FlowJo v10 Software (BD Biosciences).

4.11 Statistics

For normally distributed paired datasets of more than two groups and one independent variable, repeated measures one-way ANOVA was used, and for multiple variables two-way ANOVA was used. In non-normally distributed paired data of more than two groups, the Friedman test was used to evaluate the statistical relevance of observed differences. Statistical differences were considered significant if p-values were < 0.05. Data analyses and graphical representation were performed using GraphPad Prism 9.0 (GraphPad Software, San Diego, CA, USA).

Data availability statement

Data will be made available on request.

Ethics statement

The studies involving humans were approved by Institutional Review Board of the Leiden University Medical Center, the Netherlands. The studies were conducted in accordance with the local legislation and institutional requirements. The participants provided their written informed consent to participate in this study.

Author Contributions

GK: Writing original draft, Writing review-editing, Conceptualization, Investigation, Methodology, Formal analysis, Validation, Visualization.

THMO: Writing review-editing, Conceptualization, Supervision, Project administration, Funding acquisition.

AS: Writing review-editing, Conceptualization, Methodology, Supervision, Project administration, Funding acquisition, Visualization.

Funding

This project has received funding from the Innovative Medicines Initiative 2 Joint Undertaking (IMI2 JU) (www.imi.europa.eu) under the RespiriNTM (grant N° 853932) project within the IMI AntiMicrobial Resistance (AMR) Accelerator program. The JU receives support from the European Union's Horizon 2020 research and innovation programme and EFPIA. The funders had no role in study design, data collection and analysis, decision to publish, or preparation of the manuscript. All claims expressed

in this article reflect solely the authors' view and do not necessarily represent those of the JU. The JU is not responsible for any use that may be made of the information it contains.

Acknowledgments
The authors would like to thank Kees L. M. C. Franken for the construction of the pSMT3 construct and Kimberley V. Walburg for performing the electroporation for generating the Wasabi-expressing *Mav* strain.

Conflict of Interest
The authors declare that they have no known competing financial interests or personal relationships that could have appeared to influence the work reported in this paper.

Declaration of generative AI and AI-assisted technologies in the writing process
During the preparation of this work, the author(s) used ChatGPT v4 (OpenAI, 2024) to improve the language and readability of the manuscript. After using this tool/service, the author(s) reviewed and edited the content as needed and take(s) full responsibility for the content of the publication.

References
1. Adjemian J, Olivier KN, Seitz AE, Holland SM, Prevots DR. Prevalence of nontuberculous mycobacterial lung disease in U.S. Medicare beneficiaries. Am J Respir Crit Care Med. 2012;185(8):881-6.
2. Brode S, Daley C, Marras T. The epidemiologic relationship between tuberculosis and non-tuberculous mycobacterial disease: a systematic review. The International journal of tuberculosis and lung disease. 2014;18(11):1370-7.
3. Marras TK, Chedore P, Ying AM, Jamieson F. Isolation prevalence of pulmonary non-tuberculous mycobacteria in Ontario, 1997 2003. Thorax. 2007;62(8):661-6.
4. Ringshausen FC, Wagner D, de Roux A, Diel R, Hohmann D, Hickstein L, et al. Prevalence of Nontuberculous Mycobacterial Pulmonary Disease, Germany, 2009-2014. Emerg Infect Dis. 2016;22(6):1102-5.
5. Griffith DE, Aksamit T, Brown-Elliott BA, Catanzaro A, Daley C, Gordin F, et al. An official ATS/IDSA statement: Diagnosis, treatment, and prevention of nontuberculous mycobacterial diseases. Am J Resp Crit Care. 2007;175(4):367-416.
6. Ingen Jv, Wagner D, Gallagher J, Morimoto K, Lange C, Haworth CS, et al. Poor adherence to management guidelines in nontuberculous mycobacterial pulmonary diseases. Eur Respir J. 2017;49(2):1601855.
7. Prevots DR, Marras TK. Epidemiology of human pulmonary infection with nontuberculous mycobacteria: a review. Clin Chest Med. 2015;36(1):13-34.
8. van Ingen J, Obradovic M, Hassan M, Lesher B, Hart E, Chatterjee A, et al. Nontuberculous mycobacterial lung disease caused by Mycobacterium avium complex - disease burden, unmet needs, and advances in treatment developments. Expert Rev Resp Med. 2021;15(11):1387-401.
9. Honda JR, Knight V, Chan ED. Pathogenesis and Risk Factors for Nontuberculous Mycobacterial Lung Disease. Clinics in Chest Medicine. 2015;36(1):1-11.
10. Chan ED, Iseman MD. Underlying host risk factors for nontuberculous mycobacterial lung disease. Semin Respir Crit Care Med. 2013;34(1):110-23.
11. Huang JH, Kao PN, Adi V, Ruoss SJ. Mycobacterium avium-intracellulare Pulmonary Infection in HIV-Negative Patients Without Preexisting Lung Disease: Diagnostic and Management Limitations. Chest. 1999;115(4):1033-40.
12. Daley CL, Iaccarino JM, Lange C, Cambau E, Wallace RJ, Jr., Andrejak C, et al. Treatment of nontuberculous mycobacterial pulmonary disease: an official ATS/ERS/ESCMID/IDSA clinical practice guideline. Eur Respir J. 2020;56(1).
13. Xu HB, Jiang RH, Li L. Treatment outcomes for Mycobacterium avium complex: a systematic review and meta-analysis. Eur J Clin Microbiol. 2014;33(3):347-58.
14. Kwon YS, Koh WJ, Daley CL. Treatment of Mycobacterium avium Complex Pulmonary Disease. Tuberc Respir Dis (Seoul). 2019;82(1):15-26.
15. Kumar K, Daley CL, Griffith DE, Loebinger MR. Management of Mycobacterium avium complex and

Mycobacterium abscessus pulmonary disease: therapeutic advances and emerging treatments. Eur Respir Rev. 2022;31(163).
16. Saxena S, Spaink HP, Forn-Cuní G. Drug Resistance in Nontuberculous Mycobacteria: Mechanisms and Models. Biology. 2021;10(2):96.
17. Koh W-J. Nontuberculous Mycobacteria—Overview. Microbiology Spectrum. 2017;5(1):10.1128/microbiolspec.tnmi7-0024-2016.
18. Shamaei M, Mirsaeidi M. Nontuberculous Mycobacteria, Macrophages, and Host Innate Immune Response. Infect Immun. 2021;89(8):e0081220.
19. Lee H-J, Woo Y, Hahn T-W, Jung YM, Jung Y-J. Formation and Maturation of the Phagosome: A Key Mechanism in Innate Immunity against Intracellular Bacterial Infection. Microorganisms. 2020;8(9):1298.
20. Uribe-Querol E, Rosales C. Control of Phagocytosis by Microbial Pathogens. Front Immunol. 2017;8:1368.
21. Lv J, He X, Wang H, Wang Z, Kelly GT, Wang X, et al. TLR4-NOX2 axis regulates the phagocytosis and killing of Mycobacterium tuberculosis by macrophages. Bmc Pulm Med. 2017;17(1):194.
22. Li P, Chang M. Roles of PRR-Mediated Signaling Pathways in the Regulation of Oxidative Stress and Inflammatory Diseases. Int J Mol Sci. 2021;22(14).
23. Danelishvili L, Chinison JJJ, Pham T, Gupta R, Bermudez LE. The Voltage-Dependent Anion Channels (VDAC) of Mycobacterium avium phagosome are associated with bacterial survival and lipid export in macrophages. Scientific Reports. 2017;7(1):7007.
24. Danelishvili L, Bermudez LE. Mycobacterium avium MAV_2941 mimics phosphoinositol-3-kinase to interfere with macrophage phagosome maturation. Microbes Infect. 2015;17(9):628-37.
25. Ottenhoff TH, Verreck FA, Lichtenauer-Kaligis EG, Hoeve MA, Sanal O, van Dissel JT. Genetics, cytokines and human infectious disease: lessons from weakly pathogenic mycobacteria and salmonellae. Nat Genet. 2002;32(1):97-105.
26. Fatima S, Bhaskar A, Dwivedi VP. Repurposing Immunomodulatory Drugs to Combat Tuberculosis. Front Immunol. 2021;12:645485.
27. Czyz DM, Potluri LP, Jain-Gupta N, Riley SP, Martinez JJ, Steck TL, et al. Host-directed antimicrobial drugs with broad-spectrum efficacy against intracellular bacterial pathogens. mBio. 2014;5(4):e01534-14.
28. Boland R, Heemskerk MT, Forn-Cuni G, Korbee CJ, Walburg KV, Esselink JJ, et al. Repurposing Tamoxifen as Potential Host-Directed Therapeutic for Tuberculosis. mBio. 2023;14(1):e0302422.
29. Heemskerk MT, Korbee CJ, Esselink JJ, Dos Santos CC, van Veen S, Gordijn IF, et al. Repurposing diphenylbutylpiperidine-class antipsychotic drugs for host-directed therapy of Mycobacterium tuberculosis and Salmonella enterica infections. Sci Rep. 2021;11(1):19634.
30. Korbee CJ, Heemskerk MT, Kocev D, van Strijen E, Rabiee O, Franken K, et al. Combined chemical genetics and data-driven bioinformatics approach identifies receptor tyrosine kinase inhibitors as host-directed antimicrobials. Nat Commun. 2018;9(1):358.
31. Kilinc G, Walburg KV, Franken K, Valkenburg ML, Aubry A, Haks MC, et al. Development of Human Cell-Based In Vitro Infection Models to Determine the Intracellular Survival of Mycobacterium avium. Front Cell Infect Microbiol. 2022;12:872361.
32. Ploemen J-PHTM, Kelder J, Hafmans T, van de Sandt H, van Burgsteden JA, Salemink PJM, et al. Use of physicochemical calculation of pKa and CLogP to predict phospholipidosis-inducing potential: A case study with structurally related piperazines. Experimental and Toxicologic Pathology. 2004;55(5):347-55.
33. Jaszczyszyn A, Gasiorowski K, Swiatek P, Malinka W, Cieslik-Boczula K, Petrus J, et al. Chemical structure of phenothiazines and their biological activity. Pharmacol Rep. 2012;64(1):16-23.
34. Marques LO, Lima MS, Soares BG. Trifluoperazine for schizophrenia. Cochrane Database Syst Rev. 2004;2004(1):CD003545.
35. Channer B, Matt SM, Nickoloff-Bybel EA, Pappa V, Agarwal Y, Wickman J, et al. Dopamine, Immunity, and Disease. Pharmacol Rev. 2023;75(1):62-158.
36. Kilinc G, Boland R, Heemskerk MT, Spaink HP, Haks MC, van der Vaart M, et al. Host-directed therapy with amiodarone in preclinical models restricts mycobacterial infection and enhances autophagy. Microbiol Spectr. 2024;12(8):e0016724.
37. Liu WJ, Ye L, Huang WF, Guo LJ, Xu ZG, Wu HL, et al. p62 links the autophagy pathway and the ubiqutin-proteasome system upon ubiquitinated protein degradation. Cell Mol Biol Lett. 2016;21:29.
38. Sharma V, Verma S, Seranova E, Sarkar S, Kumar D. Selective Autophagy and Xenophagy in Infection and Disease. Front Cell Dev Biol. 2018;6:147.
39. Huang C, Lan W, Fraunhoffer N, Meilerman A, Iovanna J, Santofimia-Castano P. Dissecting the Anticancer Mechanism of Trifluoperazine on Pancreatic Ductal Adenocarcinoma. Cancers (Basel). 2019;11(12).
40. Xia Y, Jia C, Xue Q, Jiang J, Xie Y, Wang R, et al. Antipsychotic Drug Trifluoperazine Suppresses Colorectal Cancer by Inducing G0/G1 Arrest and Apoptosis. Front Pharmacol. 2019;10:1029.

41. Herb M, Schramm M. Functions of ROS in Macrophages and Antimicrobial Immunity. Antioxidants (Basel). 2021;10(2).
42. Charbonneau ME, Passalacqua KD, Hagen SE, Showalter HD, Wobus CE, O'Riordan MXD. Perturbation of ubiquitin homeostasis promotes macrophage oxidative defenses. Sci Rep. 2019;9(1):10245.
43. Aruoma OI, Halliwell B, Hoey BM, Butler J. The antioxidant action of N-acetylcysteine: its reaction with hydrogen peroxide, hydroxyl radical, superoxide, and hypochlorous acid. Free Radic Biol Med. 1989;6(6):593-7.
44. Murphy MP, Bayir H, Belousov V, Chang CJ, Davies KJA, Davies MJ, et al. Guidelines for measuring reactive oxygen species and oxidative damage in cells and in vivo. Nat Metab. 2022;4(6):651-62.
45. Pedre B, Barayeu U, Ezerina D, Dick TP. The mechanism of action of N-acetylcysteine (NAC): The emerging role of H(2)S and sulfane sulfur species. Pharmacol Ther. 2021;228:107916.
46. Tumurkhuu G, Koide N, Dagvadorj J, Hassan F, Islam S, Naiki Y, et al. MnTBAP, a synthetic metalloporphyrin, inhibits production of tumor necrosis factor-alpha in lipopolysaccharide-stimulated RAW 264.7 macrophages cells via inhibiting oxidative stress-mediating p38 and SAPK/JNK signaling. FEMS Immunol Med Microbiol. 2007;49(2):304-11.
47. Reis J, Massari M, Marchese S, Ceccon M, Aalbers FS, Corana F, et al. A closer look into NADPH oxidase inhibitors: Validation and insight into their mechanism of action. Redox Biology. 2020;32:101466.
48. Wingler K, Altenhoefer SA, Kleikers PW, Radermacher KA, Kleinschnitz C, Schmidt HH. VAS2870 is a pan-NADPH oxidase inhibitor. Cell Mol Life Sci. 2012;69(18):3159-60.
49. Barrientos A, Moraes CT. Titrating the effects of mitochondrial complex I impairment in the cell physiology. J Biol Chem. 1999;274(23):16188-97.
50. Votyakova TV, Reynolds IJ. DeltaPsi(m)-Dependent and -independent production of reactive oxygen species by rat brain mitochondria. J Neurochem. 2001;79(2):266-77.
51. Hendricks O, Butterworth TS, Kristiansen JE. The in-vitro antimicrobial effect of non-antibiotics and putative inhibitors of efflux pumps on Pseudomonas aeruginosa and Staphylococcus aureus. International Journal of Antimicrobial Agents. 2003;22(3):262-4.
52. Nehme H, Saulnier P, Ramadan AA, Cassisa V, Guillet C, Eveillard M, et al. Antibacterial activity of antipsychotic agents, their association with lipid nanocapsules and its impact on the properties of the nanocarriers and on antibacterial activity. PLoS One. 2018;13(1):e0189950.
53. Bettencourt MV, Bosne-David S, Amaral L. Comparative in vitro activity of phenothiazines against multidrug-resistant Mycobacterium tuberculosis. International Journal of Antimicrobial Agents. 2000;16(1):69-71.
54. Kristiansen JE, Vergmann B. THE ANTIBACTERIAL EFFECT OF SELECTED PHENOTHIAZINES AND THIOXANTHENES ON SLOW-GROWING MYCOBACTERIA. Acta Pathologica Microbiologica Scandinavica Series B: Microbiology. 1986;94B(1-6):393-8.
55. Advani MJ, Siddiqui I, Sharma P, Reddy H. Activity of trifluoperazine against replicating, non-replicating and drug resistant M. tuberculosis. PLoS One. 2012;7(8):e44245.
56. Amaral L, Kristiansen JE, Abebe LS, Millett W. Inhibition of the respiration of multi-drug resistant clinical isolates of Mycobacterium tuberculosis by thioridazine: potential use for initial therapy of freshly diagnosed tuberculosis. J Antimicrob Chemother. 1996;38(6):1049-53.
57. Gadre DV, Talwar V. In vitro susceptibility testing of Mycobacterium tuberculosis strains to trifluoperazine. J Chemother. 1999;11(3):203-6.
58. Gadre DV, Talwar V, Gupta HC, Murthy PS. Effect of trifluoperazine, a potential drug for tuberculosis with psychotic disorders, on the growth of clinical isolates of drug resistant Mycobacterium tuberculosis. Int Clin Psychopharmacol. 1998;13(3):129-31.
59. Ratnakar P, Murthy PS. Trifluoperazine inhibits the incorporation of labelled precursors into lipids, proteins and DNA of Mycobacterium tuberculosis H37Rv. FEMS Microbiol Lett. 1993;110(3):291-4.
60. Deshpande D, Srivastava S, Musuka S, Gumbo T. Thioridazine as Chemotherapy for Mycobacterium avium Complex Diseases. Antimicrob Agents Chemother. 2016;60(8):4652-8.
61. Ordway D, Viveiros M, Leandro C, Bettencourt R, Almeida J, Martins M, et al. Clinical concentrations of thioridazine kill intracellular multidrug-resistant Mycobacterium tuberculosis. Antimicrob Agents Chemother. 2003;47(3):917-22.
62. Andersson Jourdan A, Peniche Alex G, Galindo Cristi L, Boonma P, Sha J, Luna Ruth A, et al. New Host-Directed Therapeutics for the Treatment of Clostridioides difficile Infection. mBio. 2020;11(2):10.1128/mbio.00053-20.
63. Andersson Jourdan A, Fitts Eric C, Kirtley Michelle L, Ponnusamy D, Peniche Alex G, Dann Sara M, et al. New Role for FDA-Approved Drugs in Combating Antibiotic-Resistant Bacteria. Antimicrobial Agents and Chemotherapy. 2016;60(6):3717-29.
64. Andersson JA, Sha J, Kirtley ML, Reyes E, Fitts EC, Dann SM, et al. Combating Multidrug-Resistant

Pathogens with Host-Directed Nonantibiotic Therapeutics. Antimicrob Agents Chemother. 2018;62(1).
65. Silva T, Moreira AC, Nazmi K, Moniz T, Vale N, Rangel M, et al. Lactoferricin Peptides Increase Macrophages' Capacity To Kill Mycobacterium avium. mSphere. 2017;2(4).
66. Crowle AJ, Dahl R, Ross E, May MH. Evidence that vesicles containing living, virulent Mycobacterium tuberculosis or Mycobacterium avium in cultured human macrophages are not acidic. Infect Immun. 1991;59(5):1823-31.
67. Frehel C, de Chastellier C, Lang T, Rastogi N. Evidence for inhibition of fusion of lysosomal and prelysosomal compartments with phagosomes in macrophages infected with pathogenic Mycobacterium avium. Infect Immun. 1986;52(1):252-62.
68. Li A, Chen X, Jing Z, Chen J. Trifluoperazine induces cellular apoptosis by inhibiting autophagy and targeting NUPR1 in multiple myeloma. FEBS Open Bio. 2020;10(10):2097-106.
69. Prozialeck WC, Weiss B. Inhibition of calmodulin by phenothiazines and related drugs: structure-activity relationships. Journal of Pharmacology and Experimental Therapeutics. 1982;222(3):509.
70. Berchtold MW, Villalobo A. The many faces of calmodulin in cell proliferation, programmed cell death, autophagy, and cancer. Biochim Biophys Acta. 2014;1843(2):398-435.
71. Otreba M, Stojko J, Rzepecka-Stojko A. The role of phenothiazine derivatives in autophagy regulation: A systematic review. J Appl Toxicol. 2023;43(4):474-89.
72. Kusner DJ. Mechanisms of mycobacterial persistence in tuberculosis. Clinical Immunology. 2005;114(3):239-47.
73. Malik ZA, Iyer SS, Kusner DJ. Mycobacterium tuberculosis Phagosomes Exhibit Altered Calmodulin-Dependent Signal Transduction: Contribution to Inhibition of Phagosome-Lysosome Fusion and Intracellular Survival in Human Macrophages1. The Journal of Immunology. 2001;166(5):3392-401.
74. Zhang Y, Nguyen DT, Olzomer EM, Poon GP, Cole NJ, Puvanendran A, et al. Rescue of Pink1 Deficiency by Stress-Dependent Activation of Autophagy. Cell Chem Biol. 2017;24(4):471-80 e4.
75. Martins M, Viveiros M, Amaral L. Inhibitors of Ca2+ and K+ transport enhance intracellular killing of M. tuberculosis by non-killing macrophages. In Vivo. 2008;22(1):69-75.
76. Conway KL, Kuballa P, Song JH, Patel KK, Castoreno AB, Yilmaz OH, et al. Atg16l1 is required for autophagy in intestinal epithelial cells and protection of mice from Salmonella infection. Gastroenterology. 2013;145(6):1347-57.
77. Zhang Y, Nguyen DT, Olzomer EM, Poon GP, Cole NJ, Puvanendran A, et al. Rescue of Pink1 Deficiency by Stress-Dependent Activation of Autophagy. Cell Chemical Biology. 2017;24(4):471-80.e4.
78. Canton M, Sanchez-Rodriguez R, Spera I, Venegas FC, Favia M, Viola A, et al. Reactive Oxygen Species in Macrophages: Sources and Targets. Front Immunol. 2021;12:734229.
79. Xia Y, Xu F, Xiong M, Yang H, Lin W, Xie Y, et al. Repurposing of antipsychotic trifluoperazine for treating brain metastasis, lung metastasis and bone metastasis of melanoma by disrupting autophagy flux. Pharmacol Res. 2021;163:105295.
80. West AP, Brodsky IE, Rahner C, Woo DK, Erdjument-Bromage H, Tempst P, et al. TLR signalling augments macrophage bactericidal activity through mitochondrial ROS. Nature. 2011;472(7344):476-80.
81. Rost LM, Louet C, Bruheim P, Flo TH, Gidon A. Pyruvate Supports RET-Dependent Mitochondrial ROS Production to Control Mycobacterium avium Infection in Human Primary Macrophages. Front Immunol. 2022;13:891475.
82. Snyder SH, Banerjee SP, Yamamura HI, Greenberg D. Drugs, neurotransmitters, and schizophrenia. Science. 1974;184(4143):1243-53.
83. Stone JM, Morrison PD, Pilowsky LS. Glutamate and dopamine dysregulation in schizophrenia--a synthesis and selective review. J Psychopharmacol. 2007;21(4):440-52.
84. Nolan RA, Reeb KL, Rong Y, Matt SM, Johnson HS, Runner K, et al. Dopamine activates NF-κB and primes the NLRP3 inflammasome in primary human macrophages. Brain, Behavior, & Immunity - Health. 2020;2:100030.
85. Gaskill PJ, Carvallo L, Eugenin EA, Berman JW. Characterization and function of the human macrophage dopaminergic system: implications for CNS disease and drug abuse. J Neuroinflammation. 2012;9:203.
86. Nolan RA, Muir R, Runner K, Haddad EK, Gaskill PJ. Role of Macrophage Dopamine Receptors in Mediating Cytokine Production: Implications for Neuroinflammation in the Context of HIV-Associated Neurocognitive Disorders. J Neuroimmune Pharmacol. 2019;14(1):134-56.
87. Cooper AM, Mayer-Barber KD, Sher A. Role of innate cytokines in mycobacterial infection. Mucosal Immunology. 2011;4(3):252-60.
88. Sasindran SJ, Torrelles JB. Mycobacterium Tuberculosis Infection and Inflammation: what is Beneficial for the Host and for the Bacterium? Frontiers in Microbiology. 2011;2.
89. Park HE, Lee W, Choi S, Jung M, Shin MK, Shin SJ. Modulating macrophage function to reinforce

host innate resistance against Mycobacterium avium complex infection. Front Immunol. 2022;13:931876.
90. Lahti RA, Evans DL, Stratman NC, Figur LM. Dopamine D4 versus D2 receptor selectivity of dopamine receptor antagonists: possible therapeutic implications. European Journal of Pharmacology. 1993;236(3):483-6.
91. Salie S, Hsu N-J, Semenya D, Jardine A, Jacobs M. Novel non-neuroleptic phenothiazines inhibit Mycobacterium tuberculosis replication. J Antimicrob Chemoth. 2014;69(6):1551-8.
92. Midha KK, Korchinski ED, Verbeeck RK, Roscoe RM, Hawes EM, Cooper JK, et al. Kinetics of oral trifluoperazine disposition in man. Br J Clin Pharmacol. 1983;15(3):380-2.
93. Vibe CB, Fenaroli F, Pires D, Wilson SR, Bogoeva V, Kalluru R, et al. Thioridazine in PLGA nanoparticles reduces toxicity and improves rifampicin therapy against mycobacterial infection in zebrafish. Nanotoxicology. 2016;10(6):680-8.
94. Abukhalid N, Islam S, Ndzeidze R, Bermudez LE. Mycobacterium avium Subsp. hominissuis Interactions with Macrophage Killing Mechanisms. Pathogens. 2021;10(11).
95. Braunstein M, Espinosa BJ, Chan J, Belisle JT, Jacobs WR, Jr. SecA2 functions in the secretion of superoxide dismutase A and in the virulence of Mycobacterium tuberculosis. Mol Microbiol. 2003;48(2):453-64.
96. Ng VH, Cox JS, Sousa AO, MacMicking JD, McKinney JD. Role of KatG catalase-peroxidase in mycobacterial pathogenesis: countering the phagocyte oxidative burst. Mol Microbiol. 2004;52(5):1291-302.
97. Sherman DR, Sabo PJ, Hickey MJ, Arain TM, Mahairas GG, Yuan Y, et al. Disparate responses to oxidative stress in saprophytic and pathogenic mycobacteria. Proc Natl Acad Sci U S A. 1995;92(14):6625-9.
98. van Doorn CLR, Schouten GK, van Veen S, Walburg KV, Esselink JJ, Heemskerk MT, et al. Pyruvate Dehydrogenase Kinase Inhibitor Dichloroacetate Improves Host Control of Salmonella enterica Serovar Typhimurium Infection in Human Macrophages. Front Immunol. 2021;12:739938.
99. Kilinc G, Boland R, Heemskerk MT, Spaink HP, Haks MC, van der Vaart M, et al. Host-directed therapy with amiodarone in preclinical models restricts mycobacterial infection and enhances autophagy. Microbiol Spectr. 2024:e0016724.

Supplementary material

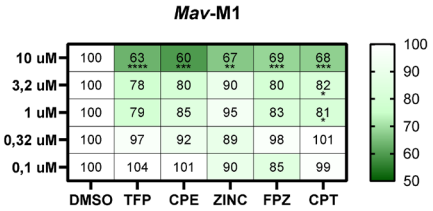

Supplementary Figure 1. Identification of phenothiazines as host-directed therapeutics against *Mav* in primary human macrophages.
Bacterial survival of *Mav* within M1 macrophages after treatment with 10, 3.2, 1, 0.32, or 0.1 µM of five phenothiazines or DMSO for 24 hours, as determined by the MGIT assay. Data represent the mean ± standard deviation (SD) from minimally four donors. Dots represent the mean from triplicate wells of a single donor. Bacterial survival is expressed as a percentage of DMSO (=100%) per donor. Statistical significance was tested using a two-way ANOVA with Dunnett's multiple comparisons test. Asterisks depict the significance of treatments.
TFP; trifluoperazine, CPE; chlorproethazine, ZINC; ZINC2187528, FPZ; fluphenazine, CPT; chlorprothixene.

* = p<0.05, ** = p<0.01, *** = p<0.001 and **** = p<0.0001.

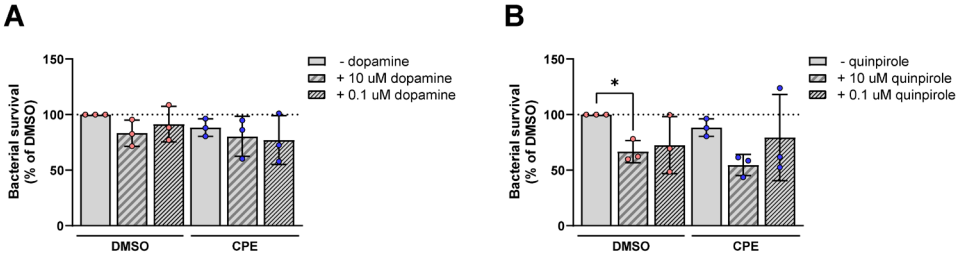

Supplementary Figure 2. Physical properties of 16 phenothiazines associated with intracellular drug accumulation.
(A) The 16 phenothiazines are graphed in relation to pKa (basic) and logP. The exclusion limits of the Ploemen models are delineated by the dotted lines. Blue dots represent the analogs that impaired the survival of *Mav* in primary human macrophages, whereas the black dots represent compounds that were not effective. **(B)** Bacterial survival in *Mav*-infected macrophages after treatment with 10 µM of the phenothiazines or DMSO for 24 hours (Figure 1A) in comparison to bacterial survival in planktonic culture (absent of macrophages) after treatment with 100 µM of the drugs or DMSO.
TFP; trifluoperazine, CPE; chlorproethazine, ZINC; ZINC2187528, FPZ; fluphenazine and CPT; chlorprothixene.

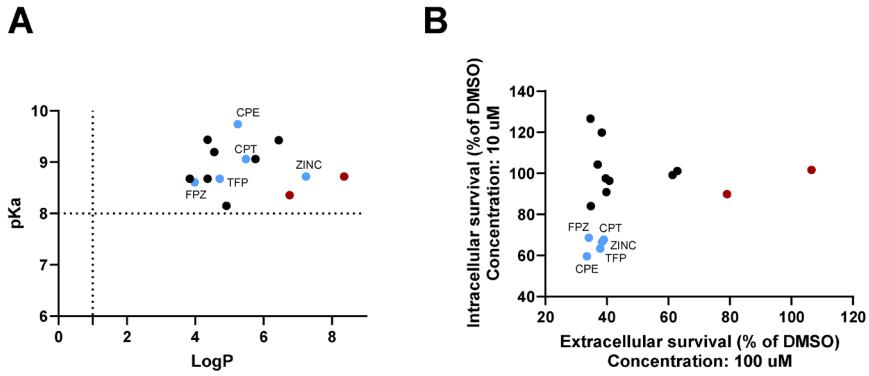

Supplementary Figure 3. Effect of dopamine agonists on intracellular *Mav* control with or without phenothiazines.
(A-B) Bacterial survival of *Mav* within M1 macrophages, where dopamine (A) or quinpirole (B) was applied alone for the first hour, followed by the addition of 10 μM of CPE or DMSO for the remainder of the treatment. After 24 hours of treatment, bacterial survival was determined by the CFU assay. Data represents the mean ± SD (n=3), and dots represent the mean from duplicate wells of a single donor. Bacterial survival is expressed as a percentage of DMSO (=100%, indicated with the dotted line) per donor. Statistical significance was tested using a repeated-measures one-way ANOVA with Bonferroni's multiple comparisons test.
CPE; chlorproethazine.
* = $p<0.05$.

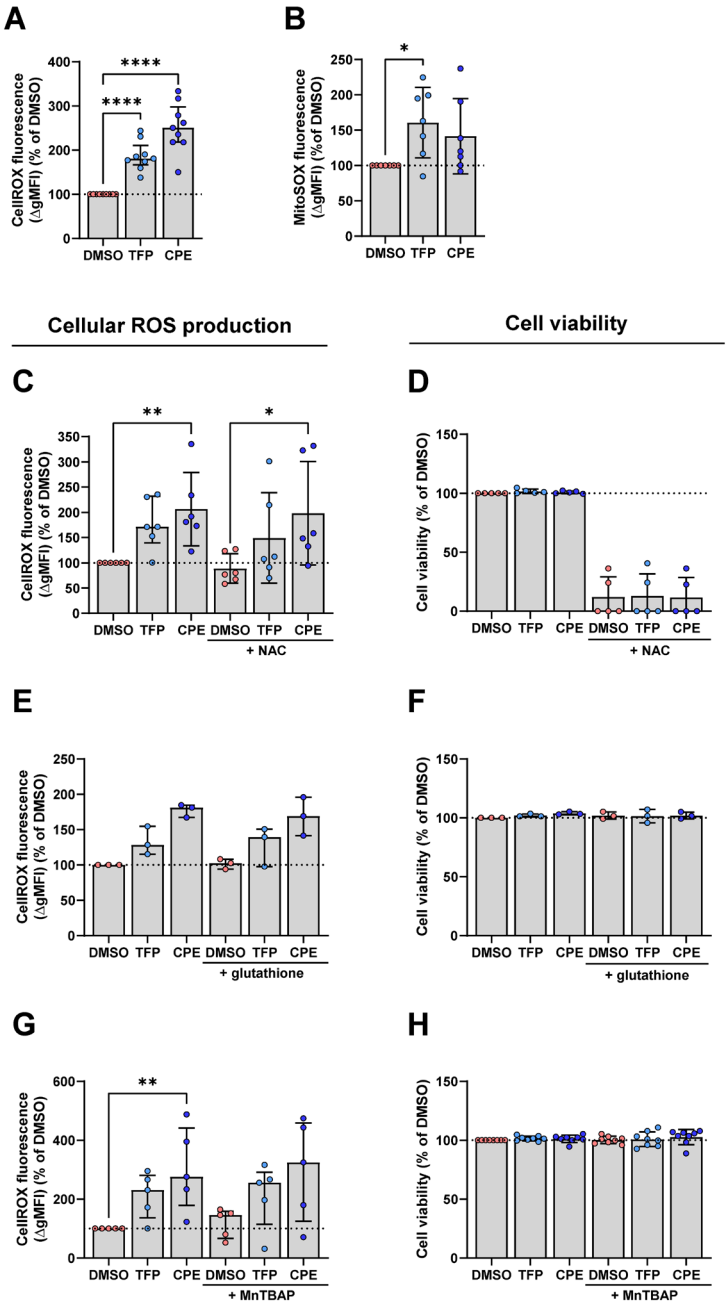

Supplementary Figure 4. Induction of NOX-derived ROS by TFP and CPE might have a limited role in their enhanced macrophage response against *Mav*.
(A-B) M1 macrophages were treated with 10 µM TFP, CPE, or DMSO for 4 hours. Total cellular ROS production (A) or mitochondrial ROS (B) production was measured by flow cytometry. Data represent the median ± interquartile range from 8 donors (A) or mean ± SD from 7 donors (B). Statistical significance was tested using a Friedman test with Dunn's multiple comparisons

test (A) or a repeated-measures one-way ANOVA with Dunnett's multiple comparisons test (B). **(C-D)** M1 macrophages were treated for 4 (C) or 24 (D) hours with 10 μM TFP, CPE, or DMSO with or without 5 mM N-acetyl-cysteine (NAC). Total cellular ROS production was detected by flow cytometry. The geometric mean fluorescence intensity (ΔgMFI) (C) or cell viability (D) were determined. Data represent the median ± interquartile range from 6 donors (C) or mean ± SD from 5 donors (D). Statistical significance was tested using a Friedman test with Dunn's multiple comparisons test (C). **(E-F)** M1 macrophages were treated with 10 μM TFP, CPE, or DMSO with or without 100 μM L-glutathione for 4 (E) or 24 (F) hours. Total cellular ROS production was detected by flow cytometry. The geometric mean fluorescence intensity (ΔgMFI) (E) or cell viability (F) were determined. Data represent the median ± interquartile range from 3 donors (E) or mean ± SD from 3 donors (F). Statistical significance was tested using a Friedman test with Dunn's multiple comparisons test (E). **(G-H)** M1 macrophages were treated with 10 μM TFP, CPE, or DMSO with or without 100 μM MnTBAP for 4 (G) or 24 (H) hours. Total cellular ROS production was detected by flow cytometry. The geometric mean fluorescence intensity (ΔgMFI) (E) or cell viability (F) were determined. Data represent the median ± interquartile range from 5 donors (G) or mean ± SD from 5 donors (H). Statistical significance was tested using a Friedman test with Dunn's multiple comparisons test (G). Dots represent the mean from duplicate wells of a single donor. Data is expressed as a percentage of vehicle control DMSO (=100%, indicated with the dotted line) per donor.
TFP; trifluoperazine, CPE; chlorproethazine. * = p<0.05, ** = p<0.01 and **** = p<0.0001.

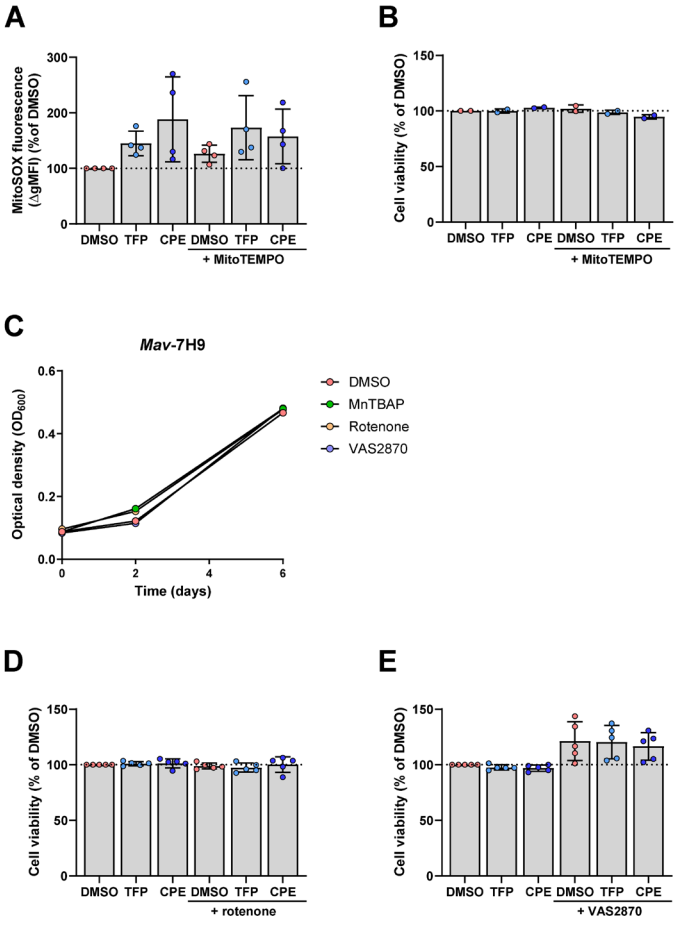

Supplementary Figure 5. Induction of NOX-derived ROS by TFP and CPE might have a limited role in their enhanced macrophage response against *Mav*.
(A-B) M1 macrophages were treated with 10 μM TFP, CPE, or DMSO with or without 10 μM MitoTEMPO for 4 (A) or 24 (B) hours after *Mav* infection. Total mitochondrial ROS production was detected by flow cytometry. The geometric mean fluorescence intensity (ΔgMFI) (A) or cell viability (B) were determined. Data represent the mean ± SD from different donors (n=4). Statistical significance was tested using a repeated-measures one-way ANOVA with Bonferroni's multiple comparisons test (A). **(C)** Growth of Mav in liquid broth up to 10 days after exposure to 100 μM MnTBAP, 5 μM rotenone, 10 μM VAS2870, or DMSO. Data represent the mean ± SD of triplicate wells from two independent experiments. **(D-E)** Percentage of viable M1 macrophages after treatment with 5 μM rotenone (D), 10 μM VAS2870 (E), or DMSO 24 hours. Data represent the mean ± SD from 5 (D). Dots represent the mean from duplicate wells of a single donor. Data is expressed as a percentage of vehicle control DMSO (=100%, indicated with the dotted line) per donor.
TFP; trifluoperazine, CPE; chlorproethazine.

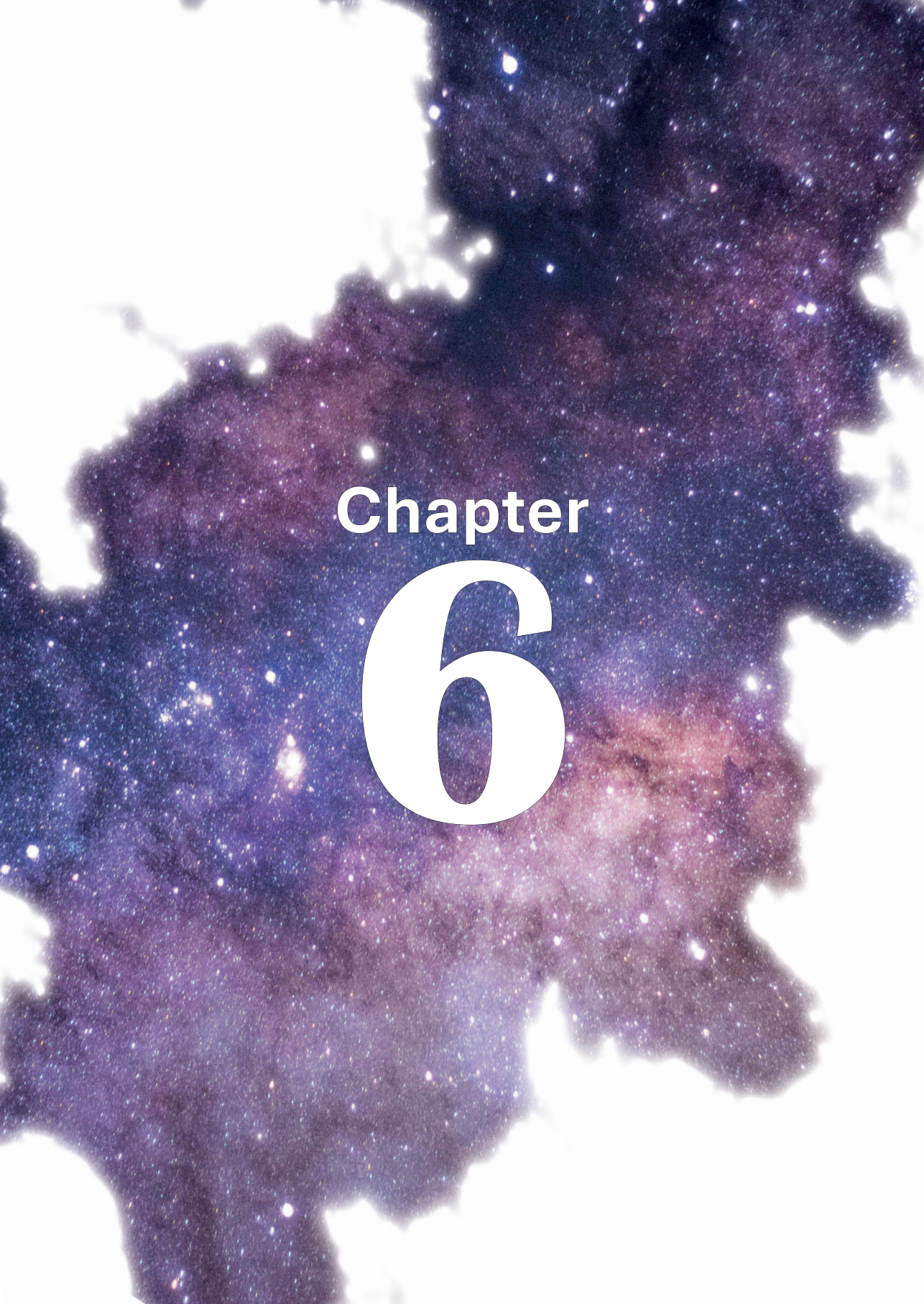
Chapter
6

Comparative transcriptomic analysis of human macrophages during *Mycobacterium avium* versus *Mycobacterium tuberculosis* infection

Gül Kilinç[1], Robin H. G. A. van den Biggelaar[1], Tom H. M. Ottenhoff[1], Leon H. Mei[2] and Anno Saris[1]

[1] Leiden University Center for Infectious Diseases, Leiden University Medical Center, Leiden, The Netherlands
[2] Department of Biomedical Data Sciences, Leiden University Medical Center, Leiden, The Netherlands

Submitted.

Abstract

The treatment of *Mycobacterium avium* (*Mav*) infection, responsible for over 80% of the chronic lung diseases caused by nontuberculous mycobacteria (NTM), remains challenging due to rising antibiotic resistance and unsatisfactory success rates. Hence, there is an urgent need for alternative treatment strategies. Host-directed therapy targets host pathways to either reduce destructive inflammation or improve antimycobacterial defenses to eradicate the infection, offering a promising approach with minimal risk of inducing drug resistance. However, compared to *Mycobacterium tuberculosis* (*Mtb*) infections, knowledge of host-pathogen interactions and development of HDT for *Mav* infection is limited. To expand our fundamental knowledge on the host response during *Mav* infections, we performed a genome-wide host transcriptomic analysis of *Mav*-infected primary human macrophages, the key players in the host immunity against *Mav*, next to *Mtb*-infected macrophages to leverage insights from *Mtb* research. Our findings show substantial overlap in the gene expression patterns between *Mav*-infected and *Mtb*-infected macrophages, including induction of cytokine responses and modulation of various G-protein coupled receptors (GPCRs) involved in (lipid-mediated) macrophage immune functions. Notably, *Mav* infection showed more pronounced modulation of nerve growth factor (NGF) signaling and genes of the GTPase of immunity-associated protein (GIMAP) family compared to *Mtb* infection. While the exact roles of these host transcriptomic responses during mycobacterial infection remain to be determined, these results may provide direction to further explore the host-pathogen interactions during *Mav*-related immunity and identify targets for HDT for the treatment of *Mav* infection.

Introduction

Mycobacterium avium (*Mav*) is the causative pathogen for the majority of the chronic lung diseases caused by nontuberculous mycobacteria (NTM) (1-3), which has seen a rise in incidence globally and is a growing public health concern (4-6). While lung disease caused by *Mav* (*Mav*-LD) particularly affects individuals with predisposing lung disorders or a compromised immune system, immunocompetent individuals with certain host characteristics have been found to develop *Mav*-LD. Improved understanding and management of NTM, in particular *Mav*, infections is therefore desirable.

The recommended treatment for *Mav*-LD consists of a three-drug antibiotic regimen comprising a macrolide, ethambutol, and a rifamycin that should be administered for at least 12 months after negative sputum conversion (7, 8). Nevertheless, even after completing the antibiotic therapy, the success rate, disappointingly, is as low as 40% (9, 10). This necessitates the development of new therapeutic strategies. One promising approach is the use of host-directed therapy (HDT), which aims to dampen destructive inflammation or to boost the host's immune responses which may be beneficial, especially for individuals who are suffering from a *Mav* infection and are immunocompromised. By targeting host immunity, HDT may help to eliminate non-replicating and drug-resistant bacteria which are hardly eradicated by antibiotic therapy. In addition, as adjunctive treatment, HDT has the potential advantage of shortening the duration or decreasing the dosage of current antibiotic regimens, which may reduce adverse drug effects. Furthermore, since host rather than bacterial pathways are targeted, the risk of de novo development of drug resistance is less likely. The development of HDT for *Mav* requires a throughout knowledge of host-pathogen interactions limited understanding of the host-pathogen interactions during *Mav* infection.

Macrophages are the immune cells that play a key role in host defense against *Mav* infection. Upon inhalation, *Mav* enters the lung alveolar space where macrophages will form the main reservoir for the mycobacteria (11, 12). Multiple macrophage receptors, including Toll-like receptors (TLRs) and C-type lectins, are involved in the initial bacterium-host cells encounter which induces phagocytosis. Upon recognition and phagocytosis, the early *Mav*-containing phagosomes undergo maturation and fusion with lysosomes containing hydrolytic enzymes to form phagolysosomes capable of eliminating the mycobacteria (13, 14). However, *Mav* is able to evade host immune surveillance and to maintain its intracellular replication and survival. For instance, the *Mav* protein *Mav*_2941 inhibits phagosome maturation, and thus prevents intracellular *Mav* killing (15, 16). The production and signaling of pro-inflammatory cytokines, including TNF, IL-12, and IL-23, by macrophages, play a vital role in further stimulating the bactericidal functions of macrophages (17). Consequently, inherited or acquired defects in the production and signaling of these cytokines lead to an increased susceptibility to *Mav*-LD (18), stressing the significant role of host immunity in deciding the outcome of *Mav* infection.

A better understanding of the mechanisms involved by which macrophages either kill *Mav* or become its breeding ground will aid the development of HDT. RNA-sequencing

has previously been used to study the macrophage host response following infection with *Mtb*, providing insights into the mechanisms of pathogenesis, potential biomarkers for disease progression, and targets for new therapeutic interventions such as HDT (19-22). In contrast, most transcriptomic studies exploring the host response to *Mav* have been conducted in cell lines, which require specific stimulation or may not accurately reflect primary human macrophage responses to mycobacteria and have relied on predefined microarray analyses that fail to reflect the complete transcriptional response (23-26). Our aim was therefore to perform genome-wide transcriptomic analysis of primary human macrophages infected with *Mav*, alongside *Mtb* as a reference to facilitate the rapid extrapolation of relevant findings from *Mtb* to *Mav*, thereby enhancing our understanding of the similarities and differences in how both pathogens interact with and are managed by the host's immune system. We hypothesized that this will ultimately contribute to the development of more effective therapies for infections caused by these mycobacteria.

In this study, we showed that the host transcriptional response is highly similar between macrophages infected with *Mav* and macrophages infected with *Mtb*. The common host response includes the expression of cytokines and other immune-related genes, but also G protein-coupled receptors involved in lipid metabolism. Furthermore, we identified genes with transcription levels that were different in magnitude between macrophages infected with *Mav* and macrophages infected with *Mtb*. These differences were linked to phospholipases, NGF signaling-related apoptosis, and the more unknown GIMAP genes.

Results

Genome-wide transcriptome analysis of primary human macrophages infected with *Mav* or *Mtb*

To investigate the induction of the early host immune response, primary human macrophages from 7 donors were infected with *Mav* or *Mtb*, with an 8th donor (*Mtb* data unavailable) maintained in the *Mav* analysis to increase power. Macrophage phagocytosis of *Mav* was higher as compared to *Mtb*, despite being exposed to a lower MOI (5.9 vs 9.9, respectively). Elimination of intracellular *Mtb* was higher at 24 hours post-infection (**Figure 1A**). Genome-wide transcriptome analysis using RNA-sequencing was performed in seven biological replicates at 2 hours and 6 hours post-infection. Expression levels were compared between infected samples and uninfected controls using unsupervised and supervised analyses. PCA analysis revealed the clustering of samples derived from different donors (**Figure 1B**), while infected samples were clustered separately from uninfected macrophages and clearly changed over time (**Figure 1C**). The transcriptome profiles of macrophages infected with either *Mav* or *Mtb* were evidently clustered together (**Figure 1D**).

Primary human macrophages infected with *Mav* or *Mtb* present similar host transcription responses

To determine the transcriptomic response upon *Mav* and *Mtb* infection, significantly differentially expressed gene (DEGs) (cutoffs: log2(fold change) ≥ 1.5 or ≤ -1.5 and false discovery rate (FDR) adjusted p-values < 0.05) were assessed by comparing gene expression levels in infected macrophages at 2 and 6 hours post-infection with uninfected controls. At 2 hours post-infection, macrophages showed downregulation

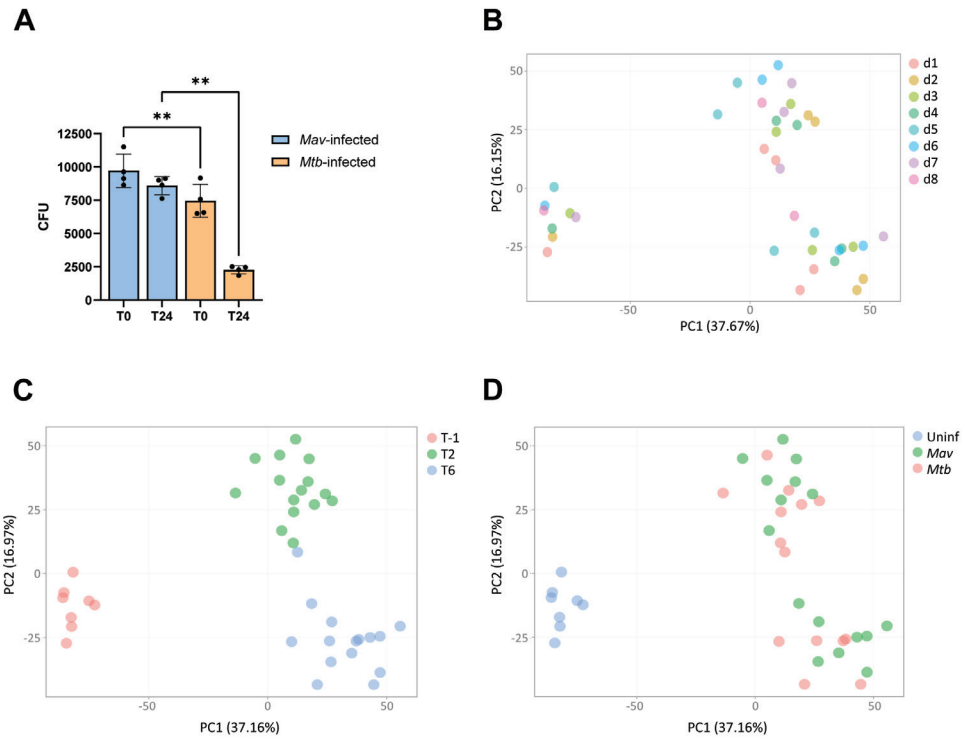

Figure 1. Transcriptome analysis of *Mav*- or *Mtb*-infected versus uninfected samples.
(A) M2 macrophages were infected with either *Mav* or *Mtb* for 1 hour. After infection, cells were washed and lysed to determine the internalization (T0) and elimination of mycobacteria after 24 hours (T24). Dots represent the mean from triplicate wells of a single donor. Data represent the mean ± standard deviation (SD) from different donors (n=4). Differences were statistically significant by repeated measures one-way ANOVA with Šídák multiple comparison test. **p < 0.005. **(B-D)** The variance of the sequencing data from *Mav*- or *Mtb*-infected M2 macrophages from different donors (n=8 or n=7, respectively) and uninfected controls was described in PCA plots, illustrating separation by donor (B), timepoint (C), or infection status (D).

and upregulation of 241 and 907 genes after *Mav* infection (**Figure 2A, Supp Table 1**) or 248 and 872 genes after *Mtb* infection, respectively (**Figure 2B, Supp Table 1**). At 6 hours post-infection, the number of downregulated and upregulated genes were 734 and 1141 for *Mav* (**Figure 2C, Supp Table 1**), and 683 and 928 for *Mtb* (**Figure 2D, Supp Table 1**), respectively. To compare the similarity between DEGs in response to infection with either *Mav* or *Mtb*, we performed a Pearson correlation and Venn diagram analysis. The correlation in gene expression data derived from *Mav*- and *Mtb*-infected macrophages was very strong (Pearson correlation coefficients: 0.98 and 0.96 at 2 and 6 hours post-infection, respectively) (**Supp Figure 1A-B**), which was stronger than the correlation within each infection between the two timepoints (Pearson correlation coefficient: 0.83 and 0.84, for *Mav* and *Mtb* infection respectively) (**Supp Figure 1C-D**). Similarly, the Venn diagram analysis showed that the majority of the DEGs was affected by both mycobacteria compared to uninfected controls (**Figure 2E and F**).

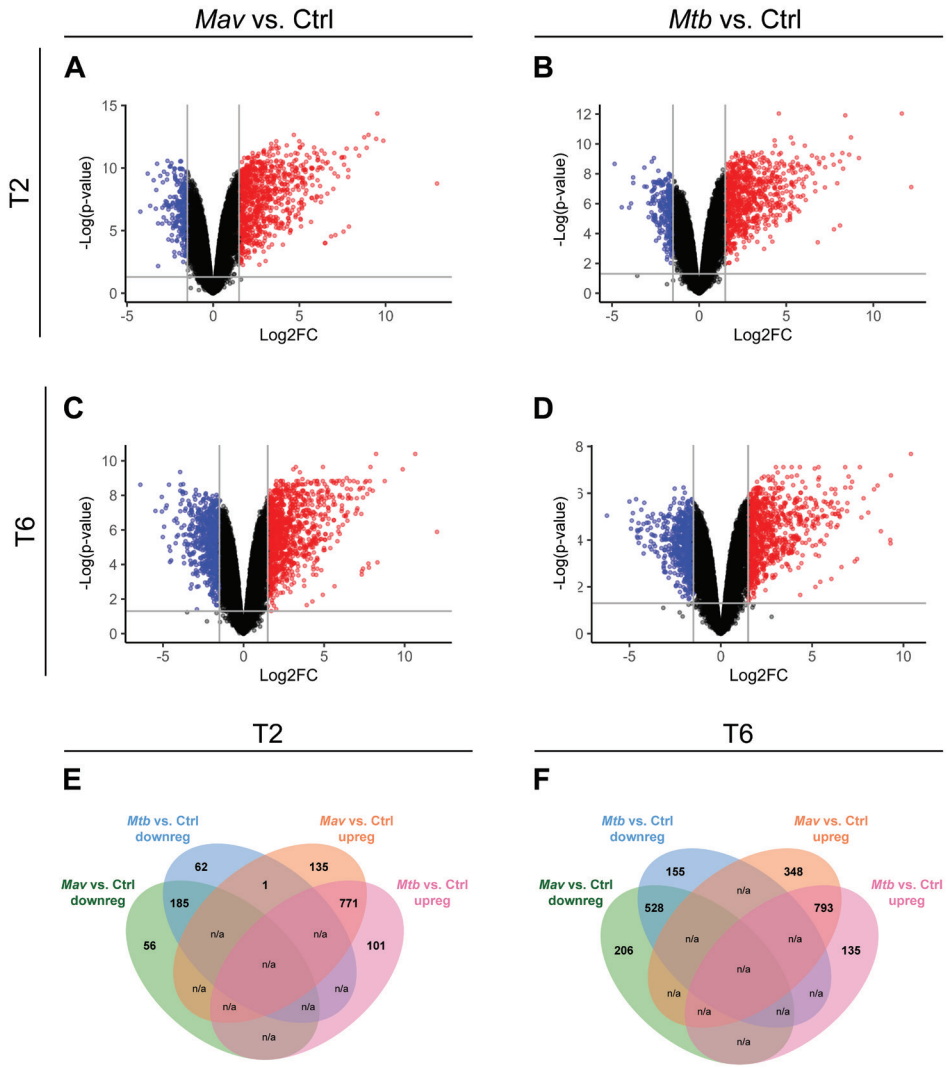

Figure 2. Differential expression analysis of primary human macrophages at 2 and 6 hours post-infection with *Mav* or *Mtb* compared to uninfected samples.
(A-D) Volcano plots showing DEGs among biological conditions of primary human macrophages at 2 (A-B) or 6 (C-D) hours post-infection with *Mav* (A-C) or *Mtb* (B-D) versus uninfected macrophages (Ctrl). Only log2 fold change (Log2FC) ≥ 1.5 or ≤ 1.5 and false discovery rate-adjusted p-values < 0.05 were analyzed. The upregulated genes are labelled red and downregulated genes are labelled blue. Non-differentially expressed genes are labeled black. **(E-F)** Venn diagram of the DEGs, showing the number of overlapping or unique down- or upregulated DEGs identified in macrophages at 2 (E) or 6 (F) hours post-infection infected with *Mav* or *Mtb* compared to the uninfected controls. N/A: comparison not applicable, as a gene cannot be down- and upregulated within the same infection and time point.

To assess the common host response against *Mav* and *Mtb*, DEGs shared after infection with both mycobacteria at either 2 or 6 hours post-infection were pooled, resulting in 610 downregulated genes and 1063 upregulated genes compared to uninfected

controls (**Supp Table 1**). Notably, one gene (FOS) was significantly upregulated by *Mav* and downregulated by *Mtb*. The 1673 DEGs shared by *Mav* and *Mtb* were subjected to Ingenuity Pathway Analysis (IPA) (**Supp table 1**). The top 20 pathways, enriched with 293 DEGs (17.5% of all DEGs), are shown in **Figure 3A**. These pathways were also among the highly ranked pathways in response to either *Mav* or *Mtb* compared to uninfected controls (**Supp Figure 2A-B**). The DEGs enriched in these top 20 pathways showed substantial overlap between pathways, predominantly in cytokines such as *IL1B*, *TNF*, *IL18*, *IL1A*, and *IL6*, as well as *NFKB1* and *NFKB2*. To comprehend the common host response, the overlapping network tool from IPA was used to identify clusters of related pathways. The analyses revealed two major nodes that were affected by both *Mav* and *Mtb* (**Figure 3B-C**). One node comprised pathways including Multiple Sclerosis Signaling Pathway, Role of Pattern Recognition Receptors in Recognition of Bacteria and Viruses, Pathogen Induced Cytokine Storm Signaling Pathway, Macrophage Classical Activation Signaling Pathway and NOD1/2 Signaling Pathway (**Figure 3B**). Gene Ontology (GO) Enrichment analysis with the 114 DEGs belonging to this node showed that most of the genes were associated with GO terms linked to a cytokine signaling response (**Figure 3D, Supp Figure 3A**), which, amongst others, included cytokines (i.e. *CXCL8*, *CSF2*, *IL36G*, *IL12B*, *IL15*, *IL10*, *CCL5* and *IL23A*), TNF superfamily ligands (*TNFSF10*, *TNFSF14*, *TNFSF15 and TNFSF9*) and Toll-like receptors (*TLR2*, *TLR3*, *TLR5* and *TLR6*) (**Figure 3E, Supp Table 1**).

The second node comprised pathways including Molecular Mechanisms of Cancer, Role of Macrophages, Fibroblasts and Endothelial Cells in Rheumatoid Arthritis, Role of Osteoblasts, Osteoclasts and Chondrocytes in Rheumatoid Arthritis, Hepatic Fibrosis Signaling Pathway, CDX Gastrointestinal Cancer Signaling Pathway, G-Protein Coupled Receptor Signaling and HMGB1 Signaling (**Figure 3C**). GO Enrichment analysis with 164 DEGs (excluding cytokines and cytokine receptors already discussed above) showed an association with mainly signal transduction by G protein-coupled receptor (GPCR) activity (**Figure 3F, Supp Figure 3B**). In total, the expression of 39 GPCRs was significantly affected by both *Mav* and *Mtb* (**Supp Table 1**). Based on the GPCR database (https://gpcrdb.org), a part of these GPCRs are involved in various signaling pathways with ligands including alicarboxylic acids (*HCAR2* and *HCAR3*) (27, 28), neurotransmitters (*CHRM3*), nucleotides (*ADORA2A*, *ADORA3* and *P2RY13*) (29-31), hormones (*SSTR2*, *OXTR*, *MAS1*, *MC1R* and *C5AR2*) (32-36) and Wnt ligands (*FZD2*, *FZD4*, *FZD6* and *LGR4*) (37). Finally, the biggest group comprised GPCRs involved in sensing lipids, including eicosanoids (*PTGIR*, *PTGER2*, *GPR31*, *CYSLTR1* and *CYSLTR2*), lysophospholipids (*LPAR5*, *LPAR6*, *GPR34*, *S1PR1*, *GPR65*, *GPR132* and *GPR82*), free fatty acids (*GPR84* and *FFAR4*) and sterols (*GPR183*) (**Figure 3G**). Taken together, these findings indicate that common changes in the host transcriptomic response upon infection with *Mav* and *Mtb* are characterized by an enhanced cytokine response and include regulation of GPCRs and likely concomitant lipid-mediated immunoregulation.

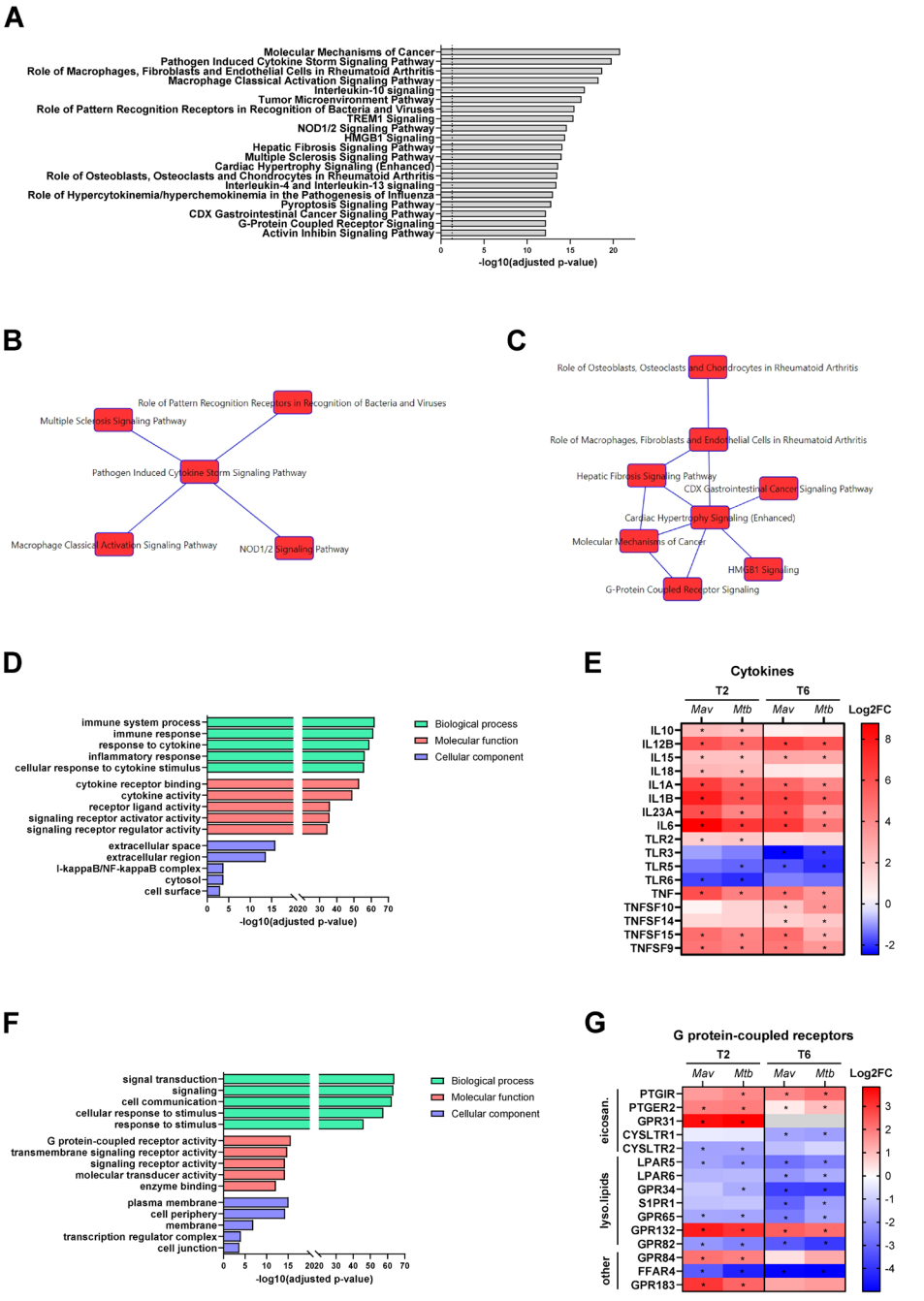

Figure 3. Enrichment analysis of DEGs shared by *Mav* and *Mtb* in primary human macrophages.

(A) The top 20 most significantly enriched IPA pathways of the 1673 commonly DEGs induced in macrophages infected with *Mav* and *Mtb* compared with uninfected controls. The enriched pathways were ranked by -log 10 p-value of gene enrichment. **(B-C)** Network analysis of enriched

pathways from A using IPA overlap networks tool. Links between indicated pathways indicates an overlap of minimum 30 DEGs. **(D)** GO enrichment analysis showing the top GO terms for biological process, molecular function and cellular component categories enriched for DEGs enriched in the pathways shown in B. The enriched ontology clusters were ranked by log10 p-value of gene enrichment. **(E)** Heatmap showing the expression patterns of various cytokines that were significantly affected by both *Mav* and *Mtb* infection at 2 (T2) and/or 6 (T6) hours post-infection, in comparison to uninfected controls. **(F)** GO enrichment analysis showing the top GO terms for biological process, molecular function and cellular component categories enriched for DEGs enriched in the pathways shown in C. The enriched ontology clusters were ranked by log10 p-value of gene enrichment. **(G)** Heatmap showing the expression patterns of lipid-binding GPCRs that were significantly affected by both *Mav* and *Mtb* infection at 2 (T2) and/or 6 (T6) hours post-infection, in comparison to uninfected controls. Grey box indicates no expression values could be determined. Ligands of genes are indicated with eicosan.: eicosanoids, lyso.lipids: lysophospholipids and other: free fatty acids and sterols.
Asterisk (*) indicates gene is differentially expressed in comparison to uninfected controls

Genes significantly regulated only by either *Mav* or *Mtb* indicate subtle, but not infection-specific, changes in host signaling pathways

To identify individual genes that were significantly regulated by either *Mav* or *Mtb*, DEGs from the two different timepoints were pooled. Although the correlation between host transcriptomic response to *Mav* and *Mtb* infection was notably high, genes were identified that were associated with either one of the infections (**Figure 2E and F**). In total, 561 genes were only differentially expressed by *Mav*, while 323 genes were only differentially regulated by *Mtb* (**Supp Table 1**). Pathway enrichment analysis revealed that the bone morphogenetic protein (BMP) signaling pathway (*BMP1*, *BMP2*, *JUN*, *MAPK8*, *RELA*, *SOS1*, *RAP1B* and *PRKAG2*), p75 neurotrophin receptor (NTR)-mediated signaling (*ARHGEF26*, *GNA13*, *ITSN1*, *MAPK8*, *PSEN2*, *RELA*, *SOS1* and *TIAM2*) and TNFR2 Signaling (*BIRC2*, *JUN*, *MAPK8* and *RELA*) were amongst the most enriched by *Mav* (**Figure 4A, Supp Table 1**). Importantly, these pathways were not specific for *Mav*, as they were also affected during *Mtb* infections (**Supp Figure 4**). GO Enrichment analysis with the 39 DEGs enriched in the top 10 pathways affected after *Mav* identified a potential more dominant role of phospholipases during *Mav* infection (**Figure 4B, Supp Table 1**). We observed that the expression of *NAPE-PLD* and *PLD6* (phospholipase D6) was significantly downregulated, while *PLCL1* (phospholipase C like 1) and PLD1 (phospholipase D1) were significantly upregulated by *Mav* and not by *Mtb* (**Figure 4C**). Interestingly, in response to both *Mav* and *Mtb*, we observed a significant downregulation of *FFAR4* (**Supp Table 1**), described to reduce lipid accumulation in macrophages (38). These observations suggest that host lipid metabolism is important for both mycobacteria, as well known for *Mtb* (39).

The genes that were significantly affected by *Mtb* were enriched in pathways associated with an immune response characterized by interferon-alpha/beta (*IFIT5*, *IFIT1*, *IFIT3*, *IRF4*, *ISG15*, *MX1*, and *MX2*) and interferon-gamma (*GBP3*, *IRF4*, *JAK2*, *OAS2*, *PTPN2*, and *TRIM5*) signaling pathways, as well as interferon-stimulated gene 15 (ISG15) signaling (*IFIT1*, *MX1*, *MX2*, *DTX3L*, *HERC5*, *IRF4*, *ISG15*, *ITGA2*, and *RIGI*) (**Figure 4D**). GO Enrichment analysis with the 29 DEGs enriched in the top 10 pathways after *Mtb* infection showed that these genes were associated with signaling in response to pathogens, consisting of mainly type I and type II interferon responses (**Figure 4E**). Like *Mtb*, *Mav* stimulated the expression of genes involved in interferon signaling (**Figure 4F**). This observation is reflected by the fact that these pathways were enriched among

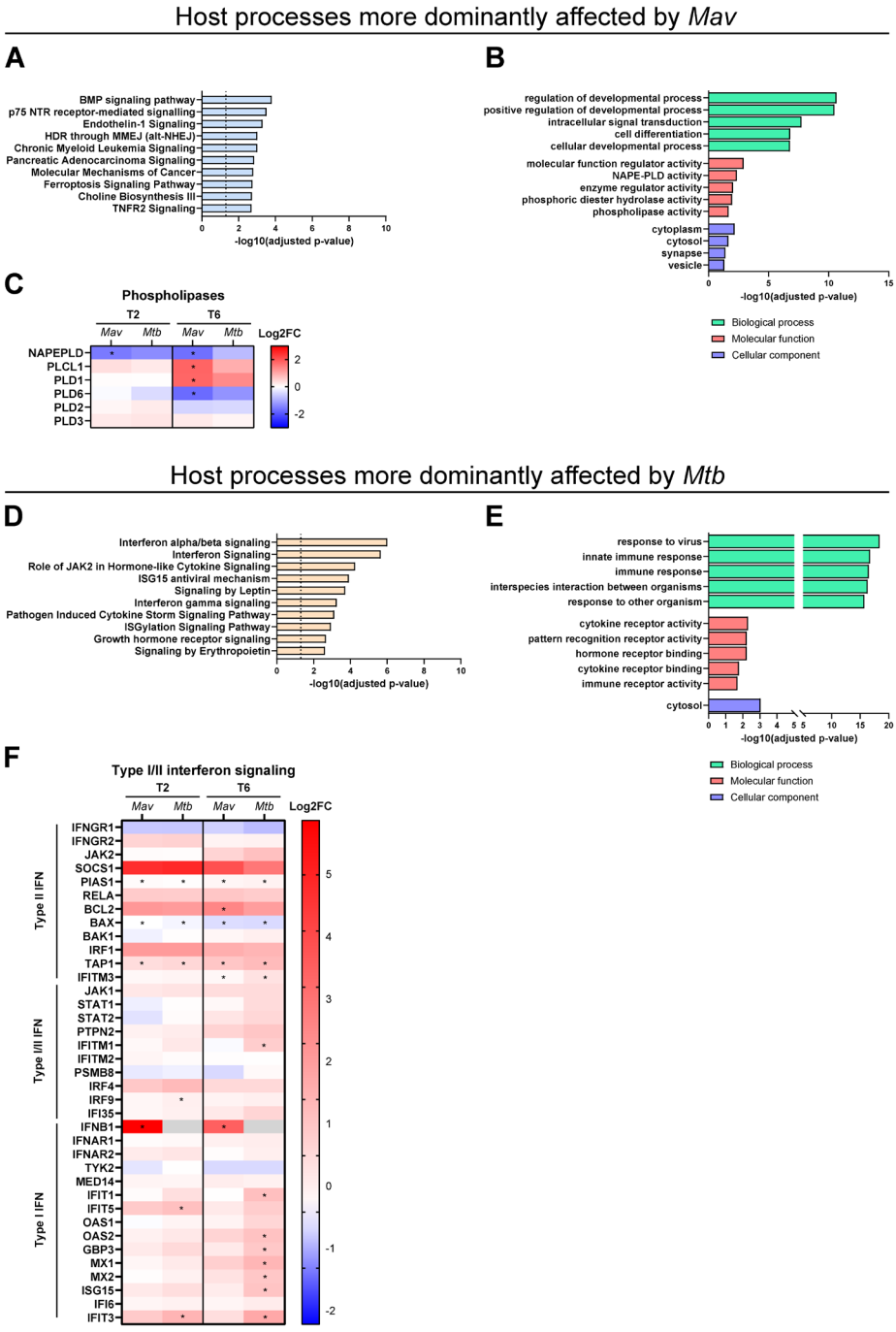

Figure 4. Genes significantly regulated only by either *Mav* or *Mtb* indicate subtle, but not infection-specific, changes in host signaling pathways
(A) The top 10 most significantly enriched IPA pathways of the 561 DEGs induced in exclusively *Mav*-

infected macrophages compared with uninfected controls. The enriched pathways were ranked by log 10 p-value of gene enrichment. **(B)** GO enrichment analysis showing the top GO terms for biological process, molecular function and cellular component categories enriched for DEGs enriched in the pathways shown in A. The enriched ontology clusters were ranked by log10 p-value of gene enrichment. **(C)** Heatmap showing the expression patterns of phospholipases that were exclusively induced by *Mav* infection at 2 (T2) and/or 6 (T6) hours post-infection, in comparison to uninfected controls, complemented with available expression data of phospholipases which were not affected by infection. Asterisk (*) indicates a DEG in comparison to uninfected controls. **(D)** The top 10 most significantly enriched IPA pathways of the 323 DEGs induced in exclusively *Mtb*-infected macrophages compared with uninfected controls. The enriched pathways were ranked by log 10 p-value of gene enrichment. **(E)** GO enrichment analysis showing the top GO terms for biological process, molecular function and cellular component categories enriched for DEGs enriched in the pathways shown in E. The enriched ontology clusters were ranked by log10 p-value of gene enrichment. **(F)** Heatmap showing the expression patterns of type I and II interferon signaling that were exclusively induced by *Mtb* infection 2 (T2) and/or 6 (T6) hours post-infection, in comparison to uninfected controls, complemented with available expression data of interferon genes which were not detected (grey). Asterisk (*) indicates a DEG in comparison to uninfected controls. Grey box indicates no expression values could be determined.

the transcriptomic response to both *Mav* and *Mtb* infections (**Supp Figure 4**). However, while *Mtb* evoked both type I and type II interferon signaling, *Mav* mainly affected type II interferon signaling. An exception was *IFNB1*, which was solely induced upon *Mav* infection.

Genes differentially expressed in macrophages infected with *Mav* compared to *Mtb* are associated with lipid metabolism, NGF-related apoptosis, and GIMAPs

In the previous analysis, we focused on the DEGs that were identified relative to uninfected controls. In the following analysis, the magnitude of gene expression was compared between the two infections to uncover significant changes between *Mav* and *Mtb* that may have been overlooked in comparison with uninfected controls. At 2 hours post-infection, this comparison revealed 14 genes that were significantly upregulated by *Mav* compared to *Mtb* and no genes that were downregulated in *Mav* (**Figure 5A, Table 1, Supp Table 1 and Supp Table 2**). At 6 hours post-infection, *Mav* infection resulted in 13 DEGs with downregulated expression levels and 17 DEGs with significantly upregulated expression levels compared to *Mtb* infection (**Figure 5B, Table 1, Supp Table 1 and Supp Table 2**). Protein-protein interaction (PPI) network analysis using the Search Tool for the Retrieval of Interacting Genes (STRING) database identified three distinct interaction networks including 24 of 38 genes: transcription regulators, GIMAPs, and cytokines (**Figure 5C**). Interestingly, among the genes that were not associated with a network, *FFAR2* and *GPR65* are related to lipid binding and/or metabolism and were significantly higher expressed in *Mav*-infected macrophages compared to those infected with *Mtb* (**Supp Table 2**) (40-42).

The first network consisted of *FOS*, *FOSB* (AP-1 transcription factor complex), *EGR1*, *EGR4* (EGR family of transcription factors), and ARC, which were all found to increase after *Mav* infection relative to *Mtb* infection (**Table 1**). *EGR1*, *EGR4*, *FOS*, and *FOSB* play key roles in regulating various biological processes including cell proliferation, differentiation and survival, and the production of pro-inflammatory cytokines (43). Furthermore, *EGR1*, *EGR4*, *FOS*, and *FOSB* are part of the Reactome pathway of nerve growth factor (NGF)-stimulated transcription (R-HSA-9031628).

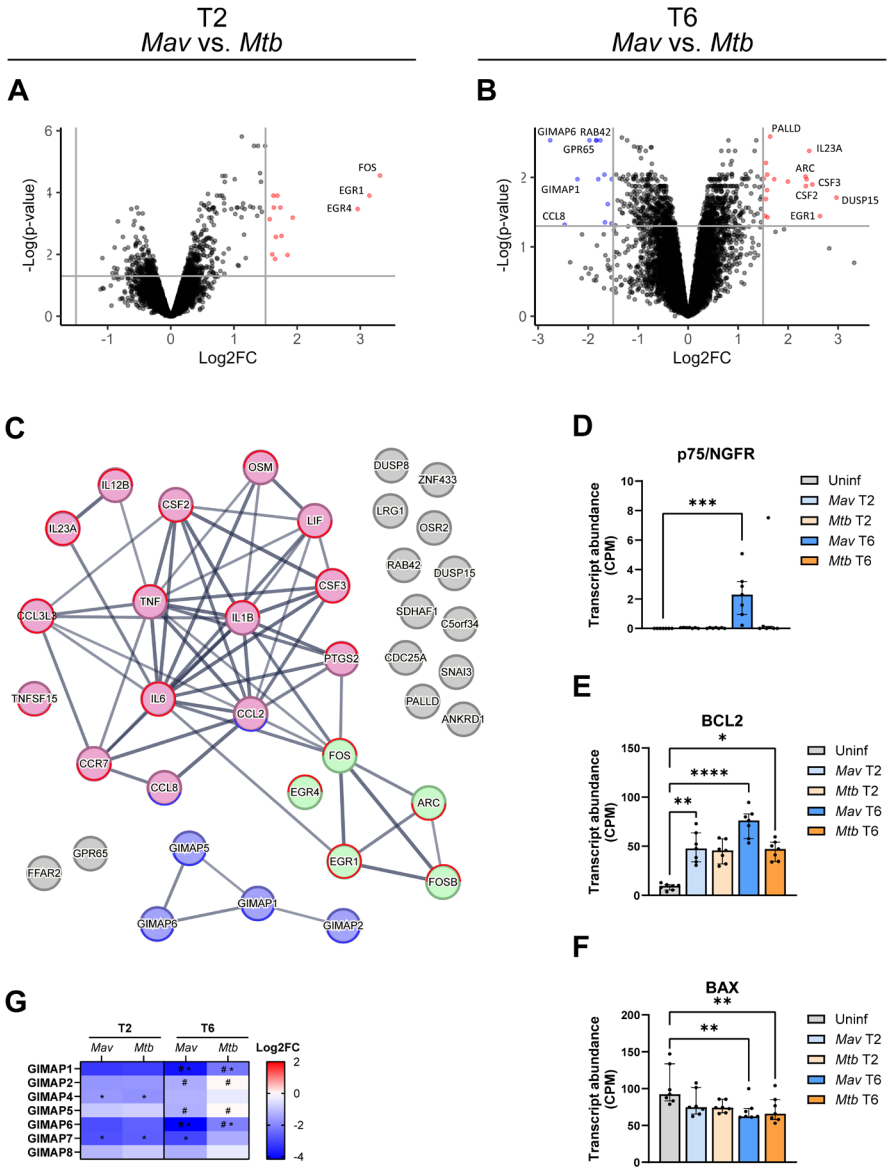

Figure 5. Genes differentially expressed in macrophages infected with *Mav* compared to *Mtb*.

(A-B) Volcano plots showing DEGs among biological conditions of primary human macrophages at 2 (A) or 6 (B) hours post-infection with *Mav* versus *Mtb* (n=7). Only log2 fold change (Log2FC) ≥ 1.5 or ≤ 1.5 and false discovery rate-adjusted p-values < 0.05 were analyzed. The upregulated genes are labelled red and downregulated genes are labelled blue. Non-differentially expressed genes are labeled black. **(C)** PPI network showing the DEGs from *Mav*-infected macrophages compared with *Mtb*-infected macrophages from A-B. The color representation indicates three distinct networks. Outline of genes indicate expression is increased (red) or decreased (blue), at 2 hours (upper circle) or 6 hours (lower circle), or both timepoints (full circle), post-infection with *Mav* compared to *Mtb* infection. **(D-F)** Transcript levels (count per million; CPM) of NGFR

(D), BLC2 (E) and BAX (F) in uninfected (grey), and *Mav* (blue shaded)- and *Mtb* (orange shaded)-infected macrophages at 2 and 6 hours post-infection. Differences were statistically significant by a Friedman test with Dunn's multiple comparison test. *p < 0.05, **p < 0.005, ***p < 0.001 and ****p < 0.0001. **(G)** Heatmap showing the expression patterns of GIMAPs that were differentially regulated in *Mav*-infected macrophages at 2 (T2) and/or 6 (T6) hours post-infection, compared to uninfected or *Mtb*-infected macrophages, complemented with available expression data of GIMAPs which were not affected by infection. Asterisk (*) indicates differential expression when compared to uninfected controls, whereas number sign (#) indicates differential expression between *Mav* and *Mtb*.

Previously, NGF-induced EGR1 downstream signaling involved *ARC*, which was also found to be significantly upregulated 6 hours post-infection with *Mav* compared to *Mtb* (**Table 1**) (44). NGF signaling involves a high-affinity receptor, TrkA, and a low-affinity receptor, p75/NGFR, which upon activation can induce either cell survival or apoptosis, respectively (45, 46). Interestingly, while no transcription of the TrkA receptor was detected in macrophages, the expression of the p75/*NGFR* gene as well as its signaling pathway were significantly upregulated 6 hours post-infection with *Mav* (**Figure 4A and 5D**). The expression of apoptosis-related genes showed significant upregulation of anti-apoptotic *BCL2*, while pro-apoptotic *BAX* was significantly downregulated in macrophages infected with *Mav* and *Mtb* (**Figure 5E-F**). Hence, these expression patterns indicate a reduced tendency of both *Mav*- and *Mtb*-infected host cells to undergo apoptosis, while the indicative pro-apoptotic p75 NTR pathway is also upregulated by *Mav*.

The second network consisted of genes of the GTPase of immunity-associated protein (GIMAP) family, which were significantly downregulated in macrophages infected with *Mav* compared to those infected with *Mtb*. *GIMAP1* and *GIMAP6* showed reduced expression in macrophages 6 hours post-infection with *Mav* and *Mtb* compared to uninfected controls, with significantly more silencing by *Mav* compared to *Mtb*. Although *GIMAP5* and *GIMAP2* were not significantly affected by mycobacterial infection when compared to uninfected controls, these genes were downregulated in macrophages infected with *Mav* compared to *Mtb*. Furthermore, while not differentially regulated between the two mycobacteria, *GIMAP4* and *GIMAP7* were significantly silenced by both *Mav* and *Mtb* 2 hours post-infection in comparison to uninfected controls.

Finally, the third PPI network consisted of genes encoding mainly cytokines. While we observed that both *Mav* and *Mtb* triggered significant early cytokine responses in macrophages compared to noninfected controls, *Mav* induced a more pronounced upregulation of several cytokines compared to *Mtb*. At 2 hours post-infection, these cytokines included *IL23A*, *IL6*, *IL1B*, *IL12B*, *CCL3L3*, *TNF* and *CSF3* (Table 1). At 6 hours post-infection, the upregulation of I*L23A*, *IL6*, *CCL3L3*, and *CSF3* persisted, along with the downregulation of *CCL8* and *CCL2* and additional upregulation of cytokines *TNFSF15*, *CSF2*, and *CCR7* in response to *Mav* compared to *Mtb* (**Table 1, Figure 5C**). The heightened expression of these molecules in response to *Mav* suggests this infection might be stimulating a more intense or swifter activation of immune pathways compared to *Mtb*. In addition, macrophages infected with *Mav* or *Mtb* showed increased expression of *PTGS2*, which was significantly higher upon *Mav* compared to *Mtb* infection.

Table 1. Genes, belonging to one of the STRING nodes, differentially modulated in primary human macrophages in response to *Mav* compared to *Mtb*.

Genes differentially expressed between *Mav* and *Mtb*				
2 hours post-infection			**DEG vs. uninfected**	
Gene	**Log2FC (*Mav* vs. *Mtb*)**	**p-value (adj)**	***Mav***	***Mtb***
Cytokines/Chemokines				
IL23A	1,85	1,05E-02	Up	Up
IL6	1,75	2,52E-03	Up	Up
OSM	1,74	3,06E-04	Up	-
IL1B	1,69	1,26E-04	Up	Up
IL12B	1,65	1,40E-02	Up	Up
CCL3L3	1,63	3,06E-04	Up	Up
TNF	1,62	1,26E-04	Up	Up
CSF3	1,57	7,26E-04	Up	Up
Transcription regulators				
FOS	3,31	2,80E-05	Up	Down
EGR1	3,14	1,26E-04	Up	-
EGR4	2,96	3,39E-04	Up	-
FOSB	1,93	6,47E-04	Up	-
Other				
PTGS2	1,66	2,72E-03	Up	Up
6 hours post-infection			**DEG vs. uninfected**	
Gene	**Log2FC (*Mav* vs. *Mtb*)**	**p-value (adj)**	***Mav***	***Mtb***
GIMAPs				
GIMAP1	-2,21	1,06E-02	Down	Down
GIMAP2	-1,66	4,45E-02	-	-
GIMAP5	-1,80	1,06E-02	-	-
GIMAP6	-2,76	2,93E-03	Down	Down
Cytokines/Chemokines				
CCL8	-2,47	4,79E-02	-	Up
CCL2	-1,67	9,12E-03	-	-
CSF3	2,49	1,26E-02	Up	Up
IL23A	2,42	4,15E-03	Up	Up
TNFSF15	2,35	1,33E-02	Up	Up
CSF2	2,35	9,73E-03	Up	Up
IL6	1,99	1,15E-02	Up	Up
CCL3L3	1,58	1,52E-02	Up	Up
CCR7	1,56	2,05E-02	Up	Up
LIF	1,52	9,98E-03	Up	Up
Transcription regulators				
EGR1	2,64	3,61E-02	-	Down
Other				
ARC	2,37	1,06E-02	Up	-

Taken together, macrophages infected with *Mav* showed upregulation of transcription factors related to NGF signaling and pro-inflammatory cytokines compared to *Mtb* infection, whereas GIMAPs were downregulated.

Validation of upregulated cytokine expression by assessing cytokine secretion by *Mav*- and *Mtb*-infected macrophages

To validate the transcriptome analysis results of cytokine production (**Supp Figure 5A**), secretion of a number of DEGs encoding cytokines in the supernatants of macrophages infected with *Mav* or *Mtb* 24 hours post-infection was measured using the Luminex assay. Compared to uninfected controls, both *Mav* and *Mtb* infection resulted in the induction of IL-6, IL-1β, TNF, IFN-γ, and to a lesser extent IL-12B and IFN-α2 (**Figure 6**). Induction of CSF2 and CSF3 by *Mav* or *Mtb* was not evident. Moreover, the transcriptome analysis between *Mav*- and *Mtb*-infected macrophages indicated the higher expression of certain cytokines after *Mav* infection (**Table 1, Supp Figure 5**). While *Mtb* rather than *Mav* appeared to induce higher levels of certain cytokines, no statistically significant differences in cytokine production were observed between *Mav* and *Mtb* infections (**Figure 6, Supp Figure 5**).

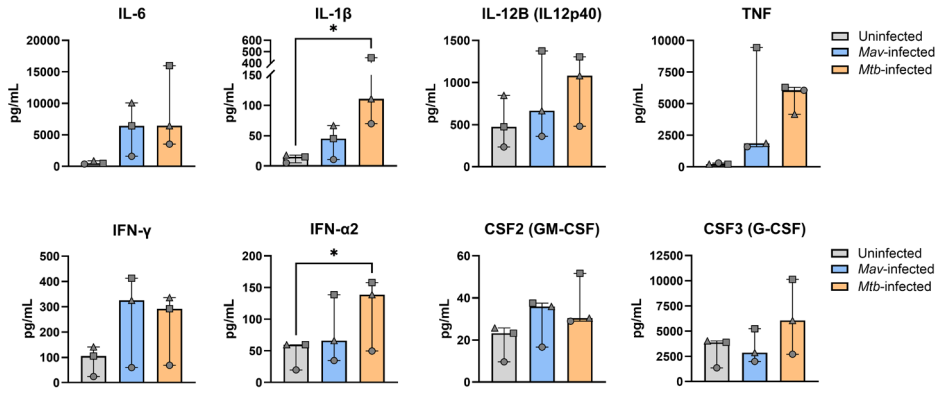

Figure 6. Cytokine production by *Mav*- and *Mtb*-infected macrophages.
Supernatants of *Mav*- and *Mtb* infected macrophages collected 24 hours post-infection were assessed for IL-6, IL-1β, IL-12B, TNF, IFN-γ, IFN-α2, CSF2 and CSF3 by the Luminex assay. Each symbol represents one donor (n=3) and data represent the median ± interquartile range. Statistical significance was tested using a Friedman test with Dunn's multiple comparisons test. *$p < 0.05$.

Discussion

There is a paucity of studies investigating the host-pathogen interactions and host transcriptomic response in *Mav*-infected primary human macrophages, cells crucial in immunity against *Mav* infection. Here, we report the first genome-wide transcriptome analysis of macrophages infected with *Mav*, and directly cross-reference these observations with *Mtb* infection. Our findings indicate that the transcriptional response to both infections largely overlaps, while some infection-specific responses are at play. The shared response to *Mav* and *Mtb* primarily involved cytokine signaling responses and GPCR signaling. In contrast, when comparing *Mav* and *Mtb* to one another and uninfected controls, differences were observed in the regulation of lipid metabolism, NGF-stimulated transcription, and the less-explored GIMAPS. Overall, we found alterations in the host response to both mycobacteria, providing insights into the shared and distinctive host processes that may play a role in the intracellular control of

Mav and *Mtb*, and which potentially offer targets for host-directed therapy.

Macrophages have a leading role in mycobacterial killing, antigen presentation, and directing immune responses. Cytokines like TNF, IL-1β, IL-6, and IL-10 produced by macrophages upon activation of pattern recognition receptors including Toll-like receptors (TLR) are crucial in bridging the innate and adaptive immune responses to mycobacterial infection (17). Consistent with previous findings, we observed a significant increase in pro-inflammatory cytokines (I*L12B*, *IL23A*, *TNF*, *IL1B*, *IL6*, *CCL20*, *CSF3*, and *CSF2*) in macrophages within hours of *Mav* or *Mtb* infection (25, 47, 48). Some of these cytokines in turn regulate TLR transcription to create feedback loops (49). We found increased *TLR2* expression and decreased *TLR5* expression in macrophages up to 6 hours post-infection with *Mav* and *Mtb*, as observed in prior studies (49, 50). In addition, *TLR3* and *TLR6* were downregulated in *Mav*- and *Mtb*-infected macrophages. Our cytokine secretion data validates that cytokine responses are a common feature of both *Mav* and *Mtb* infections. At 2 hours post-infection, however, differential expression analysis of infected macrophages showed a higher expression of pro-inflammatory cytokines such as *TNF*, *CSF3*, and *IL6* in response to *Mav* as compared to *Mtb*, which did not result in differences in cytokine secretion patterns between *Mav*- and *Mtb*-infected macrophages. Possibly, cytokine gene expression upon *Mtb* infection is slightly delayed as compared to *Mav* infection, which may be associated with the suggestion that mycobacterial virulence is inversely related to their ability to induce pro-inflammatory cytokines as an immune evasion strategy (51-53). Although *Mav* is considered less virulent than *Mtb*, we observed higher persistence of *Mav* in macrophages within 24 hours, suggesting that host cell antimycobacterial mechanisms other than cytokine production may be involved in the differential elimination of *Mav*.

Comparing the host transcriptomic response to *Mav* and *Mtb* revealed that both infections affected interferon signaling, which was more pronounced following *Mtb* infection. Both *Mav* and *Mtb* upregulated genes related to type II interferon (IFN) signaling. Interestingly, *Mav* affected type I IFN signaling only by upregulation of *IFNB1* (type I IFN), while *Mtb* induced the expression of genes downstream of type I IFN signaling (including *OAS2*, *MX1*, *MX2*, *ISG15*). In line with this, both *Mav* and *Mtb* seemed to induce secretion of IFN-γ to a similar extent, whereas secretion of IFN-α2 was slightly higher for *Mtb*-infected macrophages. While type II IFN (i.e. IFN-γ) is required for the resistance to mycobacteria, there is a lack of consensus on the role of type I IFNs in mycobacterial infections. In *Mav*-infected mice, continuous IFN-β infusion increased resistance, as evidenced by reduced bacterial loads (54). In contrast, type I IFN worsens *Mtb* infections (55), as shown by reduced bacterial loads in type I IFN receptor-deficient mice, and increased bacterial burden and pathology associated with recruitment of permissive macrophages via CCL2 when IFN-α/β was induced (56, 57). Remarkably, *CCL2* was more strongly downregulated in macrophages infected by *Mav* compared to *Mtb*. Moreover, type I IFN induces the immunosuppressive cytokine IL-10, and suppresses IL-1β production, resulting in the loss of protection against *Mtb* (58-60). *IL1B* was more strongly upregulated in *Mav*-infected cells compared to *Mtb* at 2 hours. IL-1β has a reciprocal control of type I IFN, by controlling type I IFN-induced accumulation of permissive macrophages at the site of infection through prostaglandin E2 (61). In line with the expression pattern of *IL1B*, *PTGS2*, which encodes for COX2 that mediates the production of prostaglandin E2, was more strongly upregulated by

Mav compared to *Mtb* at 2 hours. The disappearance of *IL1B* and *PTGS2* expression differences between *Mav* and *Mtb* at 6 hours post-infection may explain the comparable cytokine secretion observed following both infections. Taken together, IFN signaling was affected by both *Mav* and *Mtb* infection, with considerable variation over time.

The host transcriptomic regulation by *Mav* and *Mtb* infection also involved many genes linked to lipid metabolism, with some clear differences between both infections. Fatty acids are the most energy-dense substrates for energy production and are components of phospholipids in cell membranes (62). When nutrients are in excess, fatty acids can be stored as triglycerides, together with cholesteryl esters, in lipid droplets, which can be accessed via lipophagy (hydrolysis of lipid droplets by lipo-autophagosomes and lysosomes) or lipolysis (enzymatic hydrolysis of contents of cytosolic lipid droplets) during nutrient starvation (63). We found that infection with *Mav* and *Mtb* commonly upregulated *HCAR2* (promotes lipid accumulation associated with *Mtb* survival) (64), downregulated *FFAR4* (reduces lipid accumulation) (65), and upregulated *GPR156* (increases lipid accumulation) (66), indicating mycobacterial infection induces the accumulation and availability of lipids. Moreover, *Mav* and *Mtb* infections downregulated *GPR34* and closely related *GPR82* (both inhibit lipolysis) (67-70) and upregulated *GPR84*, *GPR132*, and *GPR183* (all three involved in sensing fatty acids or cholesterol) (71-75). In addition, expression of *FFAR2* (i.e. *GPR43*), associated with inhibition of lipolysis (40), varied in time, and was more strongly downregulated by *Mav* compared to *Mtb* infection. Lipid metabolism is known to be crucial for *Mtb* survival during infections; *Mtb* stimulates intracellular lipid accumulation and access to cytosolic lipids by escaping the phagosome or promoting the transport of lipid droplets to mycobacteria-containing vacuoles (39), creating a nutrient-rich environment that supports mycobacterial growth (76). While knowledge of the modulation of the host lipid metabolism during *Mav* infections is limited (77), our findings suggest that lipid metabolism is also essential during *Mav* infections. Indeed, there is a clear association between lower body fat mass and the development of *Mav*-LD (78, 79), and increased fatty acid metabolism has been linked to disease progression (76), indicating that altered lipid metabolism is also involved during *Mav* infection. This is supported by *Mav*-infected mice showing a correlation between increased fatty acid uptake and the formation of lipid-rich foamy macrophages with the progression of pulmonary disease (76). Notably, *Mav* but not *Mtb*, induced significant changes in the expression of phospholipases, which have a hydrolytic activity on host membrane phospholipids, resulting in the release of fatty acids for energy consumption, or anabolism of other lipids. These findings suggest that *Mav*, like *Mtb*, modulates lipid metabolism, possibly through different strategies in the battle between the host and mycobacteria for host lipids.

Another host pathway that was differentially regulated by *Mav* and *Mtb* is NGF signaling. Apoptosis of infected macrophages serves as an essential component of the host's defense mechanism against pathogens. Unlike necrosis, a type of cell death characterized by cell lysis releasing bacteria, apoptosis is a tightly regulated process that restricts bacterial growth and contributes to the activation of adaptive immunity (80). The role of apoptosis in both *Mav* and *Mtb* infection is debated, as inhibition of apoptosis is recognized as a key strategy to impair host immunity (81-84). However, mycobacteria can also benefit from the induction of apoptosis which enables them

to escape from dying cells to infect neighboring cells (85-87). Here, we observed that *Mav* infection induced expression of the neurotrophic factor receptor p75/*NGFR* 6 hours post-infection, which upon high or low affinity and activation by pro-NGF or NGF, respectively, is known to induce apoptosis in neurons (45, 46). Hence, macrophages infected with *Mav* rather than *Mtb* show a tendency towards induction of apoptosis, which is more likely to be induced during *Mav* infection compared to *Mtb* infection, which is supported by the finding that *Mtb* induced less apoptosis than other mycobacterial species including *Mav* (53). However, macrophages infected with *Mav* also showed increased expression of anti-apoptotic *BCL2*, while pro-apoptotic *BAX* was significantly silenced, as also seen in *Mtb*-infected cells, which promotes cell survival. Hence, during both *Mav* and *Mtb* infections, apoptosis may be inhibited, but macrophages upregulate NGF signaling only during *Mav* infection to promote apoptosis, resulting in differences in the cells' ability to induce apoptosis during *Mav* and *Mtb* infections.

Lastly, multiple GIMAPs were downregulated by both mycobacterial infections, and this downregulation was more pronounced during *Mav* infections. *GIMAP4* and *GIMAP7* were comparably silenced in macrophages by both *Mav* and *Mtb* 2 hours post-infection. At 6 hours post-infection, however, *Mav* showed a stronger suppression of *GIMAP1*, *GIMAP2*, *GIMAP5*, and *GIMAP6* expression compared to *Mtb*. To our knowledge, this is the first report of the differential expression of GIMAPs in human macrophages infected with mycobacteria. While the role of these proteins has mainly been described for the maintenance of lymphocytes (88-90), GIMAPs are also thought to be important in intracellular trafficking, as well as autophagy and lysosome function (91, 92), processes considered important in immune defenses against mycobacteria. GIMAP2 is found on lipid droplets to which it recruits GIMAP7, suggesting a role for these GIMAPs in lipid droplet trafficking (93). Furthermore, mutations in GIMAP5, which resides on lysosomes, are linked to increased autoimmune susceptibility (88), but its function in macrophages remains to be determined. GIMAP6 is involved in regulating efficient autophagy and facilitates antibacterial innate immunity by binding to and clearing pathogens (88, 92, 94). Finally, *GIMAP6* was downregulated in cattle infected with *Mav* subspecies paratuberculosis, while its role in disease susceptibility remains unknown (95). Taken together, while it remains unclear what the exact roles of GIMAPs are during mycobacterial infection, the more profoundly reduced expression of these proteins observed upon *Mav* infection may indicate a stronger impairment of the macrophage's ability to manage the infection. More investigation into the role of GIMAPs during mycobacterial infection is desired and may reveal novel targets for HDT.

This study has several limitations that should be considered. Firstly, as a validation strategy, cytokine regulation was assessed by a Luminex, but other differences found in the transcriptomic data were not validated further by complementary analyses. Hence, the findings from this study require further validation. Secondly, the analysis focused exclusively on early time points post-infection, which represents only a snapshot of macrophage activity shortly after infection and may not reflect the longer-term dynamic regulation of macrophage functions. Insufficient RNA yields at later time points (24 hours post-infection) unfortunately limited our ability to assess gene expression over a prolonged time course. Despite these limitations, a strength of this study was the use of RNA-seq, which, unlike microarray studies performed previously on *Mav*-infected cells (23-26), offers significant advantages including unbiased, genome-wide transcriptome

profiling of host gene expression without requiring pre-existing genome sequence information. Additionally, our study directly compares *Mav* and *Mtb* infections across primary human macrophages from matched donors, providing relevant insights into the differential responses of macrophages to these two mycobacterial infections. This direct comparison between *Mav* and *Mtb* facilitates extrapolation of shared findings given the wealth of studies that have functionally validated RNA regulation by *Mtb*.

In conclusion, this study on the host transcriptomic regulation of the human macrophage response to *Mav* and *Mtb* infection reveals a significant overlap between these infections in gene expression patterns. However, also distinct effects were observed in macrophage gene expression, being particularly pronounced during *Mav* infection. The functional implications of these expression patterns remain to be determined, in which our results provide direction to further explore host-pathogen interactions during *Mav* and *Mtb* infections.

Materials and methods

Cell culture

Buffy coats were collected from healthy anonymous Dutch adult donors after written informed consent (Sanquin Blood Bank, Amsterdam, the Netherlands). Primary human macrophages were obtained as previously described (96). In short, CD14+ monocytes were isolated from peripheral blood mononuclear cells using density gradient centrifugation with Ficoll (Pharmacy, LUMC, the Netherlands) and subsequently magnetic-activated cell sorting (MACS) with anti-CD14-coated microbeads (Miltenyi Biotec, Auburn, CA, USA). Purified CD14+ monocytes were cultured for 6 days at 37°C/5% CO_2 in Gibco Dutch modified Roswell Park Memorial Institute (RPMI) 1640 medium (ThermoFisher Scientific, Landsmeer, the Netherlands) supplemented with 10% fetal calf serum (FCS), 2 mM L-glutamine (PAA, Linz, Austria), 100 units/mL penicillin, 100 µg/mL streptomycin, and 50 ng/mL macrophage colony-stimulating factor (M-CSF, R&D Systems, Abingdon, UK) for anti-inflammatory M2 macrophage differentiation. Cytokines were refreshed at day 3 of differentiation. One day prior to experiments, macrophages were harvested and seeded into flat-bottom 96-well plates (30,000 cells/well), if not indicated otherwise, in complete RPMI medium without antibiotics or cytokines. Macrophage differentiation was validated based on cell surface marker expression (anti-human CD163-PE, CD14-PE-Cy7, and CD1a-Alexa Fluor 647 (1:20) from Biolegend (Amsterdam, the Netherlands) and anti-human CD11b-BB515 (1:20) from BD Biosciences) using flow cytometry and secretion of cytokines (IL-10 and IL-12) following 24 hours stimulation of cells with 100 ng/mL lipopolysaccharide (InvivoGen, San Diego, United States) using ELISA.

Bacterial cultures

Mav-Wasabi (laboratory strain 101) and *Mtb*-Venus (H37Rv) were cultured as described before (96, 97). Prior to experiments, bacterial concentrations were determined by measuring the optical density at 600 nm (OD_{600}).

Bacterial infection of cells

One day before infection, *Mav* and *Mtb* cultures were diluted to a density corresponding with early log-phase growth, OD_{600} of 0.25. On the day of macrophage infection, bacterial suspensions were diluted in antibiotic-free cell culture medium to consistently infect

cells with a multiplicity of infection (MOI) of 10. The accuracy of the MOI was verified using a standard CFU assay. Following inoculation of the cells, plates were centrifuged for 3 minutes at 130 rcf and incubated for 1 hour at 37°C/5% CO2. Cells were then treated with cell culture medium supplemented with 30 µg/mL gentamicin for 10 min to inactivate and remove residual extracellular bacteria, after which the medium was refreshed with medium containing 5 µg/mL gentamicin sulfate before cells were incubated at 37°C/5% CO_2 until indicated timepoints. Following incubation, supernatants were either stored at -20°C for Luminex assay or discarded, and cells were lysed using 100 µL of lysis buffer (H2O + 0.05% SDS) for the determination of intracellular bacterial burden using a CFU assay or lysed for RNA extraction as described below.

RNA isolation and sequencing
Total RNA was extracted from *Mav*- or *Mtb* infected macrophages seeded in a flat bottom 6-wells plate (900,000 cells/well) with 350 uL TRIzol™ reagent (Thermo Fisher Scientific) and using the Direct-zol RNA miniPrep kit (Zymo Research, Leiden, Netherlands) according to the manufacturer's protocol. Samples were diluted in 25 µL RNA-free water and the total RNA concentration of each sample was quantified using DeNovix DS-11 Spectrophotometer (ThermoFisher Scientific). Nanodrop (ThermoFisher Scientific) was used to determine RNA purity. Gene expressions were profiled using the NovaSeq 6000 platform (Illumina, San Diego, CA, USA) by GenomeScan (Leiden, Netherlands).

Data processing and analysis
RNA-Seq files were processed using the opensource BIOWDL RNAseq pipeline v5.0.0 (https://zenodo.org/record/5109461#.Ya2yLFPMJhE) developed at the LUMC. This pipeline performs FASTQ preprocessing (including quality control, quality trimming, and adapter clipping), RNA-Seq alignment, read quantification, and optionally transcript assembly. FastQC was used for checking raw read QC. Adapter clipping was performed using Cutadapt (v2.10) with default settings and standard illumina universal adapter "AGATCGGAAGAG". RNA-Seq reads' alignment was performed using STAR (v2.7.5a) on GRCh38 human reference genome. umi_tools (v1.1.1) was used to remove PCR duplicates detected with UMIs. The gene read quantification was performed using HTSeq-count (v0.12.4) with setting "–stranded=reverse". The gene annotation used for quantification was Ensembl version 111. Using the gene read count matrix, CPM was calculated per sample on all annotated genes. Genes with a higher log2CPM than 1 in at least 25% of all samples are kept for downstream analysis.

For the differential gene expression analysis and PCA plot creation, dgeAnalysis R-shiny application (https://github.com/LUMC/dgeAnalysis/tree/v1.4.4) was used. EdgeR (v3.34.1) with TMM normalization was used to perform differential gene expression analysis using donor as covariate. Genes with log2(fold change) ≥ 1.5 or ≤ -1.5 and Benjamini and Hochberg false discovery rate (FDR) adjusted p-values < 0.05 were designated as differentially expressed genes (DEGs).

Functional enrichment analysis
To classify the functions of the DEGs, functional enrichment analysis and clustering of biological pathways was performed through the use of QIAGEN Ingenuity Pathway Analysis (IPA) (QIAGEN Inc., https://digitalinsights.qiagen.com/IPA) (98). In addition, enrichment of Gene Ontology (GO) categories biological process, cellular component

and molecular function was analysed. Enrichment with an adjusted P value of < 0.05 was considered significantThe protein-protein interaction (PPI) networks of DEGs were predicted using the Search Tool for the Retrieval of Interacting Genes (STRING) database.

Cytokine secretion

Collected supernatants of uninfected or *Mav*- and *Mtb*-infected macrophages were filtered in FiltrEX 96-wells filter plates (Corning Costar) with pore size 0.2 µm to remove bacteria. The concentration of IL-6, IL-1β, TNF, IFN-γ, IL-12B, IFN-α2, CSF2, and CSF3 was measured by diluting the supernatants 4 times with Luminex Assay buffer (Bio-Rad, Hercules, CA, USA). Next, the Bio-Plex Pro Human Cytokine 48-plex Assay (Bio-Rad) was performed according to the manufacturer's instructions. Samples were measured on a Bio-Plex 200 System (Bio-Rad). Per analyte, a lower and upper limit of detection was determined with standard curves. Concentrations measured below the assays' detection limit were set to 1 pg/mL, and those measured over the detection limit were set to the maximum quantifiable pg/mL per analyte.

References

1. Ingen Jv, Wagner D, Gallagher J, Morimoto K, Lange C, Haworth CS, et al. Poor adherence to management guidelines in nontuberculous mycobacterial pulmonary diseases. Eur Respir J. 2017;49(2):1601855.
2. Prevots DR, Marras TK. Epidemiology of human pulmonary infection with nontuberculous mycobacteria: a review. Clin Chest Med. 2015;36(1):13-34.
3. van Ingen J, Obradovic M, Hassan M, Lesher B, Hart E, Chatterjee A, et al. Nontuberculous mycobacterial lung disease caused by Mycobacterium avium complex - disease burden, unmet needs, and advances in treatment developments. Expert Rev Resp Med. 2021;15(11):1387-401.
4. Namkoong H, Kurashima A, Morimoto K, Hoshino Y, Hasegawa N, Ato M, et al. Epidemiology of Pulmonary Nontuberculous Mycobacterial Disease, Japan. Emerg Infect Dis. 2016;22(6):1116-7.
5. Shah NM, Davidson JA, Anderson LF, Lalor MK, Kim J, Thomas HL, et al. Pulmonary Mycobacterium avium-intracellulare is the main driver of the rise in non-tuberculous mycobacteria incidence in England, Wales and Northern Ireland, 2007-2012. BMC Infect Dis. 2016;16:195.
6. Winthrop KL, Marras TK, Adjemian J, Zhang H, Wang P, Zhang Q. Incidence and Prevalence of Nontuberculous Mycobacterial Lung Disease in a Large U.S. Managed Care Health Plan, 2008-2015. Ann Am Thorac Soc. 2020;17(2):178-85.
7. Daley CL, Iaccarino JM, Lange C, Cambau E, Wallace RJ, Jr., Andrejak C, et al. Treatment of nontuberculous mycobacterial pulmonary disease: an official ATS/ERS/ESCMID/IDSA clinical practice guideline. Eur Respir J. 2020;56(1).
8. Griffith DE, Aksamit T, Brown-Elliott BA, Catanzaro A, Daley C, Gordin F, et al. An official ATS/IDSA statement: Diagnosis, treatment, and prevention of nontuberculous mycobacterial diseases. Am J Resp Crit Care. 2007;175(4):367-416.
9. Kwon YS, Koh WJ, Daley CL. Treatment of Mycobacterium avium Complex Pulmonary Disease. Tuberc Respir Dis (Seoul). 2019;82(1):15-26.
10. Xu HB, Jiang RH, Li L. Treatment outcomes for Mycobacterium avium complex: a systematic review and meta-analysis. Eur J Clin Microbiol Infect Dis. 2014;33(3):347-58.
11. Crowle AJ, Dahl R, Ross E, May MH. Evidence that vesicles containing living, virulent Mycobacterium tuberculosis or Mycobacterium avium in cultured human macrophages are not acidic. Infect Immun. 1991;59(5):1823-31.
12. Inderlied CB, Kemper CA, Bermudez LE. The Mycobacterium avium complex. Clin Microbiol Rev. 1993;6(3):266-310.
13. Lee H-J, Woo Y, Hahn T-W, Jung YM, Jung Y-J. Formation and Maturation of the Phagosome: A Key Mechanism in Innate Immunity against Intracellular Bacterial Infection. Microorganisms. 2020;8(9):1298.
14. Uribe-Querol E, Rosales C. Control of Phagocytosis by Microbial Pathogens. Front Immunol. 2017;8:1368.
15. Danelishvili L, Chinison JJJ, Pham T, Gupta R, Bermudez LE. The Voltage-Dependent Anion Channels (VDAC) of Mycobacterium avium phagosome are associated with bacterial survival and lipid export in macrophages. Scientific Reports. 2017;7(1):7007.

16. Danelishvili L, Bermudez LE. Mycobacterium avium *Mav*_2941 mimics phosphoinositol-3-kinase to interfere with macrophage phagosome maturation. Microbes Infect. 2015;17(9):628-37.
17. Park HE, Lee W, Choi S, Jung M, Shin MK, Shin SJ. Modulating macrophage function to reinforce host innate resistance against Mycobacterium avium complex infection. Front Immunol. 2022;13:931876.
18. Ottenhoff TH, Verreck FA, Lichtenauer-Kaligis EG, Hoeve MA, Sanal O, van Dissel JT. Genetics, cytokines and human infectious disease: lessons from weakly pathogenic mycobacteria and salmonellae. Nat Genet. 2002;32(1):97-105.
19. Blischak JD, Tailleux L, Mitrano A, Barreiro LB, Gilad Y. Mycobacterial infection induces a specific human innate immune response. Sci Rep. 2015;5:16882.
20. Lee J, Lee SG, Kim KK, Lim YJ, Choi JA, Cho SN, et al. Characterisation of genes differentially expressed in macrophages by virulent and attenuated Mycobacterium tuberculosis through RNA-Seq analysis. Sci Rep. 2019;9(1):4027.
21. Prombutara P, Adriansyah Putra Siregar T, Laopanupong T, Kanjanasirirat P, Khumpanied T, Borwornpinyo S, et al. Host cell transcriptomic response to the multidrug-resistant Mycobacterium tuberculosis clonal outbreak Beijing strain reveals its pathogenic features. Virulence. 2022;13(1):1810-26.
22. Pu W, Zhao C, Wazir J, Su Z, Niu M, Song S, et al. Comparative transcriptomic analysis of THP-1-derived macrophages infected with Mycobacterium tuberculosis H37Rv, H37Ra and BCG. J Cell Mol Med. 2021;25(22):10504-20.
23. Agdestein A, Jones A, Flatberg A, Johansen TB, Heffernan IA, Djonne B, et al. Intracellular growth of Mycobacterium avium subspecies and global transcriptional responses in human macrophages after infection. BMC Genomics. 2014;15:58.
24. Blumenthal A, Lauber J, Hoffmann R, Ernst M, Keller C, Buer J, et al. Common and unique gene expression signatures of human macrophages in response to four strains of Mycobacterium avium that differ in their growth and persistence characteristics. Infect Immun. 2005;73(6):3330-41.
25. Greenwell-Wild T, Vazquez N, Sim D, Schito M, Chatterjee D, Orenstein JM, et al. Mycobacterium avium infection and modulation of human macrophage gene expression. J Immunol. 2002;169(11):6286-97.
26. McGarvey JA, Wagner D, Bermudez LE. Differential gene expression in mononuclear phagocytes infected with pathogenic and non-pathogenic mycobacteria. Clin Exp Immunol. 2004;136(3):490-500.
27. Peters A, Rabe P, Liebing AD, Krumbholz P, Nordstrom A, Jager E, et al. Hydroxycarboxylic acid receptor 3 and GPR84 - Two metabolite-sensing G protein-coupled receptors with opposing functions in innate immune cells. Pharmacol Res. 2022;176:106047.
28. Zandi-Nejad K, Takakura A, Jurewicz M, Chandraker AK, Offermanns S, Mount D, et al. The role of HCA2 (GPR109A) in regulating macrophage function. FASEB J. 2013;27(11):4366-74.
29. Klaver D, Thurnher M. Control of Macrophage Inflammation by P2Y Purinergic Receptors. Cells. 2021;10(5).
30. Jacobson KA, Merighi S, Varani K, Borea PA, Baraldi S, Aghazadeh Tabrizi M, et al. A(3) Adenosine Receptors as Modulators of Inflammation: From Medicinal Chemistry to Therapy. Med Res Rev. 2018;38(4):1031-72.
31. Aggarwal NR, D'Alessio FR, Eto Y, Chau E, Avalos C, Waickman AT, et al. Macrophage A2A adenosinergic receptor modulates oxygen-induced augmentation of murine lung injury. Am J Respir Cell Mol Biol. 2013;48(5):635-46.
32. Li XX, Clark RJ, Woodruff TM. C5aR2 Activation Broadly Modulates the Signaling and Function of Primary Human Macrophages. J Immunol. 2020;205(4):1102-12.
33. Rinne P, Rami M, Nuutinen S, Santovito D, van der Vorst EPC, Guillamat-Prats R, et al. Melanocortin 1 Receptor Signaling Regulates Cholesterol Transport in Macrophages. Circulation. 2017;136(1):83-97.
34. Hammer A, Yang G, Friedrich J, Kovacs A, Lee DH, Grave K, et al. Role of the receptor Mas in macrophage-mediated inflammation in vivo. Proc Natl Acad Sci U S A. 2016;113(49):14109-14.
35. Szeto A, Sun-Suslow N, Mendez AJ, Hernandez RI, Wagner KV, McCabe PM. Regulation of the macrophage oxytocin receptor in response to inflammation. Am J Physiol Endocrinol Metab. 2017;312(3):E183-E9.
36. Elliott DE, Li J, Blum AM, Metwali A, Patel YC, Weinstock JV. SSTR2A is the dominant somatostatin receptor subtype expressed by inflammatory cells, is widely expressed and directly regulates T cell IFN-gamma release. Eur J Immunol. 1999;29(8):2454-63.
37. Schaale K, Neumann J, Schneider D, Ehlers S, Reiling N. Wnt signaling in macrophages: augmenting and inhibiting mycobacteria-induced inflammatory responses. Eur J Cell Biol. 2011;90(6-7):553-9.
38. Zhang LS, Zhang ZS, Wu YZ, Guo B, Li J, Huang XQ, et al. Activation of free fatty acid receptors, FFAR1 and FFAR4, ameliorates ulcerative colitis by promote fatty acid metabolism and mediate macrophage polarization. Int Immunopharmacol. 2024;130:111778.
39. van der Klugt T, van den Biggelaar R, Saris A. Host and bacterial lipid metabolism during tuberculosis infections: possibilities to synergise host- and bacteria-directed therapies. Crit Rev Microbiol. 2024:1-21.

40. Al Mahri S, Malik SS, Al Ibrahim M, Haji E, Dairi G, Mohammad S. Free Fatty Acid Receptors (FFARs) in Adipose: Physiological Role and Therapeutic Outlook. Cells. 2022;11(4).
41. Lin J, Liu Q, Zhang H, Huang X, Zhang R, Chen S, et al. C1q/Tumor necrosis factor-related protein-3 protects macrophages against LPS-induced lipid accumulation, inflammation and phenotype transition via PPARgamma and TLR4-mediated pathways. Oncotarget. 2017;8(47):82541-57.
42. Xu C, Sarver DC, Lei X, Sahagun A, Zhong J, Na CH, et al. CTRP6 promotes the macrophage inflammatory response, and its deficiency attenuates LPS-induced inflammation. J Biol Chem. 2024;300(1):105566.
43. Bahrami S, Drablos F. Gene regulation in the immediate-early response process. Adv Biol Regul. 2016;62:37-49.
44. Adams KW, Kletsov S, Lamm RJ, Elman JS, Mullenbrock S, Cooper GM. Role for Egr1 in the Transcriptional Program Associated with Neuronal Differentiation of PC12 Cells. PLoS One. 2017;12(1):e0170076.
45. Bruno F, Arcuri D, Vozzo F, Malvaso A, Montesanto A, Maletta R. Expression and Signaling Pathways of Nerve Growth Factor (NGF) and Pro-NGF in Breast Cancer: A Systematic Review. Curr Oncol. 2022;29(11):8103-20.
46. Dechant G, Barde YA. The neurotrophin receptor p75(NTR): novel functions and implications for diseases of the nervous system. Nat Neurosci. 2002;5(11):1131-6.
47. Casey ME, Meade KG, Nalpas NC, Taraktsoglou M, Browne JA, Killick KE, et al. Analysis of the Bovine Monocyte-Derived Macrophage Response to Mycobacterium avium Subspecies Paratuberculosis Infection Using RNA-seq. Front Immunol. 2015;6:23.
48. Kawka M, Plocinska R, Plocinski P, Pawelczyk J, Slomka M, Gatkowska J, et al. The functional response of human monocyte-derived macrophages to serum amyloid A and Mycobacterium tuberculosis infection. Front Immunol. 2023;14:1238132.
49. Wang T, Lafuse WP, Zwilling BS. Regulation of toll-like receptor 2 expression by macrophages following Mycobacterium avium infection. J Immunol. 2000;165(11):6308-13.
50. Ariel O, Gendron D, Dudemaine PL, Gevry N, Ibeagha-Awemu EM, Bissonnette N. Transcriptome Profiling of Bovine Macrophages Infected by Mycobacterium avium spp. paratuberculosis Depicts Foam Cell and Innate Immune Tolerance Phenotypes. Front Immunol. 2019;10:2874.
51. Strohmeier GR, Fenton MJ. Roles of lipoarabinomannan in the pathogenesis of tuberculosis. Microbes Infect. 1999;1(9):709-17.
52. Borrmann E, Mobius P, Diller R, Kohler H. Divergent cytokine responses of macrophages to Mycobacterium avium subsp. paratuberculosis strains of Types II and III in a standardized in vitro model. Vet Microbiol. 2011;152(1-2):101-11.
53. Feng Z, Bai X, Wang T, Garcia C, Bai A, Li L, et al. Differential Responses by Human Macrophages to Infection With Mycobacterium tuberculosis and Non-tuberculous Mycobacteria. Front Microbiol. 2020;11:116.
54. Denis M. Recombinant murine beta interferon enhances resistance of mice to systemic Mycobacterium avium infection. Infect Immun. 1991;59(5):1857-9.
55. Cooper AM, Mayer-Barber KD, Sher A. Role of innate cytokines in mycobacterial infection. Mucosal Immunol. 2011;4(3):252-60.
56. Antonelli LR, Gigliotti Rothfuchs A, Goncalves R, Roffe E, Cheever AW, Bafica A, et al. Intranasal Poly-IC treatment exacerbates tuberculosis in mice through the pulmonary recruitment of a pathogen-permissive monocyte/macrophage population. J Clin Invest. 2010;120(5):1674-82.
57. Sabir N, Hussain T, Shah SZA, Zhao D, Zhou X. IFN-beta: A Contentious Player in Host-Pathogen Interaction in Tuberculosis. Int J Mol Sci. 2017;18(12).
58. Novikov A, Cardone M, Thompson R, Shenderov K, Kirschman KD, Mayer-Barber KD, et al. Mycobacterium tuberculosis triggers host type I IFN signaling to regulate IL-1beta production in human macrophages. J Immunol. 2011;187(5):2540-7.
59. Mayer-Barber KD, Andrade BB, Barber DL, Hieny S, Feng CG, Caspar P, et al. Innate and adaptive interferons suppress IL-1alpha and IL-1beta production by distinct pulmonary myeloid subsets during Mycobacterium tuberculosis infection. Immunity. 2011;35(6):1023-34.
60. McNab FW, Ewbank J, Howes A, Moreira-Teixeira L, Martirosyan A, Ghilardi N, et al. Type I IFN induces IL-10 production in an IL-27-independent manner and blocks responsiveness to IFN-gamma for production of IL-12 and bacterial killing in Mycobacterium tuberculosis-infected macrophages. J Immunol. 2014;193(7):3600-12.
61. Mayer-Barber KD, Andrade BB, Oland SD, Amaral EP, Barber DL, Gonzales J, et al. Host-directed therapy of tuberculosis based on interleukin-1 and type I interferon crosstalk. Nature. 2014;511(7507):99-103.
62. Remmerie A, Scott CL. Macrophages and lipid metabolism. Cell Immunol. 2018;330:27-42.
63. Zechner R, Madeo F, Kratky D. Cytosolic lipolysis and lipophagy: two sides of the same coin. Nat

Rev Mol Cell Biol. 2017;18(11):671-84.
64. Naz F, Arish M. GPCRs as an emerging host-directed therapeutic target against mycobacterial infection: From notion to reality. Br J Pharmacol. 2022;179(21):4899-909.
65. Stuttgen GM, Sahoo D. FFAR4: A New Player in Cardiometabolic Disease? Endocrinology. 2021;162(8).
66. Kalam H, Chou CH, Kadoki M, Graham DB, Deguine J, Hung DT, et al. Identification of host regulators of Mycobacterium tuberculosis phenotypes uncovers a role for the MMGT1-GPR156 lipid droplet axis in persistence. Cell Host Microbe. 2023;31(6):978-92 e5.
67. Yasuda D, Hamano F, Masuda K, Dahlstrom M, Kobayashi D, Sato N, et al. Inverse agonism of lysophospholipids with cationic head groups at Gi-coupled receptor GPR82. Eur J Pharmacol. 2023;954:175893.
68. Engel KM, Schrock K, Teupser D, Holdt LM, Tonjes A, Kern M, et al. Reduced food intake and body weight in mice deficient for the G protein-coupled receptor GPR82. PLoS One. 2011;6(12):e29400.
69. Andreu N, Phelan J, de Sessions PF, Cliff JM, Clark TG, Hibberd ML. Primary macrophages and J774 cells respond differently to infection with Mycobacterium tuberculosis. Sci Rep. 2017;7:42225.
70. Liebscher I, Muller U, Teupser D, Engemaier E, Engel KM, Ritscher L, et al. Altered immune response in mice deficient for the G protein-coupled receptor GPR34. J Biol Chem. 2011;286(3):2101-10.
71. Wang J, Wu X, Simonavicius N, Tian H, Ling L. Medium-chain fatty acids as ligands for orphan G protein-coupled receptor GPR84. J Biol Chem. 2006;281(45):34457-64.
72. Hannedouche S, Zhang J, Yi T, Shen W, Nguyen D, Pereira JP, et al. Oxysterols direct immune cell migration via EBI2. Nature. 2011;475(7357):524-7.
73. Foster JR, Ueno S, Chen MX, Harvey J, Dowell SJ, Irving AJ, et al. N-Palmitoylglycine and other N-acylamides activate the lipid receptor G2A/GPR132. Pharmacol Res Perspect. 2019;7(6):e00542.
74. Foo CX, Bartlett S, Chew KY, Ngo MD, Bielefeldt-Ohmann H, Arachchige BJ, et al. GPR183 antagonism reduces macrophage infiltration in influenza and SARS-CoV-2 infection. Eur Respir J. 2023;61(3).
75. Recio C, Lucy D, Purvis GSD, Iveson P, Zeboudj L, Iqbal AJ, et al. Activation of the Immune-Metabolic Receptor GPR84 Enhances Inflammation and Phagocytosis in Macrophages. Front Immunol. 2018;9:1419.
76. Choi S, Lee JM, Kim KES, Park JH, Kim LH, Park J, et al. Protein-energy restriction-induced lipid metabolism disruption causes stable-to-progressive disease shift in Mycobacterium avium-infected female mice. EBioMedicine. 2024;105:105198.
77. Thirunavukkarasu S, de Silva K, Plain KM, R JW. Role of host- and pathogen-associated lipids in directing the immune response in mycobacterial infections, with emphasis on Mycobacterium avium subsp. paratuberculosis. Crit Rev Microbiol. 2016;42(2):262-75.
78. Kartalija M, Ovrutsky AR, Bryan CL, Pott GB, Fantuzzi G, Thomas J, et al. Patients with nontuberculous mycobacterial lung disease exhibit unique body and immune phenotypes. Am J Respir Crit Care Med. 2013;187(2):197-205.
79. Tasaka S, Hasegawa N, Nishimura T, Yamasawa W, Kamata H, Shinoda H, et al. Elevated serum adiponectin level in patients with Mycobacterium avium-intracellulare complex pulmonary disease. Respiration. 2010;79(5):383-7.
80. Behar SM, Martin CJ, Booty MG, Nishimura T, Zhao X, Gan HX, et al. Apoptosis is an innate defense function of macrophages against Mycobacterium tuberculosis. Mucosal Immunol. 2011;4(3):279-87.
81. Keane J, Shurtleff B, Kornfeld H. TNF-dependent BALB/c murine macrophage apoptosis following Mycobacterium tuberculosis infection inhibits bacillary growth in an IFN-gamma independent manner. Tuberculosis (Edinb). 2002;82(2-3):55-61.
82. Liu M, Li W, Xiang X, Xie J. Mycobacterium tuberculosis effectors interfering host apoptosis signaling. Apoptosis. 2015;20(7):883-91.
83. Bermudez LE, Danelishvili L, Babrack L, Pham T. Evidence for genes associated with the ability of Mycobacterium avium subsp. hominissuis to escape apoptotic macrophages. Front Cell Infect Microbiol. 2015;5:63.
84. Early J, Fischer K, Bermudez LE. Mycobacterium avium uses apoptotic macrophages as tools for spreading. Microb Pathog. 2011;50(2):132-9.
85. Augenstreich J, Arbues A, Simeone R, Haanappel E, Wegener A, Sayes F, et al. ESX-1 and phthiocerol dimycocerosates of Mycobacterium tuberculosis act in concert to cause phagosomal rupture and host cell apoptosis. Cell Microbiol. 2017;19(7).
86. Aguilo JI, Alonso H, Uranga S, Marinova D, Arbues A, de Martino A, et al. ESX-1-induced apoptosis is involved in cell-to-cell spread of Mycobacterium tuberculosis. Cell Microbiol. 2013;15(12):1994-2005.
87. Fratazzi C, Arbeit RD, Carini C, Remold HG. Programmed cell death of Mycobacterium avium serovar 4-infected human macrophages prevents the mycobacteria from spreading and induces mycobacterial growth inhibition by freshly added, uninfected macrophages. J Immunol. 1997;158(9):4320-7.
88. Pascall JC, Webb LMC, Eskelinen EL, Innocentin S, Attaf-Bouabdallah N, Butcher GW. GIMAP6 is

required for T cell maintenance and efficient autophagy in mice. PLoS One. 2018;13(5):e0196504.
89. Saunders A, Webb LM, Janas ML, Hutchings A, Pascall J, Carter C, et al. Putative GTPase GIMAP1 is critical for the development of mature B and T lymphocytes. Blood. 2010;115(16):3249-57.
90. Schnell S, Demolliere C, van den Berk P, Jacobs H. Gimap4 accelerates T-cell death. Blood. 2006;108(2):591-9.
91. Limoges MA, Cloutier M, Nandi M, Ilangumaran S, Ramanathan S. The GIMAP Family Proteins: An Incomplete Puzzle. Front Immunol. 2021;12:679739.
92. Yao Y, Du Jiang P, Chao BN, Cagdas D, Kubo S, Balasubramaniyam A, et al. GIMAP6 regulates autophagy, immune competence, and inflammation in mice and humans. J Exp Med. 2022;219(6).
93. Schwefel D, Frohlich C, Eichhorst J, Wiesner B, Behlke J, Aravind L, et al. Structural basis of oligomerization in septin-like GTPase of immunity-associated protein 2 (GIMAP2). Proc Natl Acad Sci U S A. 2010;107(47):20299-304.
94. Pascall JC, Rotondo S, Mukadam AS, Oxley D, Webster J, Walker SA, et al. The immune system GTPase GIMAP6 interacts with the Atg8 homologue GABARAPL2 and is recruited to autophagosomes. PLoS One. 2013;8(10):e77782.
95. Thirunavukkarasu S, Plain KM, de Silva K, Begg D, Whittington RJ, Purdie AC. Expression of genes associated with cholesterol and lipid metabolism identified as a novel pathway in the early pathogenesis of Mycobacterium avium subspecies paratuberculosis-infection in cattle. Vet Immunol Immunopathol. 2014;160(3-4):147-57.
96. Kilinc G, Walburg KV, Franken K, Valkenburg ML, Aubry A, Haks MC, et al. Development of Human Cell-Based In Vitro Infection Models to Determine the Intracellular Survival of Mycobacterium avium. Front Cell Infect Microbiol. 2022;12:872361.
97. Korbee CJ, Heemskerk MT, Kocev D, van Strijen E, Rabiee O, Franken K, et al. Combined chemical genetics and data-driven bioinformatics approach identifies receptor tyrosine kinase inhibitors as host-directed antimicrobials. Nat Commun. 2018;9(1):358.
98. Kramer A, Green J, Pollard J, Jr., Tugendreich S. Causal analysis approaches in Ingenuity Pathway Analysis. Bioinformatics. 2014;30(4):523–30.

Supplementary material

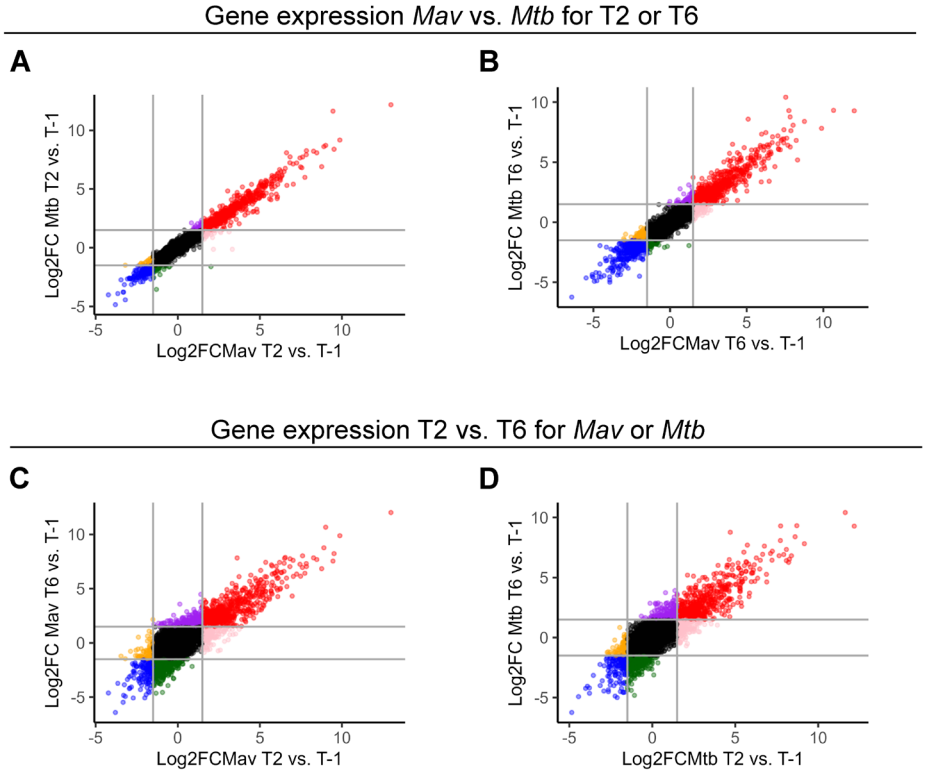

Supplementary Figure 1. Transcriptomic response of primary human macrophages infected with *Mav* or *Mtb* at 2 or 6 hours post-infection and uninfected controls.
(A-B) Scatterplot showing gene expression levels (Log2FC ≥ 1.5 or ≤ 1.5) of macrophages infected with *Mav* vs. *Mtb* at 2 hours (A) or 6 hours (B) post-infection compared to uninfected controls. Genes with Log2FC ≥ 1.5 and Log2FC ≤ 1.5 by both *Mav* and *Mtb* are expressed red and blue, respectively. **(C-D)** Scatterplot showing gene expression levels (Log2FC ≥ 1.5 or ≤ 1.5) of macrophages 2 hours vs. 6 hours post-infected with *Mav* (C) or *Mtb* (D) compared to uninfected controls. Genes with Log2FC ≥ 1.5 and Log2FC ≤ 1.5 by both timepoints post-infection are expressed red and blue, respectively.

Supplementary Table 1. Gene expression values of *Mav*- and *Mtb*-infected macrophages compared to uninfected controls.
Data will be made available on request from the authors.

Supplementary Table 2. Genes differentially expressed between *Mav* and *Mtb* not associated with a STRING-node.

Genes differentially expressed between *Mav* and *Mtb*				
2 hours post-infection			**DEG vs. uninfected**	
Gene	**Log2FC (*Mav* vs. *Mtb*)**	**p-value (adj)**	***Mav***	***Mtb***
OSR2	1,34	9,89E-03	Up	Up
6 hours post-infection			**DEG vs. uninfected**	
Gene	**Log2FC (*Mav* vs. *Mtb*)**	**p-value (adj)**	***Mav***	***Mtb***
GPR65	-1,98	2,93E-03	Down	Down
ENSG00000289424	-1,84	2,93E-03	Down	-
SNAI3	-1,84	2,93E-03	-	-
RAB42	-1,75	2,93E-03	Down	Down
FFAR2	-1,61	2,43E-02	-	Up
LRG1	-1,53	4,61E-02	-	Up
SDHAF1	-1,53	1,06E-02	Down	-
DUSP15	2,97	1,95E-02	Up	Up
CDC25A	1,72	1,06E-02	Up	-
PALLD	1,64	2,58E-03	Up	-
DUSP8	1,59	3,75E-02	Up	Up
ZNF433	1,58	9,12E-03	Up	-
ANKRD1	1,56	6,19E-03	Up	Up
C5orf34	1,54	3,58E-02	Up	-

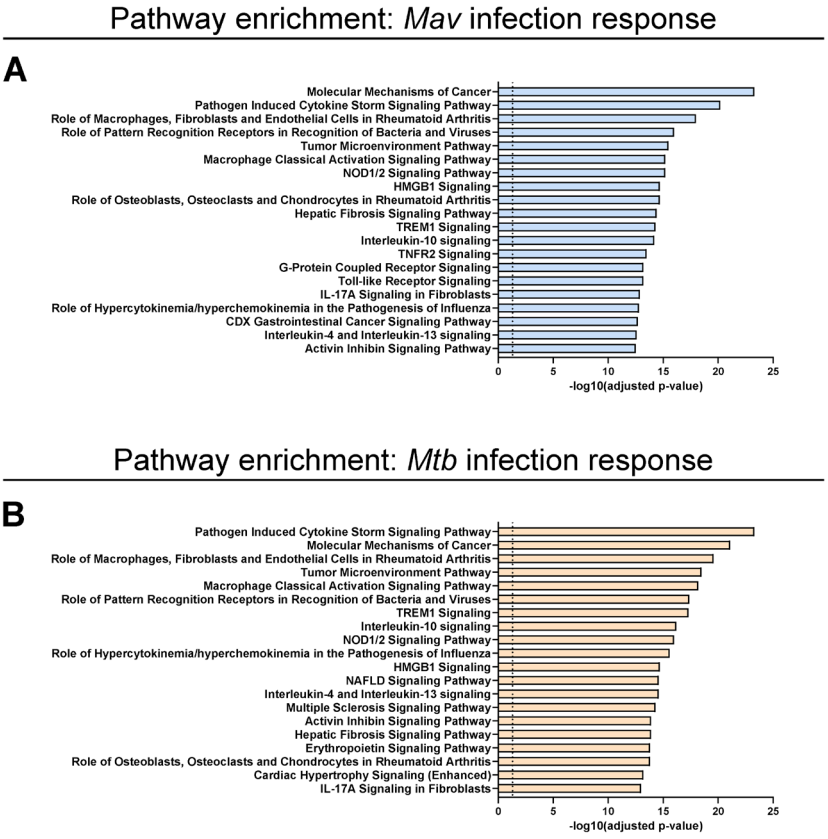

Supplementary Figure 2. Pathway enrichment analysis of the whole transcriptomic response induced by either *Mav* or *Mtb*.
(A-B) The top 20 most significantly enriched IPA pathways based on the whole host transcriptomic response consisting of all genes down- or upregulated in macrophages infected with *Mav* (A) or *Mtb* (B) compared with uninfected controls. The enriched pathways were ranked by -log 10 p-value of gene enrichment.

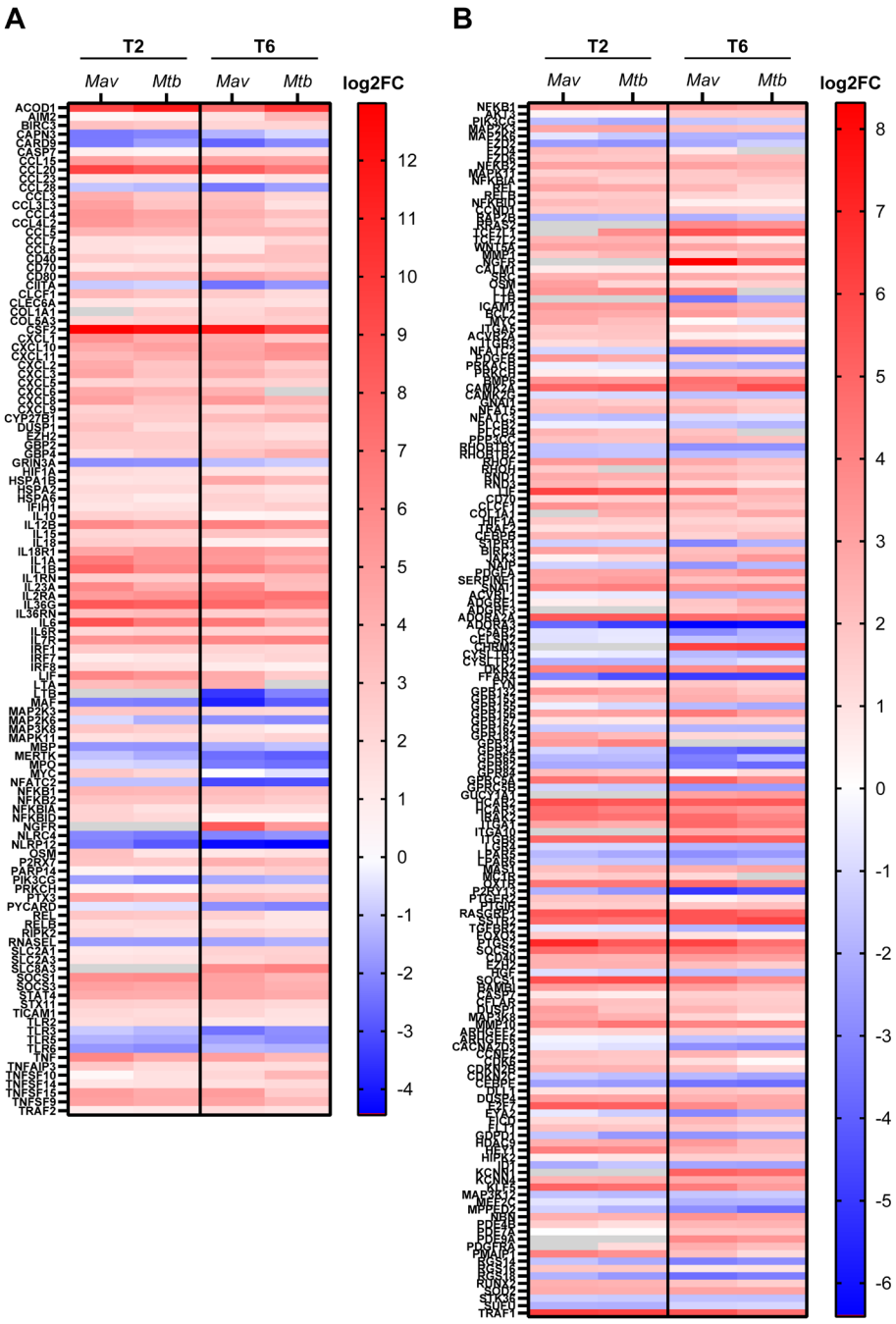

Supplementary Figure 3. Expression patterns of DEGs belonging to the cytokine response or disease-related response commonly induced by *Mav* or *Mtb*.
(A-B) Heatmap showing the expression patterns of 114 DEGs belonging to the cytokine response (A) or 164 DEGs associated with disease pathways (B) commonly induced by *Mav* and *Mtb* in

comparison to uninfected controls. Grey box indicates no expression values could be determined.

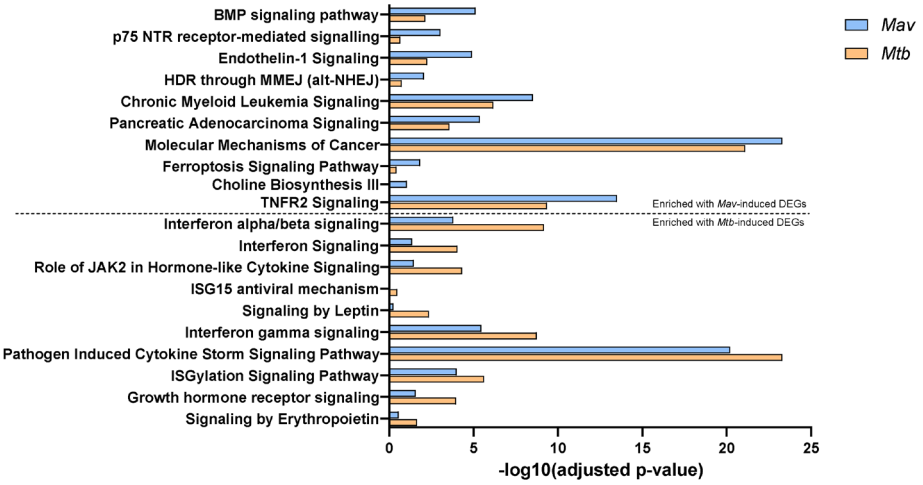

Supplementary Figure 4. Pathway analysis reveals only subtle differences in host signaling between *Mav*- and *Mtb*-infected macrophages.
The top 10 most significantly enriched IPA pathways based on the genes significantly affected in macrophages infected with either *Mav* (above dotted line) or *Mtb* (below dotted line) compared with uninfected controls, also showing the -log 10 p-value of gene enrichment values for the other infection. The enriched pathways were ranked by -log 10 p-value of gene enrichment.

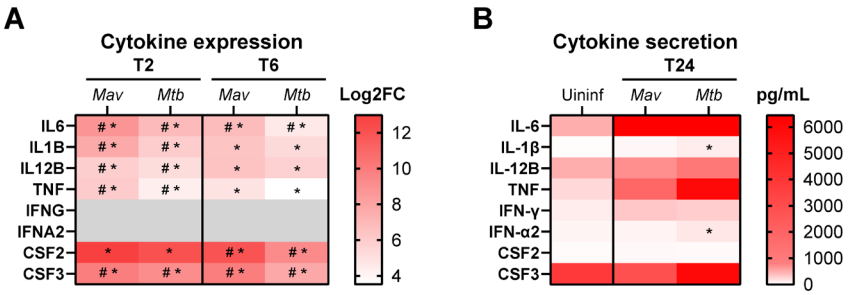

Supplementary Figure 5. Validation of cytokine expression by assessment of cytokine secretion by macrophages infected with *Mav* or *Mtb*.
(A) Heatmap showing the expression patterns of *IL6*, *IL1B*, *IL12B*, *TNF*, *IFNG*, *IFNA2*, *CSF2* and *CSF3* that were differentially regulated in Mav-infected macrophages at 2 (T2) and/or 6 (T6) hours post-infection, compared to uninfected or *Mtb*-infected macrophages. **(B)** Heatmap showing secretion of IL-6, IL-1β, IL-12B, TNF, IFN-γ, IFN-α2, CSF2 and CSF3 measured in supernatants of *Mav*- and *Mtb* infected macrophages collected 24 hours post-infection by the Luminex assay. Shown is the median from three donors.
Asterisk (*) indicates differential expression/secretion when compared to uninfected controls, whereas number sign (#) indicates differential expression/secretion between *Mav* and *Mtb*.


Chapter
7

Summary, general discussion and future directions

Gül Kilinç[1]

[1] Leiden University Center for Infectious Diseases, Leiden University Medical Center, Leiden, The Netherlands

Introduction

Mycobacterium avium (*Mav*) infections are on the rise globally and their treatment faces important challenges, including extensive and intense antibiotic regimens, severe side effects, resistance to first-line antibiotics, and unsatisfactory treatment success rates. Hence, new treatment strategies to improve treatment outcomes and decrease the risk of drug resistance development are required. Host-directed therapy (HDT), differing from conventional antibiotics in that it targets host immune mechanisms rather than the bacteria, is a promising approach to treat (intracellular) mycobacterial infections. The goal is to dampen destructive inflammation or improve host-mediated control of infection, especially by targeting mechanisms that are counteracted or modulated by the pathogen. This thesis started by providing a review of the current stage of developments in HDT for mycobacteria that notably highlights a gap in the development of HDT for *Mav* compared to *Mycobacterium tuberculosis* (*Mtb*). This lag in HDT development was concluded to reflect the limited efforts as well as the limited knowledge of the host-pathogen interactions during *Mav* infection as opposed to *Mtb*. To fill this gap in *Mav* research, this thesis had two main aims: to identify drug candidates for HDT; and to identify novel host targets to promote the development of these and other HDTs. To address these aims, we performed *in vitro* studies using a well-established primary human macrophage model to repurpose drugs as potential HDT candidates for enhanced host control of *Mav* infection (**Figure 1**). Furthermore, we investigated the intracellular host-pathogen interactions during *Mav* infection by conducting transcriptomic analysis of *Mav*-infected primary human macrophages to reveal host genes that may be involved in host pathways and therefore might represent new host targets for HDT to treat *Mav* infection.

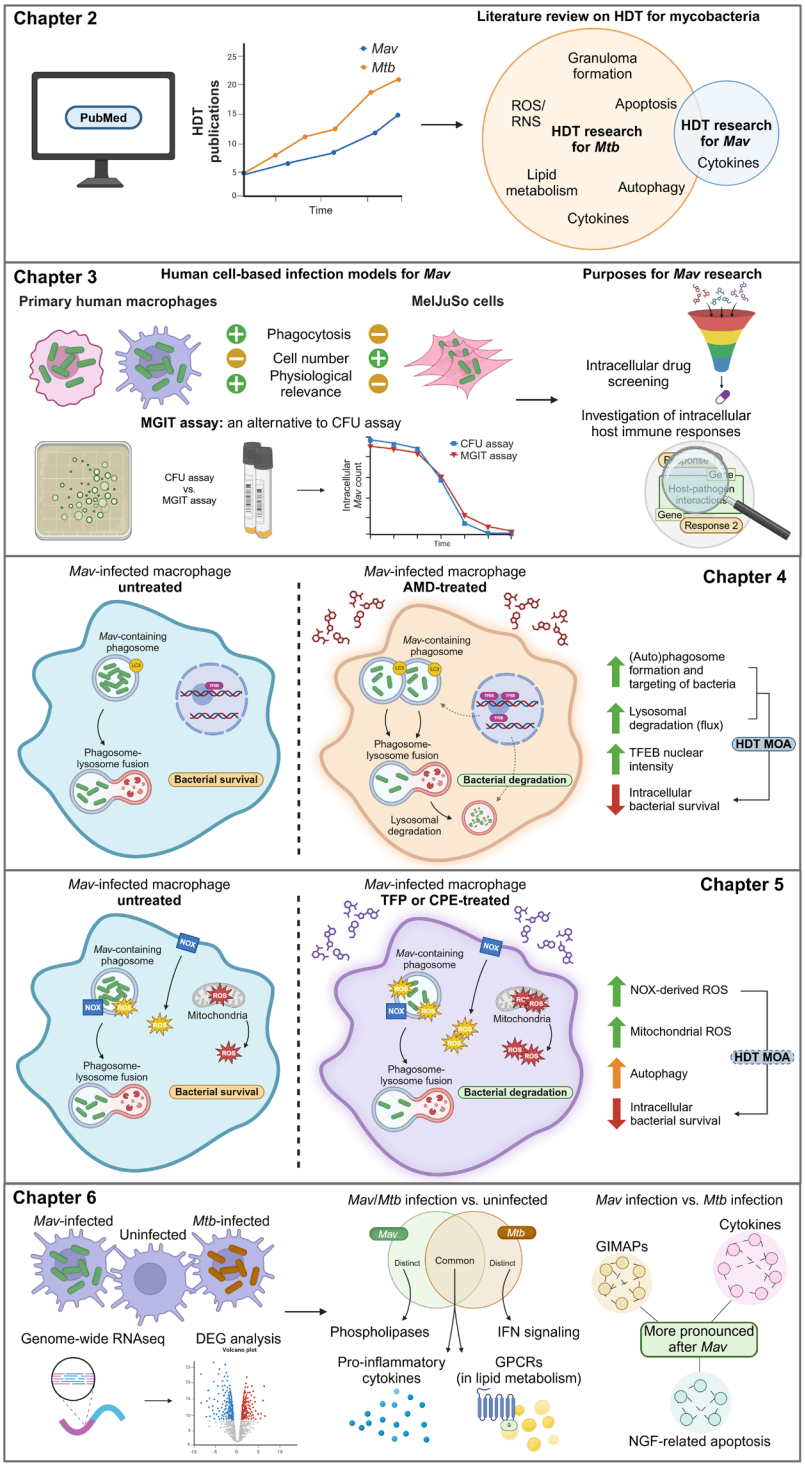

Figure 1. Schematic overview of the main findings of this thesis. *Mav*: *Mycobacterium*

avium, *Mtb*: *Mycobacterium tuberculosis*, HDT: host-directed therapy, ROS/RNS: reactive oxygen species/reactive nitrogen species, MGIT: Mycobacteria growth indicator tube, AMD: amiodarone, TFEB: transcription factor EB, MOA: mechanism of action, NOX: NADPH oxidase, TFP: trifluoperazine, CPE: chlorproethazine, RNAseq: RNA-sequencing, DEG: differentially expressed gene, IFN: interferon, GPCRs: G-protein coupled receptors, GIMAPs: GTPases of immunity-associated proteins, NGF: nerve growth factor. Created with BioRender.

Identification of HDT for *Mav*: current status

One of the aims of this thesis was to identify HDT for *Mav* since there is a compelling need for new therapies that augment the efficacy of current antibiotics and/or provide an alternative approach for decreasing host mycobacterial burden. In **chapter 2** of this thesis, we comprehensively reviewed HDT for mycobacterial infection. This review highlights the HDTs under investigation and describes host immune factors critical for controlling mycobacterial infection, which may be used as therapeutic targets. While the study of HDT in the context of *Mtb* has been extensively explored over the years, *Mav* remains understudied. Building upon the review, **Table 1** summarizes HDTs specifically investigated for *Mav* infections.

The table highlights the diversity of approaches targeting host immunity to enhance bacterial control. Most elaborate research has been performed on cytokines like GM-CSF and IFN-γ, which show potential against intracellular *Mav*, although inconsistent clinical outcomes undermine their therapeutic value. Furthermore, inducers of autophagy like lactoferrin and metformin have shown some evidence to combat *Mav* infection. While these efforts show that HDT in principle offers potential to provide the much-needed boost to the *Mav* complex (MAC) therapeutic pipeline, nearly all avenues of HDT research for *Mav* have been limited in scope and have not reached the level of efficacy to be considered an adjunctive to antibiotic treatment. In efforts to find drugs that may offer a contribution to the development of HDT for *Mav*, the next sectioof this discussion describes repurposing drugs as HDT candidates.

Table 1. HDT investigated for MAC infection.

HDT	Model	Outcome	Ref.
GM-CSF	Case report MAC*	Improvement of infection control	(1)
	In vitro and *in vivo* MAC*	Reduced bacteria burden	(2)
	In vitro MAC	Enhanced inhibition of intracellular bacteria	(3)
	In vitro Mav [x]	Enhanced inhibition of intracellular bacteria	(4)
	(R)CT MAC*,[x] Ex vivo	Enhanced inhibition of intracellular bacteria, but no clinical improvement	(5)
	Case report leukemia and MAC[x]	Improvement of skin lesions	(6)
	Case report MAC*	Clinical and histological improvement	(7)
IFN-γ	Case report MAC*,[x] *In vitro Min* *In vivo* MAC	Limited control of bacterial burden in patients Limited inhibition of intracellular bacteria No effects *in vivo*	(8)
	(R)CT *Mav*[x]	Clinical and radiographic improvement	(9)
	(R)CT MAC[x]	(Earlier) improvement in clinical, radiographic, and bacteriological assessment	(10)
	(R)CT MAC[x]	No difference in treatment outcome	(11)
	Case report MAC*	Temporary limited clinical improvement	(12)
	In vitro Mav	Enhanced inhibition of intracellular bacteria	(13)
IL-2	*In vitro* MAC	Decreased bacterial burden	(14)
	Case report MAC*	Limited effects on clinical improvement	(15)
	Case report MAC	Sputum culture conversion and improvement of CD4+ T cell count	(16)
ATP	*In vitro Min*[x]	Enhanced inhibition of intracellular bacteria	(17)
Lactoferrin	*In vitro Mav*[x]	Enhanced inhibition of intracellular bacteria	(18)
Metformin	*In vitro* and *in vivo Mav*[x]	Reduced bacterial burden in mice and cells without synergism with antibiotics	(19)
Thioridazine	*In vitro*/HFS MAC[x]	Temporary reduction of bacterial burden	(20)
	In vitro MAC[x]	Enhanced inhibition of intracellular bacteria, with synergism with antibiotics	(21)
	In vitro/HFS MAC	Enhanced inhibition of intracellular bacteria	(22)
CRL-1072	*In vitro* MAC[x] *In vivo* MAC[x]	Improved activity of antibiotics on intracellular bacteria, limited effect when administered alone	(23)
	In vitro MAC	Improved bacterial clearance by macrophages	(24)
Picolinic acid	*In vitro Mav*	Enhanced inhibition of intracellular bacteria	(25, 26)
	In vitro MAC[x]	Enhanced inhibition of intracellular bacteria, with synergism with antibiotics	(27)
Amiodarone (chapter 4)	*In vitro Mav* *In vivo* Mmar	Enhanced inhibition of bacteria in cells and zebrafish	(28)
TFP & CPE (chapter 5)	*In vitro Mav*	Enhanced inhibition of intracellular bacteria	(29)

MAC: *Mycobacterium avium* Complex, *Mav*: *Mycobacterium avium*, *Min*: *Mycobacterium intracellulare*, (R)CT: (randomized) clinical trial, HFS: hollow-fiber system, *Mmar*: *Mycobacterium marinum*. * Co-infection MAC and HIV, [x] Adjunctive to chemotherapy.

Repurposing drugs as HDT for *Mav* infection

The rise in MAC infections and the limitations of current antibiotic treatments highlight the need for alternative strategies such as HDT. Given the limited research on HDT in

this context, we aimed to identify potential HDT candidates for *Mav*.

Many studies discovering HDT for mycobacterial infections use repurposed drugs and *in vitro* cell culture models, enabling rapid screening and identification of effective agents. Hit compounds are then forwarded to more advanced infection models to validate their efficacy *in vivo*. By conducting low-throughput screenings of repurposed drugs on our primary human macrophage *Mav* infection model described in **chapter 3**, we identified HDT candidates amiodarone (**chapter 4**) and two phenothiazines, trifluoperazine (TFP) and chlorproethazine (CPE) (**chapter 5**), that enhanced macrophage-mediated control of *Mav*.

Repurposing amiodarone as HDT for *Mav*: targeting autophagy
Amiodarone is an antiarrhythmic drug that blocks calcium, sodium, and potassium channels and inhibits alpha- and beta-adrenergic receptors. Furthermore, amiodarone has been shown to induce autophagy (30-34), and by accumulating in acidic organelles amiodarone may also interact with other intracellular degradation processes, like the endocytic pathway (35). We showed that amiodarone reduces the bacterial burden of *Mav* and *Mtb* in primary human macrophages and that of *Mycobacterium marinum (Mmar)* (another NTM species, mildly pathogenic in humans) in zebrafish, proving its efficacy can be translated from *in vitro* to *in vivo* (**chapter 4**). Moreover, amiodarone promoted the activity of a major autophagy-regulating transcription factor, TFEB, and induced the formation of LC3-positive (auto)phagosomes and targeting of bacteria to these vesicles in *Mav*-infected macrophages. Amiodarone enhanced autophagic flux both in primary human macrophages and in zebrafish. Importantly, lysosomal degradation was essential for the host-protective effect of amiodarone.

Lysosomal degradation is initiated by phagocytosis capturing the bacteria within phagosomes or, when mycobacteria like *Mtb* disrupt the phagosomal membrane escaping into the cytosol (36-38), by host cargo receptors targeting the cytosolic bacteria to autophagosomes in the process of specific autophagy, i.e. xenophagy, to overcome the bacterial immune evasion strategy. *Mav* has evolved mechanisms to resist lysosomal degradation by blocking phagosome maturation, preventing phagosome-lysosome fusion, and using the modulated phagosome as a niche for replication (39-41). Nevertheless, in contrast to *Mtb*, *Mav* has shown to remain phagosomal without cytosolic translocation although the opposite has not been disproven (36). It is therefore uncertain whether autophagy occurs during *Mav* and whether it could be an HDT target. In our study (**chapter 4**), amiodarone induced the formation of LC3-associated vesicles, indicative of both LC3-associated phagocytosis (LAP) and autophagy, however, due to the limited evidence for the role of autophagy cargo receptors, we could not with certainty determine the role of autophagy in the activity of amiodarone. Nonetheless, we observed that amiodarone was able to eliminate multiple mycobacterial species, indicating it stimulates a host defense degradation regardless of the specific immune evasion strategy (e.g. phagosomal escape) conducted that *Mav* and *Mtb* may or may not share.

While amiodarone has shown promise in inducing autophagy and enhancing bacterial clearance, understanding the precise mechanisms by which it activates autophagic pathways is crucial for the development of more effective autophagy-inducing

compounds for clinical translation. We showed that amiodarone enhanced TFEB activation in *Mav*-infected macrophages (**chapter 4**). Once activated, TFEB enters the cell nucleus, stimulating the expression of autophagy-related genes and the coordinated lysosomal expression and regulation (CLEAR) gene network genes (42, 43), and TFEB overexpression strengthens autophagy (31). While it remains to be elucidated whether the autophagy-inducing property of amiodarone is mediated through the activation of TFEB, TFEB activation by itself may be an interesting target for HDT. Acacetin has been shown to activate TFEB and promote autophagic clearance of bacteria such as *Salmonella Typhimurium* (44). Similarly, trehalose is known to induce autophagy via TFEB activation, although its effects during infection have yet to be investigated (45, 46). Other compounds that activate TFEB, such as bedaquiline and molecule 2062, may also hold potential against *Mav* (47, 48). Moreover, TFEB activation is mediated by TRPML1/MCOLN1, a lysosomal calcium channel (49). Chemical agonists of TRPML1 ML-SA5 have been shown to induce TFEB activation and (auto)phagosome formation and autophagy could be blocked using TRPML1 inhibitors. In addition, the activation of TFEB can be negatively regulated, for example, by mTOR (50). Amiodarone is known to inhibit mTOR and may in that way induce TFEB-mediated activation of autophagy (51). This mechanism could parallel the activity of other autophagy-inducing compounds like rapamycin or metformin. Rapamycin, a well-known mTOR inhibitor, was shown to induce autophagy and suppress intracellular survival of *Mtb* (52). Similarly, metformin, used to treat diabetes and an mTOR inhibitor, induces autophagy and has demonstrated efficacy in improving macrophage and murine control of *Mav* infections (10). The activity of these drugs suggests that the mTOR-TFEB axis may be modulated by mycobacterial infection and further exploration could reveal novel targets for HDT. Furthermore, amiodarone can induce autophagy via mTOR-independent pathways involving cAMP. Hence, amiodarone likely interacts with multiple players from the autophagy machinery. A deeper understanding of the molecular mechanisms by which amiodarone eradicates intracellular mycobacteria will enable the identification and development of agents that modulate components of autophagy that are safer and more effective in eradicating a spectrum of mycobacteria.

Repurposing phenothiazines derivatives as HDT for *Mav*: multifaceted HDTs

The other HDT candidates we identified were phenothiazines which are currently used as antipsychotic drugs. Though multiple studies have reported the direct antibacterial effects of phenothiazine against both planktonic and intracellular bacteria, we found no direct antimycobacterial effect of phenothiazines derivatives TFP and CPE on *Mav* in the concentrations that inhibited bacterial survival in primary human macrophages. These compounds may exert direct effects at higher concentrations achieved by intracellular accumulation, however, no correlation was found between tendency to accumulate and impairment of intracellular bacterial survival, indicating host-directed mechanisms are more likely at play (**chapter 5**). Another characteristic of phenothiazines is their ability to antagonize dopamine receptors, prompting us to investigate the role of dopamine receptor activity in the HDT activity of phenothiazines. The finding that dopamine agonists enhanced control of intracellular *Mav* suggests that the ability of TFP and CPE to improve control of *Mav* infection is likely independent of their dopamine receptor antagonism (**chapter 5**). Moreover, phenothiazines have been described to both induce and impair autophagy depending on the tissue investigated.

Although our studies showed an, albeit not significant, increase in (auto)phagosome formation and bacterial targeting in *Mav*-infected primary macrophages treated with TFP and CPE, autophagy was not required for the HDT activity of these compounds (**chapter 5**).

TFP and CPE were shown to induce reactive oxygen species (ROS) production which partially explained the improved macrophage activity against *Mav* upon treatment (**chapter 5**). ROS, including superoxides, hydrogen peroxide, hydroxyl radical, and singlet oxygen, play a fundamental role in host immunity by causing oxidative damage to intracellular bacteria and enhancing clearance (53). Recognition of bacteria by macrophages leads to ROS production mainly by NADPH oxidase (NOX) into the phagosome and by mitochondria releasing ROS into the cytosol or phagosomes (54, 55). Both sources primarily produce superoxides to impair *Mav* survival (56, 57). *Mav*, however, protects itself from the superoxide attack from the host with antioxidant enzymes such as superoxide dismutase (SOD) (MAV_0182 or MAV_2043), which catalyzes the conversion of superoxide radical to hydrogen peroxide and oxygen (58, 59). The activity of SOD MAV_0182 was found to increase upon phagocytosis by macrophages, and the absence of SOD on the surface of *Mav* has been associated with a significant decrease in bacterial viability (60, 61). Once hydrogen peroxides are formed, *Mav* responds by upregulating MAV_2838 (OxyR), which regulates detoxifying enzymes such as catalase-peroxidase (KatG) that convert hydrogen peroxide to water and oxygen, thereby neutralizing oxidative stress and enabling bacterial survival (57, 58, 62). Phenothiazines were found to induce both total cellular (e.g. NOX-derived) and mitochondrial ROS, as measured by the CellROX and MitoSOX assays, respectively (**chapter 5**). Since the CellROX assay detects both superoxides and hydrogen peroxide (54), treatment with MnTBAP (a SOD mimic that converts superoxide to hydrogen peroxide) might have altered the ratio of superoxides and hydrogen peroxides but did not affect the total ROS levels induced by phenothiazines. In contrast, the MitoSOX assay, which specifically detects superoxides, showed reduced superoxide levels in cells co-treated with MnTBAP. Notably, MnTBAP neither improved nor worsened the enhanced macrophage control of *Mav* mediated by phenothiazines, suggesting that their efficacy does not rely on one specific ROS species. A pan NOX-inhibitor did partially impair the improved host control by phenothiazines (**chapter 5**), indicating NOX-derived ROS in the phagosome, regardless of the species, is partially required, highlighting HDT with phenothiazines possibly overcomes the different antioxidant bacterial defenses.

The limited reliance of phenothiazines on ROS production suggests that these drugs must also act on ROS-independent pathways (**chapter 5**). HDTs may modulate multiple interconnected host pathways, complicating the identification of their mechanism of action(s). Using repurposed drugs for HDT discovery has, in theory, the advantage that their target processes are already known. In this thesis, we used chemical modulation by interfering with specific cellular molecular processes aiming to assess their role in HDT mechanism of action. While this approach informed us about the mechanism of action of amiodarone (**chapter 4**), the exact target remains elusive. Moreover, such work is a time-consuming trial-and-error process to fully evaluate the role of host pathways, as evidenced by the phenothiazines (**chapter 5**). Transcriptomics or proteomics of cells in the presence or absence of compound treatment may provide a global view of which proteins and/or host pathways are affected during treatment.

To fully elucidate the mechanisms of action of phenothiazines, complementary approaches could be used (63), which may include host genetic manipulation with for example a (whole-genome) siRNA library to pinpoint host pathways involved in the activity of HDT (64). With repurposed drugs, some ideas on the mechanisms exist and a more targeted siRNA library or highly specific CRISPR-Cas gene knockouts may be applied to find host pathways, as shown previously (64, 65). However, knockdown or knockout may also have pleiotropic effects, making it difficult to specify compound effects. Finally, affinity-based methods detect the binding of the compound of interest to proteins. However, sometimes the compound acts through indirect mechanisms and this method will fail to identify the true target. Above all, all approaches require the validation of the causality between the observed changes and the phenotype.

While drugs that act through multiple mechanisms complicate the identification of the mechanism of action, such multimodal compounds may remain effective even when certain immune responses are compromised as is often the case in subjects suffering from *Mav* infections. Moreover, pathogens like *Mav* employ diverse survival strategies, and drugs targeting several host mechanisms can counteract these multifaced bacterial defenses, making it more difficult for the pathogen to adapt or evade host immunity. Hence, HDTs that modulate multiple host pathways, which likely apply to phenothiazines, remain valuable.

Clinical applicability of amiodarone and phenothiazine drugs

Despite their promising efficacy, the concentrations of both amiodarone and phenothiazines required for activity make their clinical applications as HDT for *Mav* uncertain due to safety concerns. Amiodarone concentrations used in **chapter 4** for macrophage control of *Mav* can be achieved in patients treated for arrhythmia (1-11 uM, depending on the route of administration) (66, 67), however, plasma levels exceeding 3.9 uM are associated with serious side effects like pulmonary toxicity, thyroid dysfunction, and liver damage, making systemic use as an HDT improbable (68-70). Similarly, the concentration of TFP and CPE used in **chapter 5** exceeds the peak plasma levels achieved with standard oral doses for psychotic disorders (71). In addition, the binding of phenothiazines to dopamine receptors raises concerns about potential off-target effects and the risk of neuropsychiatric side effects. To address these issues, alternative drug delivery strategies such as encapsulation in liposomes or nanoparticles may limit systemic exposure and reduce toxicity risks, while enabling localized drug delivery to infected macrophages. Encapsulation of amikacin in liposomes has previously enhanced its uptake by macrophages and improved its *in vitro* and *in vivo* efficacy (72, 73). Also GM-CSF showed a 100-fold increase in efficacy in enhancing macrophage control of *Mav* when encapsulated in liposomes compared to free GM-CSF (4). Nanoencapsulation of phenothiazine derivative thioridazine reduces drug toxicity while retaining its synergistic efficacy (74). Furthermore, structural modifications to phenothiazines could minimize dopamine receptor binding while enhancing their antimycobacterial activity, as shown with phenothiazine derivatives effective in inhibiting intracellular *Mtb* growth (75). Hence, the HDT activity of amiodarone and phenothiazines demonstrated in this thesis highlights the value of repurposing clinically approved compounds with host-modulating potential for the rapid identification of HDT candidates for *Mav*. While challenges such as toxicity concerns and unclear mechanisms of action necessitate further refinement, repurposing drugs

could be an efficient initial strategy, providing a solid foundation for their optimization to safe and effective HDT to treat *Mav* infections.

Unveiling the host response to *Mav*

Although our HDT studies highlighted the feasibility of targeting autophagy as an intracellular host pathway, our knowledge of the host immunity and pathogenesis of *Mav* infection remains limited, which significantly impairs the development of HDTs. Given the significant gaps in our understanding of host-pathogen interactions in *Mav* infection, the second key aim of this thesis was to investigate the host response to *Mav* infection and identify pathways that could serve as targets for novel HDT.

Transcriptomics of the host macrophage response to a range of mycobacteria like *Mtb* has greatly enriched the understanding of host-pathogen interactions involved in the pathogenesis of these infections (76, 77). Several studies investigated the host response on the transcriptional level during *Mav* infection (78-81), however, most, if not all, of this work relied on older RNA microarray technology, which is targeted and has limited sensitivity. In the last decades, RNA-sequencing (RNA-seq) has emerged as a more powerful tool for transcriptomic analysis of host cells in response to stimuli like pathogens (82). Although studies demonstrated the utility of RNA-seq in elucidating the host response to NTM infections (83-87), they often rely on animal models or cell lines, which may not fully represent the human host-pathogen response and/or do not include human-pathogenic *Mav* strains. To address this, **chapter 6** of this thesis used RNA-seq to examine the primary human macrophage transcriptomic response to *Mav* infection *in vitro*. By analyzing samples at 2 and 6 hours post-infection, we provided insights into early transcriptional changes associated with cellular pathways during *Mav* infection. Given that functional insights into transcriptional changes during *Mtb* infection are more established, we performed a comparative analysis between *Mav* and *Mtb* for interpreting and weighing the results of *Mav* infection responses.

The role of proinflammatory cytokines and cell-mediated immunity in host defense to *Mav*

Proinflammatory cytokines are important for the host response to both mycobacterial infections, by affecting the macrophage antimycobacterial activity (IFN-γ/TNF), granuloma formation and maintenance (TNF/IL-1β), inducing differentiation of T cells (IL-12), increased (IL-6) and decreased (IL-10) responses in T cells and macrophages. Indeed, infection of macrophages with *Mav* or *Mtb* elicited strong upregulation of proinflammatory cytokine expression including *TNF*, *IL1B*, *IL12B*, *IL6*, and also *IL10* (**chapter 6**). Interestingly, the induction of many of these cytokines in the initial hours upon infection was stronger by *Mav* than *Mtb*. IL-12 is important for the induction of a Th1 response which is characterized by IFN-γ-producing CD4+ T cells. The protective immune response most likely resides in the production of IFN-γ as defects in the IL-12 and IFN-γ axis are associated with higher susceptibility to *Mav*, in particular, disseminated, disease (88-90). In our study (**chapter 6**), we observed the upregulation of genes involved in IFN-γ signaling upon infection with *Mav* and *Mtb*. It remains unknown, how IFN-γ exactly protects against *Mav*. While IFN-γ is produced by both CD4+ and CD8+ T cells upon *Mav* infection in mice, depletion studies have shown that CD4+ but not CD8+ T cells were required for protection from *Mav* disease in contrast

to *Mtb* (91-95). The role of CD4+ T cells in host defense against *Mav* is supported by the observation that particularly acquired immunodeficiency syndrome (AIDS) patients with a low count of CD4+ T cells develop disseminated *Mav* disease. Moreover, a study showed that the frequencies of IFN-γ-producing CD4+ T cells do not differ between patients with MAC-lung disease and healthy controls (96). Clinical trials using IFN-γ or GM-CSF as immunotherapy in *Mav* infection showed inconclusive efficacy, with only limited potential in those with IL-12/IFN-γ deficiencies (**Table 1**), suggesting that IFN-γ alone is necessary but not sufficient for host defense against *Mav*. This may be due to the fact that the optimal host response to *Mav* also requires TNF, as anti-TNF therapy also impairs host responses to *Mav in vitro* (97), which has a much more complex role *in vivo*. Hence, despite these cytokines being known to be essential, we do not fully understand how they are involved in the host defense against *Mav*. The limited efficacy of IFN-γ and GM-CSF-based HDT suggests that simply supplementing cytokines may not be sufficient for effective therapy of *Mav* infection. A better understanding of the immunity mediated by different immune cells during *Mav* infection to determine the most critical immune pathways for protection may therefore guide the development of more effective immunomodulatory HDT strategies.

Lipid metabolism in *Mav* infection: balancing host defense and pathogen modulation

Unlike *Mtb*, the intracellular interactions between *Mav* and the host, particularly macrophage immunometabolism, remain poorly understood. Macrophages undergo significant metabolic shifts in response to mycobacterial infection, including in energy metabolism (e.g. shift from oxidative phosphorylation to (aerobic) glycolysis) and lipid metabolism, which shape immune responses (56, 98-100). In *Mtb* infections, macrophage lipid metabolism is rewired toward increased lipid uptake, mobilization, and storage, while lipolytic pathways are suppressed (101, 102). This promotes the formation of foamy macrophages with lipid droplets that are enriched in cholesteryl esters and triacylglycerols (TAGs), a storage form of fatty acids, and serve as a nutrient reservoir for *Mtb* survival. There are various indications that *Mav* affects lipid metabolism (83, 103, 104), although the role of this host pathway in *Mav* pathogenesis remains less well understood. It is therefore intriguing that our RNA-seq analysis revealed that *Mav*, like *Mtb*, regulates genes involved in lipid sensing, accumulation, storage, and catabolism (**chapter 6**).

Mtb exploits host lipids through various virulence factors. The *Mtb* lipase LipY secreted through the ESX-5 efflux pump catabolizes TAGs into fatty acids (102). The *Mtb* protein Rv3723/LucA facilitates the uptake of these lipids in *Mtb* and is required for bacterial virulence *in vivo* (105). Notably, *Mav* possesses the homologs Rv3723 membrane protein (106), suggesting a conserved mechanism of lipid transport. Moreover, *Mtb* ESAT-6 promotes lipid accumulation by activating the antilipolytic receptor GPR109A (*HCAR2*), suppressing TAG catabolism, and preserving lipid droplets (107). While *Mav* lacks ESAT-6, our data indicate that both *Mav* and *Mtb* upregulate *HCAR2* (**chapter 6**), suggesting that *Mav* may induce similar lipid metabolic effects independently of this virulence factor. During *Mtb* infection, impairing lipid accumulation has been associated with reduced intracellular bacterial survival in foamy macrophages (108, 109). Similarly, during *Mav* infection, lipid-loaded macrophages showed impaired intracellular antimicrobial capacity (110), indicating a role of dysregulated lipid

metabolism in increased susceptibility to both *Mav* and *Mtb*. Interestingly, both *Mav* and *Mtb* downregulate *GPR34*, *GPR82*, and *FFAR2,* which all inhibit lipolytic activity (**chapter 6**), and may reflect a host attempt to enhance lipid breakdown to restrict bacterial survival or may also be an approach to yield nutrients or to synthesize (immunomodulatory) lipids.

Despite the pathogen's exploitation of host lipid droplets, they serve as major sites for eicosanoid synthesis, including prostaglandin E2 (PGE2). PGE2 is synthesized from arachidonic acids via *PTGS2* (e.g. COX2) and has been described to have antimycobacterial activity (111-115). Notably, *PTGS2* expression was found to be strongly upregulated by *Mav*, even more pronounced than by *Mtb,* early after infection (**chapter 6**), which suggests PGE2 synthesis during infection is increased. However, the use of COX-2 inhibitors in tuberculosis (TB) show conflicting results regarding the role of PGE2 during infection. Some report that high PGE2 levels impair host control of infection, with COX-2 inhibition reducing mycobacterial burden and improving clinical outcomes (116, 117). Others present that COX-2 inhibitors decrease the host's ability to control mycobacterial infection (114). Although the potential role of drugs targeting the COX2-PGE2 axis has not been identified for *Mav* infection, evidence suggests that macrophages from TB patients treated with COX inhibitors have impaired antimycobacterial activity against *Mav* (118). PGE2 exerts its functions through various receptors and its host-protective effects against *Mtb* in mice are linked to signaling via the receptor PTGER2/EP2 (119). We observed that the expression of *PTGER2* was significantly upregulated in macrophages infected with *Mav* or *Mtb* (**chapter 6**). Thus, these gene expression patterns from *Mav*- and *Mtb*-infected macrophages indicate that both infections similarly engage with this pathway, warranting further investigation into the balance between host defense and pathogen benefit. Beyond COX2/PGE2 signaling, our transcriptomic analysis showed that *Mav*, but not *Mtb*, significantly regulated the expression of phospholipase D (PLD) isoforms, upregulating *PLD1* and downregulating *PLD6* (**chapter 6**). PLD's role in phospholipid hydrolysis associated with *Mtb* killing (120, 121), suggesting another lipid remodeling strategy during *Mav* infection. Taken together, our data reinforce the idea that lipid metabolism plays an important but complex role in *Mav* infection, with many parallels to *Mtb*. Given this complexity of lipid metabolism and concomitant signaling, a deeper understanding is pivotal and could ultimately inform new therapeutic strategies targeting this host pathway to enhance host defense against *Mav*.

Novel GIMAP genes identified in mycobacterial infection

In addition to identifying pathways with established roles in macrophage antimicrobial responses, our RNA-seq analysis served as a tool for uncovering genes whose role in mycobacterial infection remains unknown but may be highly relevant. Notably, we identified several GTPases of immunity-associated proteins (GIMAP) genes that were significantly affected by infection, particularly by *Mav* (**chapter 6**). Specifically, *GIMAP1*, *GIMAP4*, *GIMAP6*, and *GIMAP7* were significantly downregulated in macrophages within 6 hours of infection with either *Mav* or *Mtb*. These genes were, in addition to *GIMAP2* and *GIMAP5*, overall stronger suppressed by *Mav* than *Mtb* (**chapter 6**). GIMAPs are broadly expressed in immune cells, with specific members involved in lymphocyte development and survival (122), and are associated with inflammatory disorders (123, 124). Moreover, GIMAPs are also thought to be important in intracellular

trafficking, autophagy, and the formation of lipid droplets (125-129), processes that are critical for immune defense against mycobacteria, as also discussed in this thesis. The involvement of GIMAP proteins in key immune processes raises questions about their role in host-pathogen interactions during mycobacterial infection. The downregulation of multiple GIMAP genes in *Mav*-infected macrophages may be either beneficial for the host or an immune evasion strategy employed by the bacteria (**chapter 6**). It remains therefore important to determine whether modulating the activity or expression of specific GIMAPs directly affects the host's ability to eradicate intracellular mycobacterial infections. Future research should focus on revealing the functions of GIMAPs in macrophage antimycobacterial responses, which may ultimately reveal them as promising targets for HDT.

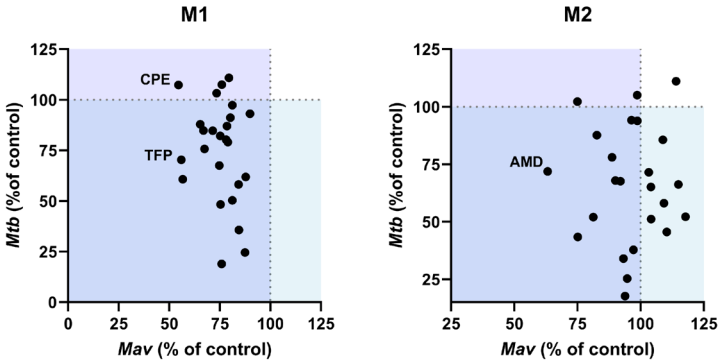

Figure 2. Efficacy of HDT against intracellular *Mav* vs. *Mtb in* primary human M1 and M2 macrophages.

Comparing host responses to *Mav* and *Mtb* infections: insights

Our RNA-seq results revealed, besides a few differences, a significant overlap in the early macrophage gene response to *Mav* and *Mtb*. While both mycobacteria can cause disease in healthy individuals, *Mav* primarily impacts individuals with immune deficiencies. This distinction in disease pathogenesis reflects differences in host-pathogen interactions. In addition to the clinical presentation, we also observed differences in the efficacy of various HDT candidates: while these treatments modulate host pathways, their efficacy in improving host control varied between *Mav* and *Mtb* infected macrophages (**Figure 2**), suggesting differential roles or manipulation of host pathways. This may suggest that the similarity observed in the host transcriptional response to *Mav* and *Mtb* (**chapter 6**) may be the result of the limited timeframe of 6 hours post-infection, with the divergence in host-pathogen interactions between *Mav* and *Mtb* occurring beyond this timepoint. However, a comparative study by McGarvey et al. also found that, eventhough only a small number of genes was evaluated by the microarray technique upon *Mav* and *Mtb* infection, there was a similarity up to 24 hours post-infection of U937 cells (81). Interestingly, a proteomics study of U937 cells showed a rather limited overlap of 35.7% (205/574) and 23.1% (682/887) of the proteins differentially expressed 24 hours after infection by *Mav* and *Mtb*, respectively (104). Furthermore, while our transcriptomic analysis provided insights into the host responses to *Mav* and *Mtb*, the findings from this study require biological validation.

Hence, further functional confirmation and multi-omics studies are therefore essential for a deeper understanding of the host-pathogen interactions and their consequences for the host control of *Mav*. Moreover, including avirulent *Mav* or *Mtb* strains may help us to understand modulation induced by bacteria which may also give us insights into new HDT strategies.

Future directions in *Mav* (HDT) research

Advancing preclinical infection models

Mav is an intracellular pathogen that evades host defenses to survive and persist within macrophages. Hence, *in vitro* human macrophage-based infection models are valuable for early drug discovery, in particular HDT, and for studying host-pathogen interactions. Commonly used cell systems in *Mav* research include human monocytic cancer cell lines THP-1 and U937 (130-132). U937 cells, however, have reduced phagocytosis activity compared to human monocyte-derived macrophages, and both THP-1 and U937 require stimulation for differentiation into mature macrophages, which may affect their cell surface markers and host response (133, 134). In addition, the human A549 alveolar epithelial cell line has been used to a limited extent (135-137), while murine macrophage cell lines RAW264.7 and J774 have been used next to *in vivo* murine studies (138-141). With regard to primary cells, human peripheral blood mononuclear cells (PBMCs) or (130, 142, 143), in studies involving mice, murine bone marrow-derived macrophages are used (144). Despite the availability of these existing cell systems, the lack of standardized and representative *in vitro* models of *Mav* infection hampers drug development. To address this, we developed primary human macrophage M1 and M2 models (**chapter 3**). Although these models are more complex to culture and limited in cell number, they offer more physiologically relevant *in vitro* systems, including macrophage spectral polarity, compared to human cell lines for *Mav* studies. These primary human macrophage models have proven valuable in studying HDT efficacy (**chapter 4 and 5**) and specific human pathways (**chapter 4**, **5 and 6**). Additionally, we developed a *Mav* infection model using the human MelJuSo cell line, which, while allowing larger drug screenings without cell number limitations and not requiring differentiation, has a lower phagocytosis capacity compared to primary human macrophages (**chapter 3**). While our primary human macrophage models are biologically relevant, the use of cells from healthy donors limits the application of results to immunocompromised conditions which is an important susceptibility factor for *Mav* disease. Developing models for *Mav* mimicking immunocompromised conditions, such as human immunodeficiency virus (HIV) co-infection (145, 146), IL-12/IFN-γ-deficient cell systems (e.g. CRISPR/Cas9-mediated knockout) (147), but also other immune defects, is therefore essential. Additionally, our model does not mimic interactions between different cell types and tissues during *Mav* infection. More advanced models like lung organoids (148-150), or gastrointestinal organoids (151) could better resemble the infection environment, but 3D cultures have yet to be developed for *Mav*. While this thesis focused on the identification of HDT candidates, our primary macrophage model has also been useful in evaluating intracellular antibiotic efficacy (**chapter 3**). Traditional drug susceptibility testing is performed in liquid broth, which lacks the role of the host immune system in affecting the bacteria, potentially explaining the poor translation of *in vitro* results to *in vivo* outcomes for many drugs used to treat *Mav* (152). This may be reflected in **chapter 3**, where the first-line *Mav* drug rifampicin effectively

impaired bacterial growth in broth, while showing limited efficacy against intracellular *Mav*. In summary, our primary human macrophage model represents a significant step forward in the development of *in vitro* infection models for *Mav* research.
The lack of standardized and reliable *in vivo* models is another hurdle in *Mav* research. Various mouse models have been used, including immunocompromised strains (beige and nude) (153-155), and immunocompetent (C57Bl/6 or Balb/c) (156). These models can develop granulomas and chronic infection as seen in human *Mav* disease (157) A head-to-head comparison of the different mouse models using one *Mav* strain showed that nude mice are highly susceptible to infection, while Balb/c mice were the most suitable to evaluate drug efficacy (158). However, a study found no correlation between the treatment outcomes in mice infected with patient-derived *Mav* strains and the treatment outcomes in those patients, which partly may be due to differences in drug dosing and determination of bacterial burdens across different tissue compartments (159), but is likely also due to the significant differences in immune responses between mice and humans (160). This discrepancy in host immune responses especially complicates studies on HDT targeting human-specific pathways. An alternative model may be zebrafish larvae, which have an innate immune system highly similar to humans (161). In **chapter 4**, we demonstrated that *in vitro* HDT activity of amiodarone could be translated to *in vivo* in *Mmar*-infected zebrafish. Furthermore, zebrafish' transparency with the use of fluorescently-labeled bacterial strains facilitates the investigation of host-pathogen interactions at a cellular level. More recently, the zebrafish model has also been developed for *Mav* infection (83), but the lack of adaptive immunity during the zebrafish larval stage may be a limitation in investigating innate and adaptive immune interactions (162). Taken together, current *in vivo* models fail to entirely recapitulate host immunity during *Mav* infection, highlighting the need for optimization of preclinical models.

Evaluation of combinatorial HDT regimens
While HDT has the potential to serve as a stand-alone treatment, particularly for patients unresponsive to standard-of-care, HDT is mainly envisioned as an adjunctive therapy to conventional antibiotics. Considering that antibiotics target bacteria and HDT target the host, they may complement each other and adjunction of HDT may shorten antibiotic treatment length or reduce the dosage of antibiotic regimens, minimizing side effects and probability of antibiotic resistance.

Evidence evaluating the efficacy of HDT, similar to treatment alone, combined with antibiotics during *Mav* infection is limited. Most available data involve combinations of HDT with cytokines and antibiotics. For instance, GM-CSF has been shown to enhance the efficacy of clarithromycin at clinically achievable concentrations, potentially due to increased intracellular uptake of clarithromycin following GM-CSF pre-treatment (4). Furthermore, it is also suggested that the impaired bacterial growth induced by cytokines, including GM-CSF, may be the result of phagosome acidification (163). Since macrolides, such as clarithromycin, accumulate in acidic vesicles, GM-CSF may enhance antibiotic activity by accumulating the drug at the site of bacteria by increasing phagosome acidification. Similarly, HDT that counteracts *Mav*-induced phagosome maturation arrest and promotes phagosome-lysosome fusion may not only enhance lysosomal degradation but also increase bacterial exposure to antibiotics localized in acidic lysosomes. However, at higher clarithromycin doses achieving serum peak

levels seen in patients, no additive effect with GM-CSF was observed (4). One possible reason is that both drugs are transported into cells via a similar uptake mechanism, and high clarithromycin concentration may saturate this process (164, 165), resulting in no enhanced antibiotic activity by GM-CSF. Alternatively, activating macrophages with cytokines like GM-CSF might render intracellular bacteria more susceptible to antibiotics, but in high clarithromycin concentrations, the bacteria are already killed, and GM-CSF has no additional effect.

Another approach in HDT as adjunctive therapy is the use of host efflux pump modulators. These pumps efflux ions and possibly antibiotics from vesicles like phagosomes and lysosomes, reducing antibiotic potency. Inhibiting these host cell pumps with HDT may therefore potentiate antibiotic efficacy. Verapamil, for example, has been shown to enhance the activity of antibiotics like rifampicin and bedaquiline against mycobacteria (166, 167), likely by inhibiting mycobacterial efflux pumps reducing drug tolerance (168, 169). This effect is linked to verapamil's ability to inhibit human p-glycoprotein (170), which may also reduce the efflux of antibiotics from vesicles where bacteria reside (171). However, verapamil may not potentiate antibiotics that have the same mechanism of action. Hence, considering the mechanism of action of both the HDT and antibiotic may inform the potential of combinations. In addition, drug metabolism should be considered in combinatorial regimens. For example, combining verapamil with clarithromycin has been observed to be fatal since clarithromycin impairs the metabolism of verapamil, leading to toxic levels (172). In summary, studying potential interactions between HDT and conventional antibiotics is critical in designing more effective and safe combinatory regimens for *Mav*.

Finally, there has been limited exploration of combining multiple HDTs. As discussed, mycobacteria like *Mav* are notorious for modulating host immune pathways via different mechanisms and a multi-targeted HDT approach could more effectively counteract these bacterial-induced modulations, resulting in improved host control of infection. For example, combining cytokines (173), or other immunomodulatory compounds have shown to have additive effects on the antimycobacterial activity of macrophages (174), including against *Mav* (175). However, combinations like vitamin D and PBA failed to show additive effects, potentially because both compounds target the same pathways, underscoring the importance of understanding the mechanism of action of HDT. Hence, further research is warranted to explore synergistic HDT combinations.

Concluding remarks

This thesis highlights the potential of HDT as a promising strategy for combating intracellular *Mav* infections, using primary human macrophage-based infection models. Repurposed amiodarone and phenothiazines were shown to improve host control of *Mav* infection through immunomodulatory effects, and optimizing their safety and efficacy could improve their clinical applicability. Further investigation of their mechanisms of action may also reveal novel strategies to eliminate intracellular *Mav* infection. In our search for new host targets for HDT, we identified the macrophage response to *Mav* infection included cytokine immune responses, although the limited cytokine-based HDT emphasizes the need for a deeper understanding of protective immune pathways during *Mav* infection. Additionally, the regulation of lipid metabolism genes upon *Mav* infection, similar to *Mtb*, reinforces its potential as a therapeutic

target, while the identification of GIMAP gene modulation suggests additional host factors that may influence infection outcomes. The next challenge lies in deciphering the precise role of these responses in *Mav* infection and their potential as host targets for the development of HDT for *Mav*. Advancing preclinical models, particularly those mimicking immunocompromised conditions or incorporating multi-cell interactions, will be crucial for improving translational relevance. Moreover, combining HDT with antibiotics or other immunomodulators may enhance treatment efficacy, but understanding synergistic mechanisms and drug interactions is essential. Ultimately, these insights and refinements will pave the way for developing more effective HDT strategies against *Mav* infections to improve patient outcomes.

References

1. Hariadi NI, Blackwood RA. Disseminated Mycobacterium Avium Complex in an Adolescent with Perinatally-Acquired HIV Infection. Infect Dis Rep. 2017;9(2):6884.
2. Kedzierska K, Mak J, Mijch A, Cooke I, Rainbird M, Roberts S, et al. Granulocyte-macrophage colony-stimulating factor augments phagocytosis of Mycobacterium avium complex by human immunodeficiency virus type 1-infected monocytes/macrophages in vitro and in vivo. J Infect Dis. 2000;181(1):390-4.
3. Bermudez LE, Young LS. Recombinant granulocyte-macrophage colony-stimulating factor activates human macrophages to inhibit growth or kill Mycobacterium avium complex. J Leukoc Biol. 1990;48(1):67-73.
4. Onyeji CO, Nightingale CH, Tessier PR, Nicolau DP, Bow LM. Activities of clarithromycin, azithromycin, and ofloxacin in combination with liposomal or unencapsulated granulocyte-macrophage colony-stimulating factor against intramacrophage Mycobacterium avium-Mycobacterium intracellulare. J Infect Dis. 1995;172(3):810-6.
5. Kemper CA, Bermudez LE, Deresinski SC. Immunomodulatory treatment of Mycobacterium avium complex bacteremia in patients with AIDS by use of recombinant granulocyte-macrophage colony-stimulating factor. J Infect Dis. 1998;177(4):914-20.
6. Nannini EC, Keating M, Binstock P, Samonis G, Kontoyiannis DP. Successful treatment of refractory disseminated Mycobacterium avium complex infection with the addition of linezolid and mefloquine. J Infect. 2002;44(3):201-3.
7. de Silva TI, Cope A, Goepel J, Greig JM. The use of adjuvant granulocyte-macrophage colony-stimulating factor in HIV-related disseminated atypical mycobacterial infection. J Infect. 2007;54(4):e207-10.
8. Squires KE, Murphy WF, Madoff LC, Murray HW. Interferon-gamma and Mycobacterium avium-intracellulare infection. J Infect Dis. 1989;159(3):599-600.
9. Holland SM, Eisenstein EM, Kuhns DB, Turner ML, Fleisher TA, Strober W, et al. Treatment of refractory disseminated nontuberculous mycobacterial infection with interferon gamma. A preliminary report. N Engl J Med. 1994;330(19):1348-55.
10. Milanes-Virelles MT, Garcia-Garcia I, Santos-Herrera Y, Valdes-Quintana M, Valenzuela-Silva CM, Jimenez-Madrigal G, et al. Adjuvant interferon gamma in patients with pulmonary atypical Mycobacteriosis: a randomized, double-blind, placebo-controlled study. BMC Infect Dis. 2008;8:17.
11. Lam PK, Griffith DE, Aksamit TR, Ruoss SJ, Garay SM, Daley CL, et al. Factors related to response to intermittent treatment of Mycobacterium avium complex lung disease. Am J Respir Crit Care Med. 2006;173(11):1283-9.
12. Lauw FN, van Der Meer JT, de Metz J, Danner SA, van Der Poll T. No beneficial effect of interferon-gamma treatment in 2 human immunodeficiency virus-infected patients with Mycobacterium avium complex infection. Clin Infect Dis. 2001;32(4):e81-2.
13. Appelberg R, Orme IM. Effector mechanisms involved in cytokine-mediated bacteriostasis of Mycobacterium avium infections in murine macrophages. Immunology. 1993;80(3):352-9.
14. Bermudez LE, Stevens P, Kolonoski P, Wu M, Young LS. Treatment of experimental disseminated Mycobacterium avium complex infection in mice with recombinant IL-2 and tumor necrosis factor. J Immunol. 1989;143(9):2996-3000.
15. Sekiguchi Y, Yasui K, Yamazaki T, Agematsu K, Kobayashi N, Koike K. Effective combination therapy using interferon-gamma and interleukin-2 for disseminated Mycobacterium avium complex infection in a pediatric patient with AIDS. Clin Infect Dis. 2005;41(11):e104-6.
16. Trojan T, Collins R, Khan DA. Safety and efficacy of treatment using interleukin-2 in a patient with idiopathic CD4(+) lymphopenia and Mycobacterium avium-intracellulare. Clin Exp Immunol.

2009;156(3):440-5.
17. Tatano Y, Yamabe S, Sano C, Tomioka H. Anti-Mycobacterium avium complex activity of clarithromycin, rifampin, rifabutin, and ethambutol in combination with adenosine 5'-triphosphate. Diagn Microbiol Infect Dis. 2017;88(3):241-6.
18. Silva T, Moreira AC, Nazmi K, Moniz T, Vale N, Rangel M, et al. Lactoferricin Peptides Increase Macrophages' Capacity To Kill Mycobacterium avium. mSphere. 2017;2(4).
19. Mediaas SD, Haug M, Louet C, Wahl SGF, Gidon A, Flo TH. Metformin improves Mycobacterium avium infection by strengthening macrophage antimicrobial functions. Front Immunol. 2024;15:1463224.
20. Srivastava S, Deshpande D, Sherman CM, Gumbo T. A 'shock and awe' thioridazine and moxifloxacin combination-based regimen for pulmonary Mycobacterium avium-intracellulare complex disease. J Antimicrob Chemother. 2017;72(suppl_2):i43-i7.
21. Ruth MM, Pennings LJ, Koeken V, Schildkraut JA, Hashemi A, Wertheim HFL, et al. Thioridazine Is an Efflux Pump Inhibitor in Mycobacterium avium Complex but of Limited Clinical Relevance. Antimicrob Agents Chemother. 2020;64(7).
22. Deshpande D, Srivastava S, Musuka S, Gumbo T. Thioridazine as Chemotherapy for Mycobacterium avium Complex Diseases. Antimicrob Agents Chemother. 2016;60(8):4652-8.
23. Jagannath C, Emanuele MR, Hunter RL. Activities of poloxamer CRL-1072 against Mycobacterium avium in macrophage culture and in mice. Antimicrob Agents Chemother. 1999;43(12):2898-903.
24. Jagannath C, Sepulveda E, Actor JK, Luxem F, Emanuele MR, Hunter RL. Effect of poloxamer CRL-1072 on drug uptake and nitric-oxide-mediated killing of Mycobacterium avium by macrophages. Immunopharmacology. 2000;48(2):185-97.
25. Pais TF, Appelberg R. Macrophage control of mycobacterial growth induced by picolinic acid is dependent on host cell apoptosis. J Immunol. 2000;164(1):389-97.
26. Pais TF, Appelberg R. Induction of Mycobacterium avium growth restriction and inhibition of phagosome-endosome interactions during macrophage activation and apoptosis induction by picolinic acid plus IFNgamma. Microbiology (Reading). 2004;150(Pt 5):1507-18.
27. Cai S, Sato K, Shimizu T, Yamabe S, Hiraki M, Sano C, et al. Antimicrobial activity of picolinic acid against extracellular and intracellular Mycobacterium avium complex and its combined activity with clarithromycin, rifampicin and fluoroquinolones. J Antimicrob Chemother. 2006;57(1):85-93.
28. Kilinc G, Boland R, Heemskerk MT, Spaink HP, Haks MC, van der Vaart M, et al. Host-directed therapy with amiodarone in preclinical models restricts mycobacterial infection and enhances autophagy. Microbiol Spectr. 2024;12(8):e0016724.
29. Kilinc G, Ottenhoff THM, Saris A. Phenothiazines boost host control of Mycobacterium avium infection in primary human macrophages. Biomed Pharmacother. 2025;185:117941.
30. Balgi AD, Fonseca BD, Donohue E, Tsang TC, Lajoie P, Proud CG, et al. Screen for chemical modulators of autophagy reveals novel therapeutic inhibitors of mTORC1 signaling. PLoS One. 2009;4(9):e7124.
31. Buratta S, Urbanelli L, Ferrara G, Sagini K, Goracci L, Emiliani C. A role for the autophagy regulator Transcription Factor EB in amiodarone-induced phospholipidosis. Biochem Pharmacol. 2015;95(3):201-9.
32. Jacquin E, Leclerc-Mercier S, Judon C, Blanchard E, Fraitag S, Florey O. Pharmacological modulators of autophagy activate a parallel noncanonical pathway driving unconventional LC3 lipidation. Autophagy. 2017;13(5):854-67.
33. Mahavadi P, Knudsen L, Venkatesan S, Henneke I, Hegermann J, Wrede C, et al. Regulation of macroautophagy in amiodarone-induced pulmonary fibrosis. J Pathol Clin Res. 2015;1(4):252-63.
34. Zhang L, Yu J, Pan H, Hu P, Hao Y, Cai W, et al. Small molecule regulators of autophagy identified by an image-based high-throughput screen. Proc Natl Acad Sci U S A. 2007;104(48):19023-8.
35. Stadler K, Ha HR, Ciminale V, Spirli C, Saletti G, Schiavon M, et al. Amiodarone alters late endosomes and inhibits SARS coronavirus infection at a post-endosomal level. Am J Respir Cell Mol Biol. 2008;39(2):142-9.
36. Houben D, Demangel C, van Ingen J, Perez J, Baldeon L, Abdallah AM, et al. ESX-1-mediated translocation to the cytosol controls virulence of mycobacteria. Cell Microbiol. 2012;14(8):1287-98.
37. Sharma V, Verma S, Seranova E, Sarkar S, Kumar D. Selective Autophagy and Xenophagy in Infection and Disease. Front Cell Dev Biol. 2018;6:147.
38. van der Wel N, Hava D, Houben D, Fluitsma D, van Zon M, Pierson J, et al. M. tuberculosis and M. leprae translocate from the phagolysosome to the cytosol in myeloid cells. Cell. 2007;129(7):1287-98.
39. Danelishvili L, Bermudez LE. Mycobacterium avium MAV_2941 mimics phosphoinositol-3-kinase to interfere with macrophage phagosome maturation. Microbes Infect. 2015;17(9):628-37.
40. Danelishvili L, Chinison JJJ, Pham T, Gupta R, Bermudez LE. The Voltage-Dependent Anion Channels (VDAC) of Mycobacterium avium phagosome are associated with bacterial survival and lipid export

in macrophages. Sci Rep. 2017;7(1):7007.
41. Sturgill-Koszycki S, Schlesinger PH, Chakraborty P, Haddix PL, Collins HL, Fok AK, et al. Lack of acidification in Mycobacterium phagosomes produced by exclusion of the vesicular proton-ATPase. Science. 1994;263(5147):678-81.
42. Settembre C, Medina DL. TFEB and the CLEAR network. Methods Cell Biol. 2015;126:45-62.
43. Song TT, Cai RS, Hu R, Xu YS, Qi BN, Xiong YA. The important role of TFEB in autophagy-lysosomal pathway and autophagy-related diseases: a systematic review. Eur Rev Med Pharmacol Sci. 2021;25(3):1641-9.
44. Ammanathan V, Mishra P, Chavalmane AK, Muthusamy S, Jadhav V, Siddamadappa C, et al. Restriction of intracellular Salmonella replication by restoring TFEB-mediated xenophagy. Autophagy. 2020;16(9):1584-97.
45. Jeong SJ, Stitham J, Evans TD, Zhang X, Rodriguez-Velez A, Yeh YS, et al. Trehalose causes low-grade lysosomal stress to activate TFEB and the autophagy-lysosome biogenesis response. Autophagy. 2021;17(11):3740-52.
46. Rusmini P, Cortese K, Crippa V, Cristofani R, Cicardi ME, Ferrari V, et al. Trehalose induces autophagy via lysosomal-mediated TFEB activation in models of motoneuron degeneration. Autophagy. 2019;15(4):631-51.
47. Bryk R, Mundhra S, Jiang X, Wood M, Pfau D, Weber E, et al. Potentiation of rifampin activity in a mouse model of tuberculosis by activation of host transcription factor EB. PLoS Pathog. 2020;16(6):e1008567.
48. Giraud-Gatineau A, Coya JM, Maure A, Biton A, Thomson M, Bernard EM, et al. The antibiotic bedaquiline activates host macrophage innate immune resistance to bacterial infection. Elife. 2020;9.
49. Zhang X, Cheng X, Yu L, Yang J, Calvo R, Patnaik S, et al. MCOLN1 is a ROS sensor in lysosomes that regulates autophagy. Nat Commun. 2016;7:12109.
50. Roczniak-Ferguson A, Petit CS, Froehlich F, Qian S, Ky J, Angarola B, et al. The transcription factor TFEB links mTORC1 signaling to transcriptional control of lysosome homeostasis. Sci Signal. 2012;5(228):ra42.
51. Fleming A, Noda T, Yoshimori T, Rubinsztein DC. Chemical modulators of autophagy as biological probes and potential therapeutics. Nat Chem Biol. 2011;7(1):9-17.
52. Gutierrez MG, Master SS, Singh SB, Taylor GA, Colombo MI, Deretic V. Autophagy is a defense mechanism inhibiting BCG and Mycobacterium tuberculosis survival in infected macrophages. Cell. 2004;119(6):753-66.
53. Canton M, Sanchez-Rodriguez R, Spera I, Venegas FC, Favia M, Viola A, et al. Reactive Oxygen Species in Macrophages: Sources and Targets. Front Immunol. 2021;12:734229.
54. Herb M, Schramm M. Functions of ROS in Macrophages and Antimicrobial Immunity. Antioxidants (Basel). 2021;10(2).
55. West AP, Brodsky IE, Rahner C, Woo DK, Erdjument-Bromage H, Tempst P, et al. TLR signalling augments macrophage bactericidal activity through mitochondrial ROS. Nature. 2011;472(7344):476-80.
56. Rost LM, Louet C, Bruheim P, Flo TH, Gidon A. Pyruvate Supports RET-Dependent Mitochondrial ROS Production to Control Mycobacterium avium Infection in Human Primary Macrophages. Front Immunol. 2022;13:891475.
57. Sherman DR, Sabo PJ, Hickey MJ, Arain TM, Mahairas GG, Yuan Y, et al. Disparate responses to oxidative stress in saprophytic and pathogenic mycobacteria. Proc Natl Acad Sci U S A. 1995;92(14):6625-9.
58. Abukhalid N, Islam S, Ndzeidze R, Bermudez LE. Mycobacterium avium Subsp. hominissuis Interactions with Macrophage Killing Mechanisms. Pathogens. 2021;10(11).
59. Braunstein M, Espinosa BJ, Chan J, Belisle JT, Jacobs WR, Jr. SecA2 functions in the secretion of superoxide dismutase A and in the virulence of Mycobacterium tuberculosis. Mol Microbiol. 2003;48(2):453-64.
60. McNamara M, Tzeng SC, Maier C, Zhang L, Bermudez LE. Surface proteome of "Mycobacterium avium subsp. hominissuis" during the early stages of macrophage infection. Infect Immun. 2012;80(5):1868-80.
61. Rosen GM, Freeman BA. Detection of superoxide generated by endothelial cells. Proc Natl Acad Sci U S A. 1984;81(23):7269-73.
62. Ng VH, Cox JS, Sousa AO, MacMicking JD, McKinney JD. Role of KatG catalase-peroxidase in mycobacterial pathogenesis: countering the phagocyte oxidative burst. Mol Microbiol. 2004;52(5):1291-302.
63. Schenone M, Dancik V, Wagner BK, Clemons PA. Target identification and mechanism of action in chemical biology and drug discovery. Nat Chem Biol. 2013;9(4):232-40.
64. Korbee CJ, Heemskerk MT, Kocev D, van Strijen E, Rabiee O, Franken K, et al. Combined chemical genetics and data-driven bioinformatics approach identifies receptor tyrosine kinase inhibitors as host-directed antimicrobials. Nat Commun. 2018;9(1):358.

65. Goncalves E, Segura-Cabrera A, Pacini C, Picco G, Behan FM, Jaaks P, et al. Drug mechanism-of-action discovery through the integration of pharmacological and CRISPR screens. Mol Syst Biol. 2020;16(7):e9405.
66. Breitenstein A, Stampfli SF, Camici GG, Akhmedov A, Ha HR, Follath F, et al. Amiodarone inhibits arterial thrombus formation and tissue factor translation. Arterioscler Thromb Vasc Biol. 2008;28(12):2231-8.
67. Pollak PT, Bouillon T, Shafer SL. Population pharmacokinetics of long-term oral amiodarone therapy. Clin Pharmacol Ther. 2000;67(6):642-52.
68. Papiris SA, Triantafillidou C, Kolilekas L, Markoulaki D, Manali ED. Amiodarone: review of pulmonary effects and toxicity. Drug Saf. 2010;33(7):539-58.
69. Park HS, Kim YN. Adverse effects of long-term amiodarone therapy. Korean J Intern Med. 2014;29(5):571-3.
70. Rotmensch HH, Belhassen B, Swanson BN, Shoshani D, Spielman SR, Greenspon AJ, et al. Steady-state serum amiodarone concentrations: relationships with antiarrhythmic efficacy and toxicity. Ann Intern Med. 1984;101(4):462-9.
71. Midha KK, Korchinski ED, Verbeeck RK, Roscoe RM, Hawes EM, Cooper JK, et al. Kinetics of oral trifluoperazine disposition in man. Br J Clin Pharmacol. 1983;15(3):380-2.
72. Zhang J, Leifer F, Rose S, Chun DY, Thaisz J, Herr T, et al. Amikacin Liposome Inhalation Suspension (ALIS) Penetrates Non-tuberculous Mycobacterial Biofilms and Enhances Amikacin Uptake Into Macrophages. Front Microbiol. 2018;9:915.
73. Winthrop KL, Flume PA, Thomson R, Mange KC, Yuen DW, Ciesielska M, et al. Amikacin Liposome Inhalation Suspension for Mycobacterium avium Complex Lung Disease: A 12-Month Open-Label Extension Clinical Trial. Ann Am Thorac Soc. 2021;18(7):1147-57.
74. Vibe CB, Fenaroli F, Pires D, Wilson SR, Bogoeva V, Kalluru R, et al. Thioridazine in PLGA nanoparticles reduces toxicity and improves rifampicin therapy against mycobacterial infection in zebrafish. Nanotoxicology. 2016;10(6):680-8.
75. Salie S, Hsu N-J, Semenya D, Jardine A, Jacobs M. Novel non-neuroleptic phenothiazines inhibit Mycobacterium tuberculosis replication. J Antimicrob Chemoth. 2014;69(6):1551-8.
76. Lee J, Lee SG, Kim KK, Lim YJ, Choi JA, Cho SN, et al. Characterisation of genes differentially expressed in macrophages by virulent and attenuated Mycobacterium tuberculosis through RNA-Seq analysis. Sci Rep. 2019;9(1):4027.
77. Nalpas NC, Park SD, Magee DA, Taraktsoglou M, Browne JA, Conlon KM, et al. Whole-transcriptome, high-throughput RNA sequence analysis of the bovine macrophage response to Mycobacterium bovis infection in vitro. BMC Genomics. 2013;14:230.
78. Agdestein A, Jones A, Flatberg A, Johansen TB, Heffernan IA, Djonne B, et al. Intracellular growth of Mycobacterium avium subspecies and global transcriptional responses in human macrophages after infection. BMC Genomics. 2014;15:58.
79. Blumenthal A, Lauber J, Hoffmann R, Ernst M, Keller C, Buer J, et al. Common and unique gene expression signatures of human macrophages in response to four strains of Mycobacterium avium that differ in their growth and persistence characteristics. Infect Immun. 2005;73(6):3330-41.
80. Greenwell-Wild T, Vazquez N, Sim D, Schito M, Chatterjee D, Orenstein JM, et al. Mycobacterium avium infection and modulation of human macrophage gene expression. J Immunol. 2002;169(11):6286-97.
81. McGarvey JA, Wagner D, Bermudez LE. Differential gene expression in mononuclear phagocytes infected with pathogenic and non-pathogenic mycobacteria. Clin Exp Immunol. 2004;136(3):490-500.
82. Mortazavi A, Williams BA, McCue K, Schaeffer L, Wold B. Mapping and quantifying mammalian transcriptomes by RNA-Seq. Nat Methods. 2008;5(7):621-8.
83. Hu W, Koch BEV, Lamers GEM, Forn-Cuni G, Spaink HP. Specificity of the innate immune responses to different classes of non-tuberculous mycobacteria. Front Immunol. 2022;13:1075473.
84. Casey ME, Meade KG, Nalpas NC, Taraktsoglou M, Browne JA, Killick KE, et al. Analysis of the Bovine Monocyte-Derived Macrophage Response to Mycobacterium avium Subspecies Paratuberculosis Infection Using RNA-seq. Front Immunol. 2015;6:23.
85. Nandanwar N, Gibson JE, Neely MN. Transcriptome profiles of macrophages upon infection by morphotypic smooth and rough variants of Mycobacterium abscessus. Microbes Infect. 2024;26(5-6):105367.
86. Park HT, Lee SM, Ko S, Kim S, Park HE, Shin MK, et al. Delineating transcriptional crosstalk between Mycobacterium avium subsp. paratuberculosis and human THP-1 cells at the early stage of infection via dual RNA-seq analysis. Vet Res. 2022;53(1):71.
87. Nakajima M, Matsuyama M, Kawaguchi M, Kiwamoto T, Matsuno Y, Morishima Y, et al. Nrf2 Regulates Granuloma Formation and Macrophage Activation during Mycobacterium avium Infection via Mediating Nramp1 and HO-1 Expressions. mBio. 2021;12(1).

88. de Jong R, Altare F, Haagen IA, Elferink DG, Boer T, van Breda Vriesman PJ, et al. Severe mycobacterial and Salmonella infections in interleukin-12 receptor-deficient patients. Science. 1998;280(5368):1435-8.
89. Dorman SE, Holland SM. Interferon-gamma and interleukin-12 pathway defects and human disease. Cytokine Growth Factor Rev. 2000;11(4):321-33.
90. Field SK, Fisher D, Cowie RL. Mycobacterium avium complex pulmonary disease in patients without HIV infection. Chest. 2004;126(2):566-81.
91. Saunders BM, Cheers C. Inflammatory response following intranasal infection with Mycobacterium avium complex: role of T-cell subsets and gamma interferon. Infect Immun. 1995;63(6):2282-7.
92. Sangari FJ, Goodman J, Petrofsky M, Kolonoski P, Bermudez LE. Mycobacterium avium invades the intestinal mucosa primarily by interacting with enterocytes. Infect Immun. 2001;69(3):1515-20.
93. Gilbertson B, Zhong J, Cheers C. Anergy, IFN-gamma production, and apoptosis in terminal infection of mice with Mycobacterium avium. J Immunol. 1999;163(4):2073-80.
94. Petrofsky M, Bermudez LE. CD4+ T cells but Not CD8+ or gammadelta+ lymphocytes are required for host protection against Mycobacterium avium infection and dissemination through the intestinal route. Infect Immun. 2005;73(5):2621-7.
95. Flynn JL, Goldstein MM, Triebold KJ, Koller B, Bloom BR. Major histocompatibility complex class I-restricted T cells are required for resistance to Mycobacterium tuberculosis infection. Proc Natl Acad Sci U S A. 1992;89(24):12013-7.
96. Han SA, Ko Y, Shin SJ, Jhun BW. Characteristics of Circulating CD4(+) T Cell Subsets in Patients with Mycobacterium avium Complex Pulmonary Disease. J Clin Med. 2020;9(5).
97. Appelberg R, Castro AG, Pedrosa J, Silva RA, Orme IM, Minoprio P. Role of gamma interferon and tumor necrosis factor alpha during T-cell-independent and -dependent phases of Mycobacterium avium infection. Infect Immun. 1994;62(9):3962-71.
98. Kim H, Shin SJ. Revolutionizing control strategies against Mycobacterium tuberculosis infection through selected targeting of lipid metabolism. Cell Mol Life Sci. 2023;80(10):291.
99. Llibre A, Dedicoat M, Burel JG, Demangel C, O'Shea MK, Mauro C. Host Immune-Metabolic Adaptations Upon Mycobacterial Infections and Associated Co-Morbidities. Front Immunol. 2021;12:747387.
100. Howard NC, Khader SA. Immunometabolism during Mycobacterium tuberculosis Infection. Trends Microbiol. 2020;28(10):832-50.
101. Gago G, Diacovich L, Gramajo H. Lipid metabolism and its implication in mycobacteria-host interaction. Curr Opin Microbiol. 2018;41:36-42.
102. van der Klugt T, van den Biggelaar R, Saris A. Host and bacterial lipid metabolism during tuberculosis infections: possibilities to synergise host- and bacteria-directed therapies. Crit Rev Microbiol. 2024:1-21.
103. Ibeagha-Awemu EM, Bissonnette N, Do DN, Dudemaine PL, Wang M, Facciuolo A, et al. Regionally Distinct Immune and Metabolic Transcriptional Responses in the Bovine Small Intestine and Draining Lymph Nodes During a Subclinical Mycobacterium avium subsp. paratuberculosis Infection. Front Immunol. 2021;12:760931.
104. Yang D, Fu X, He S, Ning X, Ling M. Analysis of Differentially Expressed Proteins in Mycobacterium avium-Infected Macrophages Comparing with Mycobacterium tuberculosis-Infected Macrophages. Biomed Res Int. 2017;2017:5103803.
105. Nazarova EV, Montague CR, La T, Wilburn KM, Sukumar N, Lee W, et al. Rv3723/LucA coordinates fatty acid and cholesterol uptake in Mycobacterium tuberculosis. Elife. 2017;6.
106. Miltner E, Daroogheh K, Mehta PK, Cirillo SL, Cirillo JD, Bermudez LE. Identification of Mycobacterium avium genes that affect invasion of the intestinal epithelium. Infect Immun. 2005;73(7):4214-21.
107. Singh V, Jamwal S, Jain R, Verma P, Gokhale R, Rao KV. Mycobacterium tuberculosis-driven targeted recalibration of macrophage lipid homeostasis promotes the foamy phenotype. Cell Host Microbe. 2012;12(5):669-81.
108. Ouimet M, Koster S, Sakowski E, Ramkhelawon B, van Solingen C, Oldebeken S, et al. Mycobacterium tuberculosis induces the miR-33 locus to reprogram autophagy and host lipid metabolism. Nat Immunol. 2016;17(6):677-86.
109. Kim YS, Lee HM, Kim JK, Yang CS, Kim TS, Jung M, et al. PPAR-alpha Activation Mediates Innate Host Defense through Induction of TFEB and Lipid Catabolism. J Immunol. 2017;198(8):3283-95.
110. Asalla S, Mohareer K, Banerjee S. Small Molecule Mediated Restoration of Mitochondrial Function Augments Anti-Mycobacterial Activity of Human Macrophages Subjected to Cholesterol Induced Asymptomatic Dyslipidemia. Front Cell Infect Microbiol. 2017;7:439.
111. Mayer-Barber KD, Sher A. Cytokine and lipid mediator networks in tuberculosis. Immunol Rev. 2015;264(1):264-75.

112. Sorgi CA, Soares EM, Rosada RS, Bitencourt CS, Zoccal KF, Pereira PAT, et al. Eicosanoid pathway on host resistance and inflammation during Mycobacterium tuberculosis infection is comprised by LTB(4) reduction but not PGE(2) increment. Biochim Biophys Acta Mol Basis Dis. 2020;1866(3):165574.
113. Mayer-Barber KD, Andrade BB, Oland SD, Amaral EP, Barber DL, Gonzales J, et al. Host-directed therapy of tuberculosis based on interleukin-1 and type I interferon crosstalk. Nature. 2014;511(7507):99-103.
114. Mortensen R, Clemmensen HS, Woodworth JS, Therkelsen ML, Mustafa T, Tonby K, et al. Cyclooxygenase inhibitors impair CD4 T cell immunity and exacerbate Mycobacterium tuberculosis infection in aerosol-challenged mice. Commun Biol. 2019;2:288.
115. Shaw TD, Krasnodembskaya AD, Schroeder GN, Doherty DF, Silva JD, Tandel SM, et al. Human mesenchymal stromal cells inhibit Mycobacterium avium replication in clinically relevant models of lung infection. Thorax. 2024;79(8):778-87.
116. Vilaplana C, Marzo E, Tapia G, Diaz J, Garcia V, Cardona PJ. Ibuprofen therapy resulted in significantly decreased tissue bacillary loads and increased survival in a new murine experimental model of active tuberculosis. J Infect Dis. 2013;208(2):199-202.
117. Byrne ST, Denkin SM, Zhang Y. Aspirin antagonism in isoniazid treatment of tuberculosis in mice. Antimicrob Agents Chemother. 2007;51(2):794-5.
118. Nore KG, Louet C, Bugge M, Gidon A, Jorgensen MJ, Jenum S, et al. The Cyclooxygenase 2 Inhibitor Etoricoxib as Adjunctive Therapy in Tuberculosis Impairs Macrophage Control of Mycobacterial Growth. J Infect Dis. 2024;229(3):888-97.
119. Kaul V, Bhattacharya D, Singh Y, Van Kaer L, Peters-Golden M, Bishai WR, et al. An important role of prostanoid receptor EP2 in host resistance to Mycobacterium tuberculosis infection in mice. J Infect Dis. 2012;206(12):1816-25.
120. Auricchio G, Garg SK, Martino A, Volpe E, Ciaramella A, De Vito P, et al. Role of macrophage phospholipase D in natural and CpG-induced antimycobacterial activity. Cell Microbiol. 2003;5(12):913-20.
121. Hawn TR, Matheson AI, Maley SN, Vandal O. Host-directed therapeutics for tuberculosis: can we harness the host? Microbiol Mol Biol Rev. 2013;77(4):608-27.
122. Ciucci T, Bosselut R. Gimap and T cells: a matter of life or death. Eur J Immunol. 2014;44(2):348-51.
123. Lee YJ, Horie Y, Wallace GR, Choi YS, Park JA, Choi JY, et al. Genome-wide association study identifies GIMAP as a novel susceptibility locus for Behcet's disease. Ann Rheum Dis. 2013;72(9):1510-6.
124. Barnes MJ, Aksoylar H, Krebs P, Bourdeau T, Arnold CN, Xia Y, et al. Loss of T cell and B cell quiescence precedes the onset of microbial flora-dependent wasting disease and intestinal inflammation in Gimap5-deficient mice. J Immunol. 2010;184(7):3743-54.
125. Limoges MA, Cloutier M, Nandi M, Ilangumaran S, Ramanathan S. The GIMAP Family Proteins: An Incomplete Puzzle. Front Immunol. 2021;12:679739.
126. Yao Y, Du Jiang P, Chao BN, Cagdas D, Kubo S, Balasubramaniyam A, et al. GIMAP6 regulates autophagy, immune competence, and inflammation in mice and humans. J Exp Med. 2022;219(6).
127. Pascall JC, Rotondo S, Mukadam AS, Oxley D, Webster J, Walker SA, et al. The immune system GTPase GIMAP6 interacts with the Atg8 homologue GABARAPL2 and is recruited to autophagosomes. PLoS One. 2013;8(10):e77782.
128. Pascall JC, Webb LMC, Eskelinen EL, Innocentin S, Attaf-Bouabdallah N, Butcher GW. GIMAP6 is required for T cell maintenance and efficient autophagy in mice. PLoS One. 2018;13(5):e0196504.
129. Schwefel D, Frohlich C, Eichhorst J, Wiesner B, Behlke J, Aravind L, et al. Structural basis of oligomerization in septin-like GTPase of immunity-associated protein 2 (GIMAP2). Proc Natl Acad Sci U S A. 2010;107(47):20299-304.
130. Bermudez LE, Kolonoski P, Wu M, Aralar PA, Inderlied CB, Young LS. Mefloquine is active in vitro and in vivo against Mycobacterium avium complex. Antimicrob Agents Chemother. 1999;43(8):1870-4.
131. Choi SR, Britigan BE, Switzer B, Hoke T, Moran D, Narayanasamy P. In Vitro Efficacy of Free and Nanoparticle Formulations of Gallium(III) meso-Tetraphenylporphyrine against Mycobacterium avium and Mycobacterium abscessus and Gallium Biodistribution in Mice. Mol Pharm. 2018;15(3):1215-25.
132. Rose SJ, Neville ME, Gupta R, Bermudez LE. Delivery of aerosolized liposomal amikacin as a novel approach for the treatment of nontuberculous mycobacteria in an experimental model of pulmonary infection. PLoS One. 2014;9(9):e108703.
133. Daigneault M, Preston JA, Marriott HM, Whyte MK, Dockrell DH. The identification of markers of macrophage differentiation in PMA-stimulated THP-1 cells and monocyte-derived macrophages. PLoS One. 2010;5(1):e8668.
134. Kohro T, Tanaka T, Murakami T, Wada Y, Aburatani H, Hamakubo T, et al. A comparison of differences in the gene expression profiles of phorbol 12-myristate 13-acetate differentiated THP-1 cells and human monocyte-derived macrophage. J Atheroscler Thromb. 2004;11(2):88-97.

135. Sato K, Tomioka H, Akaki T, Kawahara S. Antimicrobial activities of levofloxacin, clarithromycin, and KRM-1648 against Mycobacterium tuberculosis and Mycobacterium avium complex replicating within Mono Mac 6 human macrophage and A-549 type II alveolar cell lines. Int J Antimicrob Agents. 2000;16(1):25-9.
136. Sato K, Tomioka H. Antimicrobial activities of benzoxazinorifamycin (KRM-1648) and clarithromycin against Mycobacterium avium-intracellulare complex within murine peritoneal macrophages, human macrophage-like cells and human alveolar epithelial cells. J Antimicrob Chemother. 1999;43(3):351-7.
137. Tomioka H, Sato K, Sano C, Sano K, Shimizu T. Intramacrophage passage of Mycobacterium tuberculosis and M. avium complex alters the drug susceptibilities of the organisms as determined by intracellular susceptibility testing using macrophages and type II alveolar epithelial cells. Antimicrob Agents Chemother. 2002;46(2):519-21.
138. De Logu A, Saddi M, Onnis V, Sanna C, Congiu C, Borgna R, et al. In vitro antimycobacterial activity of newly synthesised S-alkylisothiosemicarbazone derivatives and synergistic interactions in combination with rifamycins against Mycobacterium avium. Int J Antimicrob Agents. 2005;26(1):28-32.
139. Zaru M, Sinico C, De Logu A, Caddeo C, Lai F, Manca ML, et al. Rifampicin-loaded liposomes for the passive targeting to alveolar macrophages: in vitro and in vivo evaluation. J Liposome Res. 2009;19(1):68-76.
140. Das S, Garg T, Chopra S, Dasgupta A. Repurposing disulfiram to target infections caused by non-tuberculous mycobacteria. J Antimicrob Chemother. 2019;74(5):1317-22.
141. Alvarez GR, Zwilling BS, Lafuse WP. Mycobacterium avium inhibition of IFN-gamma signaling in mouse macrophages: Toll-like receptor 2 stimulation increases expression of dominant-negative STAT1 beta by mRNA stabilization. J Immunol. 2003;171(12):6766-73.
142. Nozawa RT, Kato H, Yokota T, Sugi H. Susceptibility of intra- and extracellular Mycobacterium avium-intracellulare to cephem antibiotics. Antimicrob Agents Chemother. 1985;27(1):132-4.
143. Shiratsuchi H, Jacobs MR, Pearson AJ, Venkataprasad N, Klopman G, Ellner JJ. Comparison of the activity of fluoroquinolones against Mycobacterium avium in cell-free systems and a human monocyte in-vitro infection model. J Antimicrob Chemother. 1996;37(3):491-500.
144. Skinner PS, Furney SK, Jacobs MR, Klopman G, Ellner JJ, Orme IM. A bone marrow-derived murine macrophage model for evaluating efficacy of antimycobacterial drugs under relevant physiological conditions. Antimicrob Agents Chemother. 1994;38(11):2557-63.
145. Ghassemi M, Andersen BR, Reddy VM, Gangadharam PR, Spear GT, Novak RM. Human immunodeficiency virus and Mycobacterium avium complex coinfection of monocytoid cells results in reciprocal enhancement of multiplication. J Infect Dis. 1995;171(1):68-73.
146. Vijayakumar S, Finney John S, Nusbaum RJ, Ferguson MR, Cirillo JD, Olaleye O, et al. In vitro model of mycobacteria and HIV-1 co-infection for drug discovery. Tuberculosis (Edinb). 2013;93 Suppl(Suppl):S66-70.
147. Hong T, Bae SM, Song G, Lim W. Guide for generating single-cell-derived knockout clones in mammalian cell lines using the CRISPR/Cas9 system. Mol Cells. 2024;47(7):100087.
148. Iakobachvili N, Leon-Icaza SA, Knoops K, Sachs N, Mazeres S, Simeone R, et al. Mycobacteria-host interactions in human bronchiolar airway organoids. Mol Microbiol. 2022;117(3):682-92.
149. Fonseca KL, Rodrigues PNS, Olsson IAS, Saraiva M. Experimental study of tuberculosis: From animal models to complex cell systems and organoids. PLoS Pathog. 2017;13(8):e1006421.
150. Tezera LB, Bielecka MK, Chancellor A, Reichmann MT, Shammari BA, Brace P, et al. Dissection of the host-pathogen interaction in human tuberculosis using a bioengineered 3-dimensional model. Elife. 2017;6.
151. Blake R, Jensen K, Mabbott N, Hope J, Stevens J. The Development of 3D Bovine Intestinal Organoid Derived Models to Investigate Mycobacterium Avium ssp Paratuberculosis Pathogenesis. Front Vet Sci. 2022;9:921160.
152. Research Committee of the British Thoracic S. First randomised trial of treatments for pulmonary disease caused by M avium intracellulare, M malmoense, and M xenopi in HIV negative patients: rifampicin, ethambutol and isoniazid versus rifampicin and ethambutol. Thorax. 2001;56(3):167-72.
153. Gangadharam PR, Perumal VK, Parikh K, Podapati NR, Taylor R, Farhi DC, et al. Susceptibility of beige mice to Mycobacterium avium complex infections by different routes of challenge. Am Rev Respir Dis. 1989;139(5):1098-104.
154. Lounis N, Ji B, Truffot-Pernot C, Grosset J. Comparative activities of amikacin against Mycobacterium avium complex in nude and beige mice. Antimicrob Agents Chemother. 1997;41(5):1168-9.
155. Gangadharam PR, Perumal VK, Farhi DC, LaBrecque J. The beige mouse model for Mycobacterium avium complex (MAC) disease: optimal conditions for the host and parasite. Tubercle. 1989;70(4):257-71.
156. Collins FM, Stokes RW. Mycobacterium avium-complex infections in normal and immunodeficient mice. Tubercle. 1987;68(2):127-36.
157. Saunders BM, Dane A, Briscoe H, Britton WJ. Characterization of immune responses during

infection with Mycobacterium avium strains 100, 101 and the recently sequenced 104. Immunol Cell Biol. 2002;80(6):544-9.
158. Andrejak C, Almeida DV, Tyagi S, Converse PJ, Ammerman NC, Grosset JH. Characterization of mouse models of Mycobacterium avium complex infection and evaluation of drug combinations. Antimicrob Agents Chemother. 2015;59(4):2129-35.
159. Sison JP, Yao Y, Kemper CA, Hamilton JR, Brummer E, Stevens DA, et al. Treatment of Myocardium avium complex infection: does the beige mouse model predict therapeutic outcome in humans? J Infect Dis. 1996;173(3):750-3.
160. Seok J, Warren HS, Cuenca AG, Mindrinos MN, Baker HV, Xu W, et al. Genomic responses in mouse models poorly mimic human inflammatory diseases. Proc Natl Acad Sci U S A. 2013;110(9):3507-12.
161. Torraca V, Masud S, Spaink HP, Meijer AH. Macrophage-pathogen interactions in infectious diseases: new therapeutic insights from the zebrafish host model. Dis Model Mech. 2014;7(7):785-97.
162. Lam SH, Chua HL, Gong Z, Lam TJ, Sin YM. Development and maturation of the immune system in zebrafish, Danio rerio: a gene expression profiling, in situ hybridization and immunological study. Dev Comp Immunol. 2004;28(1):9-28.
163. Crowle AJ, Dahl R, Ross E, May MH. Evidence that vesicles containing living, virulent Mycobacterium tuberculosis or Mycobacterium avium in cultured human macrophages are not acidic. Infect Immun. 1991;59(5):1823-31.
164. Koga H. High-performance liquid chromatography measurement of antimicrobial concentrations in polymorphonuclear leukocytes. Antimicrob Agents Chemother. 1987;31(12):1904-8.
165. Ishiguro M, Koga H, Kohno S, Hayashi T, Yamaguchi K, Hirota M. Penetration of macrolides into human polymorphonuclear leucocytes. J Antimicrob Chemother. 1989;24(5):719-29.
166. Viljoen A, Raynaud C, Johansen MD, Roquet-Baneres F, Herrmann JL, Daher W, et al. Verapamil Improves the Activity of Bedaquiline against Mycobacterium abscessus In Vitro and in Macrophages. Antimicrob Agents Chemother. 2019;63(9).
167. Gupta S, Tyagi S, Bishai WR. Verapamil increases the bactericidal activity of bedaquiline against Mycobacterium tuberculosis in a mouse model. Antimicrob Agents Chemother. 2015;59(1):673-6.
168. Gupta S, Tyagi S, Almeida DV, Maiga MC, Ammerman NC, Bishai WR. Acceleration of tuberculosis treatment by adjunctive therapy with verapamil as an efflux inhibitor. Am J Respir Crit Care Med. 2013;188(5):600-7.
169. Adams KN, Szumowski JD, Ramakrishnan L. Verapamil, and its metabolite norverapamil, inhibit macrophage-induced, bacterial efflux pump-mediated tolerance to multiple anti-tubercular drugs. J Infect Dis. 2014;210(3):456-66.
170. Lake MA, Adams KN, Nie F, Fowler E, Verma AK, Dei S, et al. The human proton pump inhibitors inhibit Mycobacterium tuberculosis rifampicin efflux and macrophage-induced rifampicin tolerance. Proc Natl Acad Sci U S A. 2023;120(7):e2215512120.
171. Kundu A, Ghosh P, Bishayi B. Vitexin along with verapamil downregulates efflux pump P-glycoprotein in macrophages and potentiate M1 to M2 switching via TLR4-NF-kappaB-TNFR2 pathway in lipopolysaccharide treated mice. Immunobiology. 2024;229(1):152767.
172. Gandhi S, Fleet JL, Bailey DG, McArthur E, Wald R, Rehman F, et al. Calcium-channel blocker-clarithromycin drug interactions and acute kidney injury. JAMA. 2013;310(23):2544-53.
173. Rothchild AC, Stowell B, Goyal G, Nunes-Alves C, Yang Q, Papavinasasundaram K, et al. Role of Granulocyte-Macrophage Colony-Stimulating Factor Production by T Cells during Mycobacterium tuberculosis Infection. mBio. 2017;8(5).
174. Moreira JD, Koch BEV, van Veen S, Walburg KV, Vrieling F, Mara Pinto Dabes Guimaraes T, et al. Functional Inhibition of Host Histone Deacetylases (HDACs) Enhances in vitro and in vivo Anti-mycobacterial Activity in Human Macrophages and in Zebrafish. Front Immunol. 2020;11:36.
175. Denis M. Tumor necrosis factor and granulocyte macrophage-colony stimulating factor stimulate human macrophages to restrict growth of virulent Mycobacterium avium and to kill avirulent M. avium: killing effector mechanism depends on the generation of reactive nitrogen intermediates. J Leukoc Biol. 1991;49(4):380-7.

Nederlandse samenvatting
Dankwoord
List of publications
Curriculum vitae

Nederlandse samenvatting

Mycobacterium avium (*Mav*) behoort tot de groep van niet-tuberculeuze mycobacteriën (NTM) en is binnen deze groep de meest voorkomende oorzaak van ernstige en chronische longziekten. Longziekte is de meest voorkomende ziekte door een *Mav*-infectie en treft met name personen met onderliggende longaandoeningen, zoals taaislijmziekte of chronische obstructieve longziekte (COPD), maar ook ogenschijnlijk gezonde individuen kunnen aan een *Mav*-gerelateerde ziekte lijden. Alhoewel infectie van de longen het meest voorkomt, kan *Mav* ook infecties van lymfeklieren, botten, gewrichten, huid en het maagdarmkanaal veroorzaken. De incidentie van zowel *Mav*-infecties als *Mav*-geïnduceerde longziekte neemt wereldwijd toe, wat een groeiende uitdaging vormt voor de volksgezondheid.

De geadviseerde behandeling van *Mav*-infecties bestaat uit een langdurige combinatietherapie van antibiotica zoals macroliden, ethambutol en rifamycines. *Mav* is van nature echter zeer tolerant tegen deze medicijnen en vergaarde resistentie kan deze ongevoeligheid verder versterken. Hierdoor zijn deze behandelingen vaak onvoldoende effectief om de infectie volledig onder controle te krijgen. Daarnaast dragen de lange behandelduur en de bijbehorende bijwerkingen aan een verminderde therapietrouwheid, wat de effectiviteit van de behandeling verder ondermijnt. Er is daarom een dringende behoefte aan alternatieve therapeutische strategieën die deze beperkingen kunnen ondervangen en de controle van infectie kunnen verbeteren.

Het immuunsysteem van de gastheer speelt een cruciale rol in de afweer tegen mycobacteriële infecties zoals *Mav*. Na inhalatie via aerosolen bereiken *Mav*-bacteriën de longen, waar alveolaire macrofagen een essentiële verdedigingslinie vormen. Deze immuuncellen herkennen *Mav* via diverse celreceptoren, wat leidt tot opname (fagocytose) van de bacteriën. Binnen deze cellen worden de bacteriën vervolgens afgebroken in fagolysosomen, waarbij onder andere reactieve zuurstofradicalen (ROS) worden ingezet als afweermechanisme. *Mav* beschikt echter over verschillende strategieën om deze immuunresponsen te omzeilen en te kunnen overleven in de macrofagen. Een veelbelovende benadering voor de behandeling van *Mav* is daarom gastheergerichte therapie (host-directed therapy: HDT), die zich richt op het moduleren van de immuunrespons van de gastheer. HDT kan daarbij zowel weefselschade als gevolg van een overmatige immuunreactie beperken, als de intracellulaire klaring van de bacterie versterken. Doordat HDT zich niet rechtstreeks op de bacterie richt, is het risico op resistentieontwikkeling minimaal en kunnen ook resistentie bacteriën bestreden worden. HDT heeft daarmee de potentie om, als aanvulling op antibiotica therapieën, de effectiviteit van de behandeling van *Mav*-infecties te verbeteren.

Onderzoek naar HDT bij *Mav*-infecties staat echter nog in de kinderschoenen in vergelijking met onderzoek naar HDT voor *Mycobacterium tuberculosis* (*Mtb*), de veroorzaker van tuberculose. Dit wordt duidelijk in **hoofdstuk 2** van dit proefschrift, waarin we met een uitgebreid literatuuroverzicht de bestaande HDT-strategieën en veelbelovende gastheertargets bij mycobacteriële infecties presenteren. Daaruit blijkt dat, hoewel er veel bekend is over de interacties tussen gastheer en *Mtb* en HDT bij *Mtb* al uitvoerig is onderzocht, de kennis over *Mav* aanzienlijk beperkter is. Dit benadrukt de urgentie van verder onderzoek naar de gastheermechanismen die betrokken zijn bij *Mav*-infecties en die als aangrijpingspunt kunnen dienen voor de ontwikkeling van

HDT. Dit proefschrift beoogt dan ook om zowel nieuwe HDT-kandidaten ter bestrijding van *Mav*-infecties te identificeren, als het inzicht in de onderliggende gastheer-pathogeeninteracties te verkrijgen om potentiële therapeutische targets voor de ontwikkeling van nieuwe HDT-strategieën te identificeren.

Om de doelstellingen van dit proefschrift te behalen, lag in **hoofdstuk 3** de nadruk op het ontwikkelen van gestandaardiseerde en betrouwbare celmodellen voor het bestuderen van *Mav*-infecties. Hiervoor hebben we zowel primaire humane macrofagen als de MelJuSo-cellijn gebruikt. Waar macrofagen een hoge fysiologische relevantie bij *Mav*-infectie in de gastheer hebben, biedt de cellijn de mogelijkheid om experimenten uit te voeren zonder een beperking in celaantallen. Door verschillende parameters van *Mav*-infectie op gastheercellen te testen en de opname en eliminatie van bacteriën te evalueren, hebben we de infectiecondities voor toekomstige experimenten bepaald. Daarbij toonden we aan dat de MGIT-assay een objectieve, geautomatiseerde en valide alternatief is op de traditionele CFU-assay voor het kwantificeren van intracellulaire bacteriën. De ontwikkeling van deze infectiemodellen bood niet alleen waardevolle inzichten in de dynamiek van *Mav*-infecties aan, maar stelde ons ook in staat om de effectiviteit van potentiële HDT-kandidaten en de intracellulaire interacties tussen de gastheercel en de bacterie te bestuderen.

Om HDT-kandidaten voor *Mav*-infecties te identificeren, hebben we gekozen voor een herpositioneringsstrategie: het testen van al goedgekeurde geneesmiddelen die mogelijk de intracellulaire overleving van *Mav* kunnen remmen. Deze benadering zou het toekomstige ontwikkelingsproces kunnen versnellen doordat de veiligheid en farmacokinetiek van deze middelen al (grotendeels) bekend zijn. In **hoofdstuk 4** presenteren we onderzoeksresultaten van het medicijn amiodarone, dat momenteel wordt toegepast bij de behandeling van hartritmestoornissen. Behandeling van *Mav*-geïnfecteerde humane macrofagen met amiodarone resulteerde in een verhoogde klaring van intracellulaire *Mav*, zonder dat de bacterie direct werd gedood, wat suggereert dat amiodarone de afweermechanismen van de macrofaag versterkt. Onderzoek naar het mechanisme toonde aan dat amiodarone autofagie activeert, een proces dat essentieel is voor het opruimen van intracellulaire afvalstoffen, waaronder pathogenen zoals *Mav*. We ondervonden dat amiodarone de vorming van (auto)fagosomen bevorderde en de lokalisatie van bacteriën binnen deze compartimenten verhoogde. Daarnaast zagen we dat behandeling met amiodarone resulteerde in verhoogde nucleaire lokalisatie van transcriptiefactor EB (TFEB), die betrokken is bij de regulatie van autofagie-gerelateerde genen. Naast verminderde overleving in macrofagen, liet deze studie zien dat *Mav*-overleving ook sterk verlaagd was in amiodarone-behandelde zebravissen, wat de potentie van amiodarone als HDT-kandidaat verder onderbouwt.

Naast amiodarone resulteerde onze screeningsaanpak ook in de identificatie van de fenothiazines trifluoperazine (TFP) en chlorproethazine (CPE), waarvan de onderzoeksresultaten worden beschreven in **hoofdstuk 5**. Deze medicijnen worden normaliter gebruikt voor de behandeling van psychische aandoeningen maar bleken eveneens de intracellulaire overleving van *Mav* in humane macrofagen te verlagen, met beperkte directe antibacteriële werking. Dit suggereert dat TFP en CPE werken door hoogstwaarschijnlijk de antibacteriële gastheercelrespons te stimuleren. Van de verschillende mechanismen die macrofagen kunnen inzetten tegen *Mav*-infectie,

konden we aantonen dat autofagie hierin geen rol speelde. TFP en CPE verhoogden wel de productie van ROS, wat bijdroeg aan een verbeterde bacteriële klaring. Van de twee belangrijkste bronnen van ROS-productie in macrofagen, de mitochondriën en NADPH oxidase, bleek laatstgenoemde gedeeltelijk bij te dragen aan de door TFP- en CPE-geïnduceerde antibacteriële activiteit van de cel. De gedeeltelijke rol van ROS suggereert dat deze fenothiazines mogelijk ook andere gastheermechanismen moduleren om de intracellulaire bestrijding van *Mav* te stimuleren. De bevindingen in hoofstukken 4 en 5 leveren niet alleen veelbelovende HDT-kandidaten op, maar bieden ook nieuwe inzichten in de relevante mechanismen van de gastheerrespons bij de eliminatie van *Mav*, wat een belangrijke basis vormt voor de verdere ontwikkeling van veilige en effectieve HDT-strategieën.

Het tweede onderzoeksdoel van dit proefschrift was het karakteriseren van de gastheerrespons op *Mav*-infectie. Om te begrijpen welke veranderingen in genexpressie als reactie op infectie plaatsvinden, hebben we in **hoofdstuk 6** een diepgaande transcriptoomanalyse van *Mav*-geïnfecteerde humane macrofagen uitgevoerd. Gezien de bestaande kennis over de gastheerrespons bij *Mtb*, includeerden we ook *Mtb*-geïnfecteerde humane macrofagen als vergelijkingsgroep. Dit stelde ons in staat om de relevantie van bepaalde genexpressiepatronen na *Mav*-infectie beter te interpreteren. De analyse toonde substantiële overlap tussen de gastheerrespons op *Mav* en *Mtb*, waaronder de regulatie van genen die coderen voor cytokinen, bekende sleutelcomponenten van de antimicrobiële afweer. Daarnaast zagen we dat beide pathogenen genen beïnvloedden die betrokken zijn bij lipidenmetabolisme. Voor *Mtb* is bekend dat de bacterie het lipidenmetabolisme van de gastheer zodanig moduleert dat lipiden in hogere mate worden opgenomen en opgeslagen, een strategie waarmee de bacterie toegang krijgt tot deze voedingsstoffen. Onze analyse identificeerde daarnaast genen die sterker gereguleerd worden na *Mav*- dan na *Mtb*-infectie. Zo leidde *Mav*-infectie tot een sterkere expressie van cytokine-coderende genen, genen die mogelijk betrokken zijn bij apoptose, en van GIMAP-genen, waarvan de rol in mycobacteriële infecties nog grotendeels onbekend is. Deze resultaten leveren waardevolle inzichten in de gastheermechanismen die betrokken zijn bij *Mav*-infecties, en die zouden kunnen bijdragen aan de identificatie van nieuwe therapeutische targets voor HDT.

Samengevat biedt dit proefschrift nieuwe aanknopingspunten voor de ontwikkeling van HDT voor *Mav*-infecties. Enerzijds door het identificeren van veelbelovende therapeutische kandidaten die verder kunnen worden ontwikkeld, en anderzijds door het genereren van diepgaand inzicht in de gastheerrespons op *Mav*-infecties, wat kan bijdragen aan effectievere en duurzamere behandelingen met een verlaagd risico op resistentieontwikkeling.

Dankwoord

Ik heb enorm uitgekeken naar het moment dat ik mijn proefschrift in handen zou hebben, en dat moment is nu eindelijk aangebroken. Met veel emoties presenteer ik jullie mijn proefschrift. Mijn promotieonderzoek was een lange en intensieve, maar vooral leerzame reis. Hoewel het niet altijd makkelijk was, heb ik onwijs veel geleerd over het uitvoeren van onderzoek en vind ik het met name waardevol dat ik mezelf beter heb leren kennen. Deze reis had ik minder goed kunnen maken zonder de steun van de mensen om mij heen. Dit laatste stuk van mijn proefschrift wijd ik dan ook aan het bedanken van iedereen die mij in de afgelopen jaren heeft gesteund, begeleid en geïnspireerd.

Allereerst mijn promotor Tom, bedankt voor het vertrouwen in 2018 als student en de mogelijkheid om in 2019 mijn PhD in jouw groep te doen. Jouw begeleiding en waardevolle feedback hebben mij veel geholpen tijdens dit traject. Ook wil ik mijn voormalige copromotor Mariëlle bedanken voor haar bijdrage in de beginfase van mijn PhD. Mijn dank gaat ook uit naar mijn copromotor Anno voor de samenwerking en ondersteuning gedurende mijn PhD. Ik heb het laagdrempelige contact en onze ontelbare meetings, waarin we volop hebben kunnen sparren over mijn onderzoek, erg gewaardeerd.

Daarnaast wil ik ook mijn collega's van INZI/LUCID-R bedanken, en in het bijzonder de HDT-groep met Kimberley, Susan en Robin. Bedankt voor jullie kennis, input en gezelligheid. Jullie waren een heel fijne groep en ik heb mij altijd thuis gevoeld op de afdeling.

Merel, bedankt voor jouw inzet tijdens jouw stage bij de HDT groep, waarmee je hebt bijgedragen aan één van de hoofdstukken in dit proefschrift.

Diantha, van samen beginnen als bachelor studenten tot het doen van een PhD in het LUMC: een lange reis vol koffiemomentjes, lunches en mooie gesprekken. Dankjewel daarvoor.

En ook Suus, Amy, Ellen, Michella, Arthur, Daaf en Eva. Van de gezelligste lunches tot op gegeven moment ook de leukste activiteiten buiten werk. Ik heb ontzettend veel met jullie kunnen praten en lachen. In het bijzonder Suus en Amy, mijn paranimfen: dat we in het K5-kantoor met de rug naar elkaar toe zaten, weerhield ons duidelijk niet van de vele gesprekken die we hadden. Zo vormden we snel onze eigen gevarendriehoek voor afleiding, maar wat was het een fijne afwisseling van het harde werken. Ik waardeer het dat ik jullie allemaal als collega's heb leren kennen, en des te meer dat daaruit mooie vriendschappen zijn ontstaan.

Als laatste wil ik natuurlijk mijn familie bedanken. Lieve mama, Irfan abi en Cici, bedankt voor jullie liefde, geduld en dat jullie er altijd voor mij zijn. Jullie betekenen onwijs veel voor mij en ik ben heel erg dankbaar dat ik jullie om mij heen heb. Ik heb altijd mijn hart bij jullie kunnen luchten en veel steun gehad aan jullie soms troostende, maar vooral bemoedigende en motiverende woorden. Voor mij zijn jullie de onzichtbare coauteurs van dit proefschrift, want zonder jullie had dit proefschrift niet tot stand kunnen komen. Jullie zijn de beste, iyi ki varsınız, sizi çok seviyorum.

List of publications

1. **Kilinç G**, van den Biggelaar RHGA, Ottenhoff THM, Mei LH, Saris A. Comparative transcriptomic analysis of human macrophages during *Mycobacterium avium* versus *Mycobacterium tuberculosis* infection. Submitted.
2. **Kilinç G**, Ottenhoff THM, Saris A. Phenothiazines boost host control of *Mycobacterium avium* infection in primary human macrophages. Biomed Pharmacother. 2025 Feb 27;185:117941. doi: 10.1016/j.biopha.2025.117941.
3. **Kilinç G***, Boland R*, Heemskerk MT, Spaink HP, Haks MC, van der Vaart M, Ottenhoff THM, Meijer AH#, Saris A#. Host-directed therapy with amiodarone in preclinical models restricts mycobacterial infection and enhances autophagy. Microbiol Spectr. 2024 Aug 6;12(8):e0016724. doi: 10.1128/spectrum.00167-24.
4. **Kilinç G**, Walburg KV, Franken KLMC, Valkenburg ML, Aubry A, Haks MC, Saris A#, Ottenhoff THM#. Development of human cell-based *in vitro* infection models to determine the intracellular survival of *Mycobacterium avium*. Front Cell Infect Microbiol. 2022 Jun 24;12:872361. doi: 10.3389/fcimb.2022.872361.
5. Helderman NC, Elsayed FA, van Wezel T, Terlouw D, Langers AMJ, van Egmond D, **Kilinç G**, Hristova H, Farina Sarasqueta A, Morreau H, Nielsen M, Suerink M; PALGA-group collaborators. Mismatch repair deficiency and MUTYH variants in small intestine-neuroendocrine tumors. Hum Pathol. 2022 Jul;125:11-17. doi: 10.1016/j.humpath.2022.04.003.
6. Helderman NC, Suerink M, **Kilinç G**, van den Berg JG, Nielsen M, Tesselaar MET. Relation between WHO classification and location- and functionality-based classifications of neuroendocrine neoplasms of the digestive tract. Neuroendocrinology. 2024;114(2):120-133. doi: 10.1159/000534035.
7. **Kilinç G***, Saris A*, Ottenhoff THM, Haks MC. Host-directed therapy to combat mycobacterial infections. Immunol Rev. 2021 May;301(1):62-83. doi: 10.1111/imr.12951.
8. Suerink M, **Kilinç G**, Terlouw D, Hristova H, Sensuk L, van Egmond D, Farina Sarasqueta A, Langers AMJ, van Wezel T, Morreau H, Nielsen M; PALGA-group collaborators. Prevalence of mismatch repair deficiency and Lynch syndrome in a cohort of unselected small bowel adenocarcinomas. J Clin Pathol. 2021 Nov;74(11):724-729. doi: 10.1136/jclinpath-2020-207040.

*,#: Equal contribution

Curriculum vitae

Gül Kilinç was born on September 1st, 1996, in Sas van Gent, The Netherlands. After obtaining her VWO diploma at the Stedelijke Scholengemeenschap De Rede in 2014, she started her Bachelor's degree in Biomedical Sciences at Leiden University. During her studies, she completed a research internship at the department of Nephrology of the Leiden University Medical Center (LUMC). She also pursued a minor in Organ Transplantation at the Erasmus Medical Center, where she developed an interest in immunology. In 2017, she enrolled in the Research Master's program in Biomedical Sciences at Leiden University. For her first master's internship in 2018, she joined the group of Prof. Dr. Tom Ottenhoff at the department of Infectious Diseases at the LUMC. Under supervision of Matthias Heemskerk, she investigated the concept of host-directed therapy (HDT) for intracellular mycobacteria. For her second internship in 2019, she joined the group of Dr. Maartje Nielsen at the department of Clinical Genetics at the LUMC, where she studied the prevalence of specific genetic variants in small intestine adenocarcinomas. After obtaining her Master's degree in the summer of 2019, Gül decided to further pursue the development of HDT to combat mycobacterial infections. In September 2019, she returned to the group of Prof. Dr. Tom Ottenhoff and Dr. Anno Saris to start her PhD at the department of Infectious Diseases. Her PhD research focused on the identification of HDT candidates for *Mycobacterium avium* (*Mav*), and the elucidation of host transcriptomic responses to intracellular *Mav* infection to uncover novel targets, both for the ultimate goal to advance HDT for *Mav* infection. The findings of the research are presented in this thesis.